ROLE OF THYMIDYLATE SYNTHASE REGULATION OF MYC, p53 AND OTHER GENES IN MEDIATING 5-FLUOROURACIL/LEUCOVORIN RESISTANCE IN COLORECTAL CANCER AND CF10 RESPONSE

BY

CHARLES C. OKECHUKWU, MS

A Dissertation Submitted to the Graduate Faculty of

WAKE FOREST UNIVERSITY GRADUATE SCHOOL OF ARTS AND SCIENCES

in Partial Fulfillment of the Requirements

for the Degree of

DOCTOR OF PHILOSOPHY

Integrative Physiology and Pharmacology

May, 2025

Winston-Salem, North Carolina

Approved By:

William H. Gmeiner, Ph.D., MBA, Advisor

Timothy S. Pardee, MD, Ph.D., FACP, Chairperson

Kounosuke Watabe, Ph.D.

Temitope Keku, MSPH, Ph.D.

Konstantinos Votanopoulos, MD, Ph.D., FACS.

ACKNOWLEDGEMENTS

I graciously acknowledge the guidance and excellent mentorship of my advisor, Dr. William Henry Gmeiner, and I will always be forever grateful for his teachings. I am also thankful to all my committee members (Drs. Timothy Pardee, Kounosuke Watabe, Temitope Keku, and Konstantinos Votanopoulos) for their suggestions and guidance regarding my work, including the Wake Forest Comprehensive Cancer Center at Wake Forest University School of Medicine, for providing a conducive training environment.

I want to thank all the members of Dr. Gmeiner's laboratory for all their support during my study. I want to give special thanks to my wife, Sandra, and my children, Emilia and Michaelangelo, for all their support, understanding, love, prayers, and care during my PhD journey. I would like to thank my parents, Michael and Margaret Okechukwu, including my siblings, Remigius and Nicholas, for all their support. I want to give a special shout-out to the Partners program for the opportunity and for preparing me for this great journey, as well as to all my past mentors, especially Drs. Sandra White, Gwendolyn Sancar, ClarLynda Williams-DeVane, Emmanuel Awumey, and Mabel Royal, for their mentorship in multiple facets of life.

Lastly, but most importantly, I want to humbly thank my creator for providing and surrounding me with the best and most intellectual mentors, who have positively directed and structured my path to becoming an independent investigator created to contribute to the combat of metastatic colorectal cancer and also mentor the next generation of scientists.

TABLE OF CONTENTS

LIST OF FIGURES

Chapter 2

Chapter 3

.

Chapter 4

Chapter 5

Chapter 6

LIST OF TABLES

Chapter 4

Chapter 5

Chapter 6

LIST OF ABBREVIATIONS

5-FU	5-fluorouracil
3-MA	3-methyl adenine
A260	Absorbance of a solution measured at a wavelength of 260 nanometers
ABCB5	ATP-binding cassette subfamily b member 5
ABCC5	ATP-binding cassette subfamily c member 5
ABCC10	ATP-binding cassette subfamily c member 10
ACS	American cancer society
AKT	Serine/threonine-specific protein kinase
AMPK	AMP-activated protein kinase
ANOVA	Analysis of variance
AraC	Arabinosyl cytidine
AraCTP	Cytarabine triphosphate
ATCC	American type culture collection
ATM	Ataxia telangiectasia mutated
ATR	Ataxia telangiectasia mutated and Rad3-related
AUC	Area under the curve
BAK	B-cell lymphoma 2 (Bcl-2) antagonist/killer
BAX	Bcl-2-associated X protein
BCL-2	B-cell lymphoma 2
BER	Base excision repair
β-ACTIN	Beta-actin
BSA	Bovine serum albumin
CF10	AraC-FdUMP[10]
CH2 THF	5,10-methylenetetrahydrofolate

CHK1	Checkpoint kinase 1
CHK2	Checkpoint kinase 2
CO_2	Carbon dioxide
CPT	Camptothecin
CRC	Colorectal cancer
CRC-P	Parental colorectal cells
CRC-R	5FU/LV-resistant colorectal cancer cells
CRLM	Colorectal cancer liver metastasis
DDR	DNA damage response
DMEM	Dulbecco's modified eagle medium
DNA	Deoxyribonucleic acid
DPD	Dihydropyrimidine dehydrogenase deficiency
DPYD	Dihydropyrimidine dehydrogenase gene
DSB	DNA double strand break
dUMP	2'-deoxyuridine-5'-O-monophosphate
E2F	Early region 2 binding factor
E2F1	E2F Transcription Factor 1
EDTA	Ethylenediaminetetraacetic acid
EU	Ethynyl uracil
EX VIVO	Outside of the living body
F	Fluorodeoxyuridine
FANCD2	Fanconi anemia complementation group D2
FAS	Death receptor on the surface of cells that leads to programmed cell death
FASL	FAS ligand
FBAL	α-fluoro-β alanine
FBS	Fetal bovine serum

FdU	5-fluoro-2’-deoxyuridine
FdUDP	5-fluoro-2’-deoxyuridine-5’-diphosphate
FdUMP	5-Fluoro-2’-deoxyuridine-5’-O-monophosphate
FdUTP	5-fluoro-2′ deoxyuridine-5′-triphosphate
FOLFIRI	5-fluorouracil, leucovorin and irinotecan
FOLFOX	5-fluorouracil, leucovorin and oxaliplatin
FOXM1	Forkhead box M1
FP	Fluoropyrimidine
FR	Folate restricted
FUDP	5-fluorouridine diphosphosphate
FUMP	5-fluorouridine-5'-monophosphate
GAPDH	Glyceraldehyde-3-phosphate dehydrogenase
G1/S	Growth phase 1 and synthesis phase
gH2AX	Gamma-H2AX is a phosphorylated form of the histone H2AX
GI	Gastrointestinal
GI_{50}	50% inhibitory cell growth
GSEA	Gene set enrichment analysis
H&E	Hematoxylin and eosin
HSPB8	Heat shock protein family B member 8
IC_{50}	50% inhibitory drug concentration
IHC	Immunohistochemistry
IN VIVO	Within the living body
IV	Intravenously
IVIS	In Vivo imaging system
LC3	Microtubule-associated protein 1A/1B-light chain 3
LC3II	LC3-phosphatidylethanolamine conjugate
LV	Leucovorin

MCL-1	Myeloid cell leukemia 1
mCRC	Metastatic colorectal cancer
MLH1	MutL homolog
MMR-D	DNA mismatch repair deficiency
mRNA	Messenger RNA
miRNA	Micro RNA
MSH2	MutS homolog 2
MSI-H	Microsatellite instability
mTOR	Mammalian target of rapamycin
Myc	Multifunctional transcription factor
NaF	Sodium fluoride
NCI60	National Cancer Institute collection of 60 human cancer cell lines
NP-40	Nonidet P-40
NT5E	Ecto-5′-nucleotidase
O-GlcNAc	O-linked N-acetylglucosamine
p21	p53 downstream effector
p38MAPK	Mitogen-activated protein kinases that are responsive to stress stimuli
p53	Tumor suppressor
p53-/-	Two non-functional copies of the p53 gene
p53+/+	Two functional copies of the p53 gene
p62	A classical receptor of autophagy
pChk1	Phosphorylated Chk1
pChk2	Phosphorylated Chk2
PCR	Polymerase chain reaction
PDA	Pancreatic ductal adenocarcinoma
PDECGF	Platelet-derived endothelial cell growth factor

PEG	Polyethylene glycol
pH2AX	Functions same as gH2AX
PI	Propidium iodide
PI3K	Phosphoinositide 3-kinase
pRPA32	Phosphorylated RPA32
PRISM	Profiling relative inhibition simultaneously in mixtures
Rad51	Repairing double-strand breaks in DNA
RB	Retinoblastoma protein
RGD	Arginyl-glycyl-aspartic acid tripeptide sequence
RNA	Ribonucleic acid
RPA	Replication protein A complex
rRNA	Ribosomal RNA
RNR	Ribonucleotide reductase
RRM	RNA recognition motif
RT-qPCR	Real-time quantitative polymerase chain reaction
S1	Tegafur-gimeracil-potassium oxanate
SDS-PAGE	Sodium dodecyl sulfate-polyacrylamide gel electrophoresis
SEM	Standard error of the mean
SHMT2	Serine hydroxymethyl transferase
SN-38	Active metabolite of irinotecan
TAS-102	Trifluridine-tiperacil
TFT	Trifluorothymidine
TGF-βRII	Transforming growth factor-βRII
TK	Thymidine kinase
TMP	Trimethylolpropane
Top1	Topoisomerase
Top1cc	Topoisomerase 1 cleavage complexes

TP	Thymidylate phosphorylase
tRNA	Transfer RNA
TS	Thymidylate synthase
TSCC	TS classic complex or ternary complex formation
TSER	Thymidylate synthase enhancer region
TTP	Thrombotic thrombocytopenic purpura
TYMP	Thymidine phosphorylase gene
TYMS	Thymidylate synthase gene
UK	Uridine kinase
ULK1	Unc-51 Like Autophagy Activating Kinase 1
UMP	Uridine monophosphate
UMPK	UMP kinase
UMPS	UMP synthase
UV	Ultraviolet
V-FITC	Violet fluorescein isothiocyanate
WFUSM	Wake Forest university school of medicine

ANIMALS

- C57BL/6 Immunocompetent and syngeneic with the MC38 colon carcinoma cell line
- WAG/RIJ Immunocompetent and syngeneic with the CC531 colon carcinoma cell line

TUMOR CELLS

- CC531 Adenocarcinoma of the rat colon cell line
- HCT15 Human colon adenocarcinoma cell line
- HCT116 Human colorectal carcinoma cell line
- HIEC-6 Human normal intestinal epithelial cell line

- LS174T Human colorectal cancer cell line
- MC-38 Murine colon adenocarcinoma cell line
- HCT116R Human colorectal carcinoma cell line resistant to 5FU/LV
- HCT15R Human colorectal carcinoma cell line resistant to 5FU/LV
- LS174TR Human colorectal carcinoma cell line resistant to 5FU/LV
- MC-38R Murine colorectal carcinoma cell line resistant to 5FU/LV

ABSTRACT

My research explores the mechanisms underlying chemoresistance to 5-fluorouracil (5-FU)-based therapies in metastatic colorectal cancer (mCRC) and introduces CF10, a promising second-generation fluoropyrimidine (FP) polymer, as a potential treatment option. Our first paper examines the key factors contributing to 5-FU resistance, including altered anabolic metabolism, elevated thymidylate synthase (TS) expression/activity, and dysregulated programmed cell death. These resistance mechanisms can be potentially overcome with the next-generation FP polymers like CF10, which exhibit reduced dependence on anabolic metabolism and more potent TS inhibitory activity. The in-vitro and in-vivo studies demonstrate that CF10 is significantly more potent than 5-FU, causing increased apoptosis and replication stress in colorectal cancer cell lines.

Importantly, CF10 dosed to deliver equivalent FP content as 5-FU did not cause weight loss, even when combined with an inhibitor of dihydropyrimidine dehydrogenase. Additionally, CF10 was more effective than 5-FU at inhibiting tumor progression in a colorectal liver metastasis (CRLM) model. Our work delves deeper into the mechanisms of acquired resistance to 5-FU/leucovorin (5-FU/LV) in mCRC cells under physiological folate conditions. It showed that 5-FU/LV resistance was associated with elevated TS levels, increased c-Myc expression, and upregulation of the Myc-target gene ABCB5, which is linked to drug resistance.

Crucially, our findings revealed that the polymeric FP compound, CF10, remained highly potent against the 5-FU/LV-resistant CRC cells, effectively inducing TS ternary complex formation and inhibiting TS catalytic activity. In a clinically relevant

mouse model of therapy-resistant CRC liver metastasis, CF10 and CF10/LV were highly effective, completely eradicating liver metastases and providing a significant survival advantage compared to 5-FU and 5-FU/LV.

In summary, these studies provide a comprehensive understanding of the mechanisms contributing to 5-FU resistance in mCRC and present compelling preclinical evidence supporting the development of the next-generation FP polymer, CF10, as a potential treatment for 5-FU-resistant, liver-metastatic colorectal cancer.

CHAPTER 1

INTRODUCTION

Chemoresistance Challenges

Chemoresistance in metastatic colorectal cancer (mCRC) presents a significant challenge during treatment with 5-Fluorouracil (5-FU)-based therapies, contributing to high mortality rates associated with this disease. While 5-FU is a widely used chemotherapeutic agent, its efficacy is compromised in many patients due to multifactorial resistance mechanisms. One well-documented cause of this resistance is DNA mismatch repair deficiency (MMR-D), which is a critical determinant in the responsiveness to 5-FU; however, beyond this, there is no universally accepted framework to predict which patients will fail 5-FU-based treatment[1].

Mechanisms of 5-FU Resistance

Understanding the mechanistic underpinnings of 5-FU resistance is imperative for developing more effective therapeutic strategies. Research has identified many important pathways and processes contributing to resistance: (1) modified anabolic metabolism, which limits the effective formation of the active metabolite Fluorodeoxyuridylate (FdUMP); (2) increased levels of thymidylate synthase (TS), the primary enzymatic target of 5-FU; and (3) disruptions in the regulation of programmed cell death, as cancer cells adaptively override normal apoptotic signals to survive chemotherapeutic challenges[2].

5-FU functions through its conversion into active metabolites that disrupt thymidine biosynthesis, preferentially affecting rapidly proliferating cancer cells that depend more heavily on de novo pathways for nucleotide synthesis than their normal counterparts. De novo pathways refer to the synthesis of molecules from simple precursors, rather than from pre-existing molecules. When introduced into the body, only a small fraction of 5-FU is converted into FdUMP, which quantitatively limits its potential to effectively inhibit TS and subsequently leads to DNA damage through misincorporation of metabolites into both RNA and DNA. Given that roughly 80% of administered 5-FU is lost, either by liver degradation or urinary excretion, significant strides are needed in optimizing its therapeutic efficiency[3].

Thymidylate Synthase Regulation

The two main areas of resistance in mCRC are directly related to how 5-FU targets TS. Elevated TS expression is associated with reduced therapeutic efficacy, as higher levels of the enzyme necessitate greater concentrations of FdUMP for effective inhibition. This enzymatic target's expression is regulated at multiple transcriptional and post-transcriptional levels, making it a complex contributor to resistance. The major transcription factors like Myc, and FOXM1 have been shown to upregulate TS expression in response to genetic aberrations or metabolic stress, establishing a direct and urgent link between cellular signaling pathways and chemoresistance that demands our attention[4].

Genetic Factors in Resistance

The TYMS gene amplification, which encodes TS, has been shown in resistant CRC cells and correlates with poor patient outcomes due to overpowering the inhibitory effects of 5-FU. Other mechanisms include polymorphisms in TS enhancer regions and alterations in TS protein translation and degradation dynamics[5]. Meanwhile, studies have revealed that tumor cells may display intrinsic resistance by TS levels prior to therapeutic exposure, potentially leading to excessive toxicity without clinical benefit[5].

Influence of Metabolism on Toxicity

Dihydropyrimidine dehydrogenase (DPD) modulates 5-FU in its degradation is the crucial first step of 5-FU metabolism. The genetic polymorphisms of the DPYD gene significantly affect both patient's responses and toxicity profile from standard 5-FU dosing. Further than DPD, enzymes involved in the anabolic transformation of 5-FU to FdUMP also present opportunities for resistance, particularly when their activities are diminished or dysregulated.

Programmed Cell Death and Resistance

The programmed cell death pathway events to 5-FU treatment have unfolded and obscure resistance circumstances[6]. Notably, p53, a tumor suppressor gene, has been shown to mediate 5-FU-induced apoptosis, and its mutation causes apoptosis attenuation, which favors cancer cells to endure the cytotoxic effects of chemotherapy[6]. However, variability mutation levels lead to differences in therapeutic efficacy that affect treatment strategies.

A hopeful research approach is the development of the next-generation fluoropyrimidine (FP) polymers CF10, designed to bypass the metabolic limitations associated with 5-FU. CF10 has shown strong potential in both in-vitro and preclinical settings and mechanisms of action that reduce reliance on the long pathways required for 5-FU's activation. Furthermore, CF10 has potentially overcome elevated TS levels, offering hope to patients with chemoresistant tumors and fostering a sense of empathy in our pursuit of better cancer therapies.

Comparative Efficacy of CF10 Against CRC Cells

This study delves into the comparative efficacy of CF10, a second generation fluoropyrimidine polymer, against colorectal cancer (CRC) cells when compared to commonly used chemotherapeutic agents such as 5-FU and TFT (The fluoropyrimidine component of TAS-102 works by disrupting DNA synthesis in cancer cells). Our research shows that CF10 displays significantly higher potency towards CRC cells compared to 5-FU and TFT, as evidenced by lower Area Under the Curve (AUC) values across many CRC cell lines assayed in the research from the Broad Institute PRISM screen. This heightened potency of CF10 is observed consistently even under conditions of folate restriction, indicating robust effectiveness.

Mechanisms of CF10's Superior Cytotoxic Effects

Furthermore, CF10's superior cytotoxic effects on CRC cells are connected to stronger thymidylate synthase (TS) inhibition and the development of increased

Topoisomerase 1 cleavage complexes (Top1cc), which align with the mechanisms of action of Topoisomerase 1 inhibitors. Our study also is consistent with when CF10 is combined with leucovorin (LV), a modulator of 5-FU, it enhances the cytotoxicity of CF10 against CRC cells[7].

Clinical Promise of CF10 in CRC Treatment

In a CRC liver metastasis model, CF10 infusion showed a complete tumor elimination, compared to 5-FU/LV infusion which only displayed tumor regression. Furthermore, although TFT showed efficacy in this model, treatment-related scarring, and weight loss were seen, indicating potential limitations of TFT in comparison to CF10.

References

1. Gmeiner, W.H. and C.C. Okechukwu, *Review of 5-FU resistance mechanisms in colorectal cancer: clinical significance of attenuated on-target effects.* Cancer Drug Resist, 2023. **6**(2): p. 257-272.
2. Peters, G.J., et al., *Thymidylate synthase inhibition after administration of fluorouracil with or without leucovorin in colon cancer patients: implications for treatment with fluorouracil.* J Clin Oncol, 1994. **12**(10): p. 2035-42.
3. Diasio, R.B. and B.E. Harris, *Clinical pharmacology of 5-fluorouracil.* Clin Pharmacokinet, 1989. **16**(4): p. 215-37.
4. Varghese, V., et al., *FOXM1 modulates 5-FU resistance in colorectal cancer through regulating TYMS expression.* Sci Rep, 2019. **9**(1): p. 1505.

5. Wang, Y.C., et al., *An integrated analysis of the association between Ts gene polymorphisms and clinical outcome in gastric and colorectal cancer patients treated with 5-FU-based regimens.* Mol Biol Rep, 2013. **40**(7): p. 4637-44.
6. Hientz, K., et al., *The role of p53 in cancer drug resistance and targeted chemotherapy.* Oncotarget, 2017. **8**(5): p. 8921-8946.
7. Gmeiner, W.H., et al., *Improved Antitumor Activity of the Fluoropyrimidine Polymer CF10 in Preclinical Colorectal Cancer Models through Distinct Mechanistic and Pharmacologic Properties.* Mol Cancer Ther, 2021. **20**(3): p. 553-563.

CHAPTER 2

Review of 5-FU resistance mechanisms in colorectal cancer: clinical significance of attenuated on-target effects

William H. Gmeiner[1,2], Charles Chidi Okechukwu[1]

[1]Department of Cancer Biology and Comprehensive Cancer Center, Wake Forest University School of Medicine, Winston-Salem, NC 27157, USA.

[2]Integrative Physiology and Pharmacology Graduate Program, Institution, Wake Forest University School of Medicine, Winston Salem, NC 27157, USA.

Correspondence to: Prof. William H. Gmeiner, Department of Cancer Biology and Comprehensive Cancer Center, Wake Forest University School of Medicine, Medical Center Boulevard, 475 Vine Street, Winston-Salem, NC 27157, USA. E-mail: bgmeiner@wakehealth.edu

How to cite this article: Gmeiner WH, Okechukwu CC. Review of 5-FU resistance mechanisms in colorectal cancer: clinical significance of attenuated on-target effects. Cancer Drug Resist 2023;6:257-72.
https://dx.doi.org/10.20517/cdr.2022.136

Received: 30 Nov 2022 First Decision: 20 Mar 2023 Revised: 1 Apr 2023
Accepted: 17 Apr 2023 Available online: 29 Apr 2023

Academic Editor: Godefridus J. Peters Copy Editor: Dong-Li Li Production Editor: Dong-Li Li

Abstract

The emergence of chemoresistant disease during chemotherapy with 5-Fluorouracil-based (5-FU-based) regimens is an important factor in the mortality of metastatic CRC (mCRC). The causes of 5-FU resistance are multi factorial, and besides DNA mismatch repair deficiency (MMR-D), there are no widely accepted criteria for determining which CRC patients are not likely to be responsive to 5-FU-based therapy. Thus, there is a need to systematically understand the mechanistic basis for 5-FU treatment failure and an urgent need to develop new approaches for circumventing the major causes of 5-FU resistance. In this manuscript, we review mechanisms of 5 FU resistance with an emphasis on: (1) altered anabolic metabolism limiting the formation of the primary active metabolite Fluorodeoxyuridylate (5-Fluoro-2'-deoxyuridine-5'-O-monophosphate; FdUMP); (2) elevated expression or activity of the primary enzymatic target thymidylate synthase (TS); and (3) dysregulated programmed cell death as important causes of 5-FU resistance. Importantly, these causes of 5-FU resistance can potentially be overcome through the use of next-generation fluoropyrimidine (FP) polymers (e.g., CF10) that display reduced dependence on anabolic metabolism and more potent TS inhibitory activity.

Introduction

It is estimated that 1.93 million colorectal cancer (CRC) cases will be newly diagnosed in 2022 worldwide, with 0.94 million CRC-caused deaths. According to the American Cancer Society (ACS), CRC is the 2nd most common cause of cancer-related mortality in the United States, accounting for ~51,000 deaths annually[1,2]. Surgical approaches are the primary treatment modality for limited-stage CRC when there is no evidence of distant metastasis. However, in elderly patients that constitute most new CRC diagnoses, there is an increased risk of post-operative complications[3]. Adjuvant chemotherapy with 5-Fluorouracil-based (5-FU-based) combinations reduces the risk of disease recurrence in stage III and high-risk stage II CRC. Chemotherapy with 5-FU-based combinations together with biologics (e.g., bevacizumab or cetuximab) and immunotherapy in some instances are also used to treat metastatic CRC (mCRC)[4,5], which often occurs in liver and is frequently not amenable to surgical resection.

The chemotherapeutic molecule most widely used for CRC treatment is 5-fluorouracil (5-FU), a synthetic fluorinated pyrimidine (FP) analog of uracil that is used to treat > 2 million cancer patients each year worldwide[6,7]. In addition to its widespread use for CRC treatment, 5-FU is also widely used to treat pancreatic, stomach, esophageal, breast, and head-and-neck cancer. 5-FU belongs to the antimetabolite class of anti-cancer drugs[8,9],and its activity results from intracellular conversion into active metabolites that interfere in thymidine biosynthesis and affect DNA- and RNA-mediated processes[10,11]{Chen, 2019 #42}{Chen, 2019 #43}. The primary molecular target of 5-FU's anti-cancer activity

is thymidylate synthase (TS), which is required for de novo thymidylate (thymidine 5'-O-monophosphate) biosynthesis[12]. TS is a well-validated target for cancer chemotherapy[13] and aggressive malignant cells are relatively more reliant on de novo thymidylate biosynthesis than non-malignant cells that utilize the alternative salvage pathway[14]. The importance of targeting TS for 5-FU's anti-cancer activity is underscored by its invariant clinical use in combination with folinic acid (Leucovorin; LV), a reduced folate co-factor that binds TS in a ternary complex with 5-Fluoro-2'-deoxyuridine-5'-O monophosphate (FdUMP), the 5-FU metabolite that irreversibly inhibits TS enzymatic activity. TS inhibition depletes cellular stores of thymidylate, resulting in increased misincorporation of 2′ deoxyuridine-5′-triphosphate (dUTP) in DNA. In cells treated with FP drugs, 5-fluoro-2′-deoxyuridine-5′ triphosphate (FdUTP) is also misincorporated into DNA, and this causes Topoisomerase 1 (Top1) mediated DNA damage[15]. The Gmeiner lab has developed FP polymers (e.g., CF10) that directly release FdUMP without a requirement for anabolic metabolism. CF10 inhibits TS at 100-1,000-fold lower concentrations than 5-FU in CRC cells[16-18] and causes extensive Top1-mediated DNA damage to generate increased replication stress, a point of therapeutic vulnerability in CRC cells. While the anti-cancer activities of 5-FU and other FP drugs are considered to primarily result from TS inhibition and DNA damage, only a relatively small percentage of 5-FU administered to humans is converted to FdUMP and DNA-directed metabolites (< 5%[19]. Most 5-FU (~80%) is either degraded in the liver or excreted intact in the urine[20]. Among anabolic metabolites, ribonucleotides are produced at approximately 10-fold greater levels

than deoxyribonucleotides[20,21]. The importance of RNA-directed metabolites for 5-FU's anti-cancer activity remains an active area of investigation[22]; however, the systemic toxicities associated with RNA-directed metabolites are established and include gastrointestinal tract toxicity[23,24] and immunosuppression[23,25], both of which are alleviated by uridine administration[26] to dilute 5-FU's effects on RNA-mediated processes. Patients that are deficient in 5-FU catabolism are highly vulnerable to serious systemic toxicities if treated with 5-FU[27]. Approximately 5% of the human population display polymorphisms in the gene encoding dihydropyrimidine dehydrogenase (DPYD) that catalyzes the initial step in 5-FU degradation and 5-FU use at standard levels is contraindicated in these patients[28].

5-FU remains a central component of CRC treatment both in the adjuvant setting and in the treatment of mCRC[4,5], which is the cause of cancer-related lethality. While 5-FU is just one component in combination therapy regimens such as FOLFOX and FOLFIRI that combine folinic acid, 5-FU, and either oxaliplatin (FOLFOX) or irinotecan (FOLFIRI), understanding the mechanistic basis for 5-FU resistance can help guide the development of new and more effective therapeutic approaches. FOLFOX or FOLFIRI are frequently used in frontline treatment of mCRC, often in combination with a biologic, such as bevacizumab[29]. While current 5-FU-based chemotherapy regimens have contributed to significantly improved survival for mCRC patients (~20 months;[30]), 5-year survival remains rare, < 14%, indicating a critical need to understand the mechanistic basis of resistance and develop new strategies to more completely eradicate metastatic

disease[31]. Innate or acquired resistance remains a prominent cause of treatment failure for patients with metastatic cancer. 5-FU resistance can result from multiple causes; however, a critical review of the literature indicates cancer cells adapt to 5-FU's cytotoxic effects through: (1) decreasing intracellular FdUMP levels [Figure 1]; (2) elevating activity of the target enzyme, TS; and (3) dysregulating the balance between autophagy and apoptosis to favor cell survival. These endpoints are achieved via multiple mechanisms making overcoming resistance a challenging endeavor. This review focuses on addressing the causes of clinical resistance to 5-FU, considering both clinical data and cellular models of CRC. We review mechanisms by which 5-FU-based therapy fails, intending to provide insight into novel strategies to overcome resistance and improve outcomes beyond the incremental gains achieved in recent years[32].

Clinical Determinants of 5-FU Response in CRC Treatment

The applicability of 5-FU-based chemotherapy for CRC treatment depends upon several factors. For patients with stage III CRC or diagnosed with stage II CRC with risk factors consistent with an elevated likelihood for relapse, 5-FU-based adjuvant chemotherapy is recommended unless tumor biopsy demonstrates high microsatellite instability (MSI-H) or deficiency in DNA mismatch repair (MMR-D). For patients with MSI-High or MMR-D primary CRC tumors, which include familial syndromes such as Lynch syndrome, 5-FU-based regimens are ineffective and testing for MMR-D status prior to treatment is standard care. Testing for MMR-D status is also required for establishing responsiveness to immune checkpoint blockade immunotherapy, which is relatively more effective in CRC patients with

high tumor mutational burden associated with MMR-D[33]. MSI testing by polymerase chain reaction (PCR) and immunohistochemistry (IHC) is used to establish MMR-D[34]. Two antibody IHC testing for MSH6 and PMS2 is used to identify MMR-proficient CRC patients, and if deficiency is suspected, IHC for mutS homolog 2 (MSH2) and mutL homolog 1 (MLH1) are undertaken to establish MMR-D[35]. MLH1 promoter methylation testing is done for cases with MLH1-IHC loss. Relevance of MMR-D for CRC chemotherapy is that, in general, MSI-High and MMR-D in early-stage primary colon cancer confer a good prognosis and NCCN does not recommend adjuvant 5-FU for stage II CRC that is MSI-high. However, the FOLFOX regimen is beneficial in MSI-high stage III[36], and patients with Transforming growth factor-βRII (TGF-βRII) mutations in particular may be responsive to 5-FU-based therapy[37]. The TGF-β pathway also is implicated in drug resistance in pre-clinical studies and specific inhibition of TGF-βI restored the sensitivity of resistant CRC cells to 5-FU[38]. Similarly, for patients with mCRC that is MSI-H or MMR-D, alternative frontline therapy to 5-FU-based therapy is implemented,

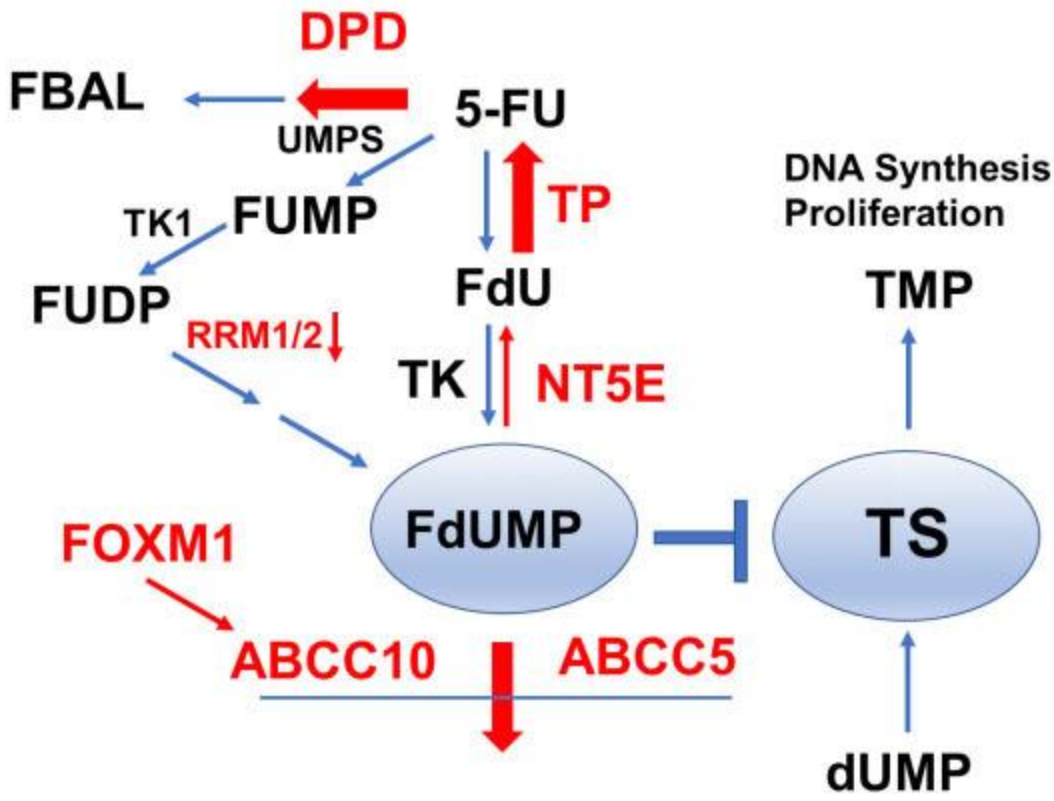

Figure 1. 5-FU Resistance can develop through either increased intratumor degradation, decreased anabolic metabolism to FdUMP and/or increased efflux of FdUMP - all of which decrease TS inhibition in tumor cells. 5-FU may be degraded via intratumor DPD, while its anabolic metabolism to FdUMP occurs primarily via UMPS/RRM1/2. Decreased FdUMP levels may result from less efficient conversion through decreased RRM1/2 expression or from increased FdUMP breakdown through elevated expression of NT5E and TP. FdUMP also undergoes efflux from tumor cells by ABC transporters, ABCC10 and ABCC5, that are upregulated upon increased FOXM1 expression in 5-FU-resistant cancer cells. Processes contributing to decreased intra-tumor FdUMP and 5-FU resistance are indicated by red arrows. 5-FU: 5-Fluorouracil; FdUMP: 5-Fluoro-2'-deoxyuridine-5'-O-monophosphate; UMPS: UMP synthase; FBAL: α-fluoro-β alanine; DPD:

dihydropyrimidine Dehydrogenase Deficiency; FUMP: 5-fluorouridine-5'-monophosphate; FUDP: 5-fluorouridine diphospho; FdU: 5-fluoro-2'-deoxyuridine; TK: thymidine kinase; TS: thymidylate synthase; TMP: Trimethylolpropane; RRM: RNA recognition motif; NT5E: ecto-5′-nucleotidase; FOXM1: forkhead box M1; dUMP: 2'-deoxyuridine-5'-O-monophosphate.

frequently immune checkpoint blockade[39]. The mechanism by which deficient MMR renders 5-FU-based regimens ineffective is not definitively known. In principle, MMR may remove 5-FU from DNA and genomic silencing or mutation of MMR genes may increase 5-FU in DNA[40], which could accentuate DNA damaging processes, which include DNA topoisomerase 1 poisoning[41]. Alternatively, MMR proficiency may contribute to cancer cell death through the activation of a futile cycling mechanism[42]. Our studies indicate MMR status does not significantly affect the response of CRC cells to either 5-FU or CF10[43], indicating the observed clinical cause of MMR dependence may not be directly related to DNA repair. Base excision repair (BER) actively removes 5-FU from DNA in CRC cells[44,45], but BER is not a determinant in 5-FU clinical response. However, CpG island methylator phenotype, and chromosome instability[46], two processes that differentiate the etiology of CRC development, are implicated in 5-FU response[47,48].

Mechanisms Increasing TS To Cause 5-FU Resistance

TS is considered the primary molecular target for the anti-cancer activities of FP drugs (5-FU, capecitabine, and floxuridine). TS also is targeted by anti-folates such as tomudex and raltitrexed[49]. The clinical success of these drugs, as well as

more recent FP-based combination approaches that target TS such as S1 (tegafur, gimeracil, potassium oxanate)[50] and Lonsurf or TAS-102 (trifluridine, Tiperacil)[51], establishes TS as a central and well-established chemotherapy target[13]. The structural basis for TS inhibition by FPs was shown to result from nucleophilic attack by Cys195 at C6 of FdUMP, resulting in irreversible enzyme inhibition via a ternary complex that also includes a reduced folate co-factor[49].

The relationship between TS levels and response to 5-FU, other FPs, or TS inhibitors is complex, in part because while elevated TS levels contribute to resistance (since more FdUMP is required for TS inhibition), but very low TS levels slow cell proliferation, which is necessary for replication-dependent DNA damage. Further, establishing elevated TS as a cause of resistance to 5-FU or other TS-targeted therapeutics is challenging because TS is regulated at multiple levels including through gene amplification, polymorphisms in the promoter, and upregulation of transcription factors that regulate its intratumor expression [Figure 2]. TS levels and activity[52] significantly correlate with response to 5-FU-based treatment and LV enhanced TS inhibition. However, incorporation of 5-FU into either DNA or RNA does not correlate with response to 5-FU[53].

Transcriptional regulation of TYMS

Transcriptionally, TYMS (encoding TS) is regulated by E2F family transcription factors[54] in an S-phase dependent manner[55]. TYMS expression is also sensitive to Myc levels and silencing TYMS decreases the oncogenic properties of elevated MYC in some cell contexts[56]. Recently, an analysis from the Cancer Genome Atlas (TCGA) database revealed lower TYMS was associated with better

response to FOLFOX/ FOLFIRI therapy in mCRC patients and MYC was identified as an upstream controller of genes that regulate response to 5-FU+folate therapy[57]. The forkhead transcription factor forkhead box M1 (FOXM1) is regulated by E2F1 and directly upregulates TYMS and is responsive to DNA damage. Elevated FOXM1 is a cause of 5-FU resistance through the upregulation of TYMS[58], and recent studies indicate targeting FOXM1 can overcome 5-FU resistance[59]. Other signaling pathways may upregulate TYMS and cause 5-FU resistance, including HSP90/Src[60]. Further, TYMS is regulated by the MALAT1-miRNA network[61] and other miRNAs that regulate drug resistance[62] and can be used as biomarkers[63].

Gene amplification of TYMS

The importance of TS gene and protein expression for 5-FU resistance was established in CRC tumors. Responsive patients had significantly lower mean TS protein and gene levels relative to non-responsive patients[64]. Further, CRC cells selected for acquired 5-FU resistance displayed elevated TS, which occurred through gene amplification[65]. Elevated TS is associated with clinical resistance to 5-FU[66], consistent with TS being the primary molecular target of FPs. Several studies[67,68], including a meta-analysis of 13 studies[69], demonstrated that elevated TS was associated with poor outcomes. However, multiple studies indicate the relationship between TS expression and 5-FU response is complex and may depend on the extent of TS nuclear localization or the expression of other genes, particularly those regulating 5-FU metabolism including dihydropyrimidine dehydrogenase deficiency (DPD) and TP[66]. TS undergoes reversible

SUMOylation[70] and localizes to the nucleus (nTS) as part of a multi-protein complex that enables efficient de novo ddP biosynthesis during S-phase[71]. Clinical studies indicate that increased intratumor nuclear localization of TS may be a better indicator of disease aggressiveness than overall TS levels[72]. TYMS gene amplification is detected in mCRC from patients pre-treated with 5-FU-based chemotherapy and was associated with shorter median survival for patients treated with chemotherapy following surgical resection[73]. A summary of studies in which TS gene amplification was implicated with 5-FU resistance is included in Table 1.

TSER and alternative causes of elevated TS In addition to TYMS gene amplification and increased transcription, at least three other processes are potential factors that could increase TS levels and contribute to 5-FU resistance [**Figure 2**]: i) TS enhancer

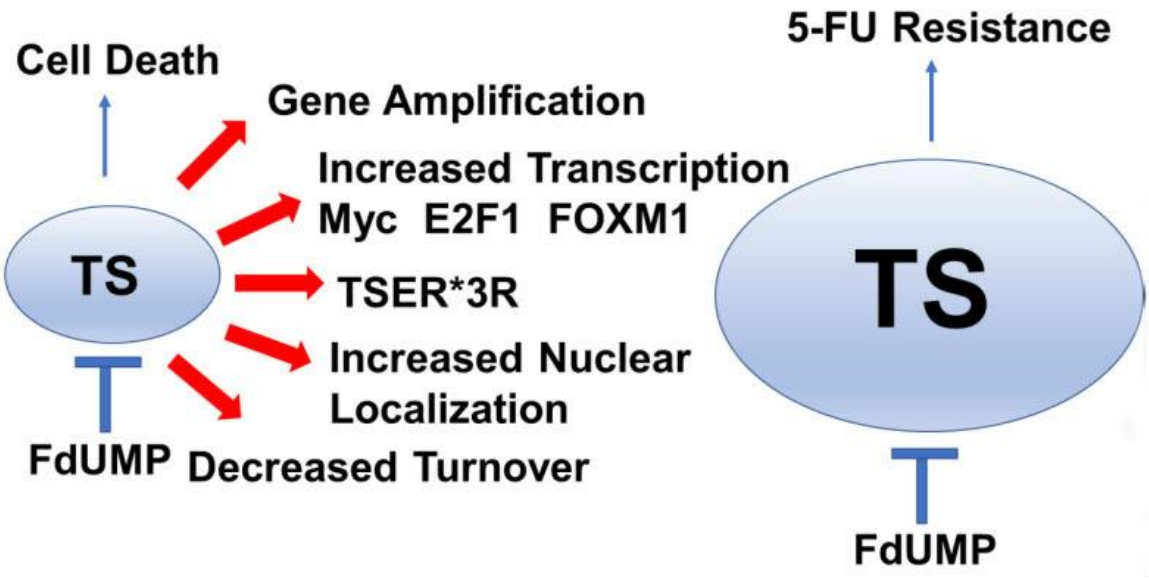

Figure 2. 5-FU Resistance develops from processes that increase thymidylate synthase (TS) activity in cancer cells. Increased TS activity can result from multiple processes including gene amplification, increased transcription, TSER*3R polymorphism, increased TS nuclear localization, and decreased TS protein degradation, which are indicated by red arrows. Increased TS activity renders cells 5-FU resistant because FdUMP levels are insufficient to inhibit all the TS available. 5-FU: 5-Fluorouracil; FdUMP: 5-Fluoro-2'-deoxyuridine-5' O-monophosphate; FOXM1: forkhead box M1.

region (TSER) polymorphisms; ii) TS translational autoregulation; iii) TS proteasomal degradation. Polymorphisms in the 5′-UTR of TYMS contribute to elevated TYMS expression in some contexts[77,78]. A triple tandem repeat (TSER*3)[79] in the 5′-UTR of the TS gene[80] resulted in elevated TYMS expression and 5-FU resistance[81]. The clinical significance of TSER genotypes remains largely unproven in CRC; however, prospective selection of patients with

gastric cancer have at least one TSER*2 allele favoring lower TYMS expression therapy resulted in an encouraging disease control rate for treatment with FOLFOX[82]. Further, TYMS polymorphisms, together with KRAS and BRAF mutation status, retrospectively, were associated with reduced relapse in CRC[83]. TS also poses a negative autoregulatory function at the translational level by binding to its own mRNA; thus, it prevents the synthesis of functional TS enzyme[73]. Autoinhibition of TS protein expression is countered by FdUMP binding and ternary complex formation. At present, there is no evidence that autoregulation of TS by this mechanism contributes to 5-FU resistance. However, another aspect of translation is affected by 5-FU, which is the efficiency and selection of proteins translated by the ribosome[84]. TS also undergoes proteasomal degradation and TS levels reflect a dynamic balance of new protein synthesis, dependent upon gene expression and translational efficiency, that is countered by the rate of degradation for expressed protein. A recent study showed that decreased O-GlcNAc transferase (OGT), an enzyme responsible for post-translational modification of multiple proteins including TS, affected TS proteasomal degradation in 5-FU-resistant cells[85].

Increased TS and intrinsic 5-FU resistance

The elevated expression of TS is commonly accepted as a primary molecular mechanism for acquired 5-FU resistance[86], but it also is important for intrinsic resistance. The stability of the ternary complex is highly dependent on 5,10-methylenetetrahydrofolate (CH2 THF) levels[78], and lack of CH2 THF creates an unstable TS: FdUMP binary complex resulting in poor inhibition[81,86,87].

Increased TS level prior to 5-FU-based treatments is associated with perturbed folate pools, which cause intrinsic resistance compared to acquired resistance associated with upregulated TYMS expression and gene amplification[73,86]. These findings suggest that patients with tumors showing TS amplification prior to treatment should not be treated with 5-FU to avoid systemic toxicity without the likelihood of clinical benefit[73,74].

Genes Modulating 5-FU Metabolism

Acquired drug resistance is a principal cause of treatment failure and significantly contributes to cancer related mortality. In the case of 5-FU, elevated TS is clinically established as a significant cause of drug resistance[69]. Still, other reasons have been identified, and prominent among them are alterations in genes that modulate 5-FU metabolism, affecting both its degradation and its conversion to FdUMP, the TS inhibitory metabolite[88] [**Figure 1**]. A key aspect of 5-FU activity, toxicity, and resistance is mediated by DPYD, the gene encoding DPD, the first and rate-limiting step in 5-FU degradation. Atypical 5-FU degradation in liver is associated with serious systemic toxicities[89]. In many countries, genetic screening is used to identify CRC patients with DPYD polymorphisms associated with decreased DPD activity that result in serious 5-FU toxicities unless the administered dose is reduced from standard dosing[90]. Since DPD is not the only potential cause of altered 5-FU toxicity or sub-optimal therapeutic response, alternative procedures such as therapeutic drug monitoring[91] are used to quantify patient response on an individualized basis and to customize 5-FU treatment to account for individual variations in drug metabolism.

Intratumor 5-FU catabolism

In addition to the role of DPYD polymorphisms in modulating 5-FU toxicity and therapeutic response by affecting systemic drug degradation, intra-tumoral DPYD expression is an important factor in modulating therapeutic response. For example, elevated intra-tumoral DPYD expression, together with elevated TYMS, is associated with poor outcomes in CRC patients treated with 5-FU-based chemotherapy[66]. A third gene, thymidine phosphorylase (TP; encoded by TYMP), was implicated together with DPYD and TYMS in this study. TP catalyzes a reversible reaction that may produce thymidine or 2'-deoxyuridine, or analogs such as 5-fluoro-2'-deoxyuridine (FdU), from their respective nucleobases (e.g., 5-FU), together with 2'-deoxyribose 1-phosphate. Alternatively, TP degrades thymidine analogs such as FdU to the nucleobase after dephosphorylation by ecto-5′-nucleotidase (NT5E)[92]. The directionality of TP catalysis depends on intra tumor substrate/product ratios; however, levels of 2'-deoxyribose 1-phosphate in plasma were also found to be predictive of chemotherapy sensitivity in gastric cancer that included a fluoropyrimidine[93]. Findings from this study[66] that elevated TYMP levels together with TYMS and DPYD are associated with decreased response to 5-FU are consistent with TP primarily catalyzing FdU degradation in CRC tumors and resistance to 5-FU is associated with elevated TYMP expression. Further, TP-mediated degradation of trifluorothymidine (TFT), the FP component of TAS-102, limits activity resulting in the inclusion of a TP inhibitor, Tipiracil[94]. TP is also known as platelet-derived endothelial cell growth factor (PDECGF), a growth factor promoting angiogenesis, and increased

PDECGF/TP is a prognostic factor for poor survival in CRC[95] that acts through the production of 2'-deoxyribose 1-phosphate from thymidine to promote chemotaxis of vascular endothelial cells[96].

Anabolic 5-FU metabolism and resistance

The anabolic biosynthesis of FdUMP from 5-FU can occur via either of two major pathways: (1) TP/ thymidine kinase (TK) in which FdUMP is produced by 5-FU in two steps; or (2) via a multi-step biosynthetic pathway (UMPS/RNR) that involves UMP synthase (UMPS), uridine kinase (UK), and UMP kinase (UMPK) to produce FUDP. FUDP is a substrate for ribonucleotide reductase (RNR) to produce FdUDP, which can be converted to 5-fluoro-2'-deoxyuridine-5'-diphosphate (FdUDP) through conversion to FdUTP followed by dUTPase cleavage. Enzymes important for the de novo biosynthesis of pyrimidines are upregulated in CRC relative to non-malignant tissue[97], and reduced activities of these enzymes which may occur via altered splicing[88,98] are associated with 5-FU resistance[99]. The importance of FdUMP biosynthesis via the UMPS/RNR pathway is demonstrated by studies that identify reduced expression and activity of enzymes in this pathway in 5-FU-resistant cells. Studies in KM12C xenograft tumors showed resistance to 5-FU was associated with decreased RNR activity[100], while analysis of clinical samples indicated 5-FU resistance was associated with high TS mRNA and low RNR activity[101].

Collectively, the preponderance of evidence indicates that altered de novo thymidine biosynthesis, either by affecting TS expression [Figure 2] or modulating genes important for 5-FU anabolic metabolism to FdUMP [Figure 1], is central to

5-FU resistance. In a few instances, 5-FU resistance is mediated by changes affecting RNA-directed processes including tRNA modifications[102,103] and rRNA[22]. However, the clinical significance of RNA-directed activities for 5-FU anti-tumor activity is not yet proven. Further evidence for anabolic metabolism of 5-FU to FdUMP being important for 5-FU resistance comes from studies demonstrating elevated expression of ABCC10[104] and ABCC5[105], two ATP binding cassette proteins[106] that mediate FdUMP efflux from 5-FU-treated cells, cause of 5-FU resistance as does elevated FOXM1, a major transcriptional regulator of ABCC10[104] [**Figure 1**].

Cell Death Signaling in 5-FU Resistance

The cytotoxicity of multiple anti-cancer drugs, including 5-FU, depends on the activation of programmed cell death that irreversibly commits drug-treated cells to destruction[107,108]. p53 is considered to be the most highly mutated gene in cancer and it plays a central role in determining if drug-treated cells undergo cell cycle arrest mediated by p53's downstream effector p21, or initiate apoptosis mediated by Bax and other p53-dependent pro-apoptotic genes[109] [Figure 3]. In the case of established DNA-damaging drugs such as Adriamycin, either p53 or p21 deficiency leads to loss of the G1/S checkpoint and efficient apoptosis[110]. However, 5-FU deletion of p53 in HCT-116 cells resulted in resistance to apoptosis and 5-FU was less effective towards p53-/- HCT-116 xenografts relative to isogenic tumors that were p53+/+. Furthermore, 5-FU induced apoptosis both required p53 and was inhibited by exogenous uridine, but not thymidine, consistent with apoptosis induction in response to an RNA-directed process under these treatment

conditions[110]. Studies from our laboratory confirm that p53 deletion causes 5-FU resistance in HCT-116 cells with expression of the R248W gain of function p53 mutation causing greater resistance, while the DNA-directed FP polymer CF10 showed reduced resistance indices relative to 5-FU[1].

However, even in cell models of CRC, there is variability in the extent that p53 is required for 5-FU-induced apoptosis. Studies report that 5-FU-induced apoptosis occurs in both wild-type and mutant p53 CRC cells with increased expression of the pro-apoptotic Bcl-2 family proteins Bax and Bak identified as being particularly important for 5-FU-induced apoptosis[111] [**Figure 3**]. The importance of p53 for regulating 5 FU-induced apoptosis has also been shown to occur via altered chromatin accessibility upon 5-FU treatment that affects the transcription of genes important for apoptosis[112]. The clinical significance of p53 mutations for 5-FU resistance is not established, although some clinical data indicate TP53 mutations confer a worse prognosis[113], while p53 together with Rb and the anti-apoptotic bcl-family member Mcl-1

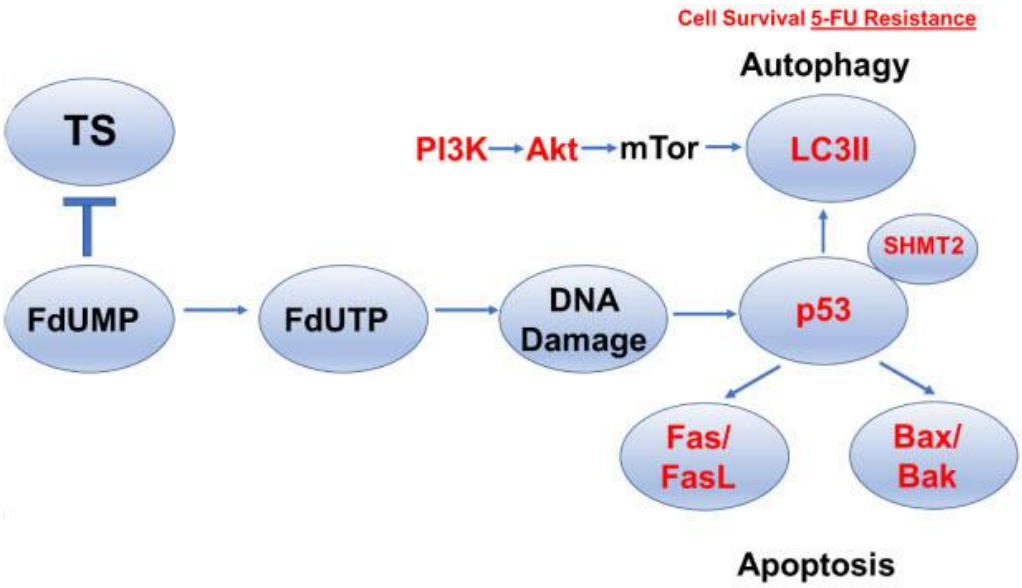

Figure 3. 5-FU Resistance develops from an altered balance between autophagy, which favors cell survival and apoptosis in 5-FU treated cells. p53 is a key regulator of autophagy/apoptosis balance in 5-FU-treated cells and is modulated by SHMT2. Increased signaling through the PI3K/Akt/mTOR pathway stimulates LC3II and upregulates autophagy to promote cell survival and 5-FU resistance. Induction of apoptosis involves upregulation of the death receptor pathway or mitochondrial pathway for programmed cell death, and downregulation of Fas/FasL or Bax/Bak decreases 5-FU-induced apoptosis and promotes cell survival and 5-FU resistance. 5-FU: 5-Fluorouracil; TS: thymidylate synthase; FdUMP: 5-Fluoro-2'-deoxyuridine-5'-O-monophosphate; FdUTP: 5-fluoro-2′ deoxyuridine-5′-triphosphate; SHMT2: serine hydroxymethyl transferase.

correlated with clinical outcomes in patients with colorectal liver metastases[114]. Factors other than p53 that are important for activating apoptosis in response to 5-FU treatment include Fas, which was shown to be induced in response to 5-FU

treatment in a p53-dependent manner and to regulate apoptosis[115] [**Figure 3**]. Houghton and co-workers showed that different CRC cell lines varied in the efficiency of Fas upregulation in response to 5-FU/LV treatment and this correlated with the efficiency of thymidine reversal, indicating 5 FU's DNA-directed effects were cell line dependent and correlated with Fas upregulation and activation of extrinsic apoptosis[116]. Resistance to 5-FU-induced Fas upregulation and apoptosis can occur via methylation of the Fas promoter, silencing its expression, which can be reversed by 5-Aza deoxycytidine[117]. Clinical significance for Fas upregulation in 5-FU response was shown by increased Fas expression in biopsy specimens following 5-FU treatment[118].

Autophagy in 5-FU Resistance

Autophagy plays an important role in tumorigenesis and modulating drug response and can either be complementary to apoptosis by promoting drug lethality or protective of the cytotoxic effects of drug treatment[119]. Activation of the PI3K/Akt/mTOR signaling pathway upregulates autophagosome formation and inhibitors of this pathway modulate drug response, in part, through downregulating autophagy. Treatment of CRC cells with 5-FU was shown to increase LC3-II levels consistent with autophagy activation and co-treatment with 3-methyl adenine (3-MA), a PI3K inhibitor, blocked autophagosome formation and promoted 5-FU-induced apoptosis implicating a protective role for autophagy in 5-FU treatment[120] [**Figure 3**]. However, reduced autophagy has also been reported in 5-FU-resistant CRC cells[121]. Overactivation of the Akt pathway is also associated with 5-FU resistance and Akt inhibition may overcome resistance in

some CRC cells[122], in part by modulating autophagy, while miRNA regulation of Akt deactivation by the PP2A phosphatase complex also regulates 5-FU resistance[123]. The autophagy inhibitor chloroquine also enhanced the lethality of 5-FU to CRC cells, and in these studies, a serine hydroxymethyl transferase (SHMT2) was shown to regulate 5-FU resistance by binding p53 and inhibiting its degradation [**Figure 3**]. Overall, SHMT2 was upregulated in CRC tissue compared to non-malignant tissue; however, patients with low SHMT2 had worse outcomes and this correlated with elevated LC3-II and p62 consistent with autophagy activation in SHMT2-low, 5-FU-resistant CRC[124]. Interestingly, trifluorothymidine (TFT), the FP used in TAS-102, differed from 5-FU in the extent of activating autophagic survival[125]. Activation of the p38MAPK pathway is also a determinant in autophagy activation and modulates cellular responses to 5 FU. Inhibition of the p38MAPK pathway correlated with attenuation in 5-FU-mediated apoptosis and promoted CRC cell resistance[126]. Thus, the p38MAPK signaling pathway modulates 5-FU resistance by regulating the pivot between autophagy and apoptosis[126]. The autophagy-regulated gene HSPB8 was found to be key in regulating interactions with the tumor microenvironment that regulate 5-FU resistance[127]. Autophagosome formation is also regulated by Rho kinases[128], which are implicated in 5-FU resistance[129]. Curcumin has been studied to inhibit AMPK/ULK1-dependent autophagy with the potential to overcome 5-FU resistance through autophagy activation[130], and studies from our laboratory indicate curcumin enhances the cytotoxicity of DNA-directed polymeric fluoropyrimidines[131,132].

Conclusion

5-FU remains central to the management of colorectal cancer and it is widely used both in the adjuvant setting to treat CRC patients with limited-stage disease and in combination with chemotherapy regimens to treat mCRC[4]. The evasion of 5-FU cytotoxicity through intrinsic or acquired resistance in patient tumors contributes to poor outcomes manifest either as a high rate of relapse despite adjuvant chemotherapy or limited survival in the metastatic setting despite multiple lines of chemotherapy that include 5-FU or other FP drugs[5]. Lack of response to 5-FU chemotherapy is predictable in patients with deficiencies in DNA MMR, or high microsatellite instability, and therapy with 5-FU is contra-indicated in these patients. 5-FU therapy is also predictably toxic in patients with polymorphisms in DPYD that limit 5-FU degradation in the liver[89], and these patients require special management[90]. Beyond these limited exclusions, there are currently no defined criteria for determining which CRC patients are not likely to be responsive to 5-FU based therapy. Thus, there is a need to systematically understand the mechanistic basis for 5-FU treatment failure, and an urgent need to develop new approaches for circumventing major causes of 5-FU resistance.

In this review, we have summarized major mechanisms that contribute to 5-FU resistance with an emphasis on those for which available data support clinical significance and that affect the on-target activity of 5-FU (TS inhibition). The causes of colorectal cancer are multi-factorial and involve both lifestyle choice and personalized genetic susceptibility[133]. Further, response to treatment also depends on multiple factors[134]. Collectively, the reviewed literature consistently

implicates resistance as developing from processes that limit the anabolic metabolism of 5-FU to FdUMP, the TS inhibitory metabolite [**Figure 1**], and from mechanisms that result in elevated TS activity that results from gene amplification, polymorphisms in the TS promoter, elevated levels of transcription factors that regulate TYMS expression, and/or altered nuclear localization of TS [**Figure 2**]. Dysregulation in the balance between cell survival and programmed cell death is also important in the development of 5-FU resistance [**Figure 3**]. We have not attempted to review miRNA regulation of TYMS [61] or other epigenetic causes of 5-FU resistance[135], and these have recently been reviewed[136-138]. We also have not directed the reader to literature focused on cellular changes that promote quiescence and stemness to escape the cytotoxic effects of 5-FU[139,140], although these are likely to be of clinical significance. Further, it is clear that the tumor microenvironment modulates therapy response by processes independent of on-target effects on cancer cells and these processes are not reviewed in this manuscript.

The focus of this review is on acquired resistance to 5-FU with decreased anabolic metabolism and elevated TS activity[49] as clinically relevant causes. In principle, these causes of 5-FU can be addressed through the translation of next-generation FP drugs that retain the anti-tumor activity associated with targeting TS in CRC, but that do not require multiple steps of anabolic metabolism required by 5-FU. TAS-102, a combination of the FP trifluorothymidine and a TP inhibitor Tiperacil, shows efficacy in 5-FU-resistant models and activity in refractory metastatic CRC[141]. TAS-102 activation requires thymidine kinase and it is not a substrate

for DPD[94]. Our laboratory has pioneered the development of DNA-based FP polymers to deliver Fluorodeoxyuridylate, the TS-inhibitory metabolite of 5-FU, without a requirement for metabolic activation. We showed that the prototype FP polymer F10 was, on average, 338-fold more potent than 5-FU across the NCI60 cell line screen[15,135], but it was still very well tolerated in vivo[142], indicating 5-FU toxicities do not necessarily arise predominantly from on-target effects. The 2nd generation FP polymer CF10 is even more potent and shows promising activity in pre-clinical models of CRC and pancreatic cancer[16,17]. Further, the cytotoxic mechanism of CF10 results from both inhibiting TS and poisoning of DNA topoisomerase 1 (Top1)[41,143], which results from a distinct mechanism distinct from current Top1 poisons in clinical use[144]. In summary, the next generation of FPs has the potential to overcome the established mechanism of resistance for 5-FU reviewed herein that has limited clinical response to FPs to date.

DECLARATIONS

Authors' contributions

Conceptualization: Gmeiner WH, Okechukwu CC

Original draft preparation: Okechukwu CC, Gmeiner WH

Writing, review, editing, visualization, supervision, and funding acquisition: Gmeiner WH Both authors have read and agreed to the published version of the manuscript.

Availability of data and material

Not applicable.

Financial support and sponsorship

This research was supported by the National Cancer Institute of the National Institutes of Health under award R41 CA254834 A1 (W.G.) P30 CA 012197 and Department of Defense Peer Reviewed Cancer Research Program CA200460. Charles Chidi Okechukwu was supported in part by R41 CA254834 A1S1.

Conflicts of interest

Gmeiner WH is an inventor on a pending patent application on CF10 for the treatment of colorectal cancer.

Ethical approval and consent to participate

Not applicable.

Consent for publication

Not applicable.

References

1. Dominijanni A, Gmeiner WH. Improved potency of F10 relative to 5-fluorouracil in colorectal cancer cells with p53 mutations. Cancer Drug Resist 2018;1:48-58. DOI PubMed PMC
2. Bray F, Ferlay J, Soerjomataram I, Siegel RL, Torre LA, Jemal A. Global cancer statistics 2018: GLOBOCAN estimates of incidence and mortality worldwide for 36 cancers in 185 countries. CA Cancer J Clin 2018;68:394-424. DOI PubMed
3. González-Senac NM, Mayordomo-Cava J, Macías-Valle A, et al. Colorectal cancer in elderly patients with surgical indication: state of the art, current management, role of frailty and benefits of a geriatric liaison. Int J Environ Res Public Health 2021;18:6072. DOI PubMed PMC
4. Gmeiner WH. Recent advances in our knowledge of mCRC tumor biology and genetics: a focus on targeted therapy development. Onco Targets Ther 2021;14:2121-30. DOI PubMed PMC
5. Punt CJ, Koopman M, Vermeulen L. From tumour heterogeneity to advances in precision treatment of colorectal cancer. Nat Rev Clin Oncol 2017;14:235-46. DOI PubMed
6. Sethy C, Kundu CN. 5-Fluorouracil (5-FU) resistance and the new strategy to enhance the sensitivity against cancer: Implication of DNA repair inhibition. Biomed Pharmacother 2021;137:111285. DOI PubMed

7. Długosz-Pokorska A, Pięta M, Janecki T, Janecka A. New uracil analogs as downregulators of ABC transporters in 5-fluorouracil resistant human leukemia HL-60 cell line. Mol Biol Rep 2019;46:5831-9. DOI PubMed
8. Chen P, Ni W, Xie T, Sui X. Meta-Analysis of 5-Fluorouracil-Based Chemotherapy Combined With Traditional Chinese Medicines for Colorectal Cancer Treatment. Integr Cancer Ther 2019;18:1534735419828824. DOI PubMed PMC
9. Luqmani YA. Mechanisms of drug resistance in cancer chemotherapy. Med Princ Pract 2005;14 Suppl 1:35-48. DOI PubMed
10. Morawska K, Goirand F, Marceau L, et al. 5-FU therapeutic drug monitoring as a valuable option to reduce toxicity in patients with gastrointestinal cancer. Oncotarget 2018;9:11559-71. DOI PubMed PMC
11. Weckbecker G. Biochemical pharmacology and analysis of fluoropyrimidines alone and in combination with modulators. Pharmacol Ther 1991;50:367-424. DOI PubMed
12. Carreras CW, Naber N, Cooke R, Santi DV. A C-terminal conformational equilibrium in thymidylate synthase observed by electron paramagnetic resonance spectroscopy. Biochemistry 1994;33:2071-7. DOI PubMed
13. Wilson PM, Danenberg PV, Johnston PG, Lenz HJ, Ladner RD. Standing the test of time: targeting thymidylate biosynthesis in cancer therapy. Nat Rev Clin Oncol 2014;11:282-98. DOI PubMed
14. Luengo A, Gui DY, Vander Heiden MG. Targeting metabolism for cancer therapy. Cell Chem Biol 2017;24:1161-80. DOI PubMed PMC

15. Liao ZY, Sordet O, Zhang HL, et al. A novel polypyrimidine antitumor agent FdUMP[10] induces thymineless death with topoisomerase I-DNA complexes. Cancer Res 2005;65:4844-51. DOI
16. Gmeiner WH, Dominijanni A, Haber AO, et al. Improved antitumor activity of the Fluoropyrimidine polymer CF10 in preclinical colorectal cancer models through distinct mechanistic and pharmacologic properties. Mol Cancer Ther 2021;20:553-63. DOI PubMed PMC
17. Haber AO, Jain A, Mani C, et al. AraC-FdUMP[10] Is a next-generation Fluoropyrimidine with potent antitumor activity in PDAC and synergy with PARG inhibition. Mol Cancer Res 2021;19:565-72. DOI PubMed PMC
18. Mani C, Pai S, Papke CM, Palle K, Gmeiner WH. Thymineless death by the fluoropyrimidine polymer F10 involves replication fork collapse and is inhanced by Chk1 inhibition. Neoplasia 2018;20:1236-45. DOI PubMed PMC
19. Miura K, Kinouchi M, Ishida K, et al. 5-fu metabolism in cancer and orally-administrable 5-fu drugs. Cancers (Basel) 2010;2:1717 30. DOI PubMed PMC
20. Diasio RB, Harris BE. Clinical pharmacology of 5-fluorouracil. Clin Pharmacokinet 1989;16:215-37. DOI PubMed
21. Longley DB, Harkin DP, Johnston PG. 5-fluorouracil: mechanisms of action and clinical strategies. Nat Rev Cancer 2003;3:330-8. DOI PubMed

22. Chalabi-Dchar M, Fenouil T, Machon C, et al. A novel view on an old drug, 5-fluorouracil: an unexpected RNA modifier with intriguing impact on cancer cell fate. NAR Cancer 2021;3:zcab032. DOI PubMed PMC
23. Gmeiner WH. Fluoropyrimidine Modulation of the Anti-Tumor Immune Response-Prospects for Improved Colorectal Cancer Treatment. Cancers (Basel) 2020;12:1641. DOI PubMed PMC
24. Pritchard DM, Watson AJ, Potten CS, Jackman AL, Hickman JA. Inhibition by uridine but not thymidine of p53-dependent intestinal apoptosis initiated by 5-fluorouracil: evidence for the involvement of RNA perturbation. Proc Natl Acad Sci U S A 1997;94:1795-9. DOI PubMed PMC
25. Groeningen CJ, Peters GJ, Leyva A, Laurensse E, Pinedo HM. Reversal of 5-fluorouracil-induced myelosuppression by prolonged administration of high-dose uridine. J Natl Cancer Inst 1989;81:157-62. DOI PubMed
26. Saif MW, Diasio RB. Benefit of uridine triacetate (Vistogard) in rescuing severe 5-fluorouracil toxicity in patients with dihydropyrimidine dehydrogenase (DPYD) deficiency. Cancer Chemother Pharmacol 2016;78:151-6. DOI PubMed
27. Saif MW, Hachem H, Purvey S, et al. Pharmacogenetic variants in the DPYD and TYMS genes are clinically significant predictors of fluoropyrimidine toxicity: are we ready for use in our clinical practice. Arch Pharmacol Ther 2020;2:6-8. DOI

28. Saif MW, Syrigos K, Mehra R, Mattison LK, Diasio RB. Dihydropyrimidine dehydrogenase deficiency (Dpd) in Gi malignancies: experience of 4-years. Pak J Med Sci 2007;23:832-9. PubMed PMC
29. Botrel TEA, Clark LGO, Paladini L, Clark OAC. Efficacy and safety of bevacizumab plus chemotherapy compared to chemotherapy alone in previously untreated advanced or metastatic colorectal cancer: a systematic review and meta-analysis. BMC Cancer 2016;16:677. DOI PubMed PMC
30. Liu Z, Xu Y, Xu G, et al. Nomogram for predicting overall survival in colorectal cancer with distant metastasis. BMC Gastroenterol 2021;21:103. DOI PubMed PMC
31. Veenstra CM, Krauss JC. Emerging systemic therapies for colorectal cancer. Clin Colon Rectal Surg 2018;31:179-91. DOI PubMed PMC
32. Shen C, Tannenbaum D, Horn R, et al. Overall survival in phase 3 clinical trials and the surveillance, epidemiology, and end results database in patients with metastatic colorectal cancer, 1986-2016: a systematic review. JAMA Netw Open 2022;5:e2213588. DOI PubMed PMC
33. André T, Cohen R, Salem ME. Immune checkpoint blockade therapy in patients with colorectal cancer harboring microsatellite instability/mismatch repair deficiency in 2022. Am Soc Clin Oncol Educ Book 2022;42:1-9. DOI PubMed

34. Adeleke S, Haslam A, Choy A, et al. Microsatellite instability testing in colorectal patients with Lynch syndrome: lessons learned from a case report and how to avoid such pitfalls. Per Med 2022;19:277-86. DOI
35. Aiyer KTS, Doeleman T, Ryan NA, et al. Validity of a two-antibody testing algorithm for mismatch repair deficiency testing in cancer; a systematic literature review and meta-analysis. Mod Pathol 2022;35:1775-83. DOI PubMed PMC
36. Tougeron D, Mouillet G, Trouilloud I, et al. Efficacy of adjuvant chemotherapy in colon cancer with microsatellite instability: a large multicenter AGEO study. J Natl Cancer Inst 2016;108:djv438. DOI
37. Watanabe T, Wu TT, Catalano PJ, et al. Molecular predictors of survival after adjuvant chemotherapy for colon cancer. N Engl J Med 2001;344:1196-206. DOI PubMed PMC
38. Romano G, Santi L, Bianco MR, et al. The TGF-β pathway is activated by 5-fluorouracil treatment in drug resistant colorectal carcinoma cells. Oncotarget 2016;7:22077-91. DOI PubMed PMC
39. Jung G, Benítez-Ribas D, Sánchez A, Balaguer F. Current treatments of metastatic colorectal cancer with immune checkpoint inhibitors-2020 update. J Clin Med 2020;9:3520. DOI PubMed PMC
40. Carethers JM, Chauhan DP, Fink D, et al. Mismatch repair proficiency and in vitro response to 5-fluorouracil. Gastroenterology 1999;117:123-31. DOI PubMed PMC

41. Gmeiner WH. Entrapment of DNA topoisomerase-DNA complexes by nucleotide/nucleoside analogs. Cancer Drug Resist 2019;2:994-1001. DOI PubMed PMC
42. Li LS, Morales JC, Veigl M, et al. DNA mismatch repair (MMR)-dependent 5-fluorouracil cytotoxicity and the potential for new therapeutic targets. Br J Pharmacol 2009;158:679-92. DOI PubMed PMC
43. Gmeiner WH, Mani C, Palle K. Abstract 2828: MMR status affects efficiency of homologous recombination repair of F10-induced DNA DSBs. Cancer Res ; 78 (13_Supplement):2828. DOI
44. Wyatt MD, Wilson DM 3rd. Participation of DNA repair in the response to 5-fluorouracil. Cell Mol Life Sci 2009;66:788-99. DOI PubMed PMC
45. An Q, Robins P, Lindahl T, Barnes DE. 5-Fluorouracil incorporated into DNA is excised by the Smug1 DNA glycosylase to reduce drug cytotoxicity. Cancer Res 2007;67:940-5. DOI PubMed
46. Bracht K, Nicholls AM, Liu Y, Bodmer WF. 5-Fluorouracil response in a large panel of colorectal cancer cell lines is associated with mismatch repair deficiency. Br J Cancer 2010;103:340-6. DOI PubMed PMC
47. Malki A, ElRuz RA, Gupta I, Allouch A, Vranic S, Al Moustafa AE. Molecular mechanisms of colon cancer progression and metastasis: recent insights and advancements. Int J Mol Sci 2020;22:130. DOI PubMed PMC
48. Cheng YW, Pincas H, Bacolod MD, et al. CpG island methylator phenotype associates with low-degree chromosomal abnormalities in colorectal cancer. Clin Cancer Res 2008;14:6005-13. DOI PubMed PMC

49. Gmeiner WH. Novel chemical strategies for thymidylate synthase inhibition. Curr Med Chem 2005;12:191-202. DOI PubMed
50. Yu J, Gao Y, Chen L, et al. Effect of S-1 plus Oxaliplatin compared with Fluorouracil, Leucovorin plus Oxaliplatin as perioperative chemotherapy for locally advanced, resectable gastric cancer: a randomized clinical trial. JAMA Netw Open 2022;5:e220426. DOI PubMed PMC
51. Tong D, Wang L, Mendis J, Essapen S. Long term real-world outcomes of Trifluridine/Tipiracil in metastatic colorectal cancer-a single UK centre experience. Curr Oncol 2021;28:2260-9. DOI PubMed PMC
52. Peters GJ, van der Wilt CL, van Groeningen CJ, Smid K, Meijer S, Pinedo HM. Thymidylate synthase inhibition after administration of fluorouracil with or without leucovorin in colon cancer patients: implications for treatment with fluorouracil. J Clin Oncol 1994;12:2035-42. DOI PubMed
53. Noordhuis P, Holwerda U, Van der Wilt CL, et al. 5-Fluorouracil incorporation into RNA and DNA in relation to thymidylate synthase inhibition of human colorectal cancers. Ann Oncol 2004;15:1025-32. DOI
54. Kasahara M, Takahashi Y, Nagata T, et al. Thymidylate synthase expression correlates closely with E2F1 expression in colon cancer. Clin Cancer Res 2000;6:2707-11. PubMed
55. Fang Z, Lin M, Li C, Liu H, Gong C. A comprehensive review of the roles of E2F1 in colon cancer. Am J Cancer Res 2020;10:757 68. PubMed PMC

56. Mannava S, Grachtchouk V, Wheeler LJ, et al. Direct role of nucleotide metabolism in C-MYC-dependent proliferation of melanoma cells. Cell Cycle 2008;7:2392-400. DOI PubMed PMC
57. Drubin DA, Hess AK, Catlett NL, Cara AD, Wettergren Y, Tell R. MYC as a candidate upstream controller involved in TYMS gene expression and 5-FU/folate treatment efficacy in colorectal cancer. Journa of Clinical Oncology 2021;39:e15512. DOI
58. Varghese V, Magnani L, Harada-Shoji N, et al. FOXM1 modulates 5-FU resistance in colorectal cancer through regulating TYMS expression. Sci Rep 2019;9:1505. DOI PubMed PMC
59. Klinhom-On N, Seubwai W, Sawanyawisuth K, Obchoei S, Mahalapbutr P, Wongkham S. FOXM1 inhibitor, Siomycin A, synergizes and restores 5-FU cytotoxicity in human cholangiocarcinoma cell lines via targeting thymidylate synthase. Life Sci 2021;286:120072. DOI PubMed
60. Ahn JY, Lee JS, Min HY, Lee HY. Acquired resistance to 5-fluorouracil via HSP P90/Src-mediated increase in thymidylate synthase expression in colon cancer. Oncotarget 2015;6:32622-33. DOI PubMed PMC
61. Matuszyk J. MALAT1-miRNAs network regulate thymidylate synthase and affect 5FU-based chemotherapy. Mol Med 2022;28:89. DOI PubMed PMC
62. Zhang Y, Wang J. MicroRNAs are important regulators of drug resistance in colorectal cancer. Biol Chem 2017;398:929-38. DOI PubMed PMC

63. Ogunwobi OO, Mahmood F, Akingboye A. Biomarkers in colorectal cancer: current research and future prospects. Int J Mol Sci 2020;21:5311. DOI PubMed PMC
64. Johnston PG, Lenz HJ, Leichman CG, et al. Thymidylate synthase gene and protein expression correlate and are associated with response to 5-fluorouracil in human colorectal and gastric tumors. Cancer Res 1995;55:1407-12. PubMed
65. Copur S, Aiba K, Drake JC, Allegra CJ, Chu E. Thymidylate synthase gene amplification in human colon cancer cell lines resistant to 5-fluorouracil. Biochem Pharmacol 1995;49:1419-26. DOI PubMed
66. Salonga D, Danenberg KD, Johnson M, et al. Colorectal tumors responding to 5-fluorouracil have low gene expression levels of dihydropyrimidine dehydrogenase, thymidylate synthase, and thymidine phosphorylase. Clin Cancer Res 2000;6:1322-7. PubMed
67. Edler D, Kressner U, Ragnhammar P, et al. Immunohistochemically detected thymidylate synthase in colorectal cancer: an independent prognostic factor of survival. Clin Cancer Res 2000;6:488-92. PubMed
68. Edler D, Glimelius B, Hallström M, et al. Thymidylate synthase expression in colorectal cancer: a prognostic and predictive marker of benefit from adjuvant fluorouracil-based chemotherapy. J Clin Oncol 2002;20:1721-8. DOI

69. Popat S, Matakidou A, Houlston RS. Thymidylate synthase expression and prognosis in colorectal cancer: a systematic review and meta-analysis. J Clin Oncol 2004;22:529-36. DOI PubMed

70. Kamynina E, Stover PJ. The roles of SUMO in metabolic regulation. In: Wilson VG, editor. SUMO regulation of cellular processes. Cham: Springer International Publishing; 2017. pp. 143-68. DOI PubMed PMC

71. Chon J, Stover PJ, Field MS. Targeting nuclear thymidylate biosynthesis. Mol Aspects Med 2017;53:48-56. DOI PubMed PMC

72. Gustavson MD, Molinaro AM, Tedeschi G, Camp RL, Rimm DL. AQUA analysis of thymidylate synthase reveals localization to be a key prognostic biomarker in 2 large cohorts of colorectal carcinoma. Arch Pathol Lab Med 2008;132:1746-52. DOI PubMed

73. Watson RG, Muhale F, Thorne LB, et al. Amplification of thymidylate synthetase in metastatic colorectal cancer patients pretreated with 5-fluorouracil-based chemotherapy. Eur J Cancer 2010;46:3358-64. DOI PubMed PMC

74. Wang TL, Diaz LA Jr, Romans K, et al. Digital karyotyping identifies thymidylate synthase amplification as a mechanism of resistance to 5-fluorouracil in metastatic colorectal cancer patients. Proc Natl Acad Sci U S A 2004;101:3089-94. DOI PubMed PMC

75. Clark JL, Berger SH, Mittelman A, Berger FG. Thymidylate synthase gene amplification in a colon tumor resistant to fluoropyrimidine chemotherapy. Cancer Treat Rep 1987;71:261-5. PubMed

76. Berger SH, Jenh CH, Johnson LF, Berger FG. Thymidylate synthase overproduction and gene amplification in fluorodeoxyuridine resistant human cells. Mol Pharmacol 1985;28:461-7. PubMed
77. Marsh S, McKay JA, Cassidy J, McLeod HL. Polymorphism in the thymidylate synthase promoter enhancer region in colorectal cancer. Int J Oncol 2001;19:383-6. DOI PubMed
78. Grumetti L, Lombardi R, Iannelli F, et al. Epigenetic approaches to overcome Fluoropyrimidines resistance in solid tumors. Cancers (Basel) 2022;14:695. DOI PubMed PMC
79. Wang YC, Xue HP, Wang ZH, Fang JY. An integrated analysis of the association between Ts gene polymorphisms and clinical outcome in gastric and colorectal cancer patients treated with 5-FU-based regimens. Mol Biol Rep 2013;40:4637-44. DOI PubMed
80. Mauritz R, Giovannetti E, Beumer IJ, et al. Polymorphisms in the enhancer region of the thymidylate synthase gene are associated with thymidylate synthase levels in normal tissues but not in malignant tissues of patients with colorectal cancer. Clin Colorectal Cancer 2009;8:146-54. DOI
81. Peters GJ, Backus HH, Freemantle S, et al. Induction of thymidylate synthase as a 5-fluorouracil resistance mechanism. Biochim Biophys Acta 2002;1587:194-205. DOI
82. Goff LW, Thakkar N, Du L, et al. Thymidylate synthase genotype-directed chemotherapy for patients with gastric and gastroesophageal junction cancers. PLoS One 2014;9:e107424. DOI PubMed PMC

83. Ntavatzikos A, Spathis A, Patapis P, et al. TYMS/KRAS/BRAF molecular profiling predicts survival following adjuvant chemotherapy in colorectal cancer. World J Gastrointest Oncol 2019;11:551-66. DOI PubMed PMC
84. Therizols G, Bash-Imam Z, Panthu B, et al. Alteration of ribosome function upon 5-fluorouracil treatment favors cancer cell drug tolerance. Nat Commun 2022;13:173. DOI PubMed PMC
85. Very N, Hardivillé S, Decourcelle A, et al. Thymidylate synthase O-GlcNAcylation: a molecular mechanism of 5-FU sensitization in colorectal cancer. Oncogene 2022;41:745-56. DOI
86. Zhang N, Yin Y, Xu SJ, Chen WS. 5-Fluorouracil: mechanisms of resistance and reversal strategies. Molecules 2008;13:1551-69. DOI PubMed PMC
87. Matuo R, Sousa FG, Escargueil AE, et al. 5-Fluorouracil and its active metabolite FdUMP cause DNA damage in human SW620 colon adenocarcinoma cell line. J Appl Toxicol 2009;29:308-16. DOI
88. Humeniuk R, Menon LG, Mishra PJ, et al. Decreased levels of UMP kinase as a mechanism of fluoropyrimidine resistance. Mol Cancer Ther 2009;8:1037-44. DOI Diasio RB, Offer SM. Testing for Dihydropyrimidine Dehydrogenase deficiency to individualize 5-Fluorouracil therapy. Cancers (Basel) 2022;14:3207. DOI PubMed PMC
89. Diasio RB, Offer SM. Testing for Dihydropyrimidine Dehydrogenase deficiency to individualize 5-Fluorouracil therapy. Cancers (Basel) 2022;14:3207. DOI PubMed PMC

90. Gmeiner WH. A narrative review of genetic factors affecting fluoropyrimidine toxicity. Precis Cancer Med 2021;4:38-38. DOI PubMed PMC
91. Lee JJ, Beumer JH, Chu E. Therapeutic drug monitoring of 5-fluorouracil. Cancer Chemother Pharmacol 2016;78:447-64. DOI PubMed PMC
92. Hu S, Meng F, Yin X, Cao C, Zhang G. NT5E is associated with unfavorable prognosis and regulates cell proliferation and motility in gastric cancer. Biosci Rep 2019;39:BSR20190101. DOI PubMed PMC
93. Wang D, Li W, Yin L, Du Y, Zhang S, Suo J. Association of serum levels of deoxyribose 1-phosphate and S-lactoylglutathione with neoadjuvant chemotherapy sensitivity in patients with gastric cancer: A metabolomics study. Oncol Lett 2020;19:2231-42. DOI PubMed PMC
94. Peters GJ. Therapeutic potential of TAS-102 in the treatment of gastrointestinal malignancies. Ther Adv Med Oncol 2015;7:340-56. DOI PubMed PMC
95. Takebayashi Y, Akiyama S, Akiba S, et al. Clinicopathologic and prognostic significance of an angiogenic factor, thymidine phosphorylase, in human colorectal carcinoma. J Natl Cancer Inst 1996;88:1110-7. DOI
96. Bijnsdorp IV, Azijli K, Jansen EE, et al. Accumulation of thymidine-derived sugars in thymidine phosphorylase overexpressing cells. Biochem Pharmacol 2010;80:786-92. DOI
97. Matsusaka S, Yamasaki H, Fukushima M, Wakabayashi I. Upregulation of enzymes metabolizing 5-fluorouracil in colorectal cancer. Chemotherapy 2007;53:36-41. DOI PubMed

98. Griffith M, Mwenifumbo JC, Cheung PY, et al. Novel mRNA isoforms and mutations of uridine monophosphate synthetase and 5 fluorouracil resistance in colorectal cancer. Pharmacogenomics J 2013;13:148-58. DOI
99. Fujii R, Seshimo A, Kameoka S. Relationships between the expression of thymidylate synthase, dihydropyrimidine dehydrogenase, and orotate phosphoribosyltransferase and cell proliferative activity and 5-fluorouracil sensitivity in colorectal carcinoma. Int J Clin Oncol 2003;8:72-8. DOI PubMed
100. Fukushima M, Fujioka A, Uchida J, Nakagawa F, Takechi T. Thymidylate synthase (TS) and ribonucleotide reductase (RNR) may be involved in acquired resistance to 5-fluorouracil (5-FU) in human cancer xenografts in vivo. Eur J Cancer 2001;37:1681-7. DOI PubMed
101. Kubota T, Watanabe M, Otani Y, KitajimaM, Fukushiuma M. Different pathways of 5-fluorouracil metabolism after continuous venous or bolus injection in patients with colon carcinoma: possible predictive value of thymidylate synthetase mRNA and ribonucleotide reductase for 5-fluorouracil sensitivity. Anticancer Res 2002;22:3537-40. PubMed
102. Gustavsson M, Ronne H. Evidence that tRNA modifying enzymes are important in vivo targets for 5-fluorouracil in yeast. RNA 2008;14:666-74. DOI PubMed PMC
103. Okamoto M, Fujiwara M, Hori M, et al. tRNA modifying enzymes, NSUN2 and METTL1, determine sensitivity to 5-fluorouracil in HeLa cells. PLoS Genet 2014;10:e1004639. DOI PubMed PMC

104. Xie T, Geng J, Wang Y, et al. FOXM1 evokes 5-fluorouracil resistance in colorectal cancer depending on ABCC10. Oncotarget 2017;8:8574-89. DOI PubMed PMC

105. Pratt S, Shepard RL, Kandasamy RA, Johnston PA, Perry W 3rd, Dantzig AH. The multidrug resistance protein 5 (ABCC5) confers resistance to 5-fluorouracil and transports its monophosphorylated metabolites. Mol Cancer Ther 2005;4:855-63. DOI PubMed

106. Marin JJG, Monte MJ, Macias RIR, et al. Expression of Chemoresistance-Associated ABC Proteins in Hepatobiliary, Pancreatic and Gastrointestinal Cancers. Cancers (Basel) 2022;14:3524. DOI PubMed PMC

107. Hientz K, Mohr A, Bhakta-Guha D, Efferth T. The role of p53 in cancer drug resistance and targeted chemotherapy. Oncotarget 2017;8:8921-46. DOI PubMed PMC

108. Fulda S, Debatin KM. Extrinsic versus intrinsic apoptosis pathways in anticancer chemotherapy. Oncogene 2006;25:4798-811. DOI PubMed

109. Bunz F, Dutriaux A, Lengauer C, et al. Requirement for p53 and p21 to sustain G2 arrest after DNA damage. Science 1998;282:1497 501. DOI PubMed

110. Bunz F, Hwang PM, Torrance C, et al. Disruption of p53 in human cancer cells alters the responses to therapeutic agents. J Clin Invest 1999;104:263-9. DOI PubMed PMC

111. Nita ME, Nagawa H, Tominaga O, et al. 5-Fluorouracil induces apoptosis in human colon cancer cell lines with modulation of Bcl-2 family proteins. Br J Cancer 1998;78:986-92. DOI PubMed PMC

112. Yang CM, Kang MK, Jung WJ, et al. p53 expression confers sensitivity to 5-fluorouracil via distinct chromatin accessibility dynamics in human colorectal cancer. Oncol Lett 2021;21:226. DOI PubMed PMC

113. Kandioler D, Mittlböck M, Kappel S, et al; p53 Research Group and the Austrian Breast and Colorectal Study Group (ABCSG). TP53 mutational status and prediction of benefit from adjuvant 5-Fluorouracil in stage III colon cancer patients. EBioMedicine 2015;2:825-30. DOI PubMed PMC

114. Backus HH, van Riel JM, van Groeningen CJ, et al. Rb, mcl-1 and p53 expression correlate with clinical outcome in patients with liver metastases from colorectal cancer. Ann Oncol 2001;12:779-85. DOI

115. Longley DB, Allen WL, McDermott U, et al. The roles of thymidylate synthase and p53 in regulating Fas-mediated apoptosis in response to antimetabolites. Clin Cancer Res 2004;10:3562-71. DOI

116. Tillman DM, Petak I, Houghton JA. A Fas-dependent component in 5-fluorouracil/leucovorin-induced cytotoxicity in colon carcinoma cells. Clin Cancer Res 1999;5:425-30. PubMed

117. Petak I, Danam RP, Tillman DM, et al. Hypermethylation of the gene promoter and enhancer region can regulate Fas expression and sensitivity in colon carcinoma. Cell Death Differ 2003;10:211-7. DOI

118. Backus HH, Dukers DF, van Groeningen CJ, et al. 5-Fluorouracil induced Fas upregulation associated with apoptosis in liver metastases of colorectal cancer patients. Ann Oncol 2001;12:209-16. DOI

119. Xie Q, Liu Y, Li X. The interaction mechanism between autophagy and apoptosis in colon cancer. Transl Oncol 2020;13:100871. DOI PubMed PMC

120. Li J, Hou N, Faried A, Tsutsumi S, Kuwano H. Inhibition of autophagy augments 5-fluorouracil chemotherapy in human colon cancer in vitro and in vivo model. Eur J Cancer 2010;46:1900-9. DOI

121. Yao CW, Kang KA, Piao MJ, et al. Reduced autophagy in 5-Fluorouracil resistant colon cancer cells. Biomol Ther (Seoul) 2017;25:315-20. DOI PubMed PMC

122. Kim EJ, Kang GJ, Kang JI, et al. Over-activation of AKT signaling leading to 5-Fluorouracil resistance in SNU-C5/5-FU cells. Oncotarget 2018;9:19911-28. DOI PubMed PMC

123. Zhang Y, Talmon G, Wang J. MicroRNA-587 antagonizes 5-FU-induced apoptosis and confers drug resistance by regulating PPP2R1B expression in colorectal cancer. Cell Death Dis 2015;6:e1845. DOI PubMed PMC

124. Chen J, Na R, Xiao C, et al. The loss of SHMT2 mediates 5-fluorouracil chemoresistance in colorectal cancer by upregulating autophagy. Oncogene 2021;40:3974-88. DOI PubMed PMC

125. Bijnsdorp IV, Peters GJ, Temmink OH, Fukushima M, Kruyt FA. Differential activation of cell death and autophagy results in an increased cytotoxic potential for trifluorothymidine compared to 5-fluorouracil in colon cancer cells. Int J Cancer 2010;126:2457-68. DOI

126. de la Cruz-Morcillo MA, Valero ML, Callejas-Valera JL, et al. P38MAPK is a major determinant of the balance between apoptosis and autophagy triggered by 5-fluorouracil: implication in resistance. Oncogene 2012;31:1073-85. DOI

127. Gao T, Yuan D, He B, et al. Identification of autophagy related genes in predicting the prognosis and aiding 5- fluorouracil therapy of colorectal cancer. Heliyon 2022;8:e09033. DOI PubMed PMC

128. Mleczak A, Millar S, Tooze SA, Olson MF, Chan EY. Regulation of autophagosome formation by Rho kinase. Cell Signal 2013;25:1-11. DOI PubMed

129. Zheng Z, He XY, Li JF, et al. RhoGDI2 confers resistance to 5-fluorouracil in human gastric cancer cells. Oncol Lett 2013;5:255-60. DOI PubMed PMC

130. Zhang P, Lai ZL, Chen HF, et al. Curcumin synergizes with 5-fluorouracil by impairing AMPK/ULK1-dependent autophagy, AKT activity and enhancing apoptosis in colon cancer cells with tumor growth inhibition in xenograft mice. J Exp Clin Cancer Res 2017;36:190. DOI PubMed PMC

131. Ghosh S, Mallick S, Das U, et al. Curcumin stably interacts with DNA hairpin through minor groove binding and demonstrates enhanced

cytotoxicity in combination with FdU nucleotides. Biochim Biophys Acta Gen Subj 2018;1862:485-94. DOI

132. Das U, Bhuniya A, Roy AK, Gmeiner WH, Ghosh S. Hairpin Oligonucleotide can functionalize gold nanorods for in vivo application delivering cytotoxic nucleotides and curcumin: a comprehensive study in combination with near-infrared laser. ACS Omega 2020;5:28463-74. DOI PubMed PMC

133. Anand P, Kunnumakkara AB, Sundaram C, et al. Cancer is a preventable disease that requires major lifestyle changes. Pharm Res 2008;25:2097-116. DOI PMC

134. Azwar S, Seow HF, Abdullah M, Faisal Jabar M, Mohtarrudin N. Recent updates on mechanisms of resistance to 5-Fluorouracil and reversal strategies in colon cancer treatment. Biology (Basel) 2021;10:854. DOI PubMed PMC

135. Gmeiner WH, Reinhold WC, Pommier Y. Genome-wide mRNA and microRNA profiling of the NCI 60 cell-line screen and comparison of FdUMP[10] with fluorouracil, floxuridine, and topoisomerase 1 poisons. Mol Cancer Ther 2010;9:3105-14. DOI PubMed PMC

136. Deng J, Wang Y, Lei J, Lei W, Xiong JP. Insights into the involvement of noncoding RNAs in 5-fluorouracil drug resistance. Tumour Biol 2017;39:1010428317697553. DOI

137. Marjaneh RM, Khazaei M, Ferns GA, Avan A, Aghaee-Bakhtiari SH. The role of microRNAs in 5-FU resistance of colorectal cancer: possible mechanisms. J Cell Physiol 2019;234:2306-16. DOI PubMed

138. Ghafouri-Fard S, Abak A, Tondro Anamag F, et al. 5-Fluorouracil: a narrative review on the role of regulatory mechanisms in driving resistance to this chemotherapeutic agent. Front Oncol 2021;11:658636. DOI PubMed PMC

139. Touil Y, Igoudjil W, Corvaisier M, et al. Colon cancer cells escape 5FU chemotherapy-induced cell death by entering stemness and quiescence associated with the c-Yes/YAP axis. Clin Cancer Res 2014;20:837-46. DOI PubMed PMC

140. Cho YH, Ro EJ, Yoon JS, et al. 5-FU promotes stemness of colorectal cancer via p53-mediated WNT/β-catenin pathway activation. Nat Commun 2020;11:5321. DOI PubMed PMC

141. Siebenhüner A, De Dosso S, Meisel A, Wagner AD, Borner M. Metastatic colorectal carcinoma after second progression and the role of Trifluridine-Tipiracil (TAS-102) in Switzerland. Oncol Res Treat 2020;43:237-44. DOI PubMed

142. Pardee TS, Gomes E, Jennings-Gee J, Caudell D, Gmeiner WH. Unique dual targeting of thymidylate synthase and topoisomerase1 by FdUMP[10] results in high efficacy against AML and low toxicity. Blood 2012;119:3561-70. DOI PubMed PMC

143. Gmeiner WH, van Waardenburg RCAM. Targeting DNA topoisomerases: past & future. Cancer Drug Resist 2021;4:758-61. DOI PubMed PMC

144. Pommier Y. Drugging topoisomerases: lessons and challenges. ACS Chem Biol 2013;8:82-95. DOI PubMed PMC

CHAPTER 3

Enhanced Therapeutic Efficacy of the Nanoscale Fluoropyrimidine Polymer CF10 in a Rat Colorectal Cancer Liver Metastasis Model

Charles Chidi Okechukwu [1,2], Xue Ma [3], Naresh Sah [4], Chinnadurai Mani [4], Komaraiah Palle [4] and William H. Gmeiner [2,*]

[1] Integrative Physiology and Pharmacology Graduate Program and Department of Cancer Biology, Wake Forest University School of Medicine, Winston-Salem, NC 27157, USA; cokechuk@wakehealth.edu.

[2]Department of Cancer Biology, Wake Forest University School of Medicine, Winston-Salem, NC 27157, USA.

[3] Department of Orthopedic Surgery, Wake Forest University School of Medicine, Winston-Salem, NC 27157, USA; xma@wakehealth.edu.

[4]Department of Cell Biology and Biochemistry, Texas Tech University Health Sciences Centre, Lubbock, TX 79430, USA; naresh.sah@ttuhsc.edu (N.S.); chinnadurai.mani@ttuhsc.edu (C.M.); komaraiah.palle@ttuhsc.edu (K.P.).

* Correspondence: bgmeiner@wakehealth.edu.

Simple Summary

Liver metastases are a major cause of colorectal cancer mortality. To combat this, chemotherapy is widely used but generally does not result in long-term survival and causes serious side effects in many patients. We tested if a new polymeric chemotherapy, CF10, was more effective than the current drug, 5-FU, in a rat model of liver metastatic disease. Our studies proved that CF10 was better tolerated in rats than 5-FU, was more potent at decreasing the viability of rat colon cancer cells, and was significantly more effective than 5-FU at inhibiting cancer progression in a rat model of liver metastasis when administered at an equivalent dose. Based on these studies, we propose advancing CF10 into clinical trials and testing it for improved activity in human patients with colorectal liver metastases.

Abstract

Combination chemotherapy regimens that include fluoropyrimidine (FP) drugs, e.g., 5-fluorouracil (5-FU), are central to the treatment of colorectal cancer liver metastases (CRLMs), a major cause of cancer mortality. We tested a second-generation FP polymer, CF10, in a CC531/WAG/Rij syngeneic orthotopic rat model of liver metastasis to determine if CF10 improved response relative to 5-FU. CF10 displayed increased potency relative to 5-FU in CC531 rat colorectal cancer cells based on clonogenic assay results and caused increased apoptosis, as shown using a live/dead assay. The increased potency of CF10 to CC531 cells was associated with increased replication stress, as assessed by Western blot for biomarkers of ATR/Chk1 and ATM/Chk2 pathway activation. CF10 dosed to deliver equivalent FP content as an established dose of 5-FU in rats (50 mg/kg) did not cause weight loss in WAGRij rats even when combined with ethynyl uracil (EU), an inhibitor of dihydropyrimidine dehydrogenase, the enzyme primarily responsible for 5-FU degradation in the liver. In contrast, 5-FU caused significant weight loss that was exacerbated in combination with EU. Importantly, CF10 was significantly more effective than 5-FU at inhibiting tumor progression (~90% reduction) in the CC531/WAG/Rij CRLM model. Our results reveal strong potential for CF10 to be used for CRLM treatment.

Keywords: colorectal cancer; liver metastasis; fluoropyrimidine; replication stress.

Introduction

Colorectal cancer (CRC) is the second leading cause of cancer-related mortality in men and women combined [1] (>940,000 deaths worldwide in 2020) and metastatic progression is almost exclusively responsible for all CRC mortality. Primary CRC most frequently metastasizes to the liver (colorectal liver metastasis (CRLM)) [2], with synchronous metastases in the liver occurring in 13.8–17.1% of cases and metachronous liver metastases in 7.6–15.1% of CRC [3]. Liver resection is a treatment that offers the best possibility for long-term survival in CRC patients with liver metastatic disease (40% 5-year survival) [4], but it is not achievable in >70% of cases [5]. Chemotherapy is crucial for disease management in most instances. A significant survival advantage for CRLM treatment was realized with the introduction of 5-FU chemotherapy and its modulation with leucovorin (LV), which resulted in survival benefits lasting 3–6 months [6]. The introduction of FP-based doublet chemotherapy regimens, in which 5-FU/LV is combined with oxaliplatin (FOLFOX) or irinotecan (FOLFIRI), further improved objective response rates and overall survival rates, which represent the current standard of care to improve survival [7]. While triplet therapy with FOLFOXFIRI is associated with further increased conversion to resectable disease and increased overall survival rates [8,9], this is achieved in only a limited percentage of CRLM patients because serious toxicities limit the use of this regimen to patients with a high-performance status. Thus, the development of new chemotherapies is important to further improve survival rates for CRLM patients. To overcome the limitations of 5-FU due to inefficient TS inhibition, we developed polymeric

fluoropyrimidines (FPs) that are more directly converted to fluorodeoxyuridylate (FdUMP), the TS-inhibitory metabolite of FPs. Thymidylate synthase (TS) is considered the primary molecular target for FP drugs because the more rapid proliferation of tumor cells increases cell reliance upon the de novo thymidylate biosynthesis pathway [10]. The importance of TS expression for developing resistance to 5-FU-based therapies [11] was shown in multiple studies, including a meta-analysis of 13 studies that demonstrated that elevated TS was associated with poor outcomes [12]. TYMS gene amplification in CRLMs was associated with shorter median survival time for patients treated with 5-FUbased chemotherapy [13]. Pre-clinical studies showed that the prototype FP polymer F10 improved antitumor activity relative to 5-FU in multiple tumor models [14,15] through a mechanism involving highly potent TS inhibition and the formation of DNA–protein crosslinks with DNA topoisomerase 1 (Top1), referred to as Top1 cleavage complexes (Top1ccs) [16,17]. We developed a second-generation FP polymer, CF10 (Figure 1), which was chemically modified to reduce exonucleolytic degradation and demonstrated that CF10 was highly effective in a mouse orthotopic model of primary colon cancer [18]. In this study, our primary objective was to test if CF10 displayed improved efficacy in a rat model of CRC liver metastatic disease. We used a modified clonogenic assay to demonstrate whether CF10 displayed improved potency relative to 5-FU in a rat colon carcinoma cell line, CC531, and we showed whether it was a potent inducer of apoptotic cell death using a live/dead assay. The CC531 cell line is of interest for evaluating potential new agents for improved CRLM treatment because it has been established as a

rodent CRLM model for sub-capsular injection into the livers of syngeneic WAG/Rij rats [5,19]. Mechanistically, CF10 is more effective than 5-FU at activating biomarkers of replication stress (e.g., pRPA and pChk1), as assessed by Western blots, and causing DNA doublestrand breaks (DSBs), consistent with the established TS/Top1 dual-targeting mechanism. CF10 was very well tolerated in vivo and intra-venous doses that delivered equivalent fluoropyrimidine content as an established dose of 5-FU in rats (50 mg/kg [20]) did not cause weight loss or systemic toxicities. CF10 demonstrated improved antitumor activity relative to an equivalent dosing of 5-FU; moreover, when combined with a favorable toxicity profile based on a lack of weight loss, further therapeutic advantages could be achieved with more aggressive dosing. Our findings are consistent with CF10 and CF10- based combination therapies having the potential to improve outcomes for CRLM patients relative to 5-FU-based therapies through distinct mechanistic and pharmacologic properties.

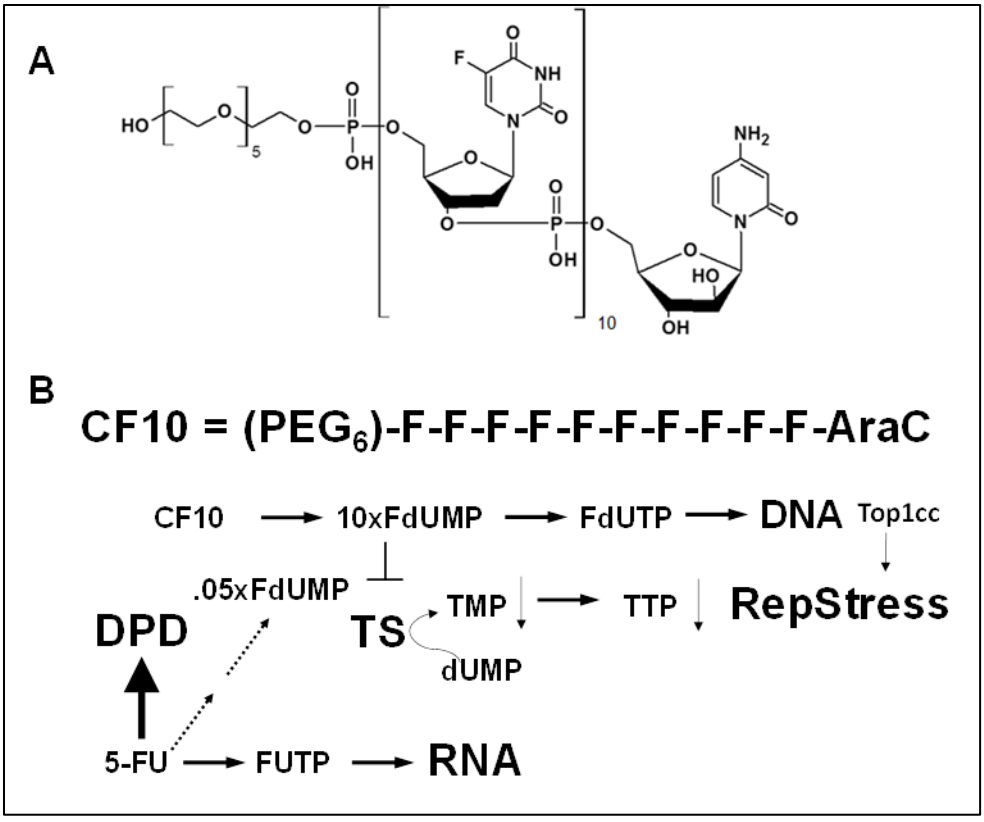

Figure 1. (A) Chemical structure of CF10; (B) scheme depicting the conversion of CF10 to 10× equivalents of fluorodeoxyuridylate, while only ~5% (0.05×) of 5-FU is converted to FdUMP. TS inhibition results in the depletion of TTP that causes replication fork stalling and collapse. The misincorporation of FdUTP into DNA causes the formation of DNA topoisomerase 1 cleavage complexes (Top1ccs) that stall replication forks.

Materials and Methods

Cell Culture and Reagents

The rat colon carcinoma cell line CC531 was derived from WAG/Rij rats exposed to 1,2-dimethyl hydrazine. CC531 cells obtained from Dr. Sarah White (University of Wisconsin—Milwaukee) were cultured in Dulbecco's modified Eagle medium (DMEM) (Life Technologies, Carlsbad, CA, USA) and supplemented with 10% fetal bovine serum in culture flasks at 37 ◦C in a humidified atmosphere containing 5% CO2. CF10 was obtained from ST Pharma and was validated by high-resolution mass spectrometry and was dissolved in 0.9% sterile saline. Clinical-grade 5-FU (50 mg/mL) was purchased from the Baptist Hospital clinical pharmacy. 5-FU concentrations were calculated based on the dilution of the established stock concentration. CF10 concentrations were matched to deliver equivalent nucleoside content based on UV absorbance at 260 nm. A modified clonogenic assay was used to assess the potency of CF10 and 5-FU in CC531 cells. CC531 cells were plated in 24-well plates, and, after 24 h, they were treated with the indicated concentration of CF10 or 5-FU for 72 h. Following drug treatment, the media were replaced, and cells were allowed to grow for 7 days. Cell proliferation was evaluated using the Aqueous One (Promega) reagent, in line with the manufacturer's instructions, after the cell solution was transferred to 96-well plates.

Western Blotting

Proteins were isolated and their differential expressions were analyzed by Western blot, as described previously [21,22]. Briefly, the cells were lysed using RIPA buffer (50 mM Tris HCl at pH 7.4, 150 mM NaCl, 1% Triton X-100 or NP-40, 0.5% sodium deoxycholate, 0.1% SDS, 1 mM EDTA, and 10 mM NaF freshly supplemented with protease and phosphatase inhibitors). Protein concentrations were quantified using a Bradford assay (Bio-Rad), and the samples were normalized for equal loading. The samples were then heated to 100 °C for 10 min in the presence of 6× Laemmli buffer (Boston BioProducts; Milford, MA, USA). The proteins were resolved by SDS-PAGE and their expression was analyzed following immunoblotting using specific antibodies. The following antibodies were used in this study: FANCD2 (R&D MAB93691), pCHK2-T68 (Invitrogen PA5-104715), pRPA 32-S33 (Cell Signaling 10148s), pCHK1-S296 (Cell Signaling 90178s), pH2AX-S139 (Millipore 05- 636), GAPDH (Santa Cruz 32233), and Vinculin (Cell Signaling 13901S).

Apoptosis Analysis with Flow Cytometry

CC531 cells underwent 48 h and 72 h treatments with a dose of CF10 that was 1 log less than the 5FU dose. After the treatment, the samples were analyzed for apoptosis using the Invitrogen™ eBioscience™ Annexin V-FITC Apoptosis Detection Kit (catalog number 509299), as described previously [23]. Following drug treatment, the cells were trypsinized and then stained with 5 µL of Annexin-V for 10 min at room temperature. After this, the samples were washed with binding buffer (following the manufacturer's instructions) and incubated with 10 µL of

propidium iodide (PI, 20 μg/mL) for 30 min at 37 ◦C. Finally, the samples were analyzed with flow cytometry for the apoptotic cells using a BD Accuri (BD Biosciences, Franklin Lakes, NJ, USA). A total of three independent experiments were performed for each time point.

Liver Tumor Cell Inoculation to Simulate CRLM Formation

All animal studies were undertaken in accordance with the protocols approved by the Institutional Animal Care and Use Committee at Wake Forest University School of Medicine (Winston-Salem, NC, USA). Immunocompetent WAG/Rij rats weighing 250–300 g were used because this strain is syngeneic with the CC531 colon carcinoma cell line. WAG/Rij rats are not commercially available in the U.S. and were obtained from Dr. Sarah White (UW-M) and bred at WFUSM for these studies. The rats had a controlled climate and light cycles, and all had free access to a standard laboratory diet and water. For the inoculation procedure, anesthesia was obtained using 2–3% isoflurane and then maintained at 1.5% for surgery. A 2 cm midline incision was made, and both the left and right hepatic lobes were mobilized. The CC531 cells were suspended at a density of 2×10^6 cells in 200 uL and 25 uL of cell suspension, mixed 1:1 with Matrigel, and injected via a 29-gauge needle into the subcapsular portion of one of the previously specified hepatic lobes. When the needle was withdrawn, a cotton swab was used to press on the puncture site to achieve hemostasis. Once hemostasis was achieved, the wound was washed with saline, the muscle layer was closed using a 6-0 Vicryl suture, and the skin was closed using staples. An abdominal bandage was applied and the rats were allowed to recover from anesthesia before returning to the animal

facility. The tumors were allowed to grow for 7 days and fluorescence imaging was performed using an RGD peptide Cy5.5 conjugate to establish tumor formation prior to initiating treatments.

Treatment and Fluorescence Imaging of Tumor Progression

Tumor formation in the liver was established using fluorescence imaging following the tail vein injection of a Cy5.5-labeled cyclic “RGD” peptide (c[fK(Cy5.5)RGD]; UNC peptide synthesis facility, Chapel Hill, NC, USA) targeting integrin avb3. (**Figure S1**) 10 nmol of peptide in 100 µL of 0.9% sterile saline were injected 4–24 h prior to imaging [24]. Attempts to label CC531 cells with luciferase using viral transduction were successful (**Figure S2**); however, we were not able to follow tumor progression in vivo afterwards by conducting bioluminescence imaging because imaging was negative for luciferase signal, even though the autopsy of rats revealed tumor formation and progression in the liver. It is likely that the luciferase-labeled CC531 cells were selected against during tumor progression in the immunocompetent host. We experienced similar issues detecting luciferase-transduced MC38 mouse CRC cells in a C57BL6/MC38 syngeneic orthotopic mouse model, and, in that model, the immunohistochemistry of liver tumor correlated with RGD peptide fluorescent signals. The fluorescence imaging of tumors was undertaken using an IVIS Lumina LT Series III system and the rats were imaged under isoflurane anesthesia. All images were analyzed using Living Image software (v4.7.4.) with an identical size region of interest for each rat. To assess the therapeutic efficacy of CF10 and 5-FU, groups of n = 5 rats with similar initial tumor levels based on fluorescence imaging (**Figure S3**) were treated with

either 5-FU (50 mg/kg) or CF10 doses to deliver equivalent nucleoside content based on UV absorbance at 260 nm. The 5-FU dose is based on similar studies in the related Sprague–Dawley rat strain [20]. Rats in each group were treated 1×/week for 4 weeks. One week after the fourth treatment, all rats underwent a final imaging procedure and were then euthanized, and their livers were extracted and imaged ex vivo.

Statistical Analysis

All statistical analyses were conducted using GraphPad Prism 10.2.0. Experiments were conducted in triplicate ± SEM. For all in vitro experiments, five biological replicates were used for analysis, and appropriate one-way ANOVA tests with recommended Tukey corrections were conducted, with $p < 0.05$ indicating significance.

Results

CF10 inhibits CC531 clonogenic survival and induces apoptosis. We previously demonstrated improved potency for CF10 relative to 5-FU in the NCI60 cell line screen [18,25] and a more potent decrease in clonogenic survival for human CRC [18] and pancreatic ductal adenocarcinoma (PDA) cell lines [26] relative to 5-FU, which correlated with improved antitumor activity in xenograft models. We performed a modified clonogenic survival assay to test if the CC531 rat CRC cell line was responsive to CF10 and observed improved potency relative to 5-FU (**Figure 2A**). We then investigated if CF10 efficiently induced apoptotic cell death based on flow cytometry analysis for Annexin V cell surface expression and

permeability to propidium iodide (PI). The percentage of early apoptotic (Annexin V +/PI−) and late apoptotic (Annexin V+/PI+) cells were increased upon CF10 treatment relative to a 10-fold higher concentration of 5-FU at 48 h (**Figure 2B**) and 72 h (**Figure 2C**). Thus, we found that CC531 cells are relatively more responsive to CF10 than 5-FU and that CF10 is a potent inducer of apoptotic cell death in this cell line.

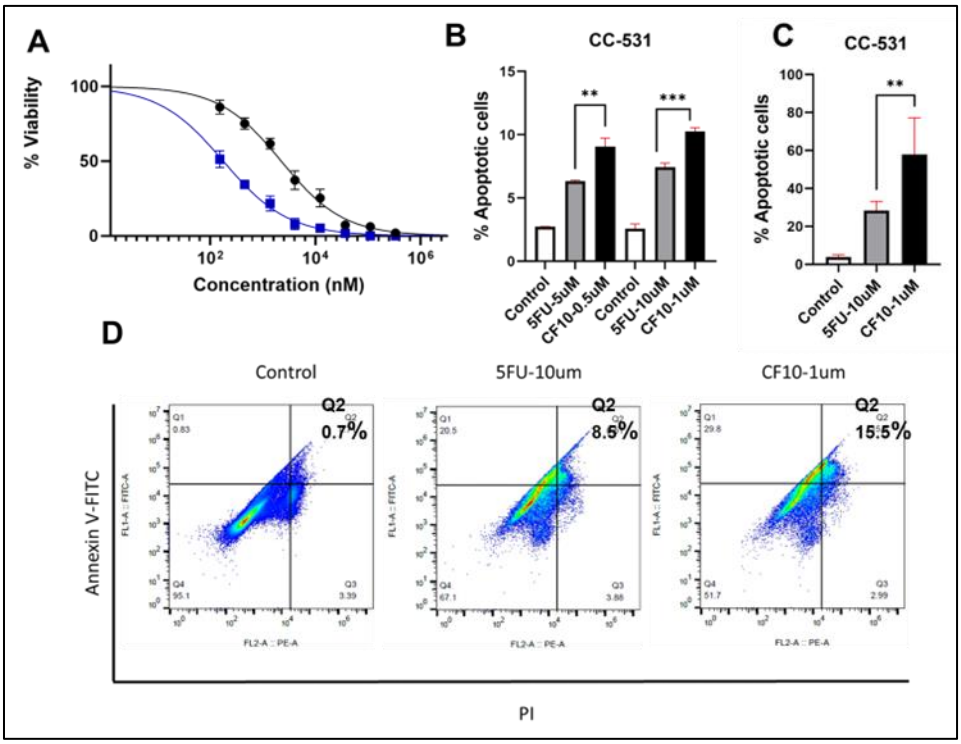

Figure 2. CF10 is potent in CC531 cells and induces apoptosis more efficiently than 5-FU. (A) Dose–response graphs for 5-FU (black) and CF10 (blue) in CC531 cells determined using a modified clonogenic assay with 48 h treatment (N = 4). (B–D) Graphs of % apoptotic CC531 cells based on Annexin V staining and flow cytometry analysis following the indicated treatment for (B) 48 h and (C) 72 h cells. (D) Representative images from flow cytometry analysis (72 h treatment) with

quantification showing increased late apoptotic (Q2; AnnexinV+/PI+) cells for CF10 with a 10-fold lower concentration than 5-FU. ** $p < 0.01$, *** $p < 0.0001$.

CF10 Causes Replication Stress and DNA DSBs in CC531 Cells We previously established that the improved potency of CF10 relative to 5-FU in human CRC cells resulted from more efficient TS inhibition and the poisoning of DNA topoisomerase 1 (Top1) [16,17], resulting in stalled replication forks and increased replication stress [18]. Replication fork collapse may result in DNA double-strand breaks (DSBs), genomic instability, and cell death [27], which is consistent with the observed increased potency of CF10 relative to 5-FU in CC531 cells (**Figure 2**). The adverse consequences of replication fork collapse may be countered by ATR/Chk1 pathway activation which decreases the initiation of new replication forks and may stimulate the activation of the homologous recombination (HR)-mediated repair of DNA DSBs generated at collapsed forks [28]. CF10 significantly stimulated increased pChk1 Serine-317 (S317) levels, consistent with ATR/Chk1 pathway activation (Figure 3A). FANCD2 mono-ubiquitination and pRPA32 Serine-S33 were also increased in CF10-treated CC531 cells to a greater extent than in CC531 cells treated with 5-FU at equivalent fluoropyrimidine concentrations (**Figure 3B, C**), consistent with the stabilization of stalled forks and the attempted repair of collapsed forks [29,30]. Further, pH2AX-S139 and pChk2 Threonine-T68 (T68) increased with CF10 treatment, consistent with the generation of DNA DSBs during the attempted repair of collapsed forks resulting in ATM/Chk2 pathway activation (**Figure 3B, C**). Our results are consistent with the increased potency of CF10 relative to 5-FU in CC531 cells resulting from DNA damage associated with

replication fork collapse, with the extent of damage mitigated through the activation of the ATR/Chk1 and ATM/Chk2 pathways.

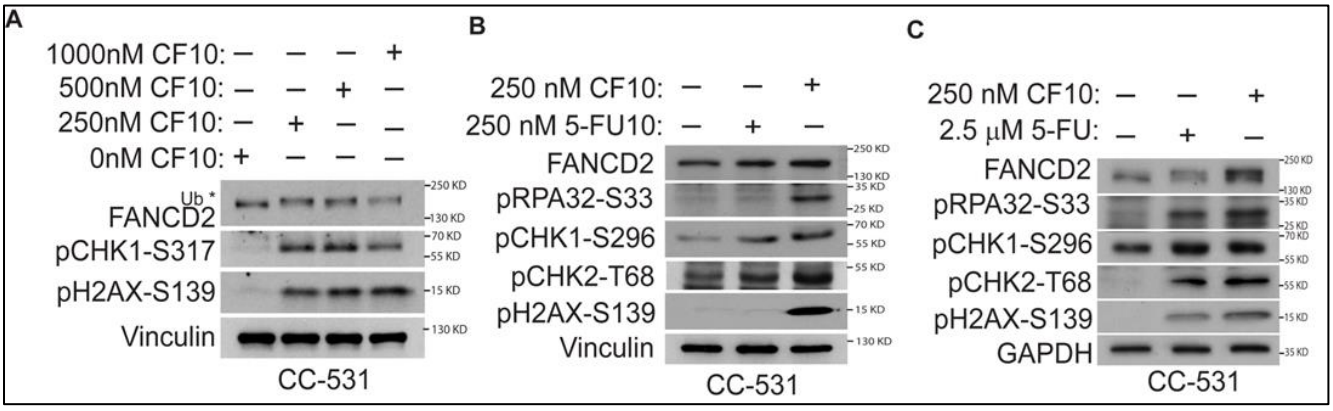

Figure 3. CF10 activates the ATR/Chk1 pathway, consistent with replication stress, and causes DNA DSBs in CC531 cells. Western blots from CC531 cell lysates: (A) CF10 dose–response graphs demonstrate that a 250 nM dose is sufficient for ATR/Chk1 pathway activation and DNA DSBs; (B) equimolar 5-FU is not effective in ATR/Chk1 activation and DNA DSBs; and (C) a 10-fold greater 5-FU dose is relatively less effective than 250 nM CF10. * indicates mono-ubiquitnated FANCD2.

CF10 is well tolerated and efficacious in the WAG/Rij Rat CRLM model.

CRC mortality is almost exclusively from metastatic progression, with the liver being the most frequent metastatic site involved in ~50% of all CRC cases [2]. Chemotherapy with 5-FU-based combination therapy regimens is central to CRLM treatment with established survival advantages for both FOLFOX and FOLFIRI regimens [31]. However, these regimens are rarely curative and are associated with serious toxicities in many cancer patients [9] and the development of drug

resistance [11], necessitating new and more effective therapies. To test if the improved potency of CF10 relative to 5-FU in CC531 rat CRC cells could translate into improved activity in a rat model of CRC liver metastasis, we evaluated both FPs using the CC531/WAGRij rat syngeneic orthotopic model. In this model, the sub-capsular injection of CC531 cells into one lobe of WAG/Rij rat liver resulted in a liver tumor mass that demonstrated the pharmacological challenges associated with chemotherapy administration for CRLM treatment [5]. 5-FU was dosed at 50 mg/kg, a dose previously used in rats [20], and i.v. tail vein injection 1×/week for 4 weeks resulted in significant weight loss (**Figure 4A**). However, the identical dosing of CF10 to deliver equivalent fluoropyrimidine based on UV A260 absorbance was not associated with weight loss, while initial weights were similar for all groups (**Figure S4**). To further investigate potential toxicity differences between CF10 and 5-FU related to altered metabolism, we tested the effects of the co-administration of ethynyl uracil (EU), an agent that inhibits the hepatic degradation of 5-FU with the dihydropyrimidine dehydrogenase (DPD) enzyme [32]. A single dose of 5-FU at 50 mg/kg resulted in significant weight loss upon co-administration with EU (2 mg/kg); however, the co-administration of CF10 dosed to deliver equivalent fluoropyrimidine content did not cause significant weight loss upon co-administration with EU. The results demonstrate that CF10 is relatively well tolerated in WAG/Rij rats and, consistent with this, is not undergoing hepatic degradation to the same extent as 5-FU.

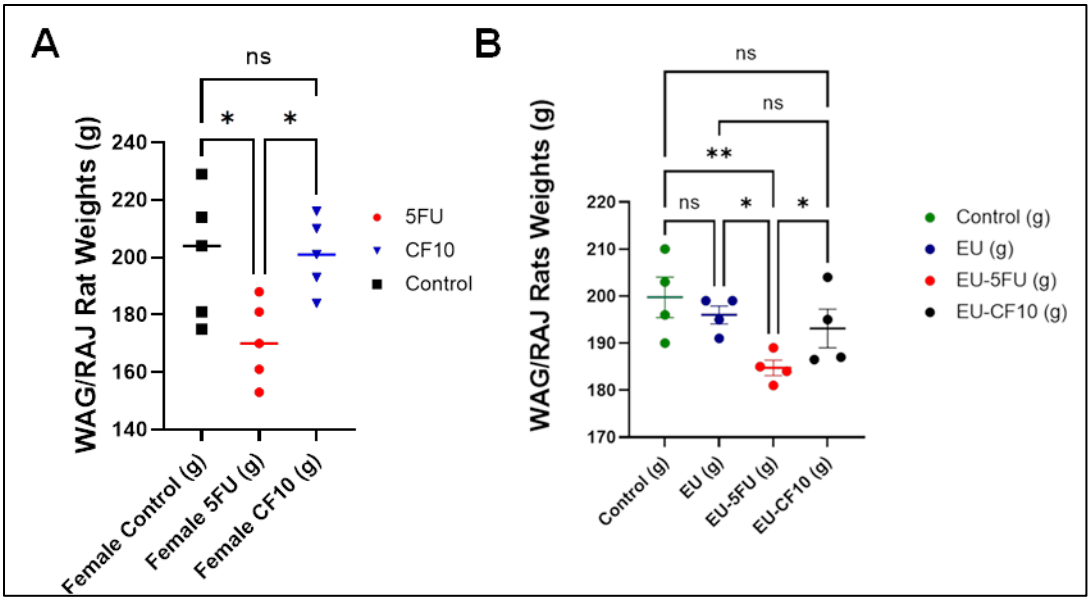

Figure 4. 5-FU (but not CF10) induced significant weight loss in WAG/Rij rats. (A) The final weights of WAG/Rij rats following treatment with 5-FU (50 mg/kg), CF10 (141 mg/kg), or vehicle (0.9% sterile saline). The rats were dosed 1×/week for 4 weeks via tail vein injection. (B) The rats were administered a single dose of ethynyl uracil (EU; 2 mg/kg), alone or in combination with a single dose of 5-FU or CF10, as shown in (A). 5-FU+EU (but not CF10+EU) caused significant weight loss (* $p < 0.05$, ** $p < 0.041$, ns - not significant), Initial average weights for all groups were not significantly different in both (A, B) (**Figure S4**).

We then evaluated the potential of CF10 to reduce the progression of liver tumor mass in the CC531 WAG/Rij rat syngeneic orthotopic CRLM model (**Figure 5**). As described previously [5,19], the subcapsular injection of CC531 rat CRC tumor cells into a hepatic lobe results in a liver-specific tumor mass that models CRLM for evaluating novel therapies. Tumor masses were identified using a fluorescent RGD peptide that binds to integrin αvβ3 [24], as luciferase expression (**Figure S2**)

was not maintained in CC531 cells in vivo following tumor formation. The establishment of a tumor was validated in all rats based on the detection of fluorescent signals in the liver (**Figure S3**). Parallel studies in a mouse CRLM model demonstrated that fluorescent imaging with the RGD peptide accurately reflected the extent of tumor progression, as assessed by histopathology. The rats were treated with either vehicle (0.9% sterile saline), 5-FU (50 mg/kg), or CF10. The CF10 dose was matched to deliver fluoropyrimidine content equivalent to the 5-FU dose based on UV A260 absorbance. The rats were dosed 1× per week for 4 weeks via tail vein injection. One week following the final treatment, all rats underwent a final in vivo imaging procedure (**Figure 4A, B**), after which the rats were humanely euthanized and their livers were extracted and imaged ex vivo (**Figure 5C, D**). Ex vivo liver imaging confirmed strong fluorescent signals throughout the liver for all rats in the control group, while for rats treated with 5-FU, fluorescent signals were primarily associated with a single lobe and were of significantly lower intensity relative to vehicle, consistent with the idea that 5-FU activity is used for inhibiting the progression of liver metastatic disease. Rats treated with CF10 did not have a detectable fluorescent signal in the liver in the final in vivo imaging and ex vivo imaging procedures, which did not indicate that any lobe displayed increased fluorescence intensity relative to background, a result consistent with the regression of liver tumor mass with CF10 treatment. The data are consistent with the notion that CF10 is more effective than 5-FU for the treatment of liver metastatic CRC in a rat model that replicates pharmacological challenges associated with CRLM treatment.

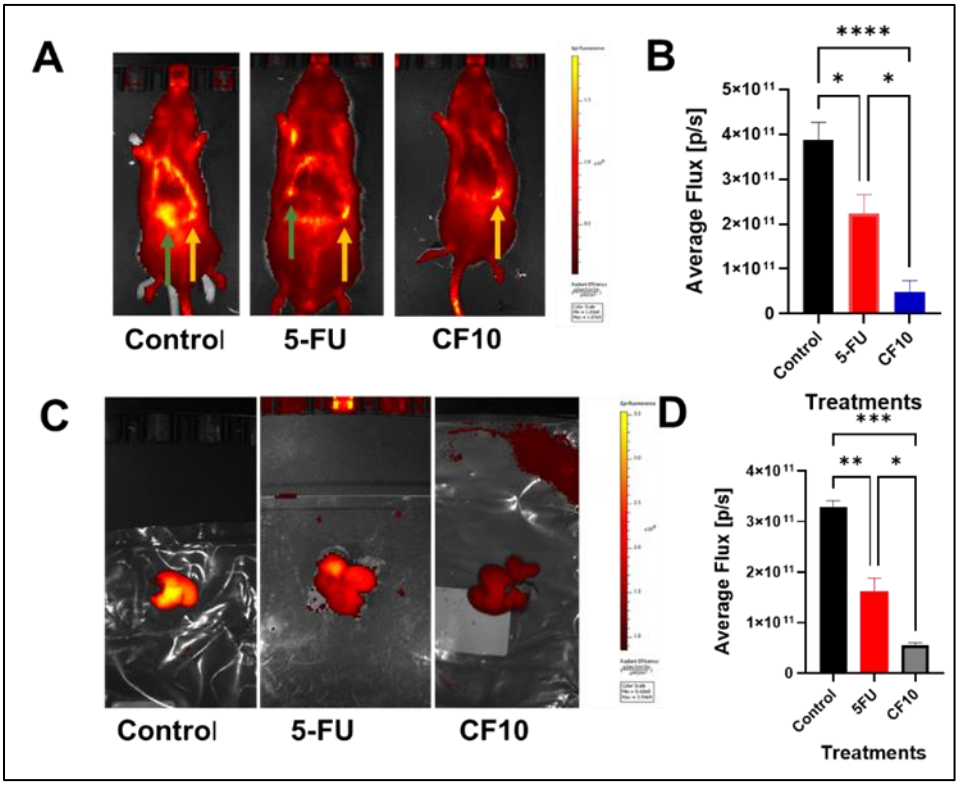

Figure 5. Imaging CRLM progression in WAG/Rij rats after 4 weeks of the indicated treatment, showing that CF10 was found to be effective in a rat CRLM model. Liver metastases were formed by injecting CC531 rat CRLM cells into the left hepatic lobe. Liver tumor masses were detected using a fluorescent (Cy5.5-labeled) RGD peptide and were similar in all rats at baseline (2 weeks after receiving an injection). Rats (n = 5 per group) were then treated for 4 weeks (1×/week via i.v. dose) with vehicle, 5-FU (50 mg/kg), or CF10 (identical to 50 mg/kg 5-FU dose based on UV A260). (A) The fluorescence imaging of rats 4 weeks after receiving treatment. Green arrows point to liver tumor signal, which is quantified in (B). Yellow arrows point to spleen autofluorescence. (C) Rats were then euthanized, and their livers were extracted and imaged ex vivo with Cy5.5

signal quantified in (D). Rats treated with CF10 displayed significantly reduced signals from CRLMs relative to both 5-FU and vehicle. * $p < 0.01$; ** $p < 0.011$; *** $p < 0.015$; **** $p < 0.002$.

Discussion

The principal cause of CRC mortality is the progression of metastatic disease, with the liver being the most frequent site for CRC metastasis [2,3]. Chemotherapy is central to the management of CRC liver metastatic disease (CRLM) and 5-FU-based combination chemotherapy regimens (including FOLFOX and FOLFIRI) have contributed to improved overall survival rates for mCRC patients in the last decade. While an increasing number of CRLM patients are surviving to receive second- and even third-line treatments with regimens that include FP drugs [31], the 5-year survival rate for mCRC remains dismal at <14% [33]. Further, FP-based chemotherapy is associated with serious systemic toxicities that limit patients' quality of life. Thus, developing the next generation of FP therapies that preserve and enhance the strong anti-tumor activity of this class of drugs, particularly in gastrointestinal malignancies, even while reducing systemic toxicities, is an important research objective. In this study, we highlighted the improved activity of CF10 (**Figure 1**), a second-generation fluoropyrimidine polymer that is advancing towards clinical development based on the promising anti-cancer activity of FP polymers in multiple preclinical models [14,15,26], including in an orthotopic mouse model of primary colon cancer [18]. Importantly for CF10 clinical translation, we demonstrated significantly improved antitumor activity relative to equivalent 5-FU dosing in a syngeneic orthotopic rat model that replicates pharmacological

challenges associated with the treatment of liver metastatic disease. Our results demonstrate that CF10 displays pharmacological properties suited for the effective treatment of liver metastatic disease. Further, strong activity was achieved without significant weight loss or other indications of systemic toxicities, while 5-FU administration was associated with significant weight loss in this rat model.

Mechanistically, CF10's substantial potency advantage relative to 5-FU in CRC cells [16,25] is associated with increased replication stress and the activation of apoptosis. We demonstrated that CF10 was more potent than 5-FU to the rat CRC cell line CC531 in a clonogenic assay (**Figure 2A**), and a 10-fold lower concentration of CF10 resulted in a significantly greater percentage of late apoptotic cells at a 72 h timepoint (**Figure 2B–D**). In previous studies, we demonstrated that CF10 inhibited thymidylate synthase (TS) more effectively than equivalent 5-FU concentrations, consistent with the direct release of fluorodeoxyuridylate (FdUMP), a TS-inhibiting metabolite. TS inhibition depletes CRC cells of thymidylate and consequently thymidine triphosphate, causing the slowing and stalling of replication forks. Consistent with increased replication stress, we demonstrated that CF10 stimulated the mono-ubiquitination of FANCD2, a marker of stalled replication forks (**Figure 3**). CF10 treatment also more effectively activated pChk1 (S296) and pRPA (S33), consistent with ATR/Chk1 pathway activation following replication fork collapse. In previous studies, we demonstrated that ATR/Chk1 inhibitors selectively enhanced F10 but not 5-FU cytotoxicity in human CRC cell lines [34], while inhibitors of the ATR/Chk1/Wee1 pathway enhanced CF10 but not 5-FU cytotoxicity in pancreatic

ductal adenocarcinoma [35]. The repair of stalled replication forks may proceed via the formation of Mus81-induced DNA DSBs [36] and our studies demonstrated that CF10 more efficiently induced pH2AX-S139 and activated the ATM/Chk2 pathway relative to 10-fold greater 5-FU concentrations (**Figure 3**). Our results are consistent with increased potency for CF10 relative to 5-FU through increased replication stress.

The efficacy of FP-based chemotherapy for the treatment of mCRC and CRLM is countered by the serious systemic toxicities that occur in many patients treated with these drugs [9]. In this study, we dosed rats with 5-FU at 50 mg/kg 1×/week for 4 weeks and, consistent with previous studies, observed significant weight loss with this dose [20]. In contrast, equivalent dosing with CF10 did not cause any weight loss (**Figure 4A**). The causes of 5-FU-induced GI-toxicity are not definitively known; however, previous studies demonstrated that 5-FU-induced intestinal damage and cell death in mice were reversed by uridine co-treatment, consistent with GI toxicity originating (at least in part) from RNA-mediated effects [37]. Thus, the improved toxicity profile for CF10 is consistent with its more direct conversion to fluorodeoxyuridylate and consequently reduced levels of RNA-directed metabolites that are primarily responsible for GI toxicity. The systemic toxicities of 5-FU are particularly severe in individuals with deficiencies in DPD activity that are associated with SNPs that occur in up to 5% of humans [9]. In these individuals, 5-FU is not degraded efficiently in the liver, resulting in relatively higher levels in tissues, including in the GI tract. To model these effects, we performed studies using the DPD inhibitor 5-ethynyluracil (EU) [32]. A single dose of 5-FU (50 mg/kg)

caused significant weight loss in WAG/Rij rats when combined with EU (2 mg/kg). In contrast, the combination of CF10+EU delivering equivalent FP and equivalent EU did not cause significant weight loss in rats (**Figure 4B**). Our results highlight the potential for CF10 to be administered at relatively higher doses than is possible with 5-FU, potentially further increasing its anticancer activity and its therapeutic advantages relative to 5-FU. Further, patients with DPD deficiency may not be as high-risk for developing serious toxicities with CF10 treatment as for 5-FU, reducing the expense associated with the increased length of hospitalization for many DPD-deficient patients.

Conclusions

In this study, we demonstrated improved anticancer activity for CF10 relative to equivalent 5-FU concentrations in a rat-based syngeneic orthotopic model of colorectal cancer liver metastatic disease (**Figure 5**). CRC is a leading cause of cancer-related mortality and liver metastasis is a principal cause of CRC mortality. Our results are consistent with the finding that there is strong potential for CF10 to treat patients with CRLMs more effectively than current 5-FU-based therapy. Our results support the further development of CF10 for improved CRLM treatment that may contribute to improved outcomes for this highly lethal malignancy.

Supplementary Materials: The following supporting information can be downloaded at: https: //www.mdpi.com/article/10.3390/cancers16071360/s1. Figure S1: Structure and analytical data for cyclic RGD peptides; Figure S2:

Validation of luciferase expression in CC531-luc cells; Figure S3: Fluorescent imaging of rats prior to treatment; Figure S4: Initial weights of rats prior to treatment.

Author Contributions: Conceptualization, W.H.G.; methodology, C.C.O., X.M., N.S., C.M. and K.P.; validation, W.H.G., C.C.O. and K.P.; investigation, C.C.O., X.M., N.S. and C.M.; resources, W.H.G., X.M. and K.P.; writing—original draft preparation, W.H.G.; writing—review and editing, C.C.O., X.M., N.S. and K.P.; supervision, W.H.G. and K.P.; project administration, W.H.G. and K.P.; funding acquisition, W.H.G. and K.P. All authors have read and agreed to the published version of the manuscript.

Funding: This research was funded by P30 CA 012197 and the Department of Defense Peer-Reviewed Cancer Research Program CA200460.

Institutional Review Board Statement: Not applicable.

Informed Consent Statement: Not applicable.

Data Availability Statement: Data will be made available on request.

Conflicts of Interest: Gmeiner is an inventor on a patent application related to the use of CF10 for the treatment of colorectal cancer (including liver metastatic disease)

References

1. Xi, Y.; Xu, P. Global colorectal cancer burden in 2020 and projections to 2040. *Transl. Oncol.* **2021**, *14*, 101174. [**Google Scholar**] [**CrossRef**] [**PubMed**]

2. Zhou, H.; Liu, Z.; Wang, Y.; Wen, X.; Amador, E.H.; Yuan, L.; Ran, X.; Xiong, L.; Ran, Y.; Chen, W.; et al. Colorectal liver metastasis: Molecular mechanism and interventional therapy. *Signal Transduct. Target. Ther.* **2022**, *7*, 70. [**Google Scholar**] [**CrossRef**] [**PubMed**]

3. Martin, J.; Petrillo, A.; Smyth, E.C.; Shaida, N.; Khwaja, S.; Cheow, H.K.; Duckworth, A.; Heister, P.; Praseedom, R.; Jah, A.; et al. Colorectal liver metastases: Current management and future perspectives. *World J. Clin. Oncol.* **2020**, *11*, 761–808. [**Google Scholar**] [**CrossRef**] [**PubMed**]

4. Chow, F.C.; Chok, K.S. Colorectal liver metastases: An update on multidisciplinary approach. *World J. Hepatol.* **2019**, *11*, 150–172. [**Google Scholar**] [**CrossRef**] [**PubMed**]

5. White, S.B.; Procissi, D.; Chen, J.; Gogineni, V.R.; Tyler, P.; Yang, Y.; Omary, R.A.; Larson, A.C. Characterization of CC-531 as a Rat Model of Colorectal Liver Metastases. *PLoS ONE* **2016**, *11*, e0155334. [**Google Scholar**] [**CrossRef**] [**PubMed**]

6. Arbuck, S.G. Overview of clinical trials using 5-fluorouracil and leucovorin for the treatment of colorectal cancer. *Cancer* **1989**, *63*, 1036–1044. [**Google Scholar**] [**CrossRef**] [**PubMed**]

7. Zeineddine, F.A.; Zeineddine, M.A.; Yousef, A.; Gu, Y.; Chowdhury, S.; Dasari, A.; Huey, R.W.; Johnson, B.; Kee, B.; Lee, M.S.; et al. Survival improvement for patients with metastatic colorectal cancer over twenty years. *NPJ Precis. Oncol.* **2023**, *7*, 16. [**Google Scholar**] [**CrossRef**]

8. Oki, E.; Ando, K.; Nakanishi, R.; Sugiyama, M.; Nakashima, Y.; Kubo, N.; Kudou, K.; Saeki, H.; Nozoe, T.; Emi, Y.; et al. Recent advances in treatment for colorectal liver metastasis. *Ann. Gastroenterol. Surg.* **2018**, *2*, 167–175. [**Google Scholar**] [**CrossRef**] [**PubMed**]

9. Gmeiner, W.H. A narrative review of genetic factors affecting fluoropyrimidine toxicity. *Precis. Cancer Med.* **2021**, *4*. [**Google Scholar**] [**CrossRef**]

10. Wilson, P.M.; Danenberg, P.V.; Johnston, P.G.; Lenz, H.J.; Ladner, R.D. Standing the test of time: Targeting thymidylate biosynthesis in cancer therapy. *Nat. Rev. Clin. Oncol.* **2014**, *11*, 282–298. [**Google Scholar**] [**CrossRef**]

11. Gmeiner, W.H.; Okechukwu, C.C. Review of 5-FU resistance mechanisms in colorectal cancer: Clinical significance of attenuated on-target effects. *Cancer Drug Resist.* **2023**, *6*, 257–272. [**Google Scholar**] [**CrossRef**] [**PubMed**]

12. Popat, S.; Matakidou, A.; Houlston, R.S. Thymidylate synthase expression and prognosis in colorectal cancer: A systematic review and meta-

analysis. *J. Clin. Oncol.* **2004**, *22*, 529–536. [**Google Scholar**] [**CrossRef**] [**PubMed**]

13. Watson, R.G.; Muhale, F.; Thorne, L.B.; Yu, J.; O'Neil, B.H.; Hoskins, J.M.; Meyers, M.O.; Deal, A.M.; Ibrahim, J.G.; Hudson, M.L.; et al. Amplification of thymidylate synthetase in metastatic colorectal cancer patients pretreated with 5-fluorouracil-based chemotherapy. *Eur. J. Cancer* **2010**, *46*, 3358–3364. [**Google Scholar**] [**CrossRef**] [**PubMed**]
14. Pardee, T.S.; Gomes, E.; Jennings-Gee, J.; Caudell, D.; Gmeiner, W.H. Unique dual targeting of thymidylate synthase and topoisomerase1 by FdUMP [10] results in high efficacy against AML and low toxicity. *Blood* **2012**, *119*, 3561–3570. [**Google Scholar**] [**CrossRef**] [**PubMed**]
15. Gmeiner, W.H.; Lema-Tome, C.; Gibo, D.; Jennings-Gee, J.; Milligan, C.; Debinski, W. Selective anti-tumor activity of the novel fluoropyrimidine polymer F10 towards G48a orthotopic GBM tumors. *J. Neurooncol.* **2014**, *116*, 447–454. [**Google Scholar**] [**CrossRef**] [**PubMed**]
16. Liao, Z.Y.; Sordet, O.; Zhang, H.L.; Kohlhagen, G.; Antony, S.; Gmeiner, W.H.; Pommier, Y. A novel polypyrimidine antitumor agent FdUMP [10] induces thymineless death with topoisomerase I-DNA complexes. *Cancer Res.* **2005**, *65*, 4844–4851. [**Google Scholar**] [**CrossRef**] [**PubMed**]

17. Gmeiner, W.H. Entrapment of DNA topoisomerase-DNA complexes by nucleotide/nucleoside analogs. *Cancer Drug Resist.* **2019**, *2*, 994–1001. [**Google Scholar**] [**CrossRef**] [**PubMed**]

18. Gmeiner, W.H.; Dominijanni, A.; Haber, A.O.; Ghiraldeli, L.P.; Caudell, D.L.; D'Agostino, R., Jr.; Pasche, B.C.; Smith, T.L.; Deng, Z.; Kiren, S.; et al. Improved Antitumor Activity of the Fluoropyrimidine Polymer CF10 in Preclinical Colorectal Cancer Models through Distinct Mechanistic and Pharmacologic Properties. *Mol. Cancer Ther.* **2021**, *20*, 553–563. [**Google Scholar**] [**CrossRef**] [**PubMed**]

19. Heskamp, S.; Heijmen, L.; Gerrits, D.; Molkenboer-Kuenen, J.D.M.; Ter Voert, E.G.W.; Heinzmann, K.; Honess, D.J.; Smith, D.M.; Griffiths, J.R.; Doblas, S.; et al. Response Monitoring with [(18)F]FLT PET and Diffusion-Weighted MRI After Cytotoxic 5-FU Treatment in an Experimental Rat Model for Colorectal Liver Metastases. *Mol. Imaging Biol.* **2017**, *19*, 540–549. [**Google Scholar**] [**CrossRef**]

20. van der Wilt, C.L.; Marinelli, A.; Pinedo, H.M.; Cloos, J.; Smid, K.; van de Velde, C.J.; Peters, G.J. The effect of different routes of administration of 5-fluorouracil on thymidylate synthase inhibition in the rat. *Eur. J. Cancer* **1995**, *31A*, 754–760. [**Google Scholar**] [**CrossRef**]

21. Mani, C.; Acharya, G.; Kshirsagar, S.; Vijayan, M.; Khan, H.; Reddy, P.H.; Palle, K. A Novel Role for BRIP1/FANCJ in Neuronal Cells Health and in

Resolving Oxidative Stress-Induced DNA Lesions. *J. Alzheimers Dis.* **2022**, *85*, 207–221. [**Google Scholar**] [**CrossRef**] [**PubMed**]

22. Mani, C.; Acharya, G.; Saamarthy, K.; Ochola, D.; Mereddy, S.; Pruitt, K.; Manne, U.; Palle, K. Racial differences in RAD51 expression are regulated by miRNA-214-5P and its inhibition synergizes with olaparib in triple-negative breast cancer. *Breast Cancer Res.* **2023**, *25*, 44. [**Google Scholar**] [**CrossRef**] [**PubMed**]

23. Schumacher, T.J.; Sah, N.; Palle, K.; Rumbley, J.; Mereddy, V.R. Synthesis and biological evaluation of benzofuran piperazine derivatives as potential anticancer agents. *Bioorg. Med. Chem. Lett.* **2023**, *93*, 129425. [**Google Scholar**] [**CrossRef**] [**PubMed**]

24. Gamage, R.S.; Li, D.H.; Schreiber, C.L.; Smith, B.D. Comparison of cRGDfK Peptide Probes with Appended Shielded Heptamethine Cyanine Dye (s775z) for Near Infrared Fluorescence Imaging of Cancer. *ACS Omega* **2021**, *6*, 30130–30139. [**Google Scholar**] [**CrossRef**] [**PubMed**]

25. Gmeiner, W.H.; Reinhold, W.C.; Pommier, Y. Genome-wide mRNA and microRNA profiling of the NCI 60 cell-line screen and comparison of FdUMP [10] with fluorouracil, floxuridine, and topoisomerase 1 poisons. *Mol. Cancer Ther.* **2010**, *9*, 3105–3114. [**Google Scholar**] [**CrossRef**] [**PubMed**]

26. Haber, A.O.; Jain, A.; Mani, C.; Nevler, A.; Agostini, L.C.; Golan, T.; Palle, K.; Yeo, C.J.; Gmeiner, W.H.; Brody, J.R. AraC-FdUMP [10] Is a Next-

Generation Fluoropyrimidine with Potent Antitumor Activity in PDAC and Synergy with PARG Inhibition. *Mol. Cancer Res.* **2021**, *19*, 565–572. [**Google Scholar**] [**CrossRef**] [**PubMed**]

27. Pommier, Y.; Nussenzweig, A.; Takeda, S.; Austin, C. Human topoisomerases and their roles in genome stability and organization. *Nat. Rev. Mol. Cell Biol.* **2022**, *23*, 407–427. [**Google Scholar**] [**CrossRef**] [**PubMed**]

28. Saldivar, J.C.; Cortez, D.; Cimprich, K.A. The essential kinase ATR: Ensuring faithful duplication of a challenging genome. *Nat. Rev. Mol. Cell Biol.* **2017**, *18*, 622–636. [**Google Scholar**] [**CrossRef**] [**PubMed**]

29. Qiu, S.; Jiang, G.; Cao, L.; Huang, J. Replication Fork Reversal and Protection. *Front. Cell Dev. Biol.* **2021**, *9*, 670392. [**Google Scholar**] [**CrossRef**]

30. Nakamura, K.; Kustatscher, G.; Alabert, C.; Hodl, M.; Forne, I.; Volker-Albert, M.; Satpathy, S.; Beyer, T.E.; Mailand, N.; Choudhary, C.; et al. Proteome dynamics at broken replication forks reveal a distinct ATM-directed repair response suppressing DNA double-strand break ubiquitination. *Mol. Cell* **2021**, *81*, 1084–1099.e1086. [**Google Scholar**] [**CrossRef**]

31. WH, G. Recent Advances in Therapeutic Strategies to Improve Colorectal Cancer Treatment. *Cancers* **2024**, *16*, 1029. [**Google Scholar**] [**CrossRef**] [**PubMed**]

32. Spector, T.; Harrington, J.A.; Porter, D.J. 5-Ethynyluracil (776C85): Inactivation of dihydropyrimidine dehydrogenase in vivo. *Biochem. Pharmacol.* **1993**, *46*, 2243–2248. [**Google Scholar**] [**CrossRef**] [**PubMed**]

33. Koroukian, S.M.; Booker, B.D.; Vu, L.; Schumacher, F.R.; Rose, J.; Cooper, G.S.; Selfridge, J.E.; Markt, S.C. Receipt of Targeted Therapy and Survival Outcomes in Patients with Metastatic Colorectal Cancer. *JAMA Netw. Open* **2023**, *6*, e2250030. [**Google Scholar**] [**CrossRef**] [**PubMed**]

34. Mani, C.; Jonnalagadda, S.; Lingareddy, J.; Awasthi, S.; Gmeiner, W.H.; Palle, K. Prexasertib treatment induces homologous recombination deficiency and synergizes with olaparib in triple-negative breast cancer cells. *Breast Cancer Res.* **2019**, *21*, 104. [**Google Scholar**] [**CrossRef**] [**PubMed**]

35. Di Niro, R.; Haber, A.O.; Jeong, K.J.; Park, S.Y.; Mills, G.B.; Gmeiner, W.H.; Brody, J.R. The polymeric fluoropyrimidine CF10 overcomes limitation of 5-UF in pancreatic ductaladenocarcinoma cells through increased replication stress. *Cancer Res.* **2022**, *82* (Suppl. S12), 3935. [**Google Scholar**]

36. Regairaz, M.; Zhang, Y.W.; Fu, H.; Agama, K.K.; Tata, N.; Agrawal, S.; Aladjem, M.I.; Pommier, Y. Mus81-mediated DNA cleavage resolves replication forks stalled by topoisomerase I-DNA complexes. *J. Cell Biol.* **2011**, *195*, 739–749. [**Google Scholar**] [**CrossRef**]

37. Pritchard, D.M.; Watson, A.J.; Potten, C.S.; Jackman, A.L.; Hickman, J.A. Inhibition by uridine but not thymidine of p53-dependent intestinal apoptosis initiated by 5-fluorouracil: Evidence for the involvement of RNA perturbation. *Proc. Natl. Acad. Sci. USA* **1997**, *94*, 1795–1799. [**Google Scholar**] [**CrossRef**]

P4409v2 I, **c[fK(Cy5.5)RGD]**, 1169.46, HPLC purity 99%, 4.07 mg MS ok (585.0 Da $[M+H]^{++}$)

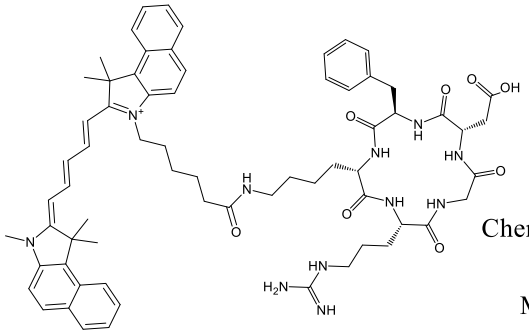

Chemical Formula: $C_{67}H_{82}N_{11}O_8^+$
Exact Mass: 1168.63
Molecular Weight: 1169.46

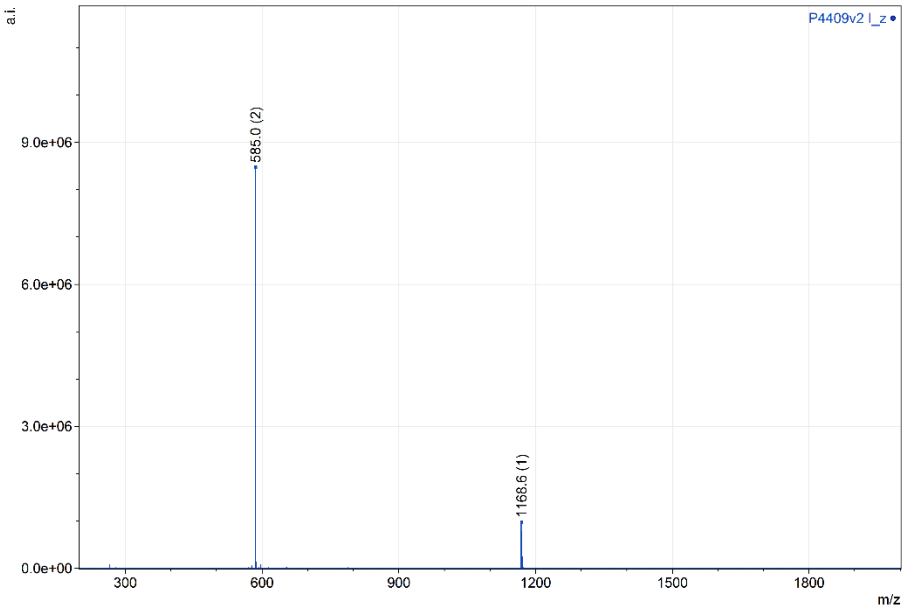

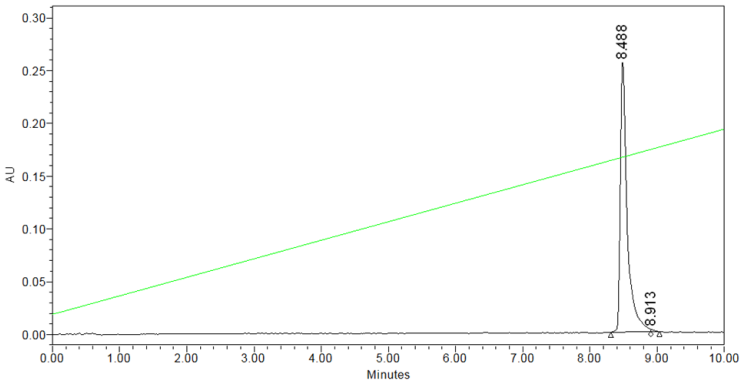

	RT	% Area	Area	Height
1	8.488	99.62	1837390	257499
2	8.913	0.38	6993	2308

Figure S1. Structure and analytical data for cyclic RGD peptide. Peptide was labeled with Cy5.5 for tumor imaging in the CC531/WAGRij rat model. Shown are mass spectrometry identification (middle) and HPLC validation of peptide purity (bottom).

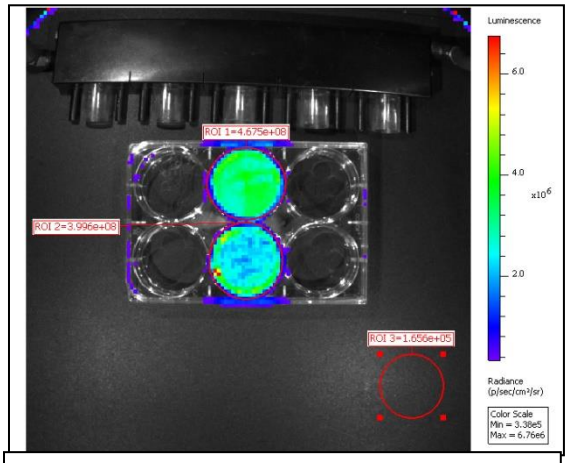

Figure S2. Validation of luciferase expression in CC531-luc cells. The cells robustly express luciferase *in vitro*.; however, expression was lost *in vivo*.

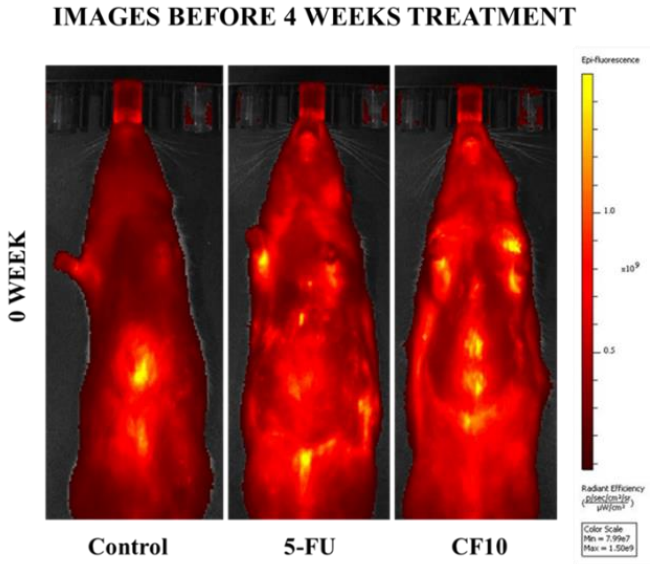

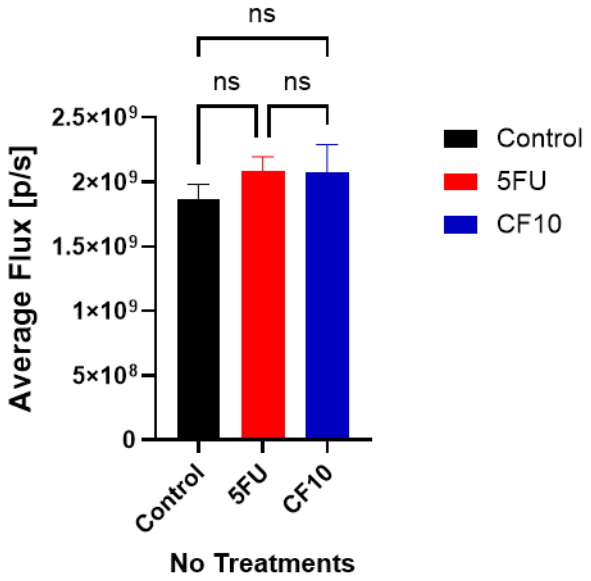

Figure S3. Fluorescent imaging of rats prior to treatment.

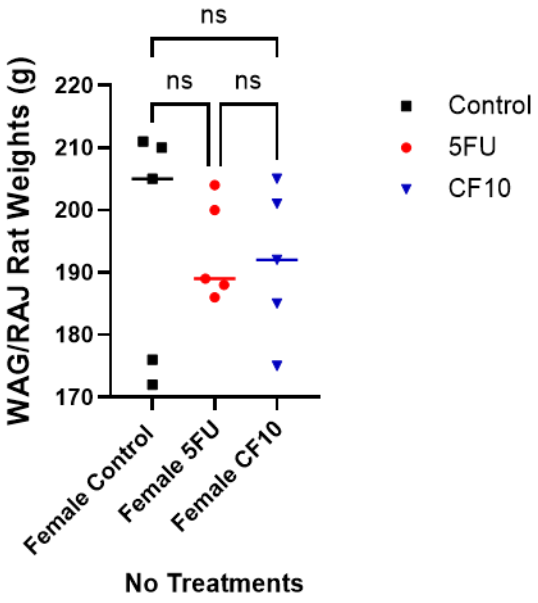

Figure S4. Initial weights for rats prior to treatment.

CHAPTER 4

CF10 Displays Improved Activity Relative to 5-FU in a Mouse CRLM Model Under Conditions of Physiological Folate

Charles Chidi Okechukwu[1,2], Xue Ma[3], Wencheng Li[4], Ralph D'Agostino[5], Jr., Matthew G. Rees[6], Melissa M. Ronan[6], Jennifer A. Roth[6], and William H. Gmeiner[2*]

[1]Integrative Physiology and Pharmacology Graduate Program. Wake Forest University School of Medicine, Winston-Salem, NC 27157 USA;

[2]Department of Cancer Biology, Wake Forest University School of Medicine, Winston-Salem, NC 27157 USA;

[3]Department of Orthopedic Surgery. Wake Forest University School of Medicine, Winston-Salem, NC 27157 USA;

[4]Department of Pathology, Wake Forest University School of Medicine, Winston-Salem, NC 27157 USA;

[5]Department of Public Health Sciences and Comprehensive Cancer Center, Wake Forest University School of Medicine, Winston-Salem, NC 27157 USA;

[6]Broad Institute of MIT and Harvard, Cambridge, MA 02142

Running Title: Improved Efficacy of CF10 in Liver-metastatic CRC

Key Words: Colorectal cancer, fluoropyrimidine, leucovorin, replication stress, thymidylate synthase, topoisomerase 1

Financial support: NIH-NCI R42 CA254834, NIH-NCI P30 CA012197, DoD PRCRP CA200460

* Corresponding Author: William H. Gmeiner, Wake Forest University School of Medicine, Medical Center Blvd, Winston-Salem, NC 27055. Phone: 336-716-6216; Fax: 336-716-0255; E-mail bgmeiner@wakehealth.edu.

Conflict of interest: W. Gmeiner is an inventor on a patent application for CF10 in colon cancer. No disclosures were reported by the other authors.

Word count: 6,274. Total number Figures and Tables: 6

Abstract

At least 25% of colorectal cancer (CRC) patients develop liver metastases (CRLM) and chemotherapeutic regimens based on the fluoropyrimidine (FP) drug 5-fluorouracil (5-FU) provide a survival advantage, but long-term survival is uncommon. The primary molecular target of FP drugs is thymidylate synthase (TS). We demonstrated that a nanoscale FP polymer, CF10, displayed greater potency than expected based on FP content in part through more direct conversion to the TS-inhibitory metabolite, FdUMP. In this study, we tested CF10 for potency advantages relative to 5-FU and trifluorothymidine (TFT, the FP component of TAS-102), and confirm a general potency advantage for CF10 in CRC cell lines in the Broad Institute PRISM screen. We demonstrate that this potency advantage is retained in CRC cells cultured with human-like folate levels and is enhanced by LV co-treatment to a similar extent as 5-FU. Our results confirm CF10 development proceeding as a CF10/LV combination. Mechanistically, CF10 cytotoxicity closely correlates with poisons of DNA topoisomerase 1 (Top1) in the PRISM screen relative to 5-FU and TFT. A TS/Top1 dual targeting cytotoxic mechanism for CF10/LV was confirmed by TS ternary complex detection by Western blot and by immunofluorescence detection of Top1cleavage complexes. CF10/LV activated the ATR/Chk1 pathway consistent with enhanced replication stress and induced apoptosis. In vivo studies showed CF10 and CF10/LV eradicated liver metastasis in a CRLM model without scarring or weight loss displaying therapeutic advantages relative to legacy FPs. Our pre-clinical data support an early-phase clinical trial for CF10 for treating liver-metastatic CRC.

Introduction

The introduction of the fluoropyrimidine (FP) drug 5-fluorouracil (5-FU) into clinical use for the treatment of colorectal cancer (CRC) >60 years ago was an inflection point, with 5-FU-based adjuvant chemotherapy improving outcomes in patients with localized disease and 5-FU-based regimens improving survival for patients with metastatic CRC (mCRC) (1). The optimization of 5-FU-based chemotherapy through improved scheduling and the development of more effective combination therapy regimens has, in recent decades, substantially further improved outcomes, with mCRC patients now surviving an average of 32 months during which many receive three or more lines of chemotherapy, each of which usually includes an FP drug (5-FU or trifluorothymidine (TFT), the FP component of TAS-102) (2). Unfortunately, long-term survival remains uncommon for mCRC patients (<14% 5-year survival), and new therapeutic options are needed.

The proven activity of 5-FU-based chemotherapy regimens in mCRC has stimulated continued exploration of the mechanism responsible for antitumor activity and the development of next-generation FPs that further extend survival (3). We previously reported that a 2nd generation FP polymer, CF10, displayed significantly greater cytotoxicity to CRC cells relative to 5-FU. Despite having only, a 10-fold greater FP content CF10 was >300-fold more potent than 5-FU, on average, based on GI_{50} values across all cell lines included in the NCI60 cell line screen (4). Consistent with its strong clinical potential, we demonstrated that CF10 displayed improved antitumor activity relative to 5-FU in a mouse orthotopic model of primary colon cancer (4) and in a rat syngeneic orthotopic model of CRC liver

metastasis (CRLM) (5). CF10 also displayed reduced toxicity relative to 5-FU in both mouse and rat models, which is consistent with reduced conversion to ribonucleotide metabolites that contribute to GI-tract and hematological toxicities (6) (7).

The advancement of CF10 into clinical development requires establishing therapeutic advantages relative to legacy FPs (5-FU, TFT) in experimental models of CRC relevant to translation. In clinical regimens for mCRC, 5-FU is co-administered with leucovorin (LV). LV is converted to N^5,N^{10}-tetrahydrofolate, a reduced folate co-factor for TS which promotes the formation of a stable ternary complex consisting of FdUMP, the reduced folate co-factor, and the enzyme that irreversibly inhibits TS (**Fig. 1**). In contrast, TFT which is used primarily in 3rd line treatment of mCRC inhibits TS without a requirement for a reduced folate co-factor (8) and TFT is used without LV in clinical regimens for mCRC. Whether CF10 development should proceed with LV co-treatment requires clarification prior to initiating clinical studies. Since CF10 inhibits TS through release of FdUMP, the same FP metabolite responsible for TS inhibition by 5-FU, CF10 would be anticipated to benefit from LV co-treatment. However, CF10 is cytotoxic at much lower concentrations than 5-FU and endogenous levels of reduced folates in cancer cells could be sufficient to promote ternary complex formation without LV co-treatment. Resolution of whether CF10 benefits from LV co-treatment is complicated by the fact that most media used to culture cancer cells contains supra-physiological folate levels (9). One approach, which is adopted in these

studies, is to perform assays in folate-controlled media to simulate human physiological levels (10).

While TS is recognized as a primary target for FPs (4) (**Fig. 1**) the potency advantage of CF10 (**Fig. 1**; Supplementary Fig. S1) relative to legacy FPs results from factors other than TS inhibition.

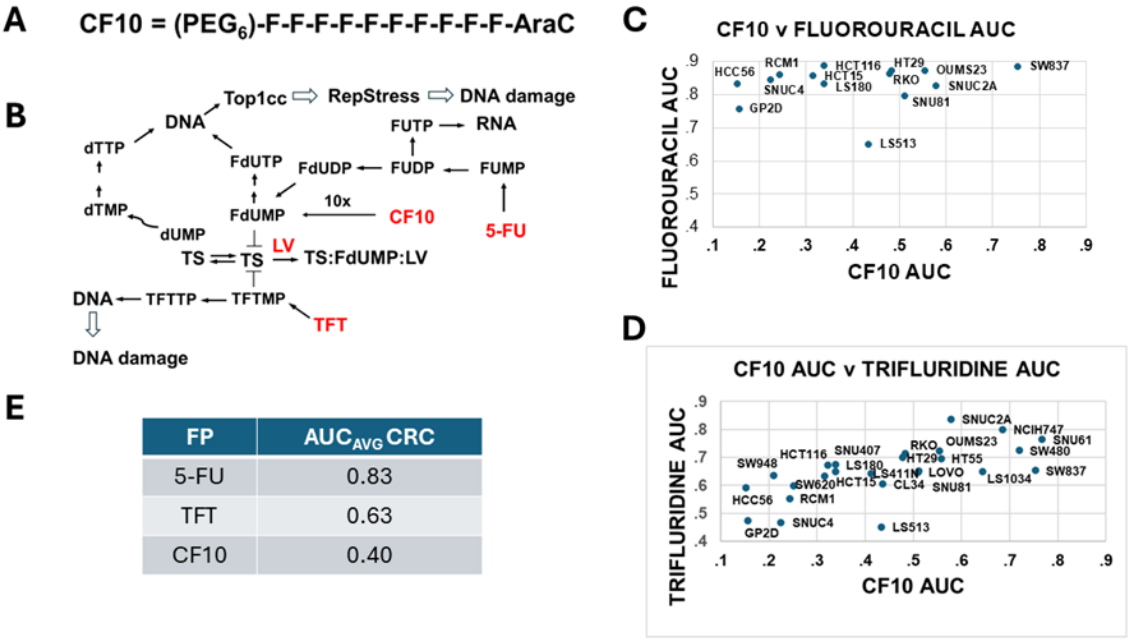

E

FP	AUC_{AVG} CRC
5-FU	0.83
TFT	0.63
CF10	0.40

Figure 1. The activity of FPs converges on TS inhibition and DNA damage. **A**, Structure of CF10 (PEG=polyethylene glycol, F = Fluorodeoxyuridine, AraC = arabinosyl cytidine). **B**, Scheme summarizing pathways for the three FPs included in the present study (CF10, 5-FU, TFT) that result in TS inhibition and cause DNA damage. **C, D**, Plots of AUC for **C**, 5-FU vs CF10 and **D**, TFT vs 5-FU. AUC values were from testing in the Broad Institute PRISM screen (data included in Supplementary Fig. S2A-C). **E**, Summary of AUC values from the Broad Institute

PRISM screen for 5-FU, CF10, and TFT in n=16 CRC cell lines in which all drugs were tested (data shown in Suppl Tables S1-S3 and Suppl Fig. 2).

Insight into the mechanistic basis for CF10's increased potency advantage relative to 5-FU came from a COMPARE analysis of data from the NCI60 cell line screen that revealed the most closely related compounds were not TS inhibitors but DNA Topoisomerase 1 (Top1) poisons (e.g. camptothecin) (11). The mechanism by which CF10 poisons Top1 is distinct from CPTs and involves the misincorporation of FdUTP into genomic DNA under conditions of Thy depletion resulting from strong TS inhibition. In collaboration with Pommier we showed that FdU inhibits the re-ligation step of Top1 catalysis leading to accumulation of trapped Top1 cleavage complexes (Top1cc) proximal to FdU-substitution in DNA. Thus, CF10 is cytotoxic to CRC cells through dual targeting of TS and Top1 (11-14) resulting in Top1-mediated DNA double-strand breaks (DSBs) and enhanced replication stress (4,15). In contrast, COMPARE analysis did not demonstrate a strong correlation of 5-FU with Top1 poisons (11) and significantly lower levels of Top1cc were detected in 5-FU-treated cancer cells and these were reversed with Urd (15) consistent with an RNA-mediated process in their formation. While TFT is known to cause DNA damage it has not been shown to cause Top1cc formation and the increased potency of CF10 relative to TFT could result from CF10 causing increased DNA damage through a Top1-mediated process that is not relevant to the cytotoxic activity of TFT or 5-FU. Thus, the TS/Top1 dual targeting mechanism of CF10 could differentiate CF10 from legacy FPs and result in more effective treatment of mCRC

and other malignancies including effective treatment of disease that has progressed with prior FP treatment.

In this study, we tested CF10 and legacy FPs in additional CRC cell lines and under folate-restricted conditions to determine if CF10 is likely to provide an improved therapeutic response in clinical studies. Results from the Broad Institute PRISM screen confirm a potency advantage for CF10 relative to 5-FU and TFT that is general across multiple CRC cell lines and consistent with broad spectrum clinical activity. We also demonstrated that CF10 is more potent than 5-FU and TFT in CRC cells cultured with human-like folate levels and established the improved potency of CF10 is enhanced with LV co-treatment to a similar extent as 5-FU, a result consistent with CF10 clinical development proceeding with LV co-treatment. Mechanistically, endpoints of TS inhibition, Top1cc formation, DNA damage, increased replication stress and induction of apoptosis are established for CF10 and CF10+LV under conditions of folate restriction providing a rationale for pharmacodynamic endpoint selection for clinical development. To test if the potency advantage for CF10 demonstrated in CRC cells results in improved antitumor activity we simulated challenges associated with clinical CRLM treatment with FPs by (i) adapting mice to an FR diet to simulate human plasma folate levels (9); (ii) testing antitumor activity in a syngeneic, orthotopic liver metastasis mouse model (5,16); (iii) evaluated three FPs (CF10, 5-FU, TFT) under conditions that delivered equivalent FP amounts on a molar basis and via the same route to assess intrinsic anti-tumor activity; and (iv) included LV co-treatment (17). We found that CF10 and CF10+LV are highly potent in eradicating liver-

metastatic CRC and that efficacy was achieved without weight-loss or other signs of toxicity under conditions where equivalent levels of 5-FU and TFT offered less therapeutic benefit. Our studies indicate that CF10 and CF10/LV show promising activity for CRLM treatment under conditions that simulate human folate physiology and support CF10 clinical development.

Materials and Methods

Cell lines, Reagents and Clonogenic assay

HCT116 (RRID:CVCL_0291), HCT15 (RRID:CVCL_0292), LS174T (RRID:CVCL_1384), and MC38 (RRID:CVCL_B288) colorectal cancer (CRC) cells were from ATCC and were cultured using recommended media or folate-restricted media (FR)(10), validated by short tandem repeat analysis, and regularly confirmed negative for Mycoplasma. CF10 was obtained from ST Pharma, validated by high-resolution mass spectrometry, and dissolved in 0.9% sterile saline. Clinical-grade 5-FU (50 mg/mL) was purchased from the Baptist Hospital clinical pharmacy, while Trifluridine (TFT) was purchased from MedChemExpress. 5-FU concentrations were calculated based on the dilution of the established stock concentration. CF10 concentrations were matched to deliver equivalent nucleoside content based on UV absorbance at 260 nm. A modified clonogenic assay assessed the potency of CF10, TFT, and 5-FU in CRC cells. CRC cells were plated in 24-well plates in both standard and folate-restricted media, and after 24 hours, they were treated with the indicated concentration of CF10, TFT, or 5-FU for 72 hours. The media were replaced after drug treatment, while the cells were allowed to grow for 168 hours. Cell proliferation was evaluated using the Aqueous

One (Promega) reagent, following the manufacturer's instructions, after the cell solution was transferred to 96-well plates. Apoptosis was evaluated using Caspase 3/7-Glo reagent (Promega) following the manufacturer's instructions.

Western Blotting

Proteins were isolated, and their differential expressions were analyzed by Western blot, as described previously(5). Briefly, the cells were lysed using RIPA buffer (50 mM Tris HCl at pH 7.4, 150 mM NaCl, 1% Triton X-100 or NP-40, 0.5% sodium deoxycholate, 0.1% SDS, 1 mM EDTA, and 10 mM NaF freshly supplemented with protease and phosphatase inhibitors). The protein concentrations were quantified using a Bradford assay (Bio-Rad), and the samples were normalized for equal loading. All samples were then heated to 100°C for 10 minutes in the presence of 6x Laemmli buffer (Boston Bio-Products; Milford, MA, USA). SDS-PAGE resolved the proteins, and their expression was analyzed following immunoblotting using specific antibodies. The following antibodies were used in this study: Rad51 (Cell Signaling Technology Cat# 8875, RRID:AB_2721109), Chk2 (Thermo Fisher Scientific Cat# MA5-35294, RRID:AB_2849196), pCHK2-T68 (Thermo Fisher Scientific Cat# PA5-104715, RRID:AB_2816188), RPA32/RPA2 (Cell Signaling Technology Cat# 52448, RRID:AB_2750889), pRPA32-S33 (Cell Signaling Technology Cat# 10148, RRID:AB_3099645), Chk1 (Thermo Fisher Scientific Cat# MA1-23336, RRID:AB_558392), pCHK1-S317 (Cell Signaling Technology Cat# 2344, RRID:AB_331488), cleaved caspase 3-D175 (Cell Signaling Technology Cat# 9664, RRID:AB_2070042), Thymidylate synthase (Cell Signaling Technology Cat#

9045, RRID:AB_2797693), and β-actin (Santa Cruz Biotechnology Cat# sc-47778 HRP, RRID:AB_2714189).

Cell Viability and Rescue Assay

HCT116 (RRID:CVCL_0291), HCT15 (RRID:CVCL_0292), LS174T (RRID:CVCL_1384), and MC38 (RRID:CVCL_B288) cells were plated on 96-well, white flat bottom plates, allowing 48 h for the cells to adhere to the plate and begin to grow exponentially until they reached about 25% confluency. Exogenous uridine (Sigma) and thymidine (Sigma) were added to their designated wells. The plates were then shaken for 2 minutes by hand to mix appropriately without disrupting cell growth before being placed back in the incubator at 37°C and with 5% CO_2. After 48 hours in the incubator, the media was evacuated, and cell viability was determined using Promega kits as described(4,18). The rescue experiments were done in triplicate with four data points in each experiment per tested condition.

TS Activity Assay

A TS *in situ* activity assay was performed as previously described (19) to provide a quantitative indication of intracellular inhibition of TS activity following drug treatment. ~$0.5x10^6$ HCT-116 (RRID:CVCL_0291) cells were plated in each well of a 6-well plates and cells were allowed to attach for 24h then treated with either 5-FU, 5-FU/LV, CF10, CF10/LV, TFT, or TFT/LV for 48h. For the last 2h [5-^{3}H]-2'-deoxyuridine (Moravek) 0.16 Ci/mmol; final concentration 2.5 uM was present. 150 µL of media from each well was added to an ice-cold suspension containing 750 µL of charcoal with 0.5% T-70 dextran and 2.5% BSA) and 150 µL of 35%

trichloroacetic acid. After centrifugation a portion of the supernatant was counted by liquid scintillation counting and enzyme activities were expressed as a percent relative to drug-free control.

Liver Tumor Cell Inoculation to Simulate CRLM Formation

All animal studies were undertaken in accordance with the protocols approved by the Institutional Animal Care and Use Committee at Wake Forest University School of Medicine (Winston-Salem, NC, USA). Immunocompetent C57BL6 (RRID:IMSR_JAX:000664) mice weighing 21–24g were used because this strain is syngeneic with the MC38 colon carcinoma cell line. C57BL6 mice were commercially available in the U.S. and were obtained from Charles River Laboratories for these studies. The mice had a controlled climate and light cycles, and all had free access to a standard laboratory diet and water. For the inoculation procedure, anesthesia was obtained using 2–3% isoflurane and then maintained at 1.5% for surgery. A 2 cm midline incision was made, and both the left and right hepatic lobes were mobilized. The MC38 (RRID:CVCL_B288) cells were suspended at a density of 2×10^6 cells in 200 µL and 25 µL of cell suspension, mixed 1:1 with Matrigel, and injected via a 29-gauge needle into the subcapsular portion of one of the previously specified hepatic lobes. When the needle was withdrawn, a cotton swab was used to press on the puncture site to achieve hemostasis. Once hemostasis was achieved, the wound was washed with saline, the muscle layer was closed using a 6-0 Vicryl suture, and the skin was closed using staples. An abdominal bandage was applied, and the mice were allowed to recover from anesthesia before returning to the animal facility. The tumors were

allowed to grow for a week and fluorescence imaging was performed using an RGD peptide Cy5.5 conjugate to establish tumor formation prior to initiating treatments(5).

Treatment and Fluorescence Imaging of Tumor Progression

The C57BL6/MC38 syngeneic orthotopic mouse model fluorescence tumor images were undertaken using an IVIS Lumina LT Series III system (RRID:SCR_014247) under isoflurane anesthesia. All images were analyzed using Living Image software (v4.7.4.) with an identical size region of interest for each mouse. To assess therapeutic efficacy, groups of $n = 4$ mice with similar initial tumor levels based on fluorescence imaging were treated with (1) no treatment, (2) 5-FU, (3) CF10, (4) TFT, (5) LV, (6) 5-FU+LV, (7) CF10+LV, (8) TFT+LV. 5-FU was administered at 100 mg/kg (20) and TFT and CF10 were dosed to deliver equivalent nucleoside content based on UV absorbance at 260 nm. Leucovorin was infused together with the FP (21). Mice in each group were treated on a 7-day mini-osmotic pump. All mice underwent a final imaging procedure at the end of the seventh day and were then euthanized, and their vital organs (livers, etc.) were extracted and prepped for other procedures. For each of the eight treatments, the difference in flux or weight values were calculated (Day 7 minus Day 0). Next, a general linear model was fit to compare the 8 groups (Control, 5FU, LV, CF10, TFT, 5FU+LV, CF10+LV, TFT+LV). We first examined the overall test for the model and if that was significant, pairwise comparison between groups were made. Given the large number of potential pairwise comparisons that could be made, we conservatively used a Bonferonni Correction when comparing groups. The

adjusted p-value for significance using a Bonferonni correction was 0.017 (0.05/3). For maintaining mice on a folate-restricted (FR) diet the FR diet purchased from Envigo Teklad Diets (Madison, WI) composed of 35.0g/Kg AIN-93G-MX (94046), 10.0g/Kg Succinyl sulfathiazole, 195.0g/Kg Casein, 3.0g/Kg L-Cystine, 304.488g/Kg Corn Starch, 0.016g/Kg Calcium Pantothenate, 0.006g/Kg Thiamin (81%), 209.749g/Kg Sucrose, 130.0g/Kg Maltodextrin, 60.0g/Kg Soybean Oil, 50.0g/Kg Cellulose, 0.007g/Kg Pyridoxine HCl, 0.012g/Kg TBHQ (antioxidant), 2.5g/Kg Choline Bitartrate, 0.03g/Kg Niacin, 0.006g/Kg Riboflavin, 0.0002g/Kg Biotin, 0.025g/Kg Vitamin B12 (0.1% in mannitol), 0.0008g/Kg Vitamin K1 phylloquinone, 0.15g/Kg Vitamin E, DL-alpha tocopheryl acetate (500 IU/g), 0.008g/Kg Vitamin A Palmitate (500,000 IU/g), and 0.002g/Kg Vitamin D3 cholecalciferol (500,000 IU/g).

PRISM Assay

PRISM, known as the Profiling Relative Inhibition Simultaneously in Mixtures assay, is a high-throughput, multiplexed screening method created for drug development and discovery, especially in cancer research. It can be used to investigate fluoropyrimidines' effects and identify their predictive biomarkers. CF10 was screened in 873 PRISM DNA-barcoded cell lines established by the Broad Institute. In brief, 20–25 cell lines per pool were plated in 384 well plates and treated with CF-10 at 8 doses in three-fold dilutions starting at 9.6 μM for 5 days. Two PRISM cell line collections were used in the assay: PR500 (including only adherent cell lines), and PR300+ (including adherent and suspension cell lines). Cells were then lysed in TCL mRNA lysis buffer, and then PCR with reverse

transcription was performed. Detection of the barcodes and univariate and multivariate analysis was then performed as previously described (22). Benchmark test agents were also tested at dose to ensure high data quality. All test agents were run in triplicate, and each plate contained positive (Bortezomib at 20μM) and negative (DMSO) controls. Comparisons of drug potency between CF10 and other drugs tested in the PRISM screen were made based on area-under-the-curve (AUC), a metric in which more potent drugs display lower values reflecting decreased cell viability across the range of drug concentrations tested (23).

Statistical Analysis

GraphPad Prism 10.2.0 (RRID:SCR_002798) was used for statistical analyses of cell-based assays. Experiments were conducted in triplicate ± SEM. For all in vitro experiments, four biological replicates were used for analysis, and appropriate one-way ANOVA tests with recommended Tukey corrections were conducted, with $p < 0.05$ indicating significance. For in vivo studies two one-way analysis of variance (ANOVA) models were fit to compare the 8 groups on the outcomes of change in treatment response based on IVIS imaging (TRT) and weight (delta TRT and delta Weight were the outcomes). In these models, pair-wise comparisons were then made between groups accounting for multiple comparisons by using a Bonferroni adjusted for the p-value to determine significance. (0.05/28 = 0.00178 (total number of possible pair-wise comparisons)). Thus, all pair-wise comparisons that had p-values less than 0.0017 were considered statistically significant. The post-hoc comparisons between groups were performed using the ANOVA models

so that the variance for the testing was based on all data provided from all eight groups of interest.

Data Availability

Data are available on request from the corresponding author.

Results

CF10 displays enhanced potency to CRC cells relative to 5-FU and TFT.

Previous studies including analysis in the NCI60 cell line screen (11,12) demonstrated that CF10 (**Fig. 1;** Supplementary Fig. S1) displayed greatly enhanced potency to CRC cell lines relative to 5-FU, Floxuridine, and TFT that significantly exceeded that anticipated based upon a 10-fold greater FP content and exceeded 100-fold relative to TFT and 5-FU (11,12). Further, CF10 was highly potent regardless of MSI/MSS status or *KRAS* mutation status, consistent with its broad use for CRC treatment regardless of factors used to stratify CRC patients for 5-FU-based chemotherapy (4). To gain further insights into the activity of CF10 in cancer cells, we provided a sample to the Broad Institute PRISM screen for testing. Analysis of AUC values for CF10 revealed that relative to other FPs for which PRISM screen data were available, CF10 was highly potent with AUC values for many CRC cell lines <0.4 consistent with strong activity (**Fig. 1C** and **D**). The average AUC value for CF10 in the 14 CRC cell lines tested in the PRISM screen was 0.40 while for 5-FU the average AUC value was 0.83 (Supplementary Table S1) and for trifluridine the average AUC value was 0.63 (Supplementary Fig. S2,

Supplementary Table S2, S3). Since previous studies including analysis of NCI60 cell line screen data revealed surprisingly strong mechanistic correlations between F10 and CF10 with DNA topoisomerase 1 poisons, we performed regression analysis of the AUC correlation data from the PRISM screen between FPs and Top1 poisons (Supplementary Fig. S3). Strong correlation between camptothecin (CPT) and SN-38 (the active metabolite of irinotecan) was observed (5e-37), as expected (Supplementary Table S4). Consistent with previous studies the correlation between CF10 and Top1 poisons was very strong (11,12) the AUC correlation for CF10 and SN-38 was very strong (5e-24) which was much stronger than for either TFT or 5-FU with SN-38 (1.1e-16 and 1.1e-4; (Supplementary Table S4). These results are consistent with the increased potency for CF10 resulting from a TS/Top1 dual targeting mechanism that is more pronounced for CF10 than for other FPs.

FP potency is enhanced by folate restriction and LV co-treatment.

While screens involving large numbers of cell lines are highly valuable in assessing compound potency and identifying genomic determinants of drug response, a limitation of screens such as the NCI60 (24) and the Broad Institute Prism screen (25) is that drug response is evaluated using media that may not reflect human physiology. This is a concern for FP drugs that are highly dependent on folate levels since ATCC-recommended media includes much higher folate concentrations than human plasma. To investigate if the potency advantage for CF10 relative to alternative FPs was realized in cells cultured using media with human-like folate levels, we adapted three human CRC cell lines (HCT116,

LS174T, HCT15) and MC38 mouse CRC cells to culture media developed for testing drug activities under conditions of physiological folate (10). Cells adapted to folate-restricted media appeared healthy (Supplementary Fig S4A) and had growth characteristics similar to those of the same cell line cultured in ATCC-recommended media (Supplementary Fig S4B). However, culture using FR media caused all three CRC cell lines to display increased sensitivity to the three FPs tested (CF10, 5-FU, TFT) (Supplementary Fig. S4C).

We then performed dose-response studies evaluating the response of these three CRC cell lines to CF10, 5-FU, and TFT with studies conducted using both complete (DMEM+10% FBS) and FR media. Results for HCT116 are summarized in **Fig. 2A-F** and results for LS174T, HCT15, and MC38 are displayed in Supplementary Figs S5-S7A-F, Supplementary Tables S5-S7.

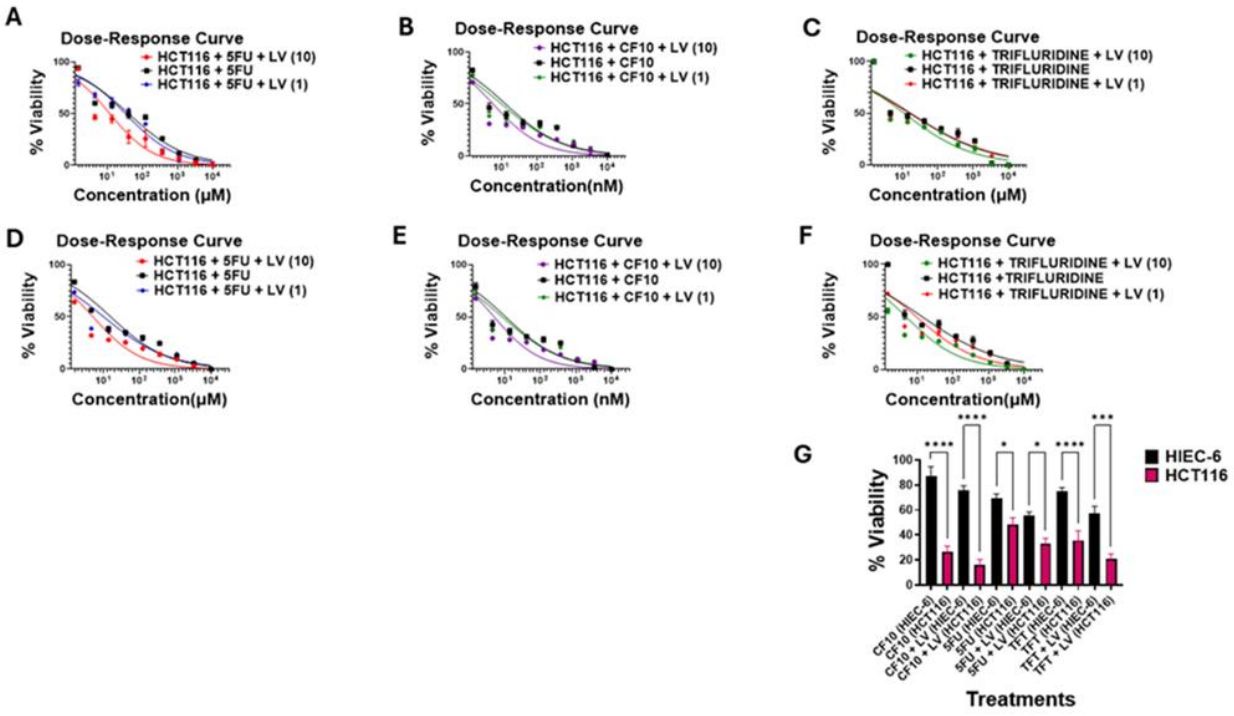

Figure 2. CF10 displays greatly increased potency to HCT116 cells relative to 5-FU and TFT under standard and folate-restricted cell culture conditions. **A-G**, Dose-response curves for **A and D**, 5-FU (black) + LV (1 uM (blue) or 10 uM (red); **B and E**, CF10 (black) + LV (1 μM (green) or 10 uM (purple); **C and F**, TFT (black) + LV (1 μM (red) or 10 μM (green). **A, B,** and **C** HCT116 cells were cultured in complete media; **D, E**, and **F** HCT116 cells were cultured in folate-restricted media. **G**,. Graphs of % viability in HCT-116 (red) and HIEC-6, a normal intestinal cell line following 48h treatment with CF10 (1 μM), 5-FU (10 μM), TFT (10 μM), LV (1 μM).

Results for HCT-116 relative to the normal intestinal cell line HIEC-6 are shown in **Fig. 2G**. Results for HCT116 cultured in complete media were similar to those reported in previous studies and from the NCI60 cell line screen and were consistent with PRISM screen data (**Fig. 1 B** and **C**). CF10 is by far the most potent of the three FPs tested (IC50=13.1nM in HCT-116). TFT is approximately 127-fold

less potent than CF10 (IC50=1.66uM), and TFT is only slightly more potent (2.46-fold) than 5-FU (IC50=4.08 uM) under these culture conditions. CF10 was slightly more potent to HCT116 cells cultured in FR-media (IC50=10.5 nM) than in complete media, with similar trends and similar relative potencies in FR-media for TFT and 5-FU. All three FPs displayed increased cytotoxicity to HCT-116 relative to the normal intestinal cell line HIEC-6, however the relative differential was greatest for CF10 (**Fig. 2G**).

In clinical regimens for CRC, 5-FU is almost always co-administered with leucovorin (LV). LV potentiates 5-FU cytotoxicity to CRC cells by promoting ternary complex formation involving (i) the active FP metabolite Fluorodeoxyuridylate, (ii) the target enzyme, thymidylate synthase (TS), and (iii) the reduced folate co-factor N^5,N^{10}-tetrahydrofolate, to irreversibly inhibit TS activity and *de novo* thymidylate biosynthesis (**Fig. 1B**) (26). We evaluated the effects of LV co-treatment on the cytotoxicity of all three FPs in HCT116 (**Fig. 2A-F, Table 1**), normal intestinal cell line, HIEC-6 (**Fig 2G**), LS174T (Supplementary Fig S5 and Supplementary Table S5), HCT15 cells (Supplementary Fig S6 and Supplementary Table S6), and MC38 (Supplementary Fig S7 and Supplementary Table S7).

FR Drug	Media	IC_{50} (μM) ± SEM	IC_{50} (μM) + LV (1μM) ± SEM	IC_{50} (μM) + LV (10μM) ± SEM	LV Effect (1μM)	LV Effect (10μM)
5FU	DMEM	4.08 ± 0.0133	3.30 ± 0.0151	1.20 ± 0.0122	1.24	3.40
5FU	FR	1.58 ± 0.0177	1.01 ± 0.0136	0.506 ± 0.0157	1.56	3.12
CF10	DMEM	0.0131 ± 0.000125	0.0101 ± 0.000132	0.00583 ± 0.000138	1.30	2.25
CF10	FR	0.0105 ± 0.000132	0.00842 ± 0.000145	0.00501 ± 0.000144	1.25	2.10
TFT	DMEM	1.66 ± 0.0105	1.54 ± 0.0105	1.09 ± 0.0112	1.08	1.52
TFT	FR	1.41 ± 0.0114	0.967 ± 0.0146	0.495 ± 0.0150	1.46	2.85

Table 1. Summary of IC50 values and LV potentiation effects for HCT116 cells.

Co-treatment of any of the three FPs with 1 μM LV resulted in slightly increased potency. For 5-FU towards HCT116 cells cultured in DMEM 5-FU/LV was approximately 1.24-fold more potent than 5-FU (IC50 = 3.30μM vs 4.08 μM,) and for HCT116 cells cultured in FR media the LV effect was slight greater (approximately 1.56-fold, IC50 = 1.01μM vs 1.58 μM). Similar trends were found for CF10 and TFT. For HCT116 cells co-treated with 10 μM LV the effects were larger with a 3.40-fold potentiation for 5-FU in DMEM and a 3.12-fold potentiation for 5-FU in FR media. The LV potentiation effects were slightly reduced but still significant for CF10 (2.25, 2.10-fold) and TFT (1.52, 2.85-fold) in DMEM and FR media, respectively. These results are consistent with LV potentiating CF10 as is established for 5-FU, but with slightly attenuated effects. Although LV is not presently used in clinical regimens in which TFT is the FP (e.g. TAS-102), LV also potentiates TFT, potentially by affecting nucleotide biosynthesis.

LV Stimulates TS ternary complex formation for CF10, 5-FU but not TFT.

To determine if LV co-treatment with 5-FU, CF10 and TFT stimulated TS ternary complex formation (FdUMP/TS/5,10-methylene THF), we performed Western blots using an anti-TS antibody under conditions that resolved the ternary complex (aka TS classic complex (TS CC) (27)) and the unbound enzyme. Results in HCT116 cells are displayed in **Fig 3A**, and quantification of TS CC and total TS is displayed in **Fig 3B,C**.

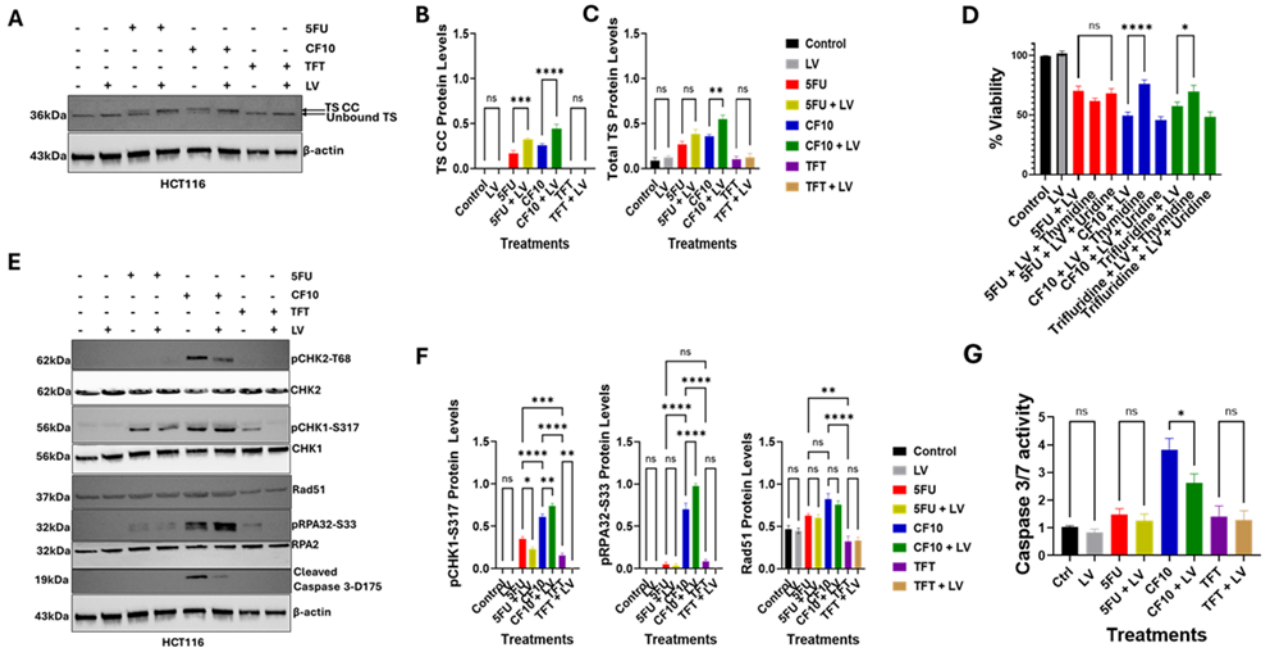

Figure 3. CF10 promotes TS classic complex (TS CC) formation and activates the ATR/Chk1 and ATM/Chk2 DNA damage response pathways in HCT-116 cells under folate-restricted culture conditions. **A**, Western blot for 5-FU ± LV, CF10 ± LV, and TFT ± LV detecting the TS CC and unbound TS; **B,C** Quantification of TS CC and total TS levels; **D**, effect of thymidine (80 μMol) and uridine (1 mMol) co-treatment on HCT-116 cell viability in FR media for 5-FU+LV (red), CF10+LV (blue), and TFT+LV (green). FP+LV was dosed at IC50 for 48h shown in Figure 2. Experiments done in triplicate ± SEM (***p ≤ 0.0002, **p ≤0.002, *p ≤ 0.03).

The results in LS174T, HCT15, and MC38 cells are shown in Supplementary Fig. S8, S9, and S10. In the absence of any FP treatment, TS CC was not detected. However, TS CC was detected as a minor component with 5-FU treatment, and with CF10 TS CC was the predominant form present. Interestingly, total TS levels were reduced with CF10 treatment relative to no treatment (**Fig 3B,C**), which is

consistent with CF10 stimulating increased TS degradation (28). While TFT is a substrate for thymidine kinase and known to inhibit TS, TFT treatment did not result in detectable TS CC either as a single drug or with TFT+LV co-treatment (**Fig 3A**). Consistent with clinical objectives LV co-treatment with 5-FU did increase TS CC levels and, in contrast to observed effects of CF10 in decreasing TS intensity with LV co-treatment, 5-FU intensified the TS CC band, which was the predominant form (**Fig 3B,C**), a result consistent with 5-FU potentially stabilizing TS from proteasomal degradation (28). Consistent with results showing CF10 and CF10/LV were effective at increasing TS CC formation and reducing TS levels TS enzymatic activity was strongly reduced with these treatments (Supplementary Fig. 11).

To determine if LV co-treatment altered the effects of a thymineless state in promoting FP cytotoxicity we performed reversal studies in which added thymidine or uridine were included in the culture medium during treatment. Results for HCT116 cells are displayed in **Fig 3D** and results for LS174T, HCT15, and MC38 cells are displayed in Supplementary Fig. S8, S9, and S10. 5-FU cytotoxicity can occur through either an RNA- or DNA-directed mechanism, depending on the cell type. While TS CC is evident as the predominant TS form in HCT116 cells with 5-FU/LV co-treatment cytotoxicity was not reversed with either Thy or Urd. Consistent with CF10 cytotoxicity resulting from TS inhibition co-treatment with Thy reduced CF10 cytotoxicity while Urd co-treatment had no effect. Thy co-treatment also reversed TFT cytotoxicity despite the absence of detectable TS CC, but effects were attenuated relative to CF10. Similar effects were detected in HCT15, LS174T, and MC38 cells (Supplementary Fig S8, S9, and S10).

CF10 is a potent inducer of replication stress and apoptosis.

In previous studies, we established that CF10 enhanced replication stress in CRC cells as shown by increased stalling and collapse of replication forks (4). CF10 induces replication stress through the dual targeting of TS and Top1 (11,29), which results in trapped Top1 cleavage complexes (Top1cc) (14,30-32) that impede replication fork progression while reduced thymidine levels due to TS inhibition hinder DNA repair. Top1cc are converted to DNA double-strand breaks (DSBs) upon collision with advancing replication forks or during transcription (33), and this contributes to genomic instability and can activate programmed cell death. In these studies, we showed that CF10 is much more potent than 5-FU or TFT to CRC cells (**Fig. 2A-F, Table 1**), including culture under conditions of folate restriction (**Table 1**). To determine if CF10 enhanced markers of replication stress in CRC cells cultured in folate-restricted media and if LV co-treatment affected DNA damage checkpoint activation, we performed Western blots for markers of DNA damage response (DDR) checkpoint activation with results shown for HCT116 cells in (**Fig. 3E**) and results for LS174T, HCT15, and MC38 cells are in Supplementary Fig. S8, S9, and S10. Replication fork stalling activates the ATR/Chk1 pathway and enables the intra-S-phase DDR checkpoint which inhibits the initiation of new replication forks and provides time to re-start stalled replication forks and repair DNA DSBs. CF10 treatment significantly increased pChk1 Serine-317 (pS317) levels and pRPA32 Serine-33 (pS33) consistent with ATR/Chk1 pathway activation. Treatment with 5-FU also activated the ATR/Chk1 pathway, however quantification of Western blot intensity by densitometry showed

significantly reduced intensity for pChk1(S317) and pRPA32(S33) for 5-FU relative to CF10. For TFT, the intensities for these bands were reduced further (**Fig. 3F**). Since Top1cc formation can cause replication fork stalling and activation of the ATR/Chk1 pathway we evaluated Top1cc and showed increased levels in HCT116 cells with CF10 and CF10/LV relative to other treatments (Supplementary Fig. S12).

The ATM/Chk2 pathway was also selectively activated with CF10 treatment in HCT116 cells cultured in FR media relative to 5-FU and TFT as shown by Western blot for pChk2-threonine68 (T68) (**Fig. 3E**). Immunofluorescence for gH2AX was also greatest for CF10 relative to other FPs (Supplementary Fig. S12B). Consistent with generation of DNA DSBs with CF10 treatment, Rad51 levels were increased but were not increased in CRC cells treated with either 5-FU or TFT. To determine if LV co-treatment affected activation of the ATR/Chk1 or ATM/Chk2 pathways we also analyzed lysates from CRC cells with FP+LV co-treatment for all three FPs tested (CF10, 5-FU, TFT). LV co-treatment enhanced pRPA32-S33 and pChk1-S317 levels in CF10-treated cells consistent with increased ATR/Chk1 pathway activation. However, levels of pChk2-T68 and Rad51 were decreased with CF10+LV treatment relative to CF10-only, which is consistent with reduced DNA DSBs.

The extent of apoptosis in FP-treated CRC cells was assessed by Western blot for cleaved caspase 3 (**Fig. 3E**) and caspase 3/7-Glo assay (**Fig. 3G**). Cleaved caspase 3 was not detected with either 5-FU or TFT treatment in HCT-116 cells with or without LV co-treatment (**Fig. 3E**) or LS174T, HCT15, and MC38 cells are

in Supplementary Fig. S8, S9, and S10. Cleaved caspase 3 was detected with CF10 treatment and CF10 also induced apoptosis relative to other treatments based on Caspase 3/7-Glo. Surprisingly although LV co-treatment with CF10 decreased cell viability relative to single agent CF10 the extent of apoptosis induced by CF10+LV relative to CF10 was less (**Fig 3E, G**). Our results are consistent with the increased potency of CF10 relative to 5-FU and TFT in human and mouse CRC cells resulting from increased replication stress with ATR/Chk1 and ATM/Chk2 DNA damage response pathways activated to counter the deleterious consequences of CF10-induced Top1cc and replication fork collapse resulting in apoptosis although non-apoptotic cell death processes may be stimulated by CF10/LV since increased potency correlates with reduced apoptosis.

CF10 is highly effective at eradicating liver-metastatic tumor burden.

In previous studies, we established that CF10 displayed more potent antitumor activity than 5-FU in a mouse orthotopic model of primary colon cancer (HCT-116/Balbc nu/nu) (4) and in a rat CRLM model (CC531/WAGRij) (5). In the latter study, rats were injected 1x/wk with 5-FU or CF10. To better emulate clinical dosing with 5-FU, which is usually done with infusion or bolus + infusion as in FOLFOX6 (34), we evaluated the antitumor activity of 5-FU or CF10 infused over 7-days using an osmotic pump. Further, mice were adapted to a folate-restricted diet to study tumor progression and treatment response under more human-like folate levels. We compared the antitumor activity of 5-FU and CF10 with and without LV since 5-FU is generally used with LV for CRC and our studies demonstrate that LV co-treatment potentiates CF10 (**Table 1**). TFT, which is used to treat 3rd line mCRC at

part of TAS-102, was also tested in these studies. TFT was administered as a single agent (TAS-102 includes the Thymidine Phosphorylase inhibitor Tiperacil) and was infused over 7-days, identical to the schedule used for 5-FU and CF10 in these studies. All treatment groups received equivalent amounts of FP based on UV activity to account for the 10-fold higher FP content of CF10 on a molar basis. The results following 7-day infusion for 5-FU±LV and CF10±LV are shown in **Fig. 4** and for TFT±LV are shown in Supplementary Fig. S13.

Liver-metastatic tumor burden was initiated by injecting MC38 cells into one lobe in the liver of C57Bl/6 mice (5,16). Seven days prior to tumor cell injection mice were adapted to a folate-restricted diet to develop human-like folate physiology which is important for evaluating the activity of FP drugs in rodents (35). Seven days post-injection tumor formation was validated in mice by fluorescence imaging using IVIS following injection of a fluorescent RGD peptide. Initial tumor levels were similar in all mice and tumor was localized to the liver (**Fig. 4A**).

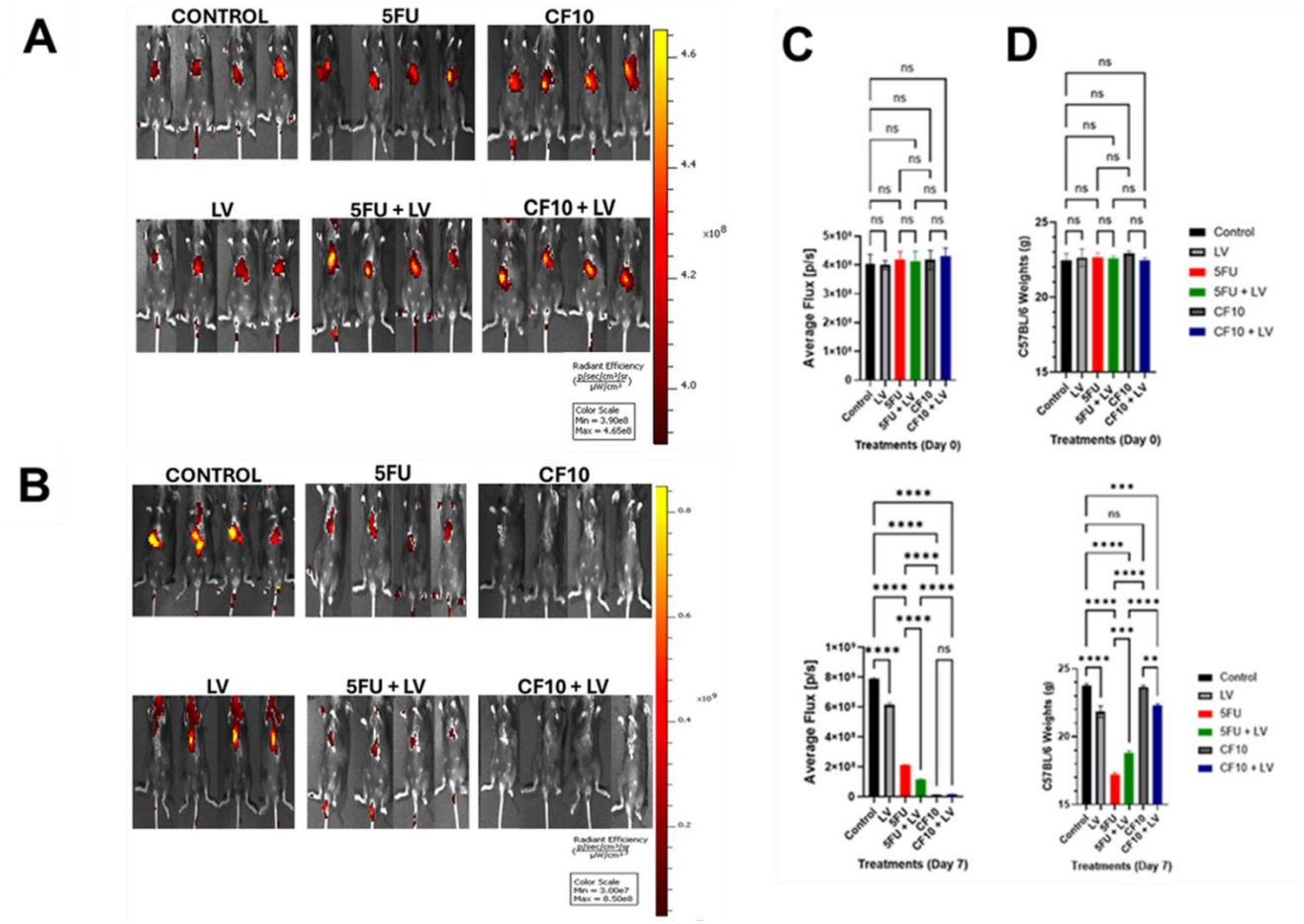

Figure 4. CF10/LV is more effective than 5-FU/LV in a liver-metastatic CRC model under conditions of human-like folate levels. **A,B** IVIS images of tumor burden for indicated treatments at day 0 (**A**) and day 7 (**B**) post-treatment. (**C**) Tumor flux pre-treatment (top) and post-treatment (bottom). (**D**) Mice weights pre-treatment (top) and post-treatment (bottom).

Mice were treated with a 7-day infusion of one of the FPs (5-FU, CF10, TFT) via an Alzet mini-pump fitted with a jugular vein catheter. 5-FU was administered at 100 mg/kg and doses of CF10 and TFT were matched to the 5-FU dose based on equal A260 absorbance. Groups of n=4 mice received (i) no treatment, (ii) single-agent 5-FU, (iii) single-agent CF10, (iv) single-agent TFT, (v) single-agent LV, (vi)

5-FU+LV, (vii) CF10+LV, or (viii) TFT+LV. The effects of treatment on tumor progression were evaluated by IVIS imaging following completion of the 7-day infusion (**Fig. 4B**). All treatment groups, including single-agent LV, displayed reduced flux values consistent with tumor reduction (**Fig. 4C**). Among the three FP treatment groups, the flux decrease was least for single-agent 5-FU and while this decreased with LV co-treatment flux reduction with 5-FU+LV treatment was still not as large as for CF10 or TFT, either as single agents or in combination with LV. Substantial flux reduction was observed with CF10 and TFT treatment as single agents and in combination with LV (**Fig 4C**) (Supplementary Table S8).

Mice in all groups tolerated treatment; however, weight loss was observed for all treatment groups except for single-agent CF10, for which mice gained weight during treatment. Weight loss was significant for 5-FU, 5-FU+LV, TFT, and TFT+LV (Supplementary Table S9). The largest weight loss occurred with 5-FU, and despite mice treated with single-agent LV losing weight, mice treated with 5-FU+LV lost less weight than for single-agent 5-FU. Weight loss for mice treated with CF10+LV was slightly less than for single-agent LV. Mice treated with single-agent TFT underwent significant weight loss but not as great as with 5-FU treatment and combining TFT+LV did not increase weight loss (Supplementary Table S9).

To gain further insight into the effects of treatment on tumor progression, mice were euthanized 7-day post-treatment following IVIS imaging and livers were excised. H&E-stained sections from livers of all treatment groups were blindly analyzed by a pathologist to evaluate tumor progression (**Fig. 5A**).

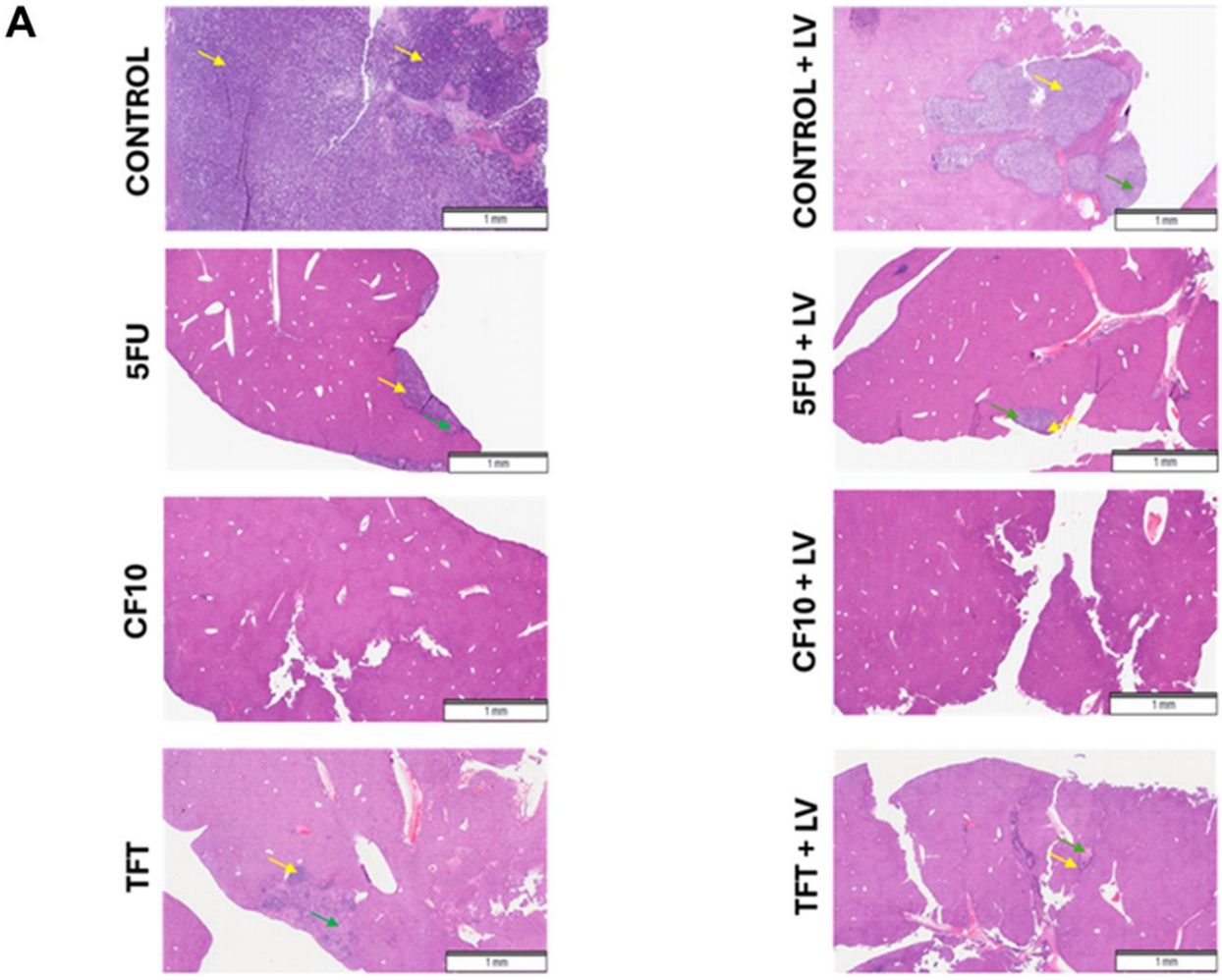
A
CONTROL
5FU
CF10
TFT
CONTROL + LV
5FU + LV
CF10 + LV
TFT + LV

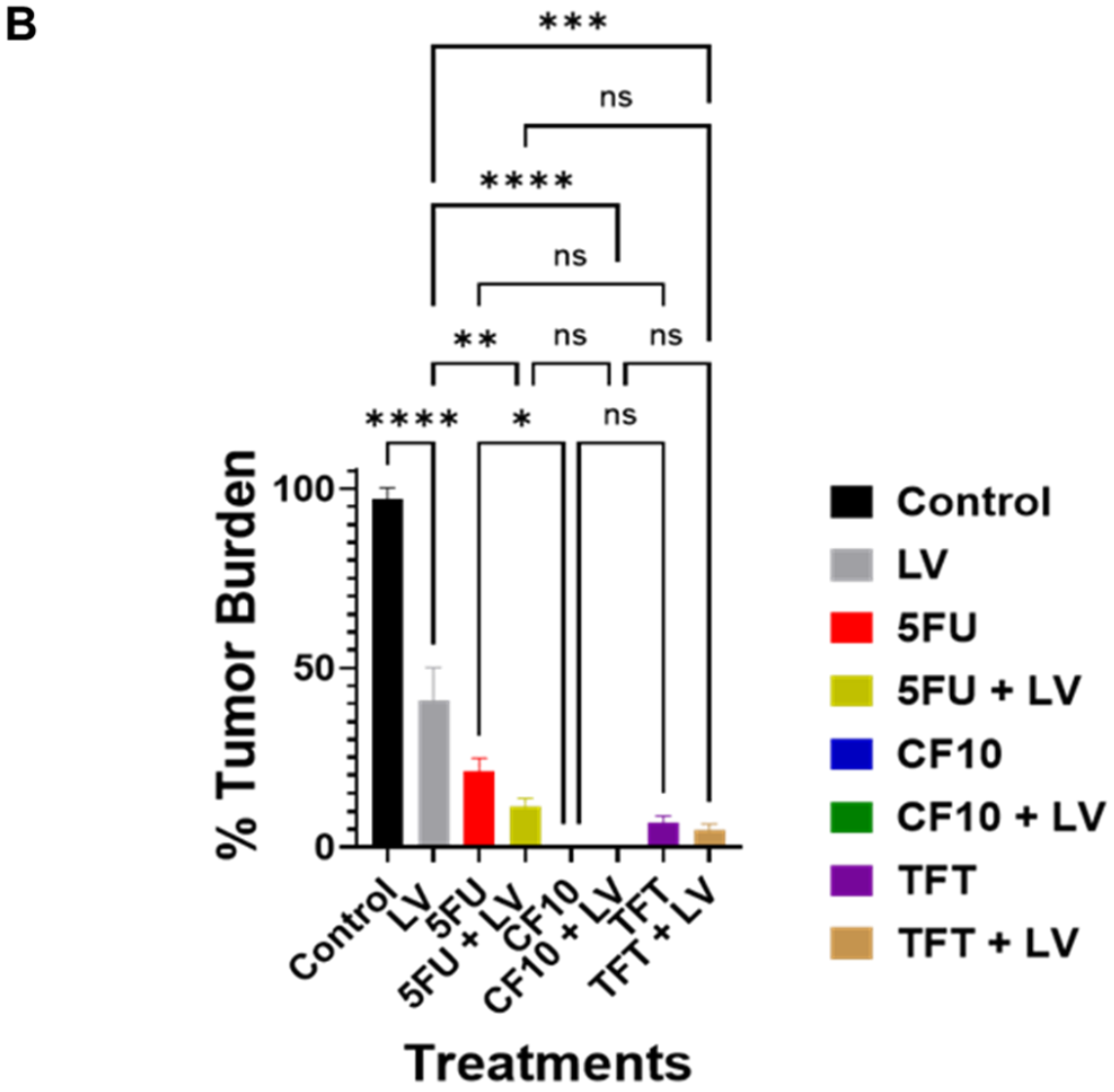

Figure 5. Pathological review of liver H&E sections from mouse liver metastasis study demonstrates CF10±LV eradicates liver metastases without scarring. (A) H&E-stained liver sections from mice with the indicated treatments (yellow arrows point to residual tumor and green arrows to scarring/inflammation). (B) Quantification of residual tumor from (A) was calculated by dividing the tumor area by the total area and multiplied by 100. p-values (n=4, ****p≤0.0001, *** p≤0.001, ** p≤0.02).

Extensive tumors were found in livers from all control mice. However, all treatment groups, including single-agent LV, displayed reduced tumor burden relative to control (Supplementary Table S10). Treatment with 5-FU and 5-FU/LV was less effective relative to CF10 and TFT. CF10 as single agent and in combination with LV completely eradicated tumor with no early scarring or inflammation noted upon pathological review (**Fig. 5A.B)**. TFT was effective in this tumor model however inflammation and early scar formation were noted (**Fig. 5A, Supplementary Table S10)** and unlike for CF10 and CF10/LV residual tumor was evident (**Fig. 5A,Supplementary Table S10)**. These results are consistent with the established clinical efficacy for 5-FU/LV and TFT (as part of Tiperacil) in CRLM treatment and indicate CF10 as single agent or as CF10+LV is likely to be highly active in treating liver-metastatic burden.

Discussion

Fluoropyrimidine (FP) drugs are central to disease management for metastatic CRC patients, and treatment with FP-based regimens provides proven survival benefits. Many mCRC patients survive to receive three or more lines of chemotherapy, with each including an FP drug (2). The 5-FU/LV-based regimens FOLFOX and FOLFIRI are widely used in first- and second-line chemotherapy for mCRC, while TAS-102 that combines the FP TFT with the thymidine phosphorylase (TP) inhibitor Tiperacil is approved for 3rd line mCRC treatment for patients previously treated with 5-FU/LV and other drugs (2). While mCRC patients are increasingly living longer through optimizing drug scheduling and sequential order, long-term survival remains rare, with only <14% of mCRC patients surviving

five years post-diagnosis. In this study, we highlighted the improved activity of a nanoscale DNA-based FP polymer, CF10, relative to the legacy FP drugs widely used in mCRC treatment, 5-FU and TFT. Importantly, we establish therapeutic benefit for CF10 relative to 5-FU with infusion dosing demonstrating the therapeutic advantages of CF10 cannot be achieved with 5-FU simply through schedule optimization.

In previous testing in our laboratory (4) and in the NCI60 cell line screen (11), CF10 and F10 displayed potency advantages substantially greater than anticipated based upon a 10-fold greater FP content exceeding 1,000-fold relative to 5-FU in some cancer cell lines (12). In these studies, we extended these findings in the Broad Institute PRISM screen. AUC values, an indicator of drug potency with strong potency correlated with low AUC revealed much lower values for CF10 relative to 5-FU and TFT consistent with increased potency broadly across all CRC cell lines tested (**Fig. 1C,D**; Supplementary TablesS1-3). While results from large cell screens can be extremely valuable and potentially enable dose-response data to be correlated with genomic and proteomic factors, screen data must be interpreted with caution since cell-compound interactions that may be important for predicting *in vivo* efficacy may not be represented ideally under the screening conditions. One factor identified as important for FP cytotoxicity is folate levels in culture media (9). In these studies, we tested the relative potency of CF10, 5-FU, and TFT in both complete media and in media with restricted folate (FR media) to better simulate human physiology. The potency advantage for CF10 relative to 5-FU and TFT was retained to CRC cells in FR conditions (**Fig. 2A-F, Table 1**)

without causing increased cytotoxicity to non-malignant cells (**Fig. 2G**). A potentiating effect of LV co-treatment was also evident for CF10 in CRC cells cultured under FR conditions and was similar as for 5-FU (2.10- vs 3.12-fold for HCT-116) (**Fig. 2A-F**). The data support LV co-treatment being beneficial during CF10 clinical development. TFT potency was also increased by LV co-treatment, and although TAS-102 is not combined with LV, our studies indicate that doing so could benefit CRC patients.

The cytotoxic mechanism responsible for CF10's enhanced potency to CRC cells involves dual targeting of TS and Top1. The effects of CF10 on these enzymes are mediated through three metabolites, FdUMP, FdUTP, and AraCTP. Nuclease degradation of CF10 releases FdUMP without the multiple steps of anabolic metabolism required for the inefficient conversion of 5-FU to FdUMP (36,37). Western blots of TS from FP-treated cells cultured under FR conditions showed that with CF10, but not 5-FU treatment, TS was predominantly complexed with FdUMP and migrated as a band with slightly reduced intensity (TS CC; **Fig 3A**) a result consistent with higher FdUMP levels in CF10-treated cells. FdUMP not complexed with TS may be metabolized to FdUTP, and under the thymineless conditions caused by TS inhibition, FdUTP is incorporated into DNA during replication in place of thymidine. We previously established that FdU interferes with the re-ligation step of Top1 catalysis (11,14), resulting in the formation of a DNA:protein complex (i.e., Top1 cleavage complex (Top1cc). Similarly, AraCTP misincorporation into DNA results in Top1cc formation by a similar mechanism (14). Top1cc formed with either nucleoside analogs or classic Top1 poisons (e.g.,

camptothecin) are converted to DNA double-strand breaks (DSBs) by collision with either an advancing replication fork or during transcription of the DNA containing the Top1cc (30-32). Our data show CF10/LV causes formation of Top1cc as evidenced from immunofluorescence (Supplementary Figure S12). Analysis of correlations from PRISM screen data for FPs (CF10, 5-FU, TFT) and SN-38 (the active metabolite of irinotecan - Supplementary Fig. S3), showed much stronger correlation for CF10 with SN-38 (5e-24), that for TFT (1.1e-16) or 5-FU (1.1e-4) (Supplementary Table S4). These results are consistent with CF10 inducing enhanced replication stress (**Fig 3E,F**) resulting from TS/Top1 dual targeting. This dual targeting contributes to CF10's increased potency of CF10 relative to clinically used FPs. Our data demonstrate this mechanism occurs for CF10/LV and under folate-restricted conditions.

The present studies also addressed whether CF10 could be more effective than 5-FU in the treatment of CRC liver metastasis under conditions of physiological folate. In clinical regimens, 5-FU may be administered by bolus injection, infusion, or both, with infusion often performed over ~46h (38). CF10 is a DNA-based FP polymer, and while clinical data are not available for CF10, there is clinical precedent for oligonucleotide activity with long infusions, such as 21 days (39). In the present studies, we tested CF10 and 5-FU with delivery of equivalent FP levels based on A260 absorbance and with infusion over seven days using an osmotic mini-pump fitted with a jugular vein catheter. We elected to test TFT under identical conditions. Thus, while TFT is orally administered as part of TAS-102 (40), we delivered the equivalent amount based on fluoropyrimidine monomer via the

same route to enable direct comparison of *in vivo* antitumor activity under similar conditions. Liver tumor masses were formed by the injection of MC38 mouse CRC cells into one lobe of the liver in syngeneic host C57BL/6 mice, similar to our previous study using a syngeneic rat model of orthotopic CRC liver metastasis (5,16). Mice have considerably higher folate levels than humans, and mice were fed a diet shown previously to reduce folate to more human-like levels (41). 5-FU and 5-FU/LV reduced tumor progression in this CRC liver metastasis model consistent with the clinical efficacy of 5-FU/LV in mCRC treatment. Consistent with previous studies in which we evaluated CF10 and 5-FU in primary colon cancer (4) and in a rat CRC liver metastasis model (5), CF10 was more effective than 5-FU. These results extend previous findings in several ways important for CF10 translation. The improved activity of CF10 relative to 5-FU is achieved in the context of relatively lower folate levels, more similar to human physiology. The strong antitumor activity of CF10 was also achieved without weight loss, while equivalent amounts of both 5-FU and TFT caused significant weight loss in treated mice. CF10 also caused no scarring of the liver which was evident with both 5-FU and TFT. Importantly, CF10 completely eradicated the liver tumor mass in this liver metastatic model which neither 5-FU±LV or TFT were able to do. Since infusion dosing was used for all treatments in this study and previous studies have shown increased efficacy for CF10 relative to 5-FU with bolus dosing our studies demonstrate an improved therapeutic benefit for CF10 regardless of schedule. CF10/LV displayed equivalent antitumor activity as single agent CF10 also without

weight loss or liver scarring and based on enhanced potency in cell-based assays the data support CF10/LV clinical development.

Overall, our findings demonstrate that CF10 is much more potent to CRC cells than FPs used in treatment regimens for mCRC. The increased potency for CF10 relative to 5-FU and TFT is general, as evidenced by lower AUC values over multiple CRC cell lines included in the Broad Institute PRISM screen, is maintained with folate restriction, and is associated with stronger TS inhibition and potent Top1cc formation consistent with mechanistic similarities to Top1 poisons. LV co-treatment enhances CF10 cytotoxicity to CRC cells, and while the effect is less pronounced than for 5-FU, our results support LV co-treatment during CF10 development. The finding of complete eradication of tumor mass in a CRC liver metastasis model with CF10 infusion while 5-FU/LV infusion only induced tumor regression but not eradication is encouraging for the clinical development of CF10. TFT was highly effective in this model, consistent with clinical activity, but treatment-related scarring was detected with TFT, which also caused weight loss. Our findings support advanced pre-clinical testing of CF10 and initiation of clinical studies with strong potential for CF10 to contribute to long-term survival in mCRC patients.

Disclosure of Potential Conflicts of interest

W. Gmeiner is inventor on a patent application for CF10 in colon cancer.

Authors' Contributions

Conception and design: W.H. Gmeiner

Development of methodology:

Acquisition of data (provided animals, acquired and managed patients, provided facilities, etc.): W.H. Gmeiner, X. Ma, C. Okechukwu

Analysis and interpretation of data (e.g. statistical analysis, biostatistics, computational analysis): R. D'Agostino Jr, W.H. Gmeiner, W. Li, C. Okechukwu

Writing, review, and/or revision of the manuscript: R. D'Agostino Jr, W.H. Gmeiner, W. Li, C. Okechukwu, X. Ma

Administrative, technical, or material support (i.e., reporting or organizing data, constructing databases): W.H. Gmeiner

Study Supervision: W.H. Gmeiner

Acknowledgements

This study was performed with grant support from 1R42 CA254843 (to W.H. Gmeiner), Department of Defense Peer Reviewed Cancer Research Program CA200460 (to W.H. Gmeiner). This work was also supported, in part, by a National Cancer Institute of the National Institutes of Health Cancer Center Support Grant P30CA012197 (AHWFBCCC). The authors wish to acknowledge the support of the Wake Forest Baptist Comprehensive Cancer Center Biostatistics Shared Resource, Cell, and Viral Vector Shared Resource, the Proteomics and Metabolomics Shared Resource, and the WFU Mass Spectrometry facility.

References

1. Wilson PM, Danenberg PV, Johnston PG, Lenz HJ, Ladner RD. Standing the test of time: targeting thymidylate biosynthesis in cancer therapy. *Nat Rev Clin Oncol* 2014;**11**(5):282-98 doi 10.1038/nrclinonc.2014.51.

2. Gmeiner WH. Recent Advances in Therapeutic Strategies to Improve Colorectal Cancer Treatment. *Cancers (Basel)* 2024;**16**(5) doi 10.3390/cancers16051029.

3. Sarkar S, Kiren S, Gmeiner WH. Review of Prodrug and Nanodelivery Strategies to Improve the Treatment of Colorectal Cancer with Fluoropyrimidine Drugs. *Pharmaceutics* 2024;**16**(6) doi 10.3390/pharmaceutics16060734.

4. Gmeiner WH, Dominijanni A, Haber AO, Ghiraldeli LP, Caudell DL, D'Agostino R, Jr.*, et al.* Improved Antitumor Activity of the Fluoropyrimidine Polymer CF10 in Preclinical Colorectal Cancer Models through Distinct Mechanistic and Pharmacologic Properties. *Mol Cancer Ther* 2021;**20**(3):553-63 doi 10.1158/1535-7163.MCT-20-0516.

5. Okechukwu CC, Ma X, Sah N, Mani C, Palle K, Gmeiner WH. Enhanced Therapeutic Efficacy of the Nanoscale Fluoropyrimidine Polymer CF10 in a Rat Colorectal Cancer Liver Metastasis Model. *Cancers (Basel)* 2024;**16**(7) doi 10.3390/cancers16071360.

6. Pritchard DM, Watson AJ, Potten CS, Jackman AL, Hickman JA. Inhibition by uridine but not thymidine of p53-dependent intestinal apoptosis initiated by 5-

fluorouracil: evidence for the involvement of RNA perturbation. *Proc Natl Acad Sci U S A* 1997;**94**(5):1795-9.

7. Ma WW, Saif MW, El-Rayes BF, Fakih MG, Cartwright TH, Posey JA*, et al.* Emergency use of uridine triacetate for the prevention and treatment of life-threatening 5-fluorouracil and capecitabine toxicity. *Cancer* 2017;**123**(2):345-56 doi 10.1002/cncr.30321.

8. Temmink OH, de Bruin M, Comijn EM, Fukushima M, Peters GJ. Determinants of trifluorothymidine sensitivity and metabolism in colon and lung cancer cells. *Anticancer Drugs* 2005;**16**(3):285-92 doi 10.1097/00001813-200503000-00007.

9. Fischel JL, Formento P, Ciccolini J, Rostagno P, Etienne MC, Catalin J*, et al.* Impact of the oxaliplatin-5 fluorouracil-folinic acid combination on respective intracellular determinants of drug activity. *Br J Cancer* 2002;**86**(7):1162-8 doi 10.1038/sj.bjc.6600185.

10. Fischel JL, Rostagno P, Formento P, Dubreuil A, Etienne MC, Milano G. Ternary combination of irinotecan, fluorouracil-folinic acid and oxaliplatin: results on human colon cancer cell lines. *Br J Cancer* 2001;**84**(4):579-85 doi 10.1054/bjoc.2000.1600.

11. Liao ZY, Sordet O, Zhang HL, Kohlhagen G, Antony S, Gmeiner WH*, et al.* A novel polypyrimidine antitumor agent FdUMP[10] induces thymineless death with topoisomerase I-DNA complexes. *Cancer Res* 2005;**65**(11):4844-51 doi 65/11/4844 [pii]

10.1158/0008-5472.CAN-04-1302.

12. Gmeiner WH, Reinhold WC, Pommier Y. Genome-wide mRNA and microRNA profiling of the NCI 60 cell-line screen and comparison of FdUMP[10] with fluorouracil, floxuridine, and topoisomerase 1 poisons. *Mol Cancer Ther* 2010;**9**(12):3105-14 doi 10.1158/1535-7163.MCT-10-0674

9/12/3105 [pii].

13. Gmeiner WH, Gearhart PJ, Pommier Y, Nakamura J. F10 cytotoxicity via topoisomerase I cleavage complex repair consistent with a unique mechanism for thymineless death. *Future Oncol* 2016;**12**(19):2183-8 doi 10.2217/fon-2016-0127.

14. Gmeiner WH, van Waardenburg R. Targeting DNA topoisomerases: past & future. *Cancer Drug Resist* 2021;**4**:758-61 doi 10.20517/cdr.2021.65.

15. Haber AO, Jain A, Mani C, Nevler A, Agostini LC, Golan T*, et al.* AraC-FdUMP[10] (CF10) is a next generation fluoropyrimidine with potent antitumor activity in PDAC and synergy with PARG inhibition. *Mol Cancer Res* 2021 doi 10.1158/1541-7786.MCR-20-0985.

16. White SB, Procissi D, Chen J, Gogineni VR, Tyler P, Yang Y*, et al.* Characterization of CC-531 as a Rat Model of Colorectal Liver Metastases. *PLoS One* 2016;**11**(5):e0155334 doi 10.1371/journal.pone.0155334.

17. Machover D. A comprehensive review of 5-fluorouracil and leucovorin in patients with metastatic colorectal carcinoma. *Cancer* 1997;**80**(7):1179-87 doi 10.1002/(sici)1097-0142(19971001)80:7<1179::aid-cncr1>3.0.co;2-g.

18. Dominijanni A, Gmeiner WH. Improved potency of F10 relative to 5-fluorouracil in colorectal cancer cells with p53 mutations. *Cancer Drug Resist* 2018;**1**:48-58 doi 10.20517/cdr.2018.01.

19. Peters GJ, Smitskamp-Wilms E, Smid K, Pinedo HM, Jansen G. Determinants of activity of the antifolate thymidylate synthase inhibitors Tomudex (ZD1694) and GW1843U89 against mono- and multilayered colon cancer cell lines under folate-restricted conditions. *Cancer Res* 1999;**59**(21):5529-35.

20. Milczarek M, Psurski M, Kutner A, Wietrzyk J. Vitamin D analogs enhance the anticancer activity of 5-fluorouracil in an in vivo mouse colon cancer model. *BMC Cancer* 2013;**13**:294 doi 10.1186/1471-2407-13-294.

21. Klubes P, Cerna I, Meldon MA. Effect of concurrent calcium leucovorin infusion on 5-fluorouracil cytotoxicity against murine L1210 leukemia. *Cancer Chemother Pharmacol* 1981;**6**(2):121-5 doi 10.1007/BF00262328.

22. Corsello SM, Nagari RT, Spangler RD, Rossen J, Kocak M, Bryan JG*, et al.* Discovering the anti-cancer potential of non-oncology drugs by systematic viability profiling. *Nat Cancer* 2020;**1**(2):235-48 doi 10.1038/s43018-019-0018-6.

23. Gutierrez JG, Lau E, Dharmapalan S, Parker M, Chen Y, Alvarez MA*, et al.* Multi-output prediction of dose-response curves enables drug repositioning and biomarker discovery. *NPJ Precis Oncol* 2024;**8**(1):209 doi 10.1038/s41698-024-00691-x.

24. Holbeck SL, Collins JM, Doroshow JH. Analysis of Food and Drug Administration-approved anticancer agents in the NCI60 panel of human tumor cell lines. *Mol Cancer Ther* 2010;**9**(5):1451-60 doi 10.1158/1535-7163.MCT-10-0106.

25. Xia Y, Ji X, Jang IS, Surka C, Hsu C, Wang K*, et al.* Genetic and pharmacological interrogation of cancer vulnerability using a multiplexed cell line screening platform. *Commun Biol* 2021;**4**(1):834 doi 10.1038/s42003-021-02352-2.

26. Gmeiner WH. Novel chemical strategies for thymidylate synthase inhibition. *Curr Med Chem* 2005;**12**(2):191-202 doi 10.2174/0929867053363432.

27. Brody JR, Gallmeier E, Yoshimura K, Hucl T, Kulesza P, Canto MI*, et al.* A proposed clinical test for monitoring fluoropyrimidine therapy: detection and stability of thymidylate synthase ternary complexes. *Cancer Biol Ther* 2006;**5**(8):923-7 doi 10.4161/cbt.5.8.2976.

28. Very N, Hardiville S, Decourcelle A, Thevenet J, Djouina M, Page A*, et al.* Thymidylate synthase O-GlcNAcylation: a molecular mechanism of 5-FU sensitization in colorectal cancer. *Oncogene* 2022;**41**(5):745-56 doi 10.1038/s41388-021-02121-9.

29. Pardee TS, Gomes E, Jennings-Gee J, Caudell D, Gmeiner WH. Unique dual targeting of thymidylate synthase and topoisomerase1 by FdUMP[10] results in high efficacy against AML and low toxicity. *Blood* 2012;**119**(15):3561-70 doi 10.1182/blood-2011-06-362442

blood-2011-06-362442 [pii].

30. Pommier Y. Drugging topoisomerases: lessons and challenges. *ACS Chem Biol* 2013;**8**(1):82-95 doi 10.1021/cb300648v.

31. Pommier Y, Leo E, Zhang H, Marchand C. DNA topoisomerases and their poisoning by anticancer and antibacterial drugs. *Chem Biol* 2010;**17**(5):421-33 doi 10.1016/j.chembiol.2010.04.012.

32. Pommier Y, Nussenzweig A, Takeda S, Austin C. Human topoisomerases and their roles in genome stability and organization. *Nat Rev Mol Cell Biol* 2022;**23**(6):407-27 doi 10.1038/s41580-022-00452-3.

33. Sordet O, Nakamura AJ, Redon CE, Pommier Y. DNA double-strand breaks and ATM activation by transcription-blocking DNA lesions. *Cell Cycle* 2010;**9**(2):274-8 doi 10.4161/cc.9.2.10506.

34. Ocvirk J, Brodowicz T, Wrba F, Ciuleanu TE, Kurteva G, Beslija S*, et al.* Cetuximab plus FOLFOX6 or FOLFIRI in metastatic colorectal cancer: CECOG trial. *World J Gastroenterol* 2010;**16**(25):3133-43 doi 10.3748/wjg.v16.i25.3133.

35. van der Wilt CL, Backus HH, Smid K, Comijn L, Veerman G, Wouters D*, et al.* Modulation of both endogenous folates and thymidine enhance the therapeutic efficacy of thymidylate synthase inhibitors. *Cancer Res* 2001;**61**(9):3675-81.

36. Liu J, Skradis A, Kolar C, Kolath J, Anderson J, Lawson T*, et al.* Increased cytotoxicity and decreased in vivo toxicity of FdUMP[10] relative to 5-FU. *Nucleosides Nucleotides* 1999;**18**(8):1789-802.

37. Bijnsdorp IV, Comijn EM, Padron JM, Gmeiner WH, Peters GJ. Mechanisms of action of FdUMP[10]: metabolite activation and thymidylate synthase inhibition. *Oncol Rep* 2007;**18**(1):287-91.

38. Redman JM, Rhea LP, Brofferio A, Whelpley M, Gulley JL, Gatti-Mays ME*, et al.* Successful 5-fluorouracil (5-FU) infusion re-challenge in a metastatic colorectal cancer patient with coronary artery disease who experienced symptoms consistent with coronary vasospasm during first 5-FU infusion. *J Gastrointest Oncol* 2019;**10**(5):1010-4 doi 10.21037/jgo.2019.07.04.

39. Cunningham CC, Holmlund JT, Schiller JH, Geary RS, Kwoh TJ, Dorr A*, et al.* A phase I trial of c-Raf kinase antisense oligonucleotide ISIS 5132 administered as a continuous intravenous infusion in patients with advanced cancer. *Clin Cancer Res* 2000;**6**(5):1626-31.

40. Lenz HJ, Stintzing S, Loupakis F. TAS-102, a novel antitumor agent: a review of the mechanism of action. *Cancer Treat Rev* 2015;**41**(9):777-83 doi 10.1016/j.ctrv.2015.06.001.

41. Raghunathan K, Schmitz JC, Priest DG. Impact of schedule on leucovorin potentiation of fluorouracil antitumor activity in dietary folic acid deplete mice. *Biochem Pharmacol* 1997;**53**(8):1197-202 doi 10.1016/s0006-2952(96)00829-5.

Figure Legends

Supplementary Table S1. AUC values for CF10 and 5-FU from the PRISM screen (data are plotted in Fig 1C).

Bowel cell lines PRISM 5FU CF10 AUC 09022024					
Depmap ID	**CF10 AUC AUC**	**FLUOROURACIL (BRD:BRD-K24844714-001-24-5) AUC Drug sensitivity AUC (PRISM Repurposing Secondary Screen)**	**Primary Disease**	**Cell Line Name**	**Lineage**
ACH-000982	0.16	0.76	Colorectal Adenocarcinoma	GP2D	Bowel
ACH-000467	0.15	0.83	Colorectal Adenocarcinoma	HCC56	Bowel
ACH-000971	0.34	0.89	Colorectal Adenocarcinoma	HCT116	Bowel
ACH-000997	0.32	0.86	Colorectal Adenocarcinoma	HCT15	Bowel
ACH-000552	0.48	0.87	Colorectal Adenocarcinoma	HT29	Bowel
ACH-000957	0.34	0.83	Colorectal Adenocarcinoma	LS180	Bowel
ACH-000007	0.43	0.65	Colorectal Adenocarcinoma	LS513	Bowel
ACH-000296	0.55	0.87	Colorectal Adenocarcinoma	OUMS23	Bowel
ACH-000565	0.24	0.86	Colorectal Adenocarcinoma	RCM1	Bowel
ACH-000943	0.48	0.86	Colorectal Adenocarcinoma	RKO	Bowel
ACH-000991	0.51	0.80	Colorectal Adenocarcinoma	SNU81	Bowel
ACH-000967	0.58	0.83	Colorectal Adenocarcinoma	SNUC2A	Bowel
ACH-000959	0.22	0.85	Colorectal Adenocarcinoma	SNUC4	Bowel
ACH-000421	0.75	0.89	Colorectal Adenocarcinoma	SW837	Bowel
average	0.40	0.83			

Supplementary Table S3. AUC values for Trifluorothymidine and 5-FU from the PRISM screen (data are plotted in Supplementary Fig. S2).

CF10 AUC AUC vs TRIFLURIDINE (BRD_BRD-K03243820-001-23-8)…					
Depmap ID	**CF10 AUC AUC**	**TRIFLURIDINE (BRD:BRD-K03243820-001-23-8) AUC Drug sensitivity AUC (PRISM Repurposing Secondary Screen)**	**Primary Disease**	**Cell Line Name**	**Lineage**
ACH-000982	0.16	0.47	Colorectal Adenocarcinoma	GP2D	Bowel
ACH-000467	0.15	0.59	Colorectal Adenocarcinoma	HCC56	Bowel
ACH-000971	0.34	0.67	Colorectal Adenocarcinoma	HCT116	Bowel
ACH-000997	0.32	0.63	Colorectal Adenocarcinoma	HCT15	Bowel
ACH-000552	0.48	0.71	Colorectal Adenocarcinoma	HT29	Bowel
ACH-000957	0.34	0.65	Colorectal Adenocarcinoma	LS180	Bowel
ACH-000007	0.43	0.45	Colorectal Adenocarcinoma	LS513	Bowel
ACH-000296	0.55	0.72	Colorectal Adenocarcinoma	OUMS23	Bowel
ACH-000565	0.24	0.55	Colorectal Adenocarcinoma	RCM1	Bowel
ACH-000943	0.48	0.70	Colorectal Adenocarcinoma	RKO	Bowel
ACH-000991	0.51	0.65	Colorectal Adenocarcinoma	SNU81	Bowel
ACH-000967	0.58	0.84	Colorectal Adenocarcinoma	SNUC2A	Bowel
ACH-000959	0.22	0.47	Colorectal Adenocarcinoma	SNUC4	Bowel
ACH-000421	0.75	0.65	Colorectal Adenocarcinoma	SW837	Bowel

average	0.40	0.63			

Supplementary Table S4. Summary of p-values for the correlations of SN-38 with indicated drugs from the Broad Institute PRISM screen (all cell lines). Data plots are shown in Supplementary Fig S3.

Drug	p- value vs SN-38
CPT	5e-37
CF10	5e-24
TFT	1.1e-16
5-FU	1.1e-4

Supplementary Table S5. Summary of GI50 values for LS174T CRC cell line for CF10, 5FU, TFT, and ± LV combination. Plots of data are shown in Supplementary Fig. S5.

FR Drug	Media	IC_{50} (μM) ± SEM	IC_{50} (μM) + LV (1μM) ± SEM	IC_{50} (μM) + LV (10μM) ± SEM	LV Effect (1μM)	LV Effect (10μM)
5FU	DMEM	4.54 ± 0.0125	3.72 ± 0.000999	1.71 ± 0.0101	1.22	2.66
5FU	FR	1.84 ± 0.0165	1.48 ± 0.0126	0.770 ± 0.0137	1.25	2.39
CF10	DMEM	0.0145 ± 0.000124	0.0139 ± 0.000122	0.00697 ± 0.000120	1.04	2.08
CF10	FR	0.0120 ± 0.000127	0.00985 ± 0.000136	0.00602 ± 0.00138	1.21	1.99
TFT	DMEM	2.16 ± 0.0120	2.01 ± 0.0134	1.33 ± 0.0129	1.08	1.62
TFT	FR	1.73 ± 0.0138	1.35 ± 0.0136	0.733 ± 0.0143	1.28	2.36

Supplementary Table S6. Summary of GI50 values for HCT15 CRC cell line for CF10, 5FU, TFT, and ± LV combination. Plots of data are shown in Supplementary Fig. S6.

FR Drug	Media	IC_{50} (μM) ± SEM	IC_{50} (μM) + LV (1μM) ± SEM	IC_{50} (μM) + LV (10μM) ± SEM	LV Effect (1μM)	LV Effect (10μM)
5FU	DMEM	4.98 ± 0.0124	3.66 ± 0.00989	1.50 ± 0.0104	1.36	3.32
5FU	FR	1.49 ± 0.0179	0.946 ± 0.0138	0.480 ± 0.0160	1.58	3.10
CF10	DMEM	0.0117 ± 0.000127	0.0100 ± 0.000132	0.00562 ± 0.000140	1.17	2.08
CF10	FR	0.0108 ± 0.000130	0.00896 ± 0.000139	0.00497 ± 0.000145	1.21	2.17
TFT	DMEM	2.56 ± 0.0117	2.13 ± 0.0132	1.18 ± 0.0132	1.20	2.17
TFT	FR	1.35 ± 0.0115	0.950 ± 0.0145	0.488 ± 0.0151	1.42	2.77

Supplementary Table S7. Summary of GI50 values for MC38 CRC cell line for CF10, 5FU, TFT, and ± LV combination. Plots of data are shown in Supplementary Fig. S7.

FR Drug	Media	IC_{50} (μM) ± SEM	IC_{50} (μM) + LV (1μM) ± SEM	IC_{50} (μM) + LV (10μM) ± SEM	LV Effect (1μM)	LV Effect (10μM)
5FU	DMEM	4.98 ± 0.0124	3.66 ± 0.00989	1.50 ± 0.0104	1.36	3.32
5FU	FR	1.49 ± 0.0179	0.946 ± 0.0138	0.480 ± 0.0160	1.58	3.10
CF10	DMEM	0.0117 ± 0.000127	0.0100 ± 0.000132	0.00562 ± 0.000140	1.17	2.08
CF10	FR	0.0108 ± 0.000130	0.00896 ± 0.000139	0.00497 ± 0.000145	1.21	2.17
TFT	DMEM	2.56 ± 0.0117	2.13 ± 0.0132	1.18 ± 0.0132	1.20	2.17
TFT	FR	1.35 ± 0.0115	0.950 ± 0.0145	0.488 ± 0.0151	1.42	2.77

Supplementary Table S8. Least squares means analysis of change in IVIS flux intensities during treatment (Delta IVIS Flux – 7 groups.

group	Mean delta_trt
Control	385500000
CF10	-402775000
CF10LV	-416250000
FU	-204500000
FULV	-298500000
LV	216000000
TFT	-404100000
TFT+LV	-398025000

Pairwise Comparison – Using Bonferroni Adjusted P-value for significance (P<0.0017 is statistically significant (yellow)) Dependent Variable: delta_trt T-statistics and P-values Shown								
i/j	**Control**	**CF10**	**CF10LV**	**FU**	**FULV**	**LV**	**TFT**	**TFT+LV**
Control		18.1 <.0001	18.45 <.0001	13.58 <.0001	15.7 <.0001	3.9 0.0007	18.17 <.0001	18.03 <.0001
CF10	-18.1 <.0001		0.31 0.7591	-4.56 0.0001	-2.40 0.0245	-14.24 <.0001	0.03 0.97	-0.109 0.91
CF10LV	-18.45 <.0001	-0.31 0.75		-4.87 <.0001	-2.71 0.0122	-14.55 <.0001	-0.279 0.78	-0.419 0.67
FU	-13.58 <.0001	4.564 0.0001	4.87 <.0001		2.16 0.0406	-9.68 <.0001	4.59 0.0001	4.45 0.0002
FULV	-15.7 <.0001	2.40 0.0245	2.71 0.0122	-2.16 0.0406		-11.84 <.0001	2.43 0.0229	2.29 0.0310
LV	-3.9 0.0007	14.24 <.0001	14.55 <.0001	9.68 <.0001	11.84 <.0001		14.27 <.0001	14.13 <.0001
TFT	-18.17 <.0001	-0.03 0.97	0.279 0.78	-4.59 0.0001	-2.43 0.0229	-14.27 <.0001		-0.139 0.889
TFT+LV	-18.03 <.0001	0.109 0.91	0.419 0.67	-4.45 0.0002	-2.29 0.0310	-14.13 <.0001	0.139 0.889	

Supplementary Table S9. Least squares means analysis of change in weight during treatment. Delta weight – 7 groups.

group	Mean delta_weight
Control	1.33750000
CF10	0.72500000
CF10LV	-0.14000000
FU	-5.41250000
FULV	-3.79250000
LV	-0.78500000
TFT	-1.62500000
TFT+LV	-2.12500000

Pairwise Comparison – Using Bonferroni Adjusted P-value for significance (P<0.0017 is statistically significant (yellow)) Dependent Variable: delta_weight T-statistics and P-values Shown								
i/j	**Control**	**CF10**	**CF10LV**	**FU**	**FULV**	**LV**	**TFT**	**TFT+LV**
Control		1.53 0.1377	3.704662 0.0011	16.92485 <.0001	12.86289 <.0001	5.321925 <.0001	7.428129 <.0001	8.681822 <.0001
CF10	-1.53 0.1377		2.168888 0.0402	15.38908 <.0001	11.32711 <.0001	3.786152 0.0009	5.892355 <.0001	7.146048 <.0001
CF10LV	-3.70466 0.0011	-2.16889 0.0402		13.22019 <.0001	9.158225 <.0001	1.617264 0.1189	3.723467 0.0011	4.97716 <.0001
FU	-16.9249 <.0001	-15.3891 <.0001	-13.2202 <.0001		-4.06196 0.0005	-11.6029 <.0001	-9.49672 <.0001	-8.24303 <.0001
FULV	-12.8629 <.0001	-11.3271 <.0001	-9.15822 <.0001	4.061964 0.0005		-7.54096 <.0001	-5.43476 <.0001	-4.18106 0.0003
LV	-5.32193 <.0001	-3.78615 0.0009	-1.61726 0.1189	11.60293 <.0001	7.540961 <.0001		2.106204 0.0458	3.359896 0.0026
TFT	-7.42813 <.0001	-5.89236 <.0001	-3.72347 0.0011	9.496722 <.0001	5.434758 <.0001	-2.1062 0.0458		1.253693 0.2220
TFT+LV	-8.68182 <.0001	-7.14605 <.0001	-4.97716 <.0001	8.243029 <.0001	4.181065 0.0003	-3.3599 0.0026	-1.25369 0.2220	

Supplementary Table S10. Summary of pathological review of liver scarring/inflammation and % tumor burden

Treatment Group	Early Scarring/ Inflammation	% Tumor Burden
Control	Negative	97.00 ± 3.22
LV	Positive	41.00 ± 9.07
5FU	Positive	21.33 ± 3.48
5FU + LV	Positive	11.33 ± 2.40
CF10	Negative	0.00 ± 0.00
CF10 + LV	Negative	0.00 ± 0.00
TFT	Positive	7.00 ± 1.73
TFT + LV	Positive	4.93 ± 1.55

A

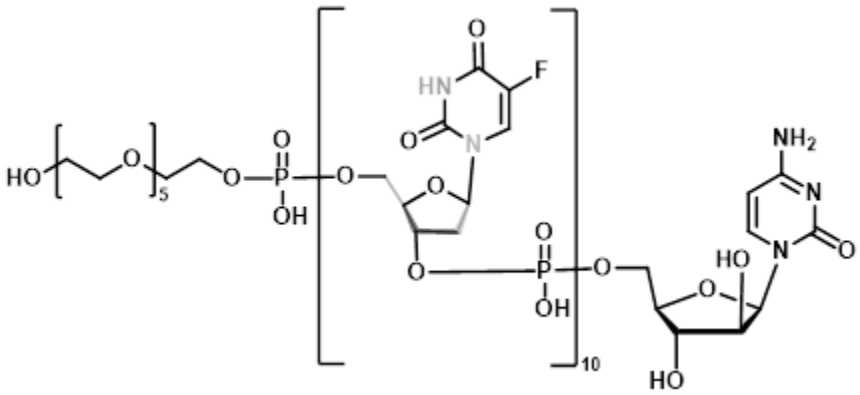

Supplementary Fig S1. Structure of CF10.

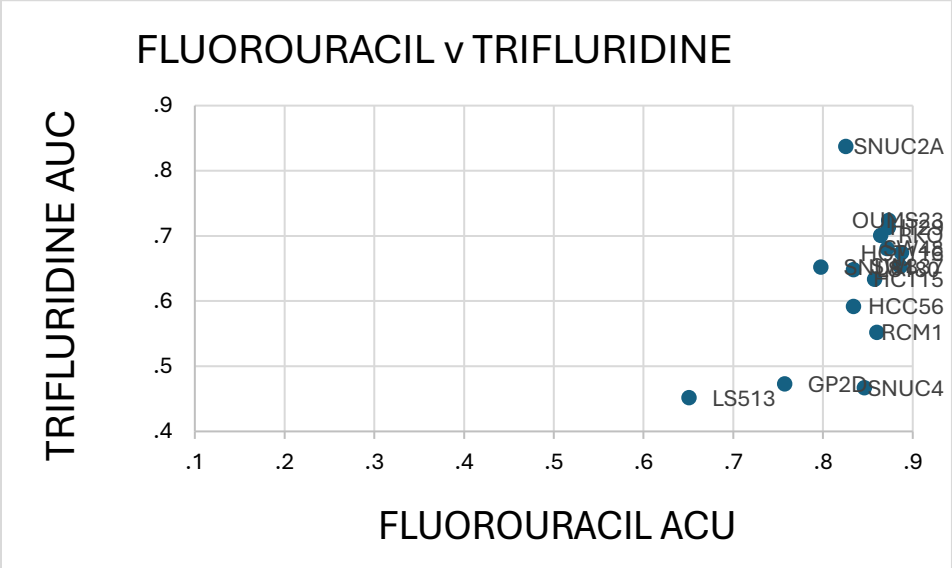

Supplementary Fig S2. AUC values for Trifluorthymidine and 5-FU from the PRISM screen.

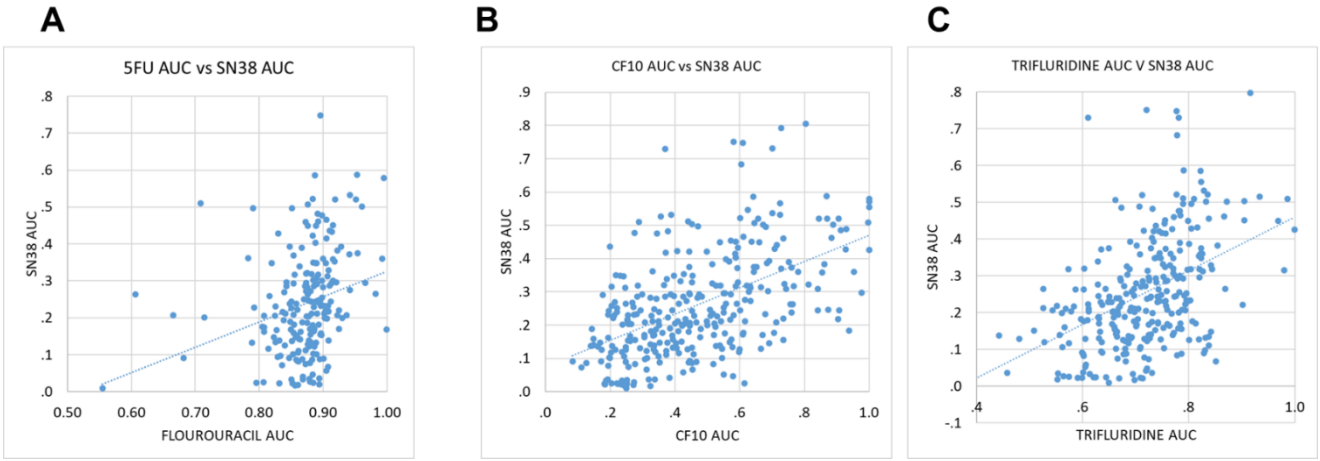

Supplementary Fig. S3. Plots of AUC for SN-38 vs (A) 5-FU, (B) CF10, and C TFT. P-values are summarized in Supplementary Table S4.

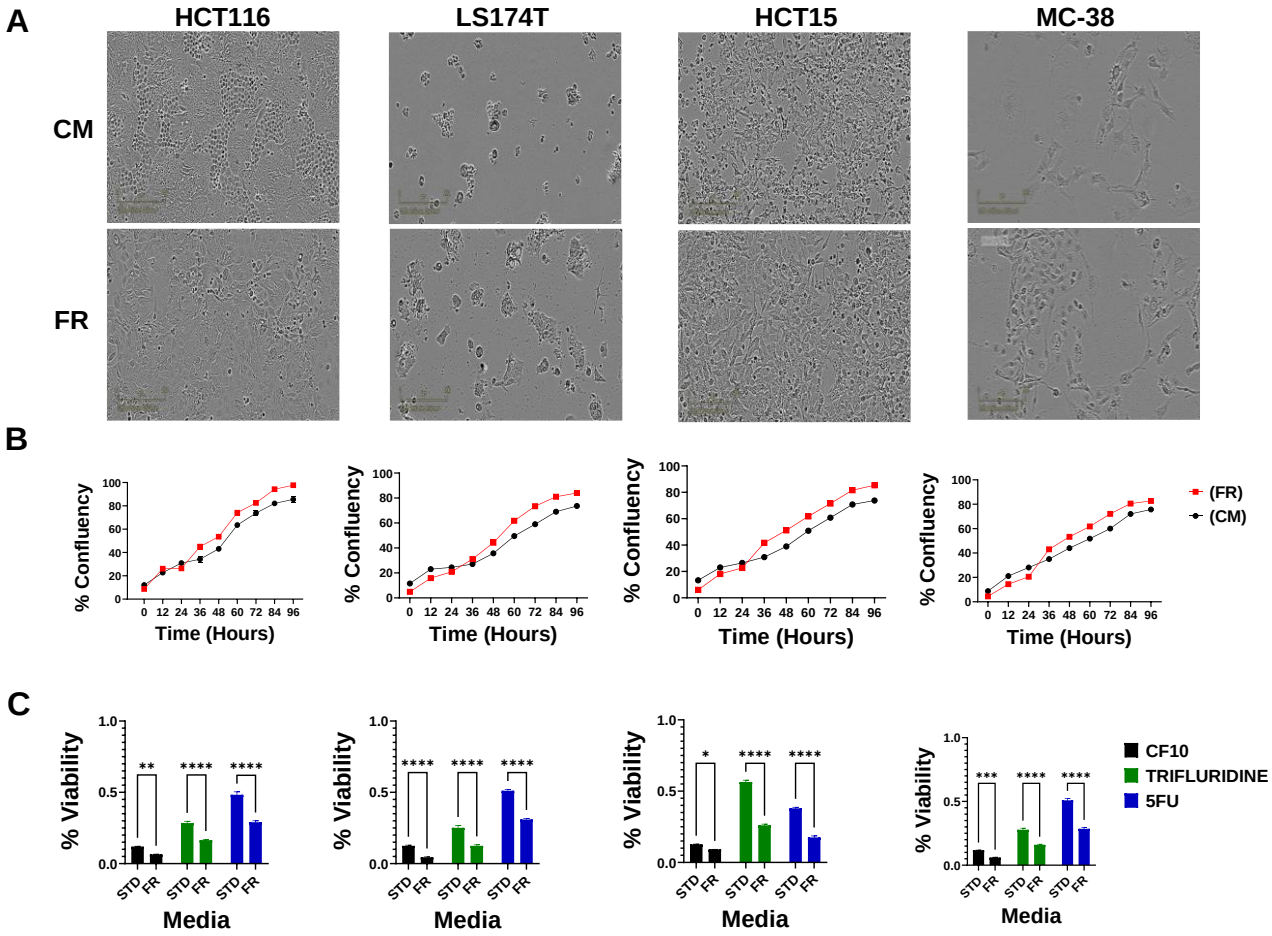

Supplementary Fig. S4. Comparison of cell viability in ATCC-recommended media (CM) and media with human-like folate levels (FR). (A) Photomicrographs of cells showing similar morphology and viability in CM and FR media; (B) % confluency in 96 well plates as a function of time showing similar growth rates in FR and ATCC-recommended media; (C) % viability for the indicated cell line in response to treatment with each of the three FPs (CF10, TFT, 5-FU) in ATCC-recommended and FR media.

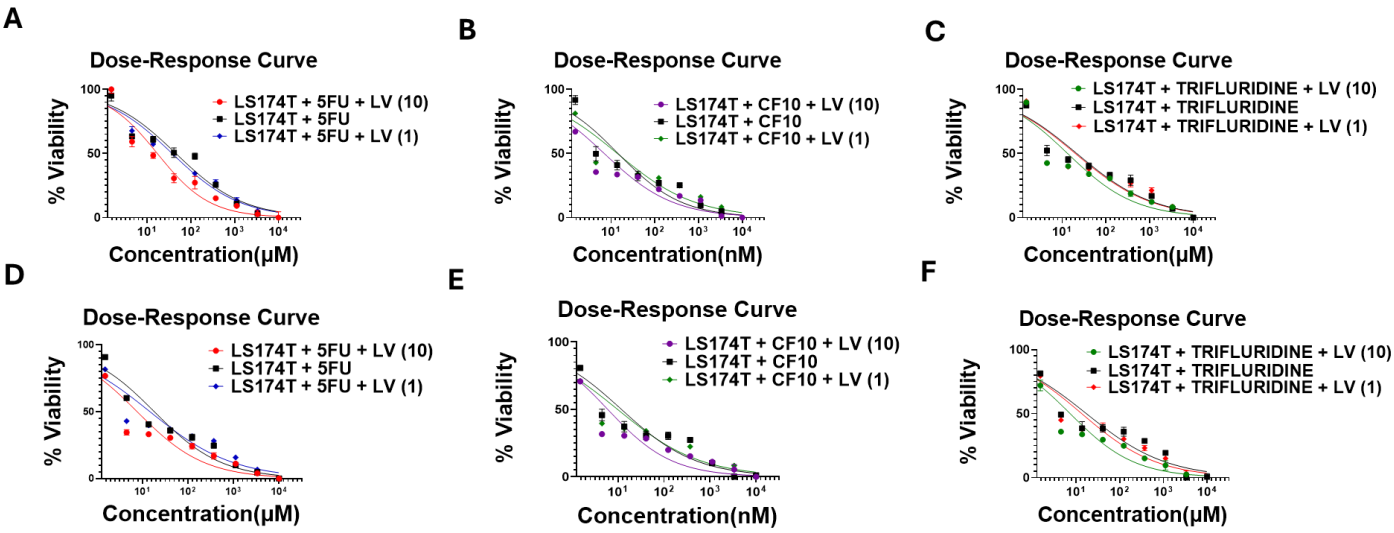

Supplementary Fig. S5. Summary of GI50 values for LS174T CRC cell line for CF10, 5FU, TFT, and ± LV combination. CF10 is much more potent to CRC cell than 5-FU and TFT on both standard media and folate-restricted media. LV potentiates the cytotoxicity of CF10 to a similar extent as 5-FU.

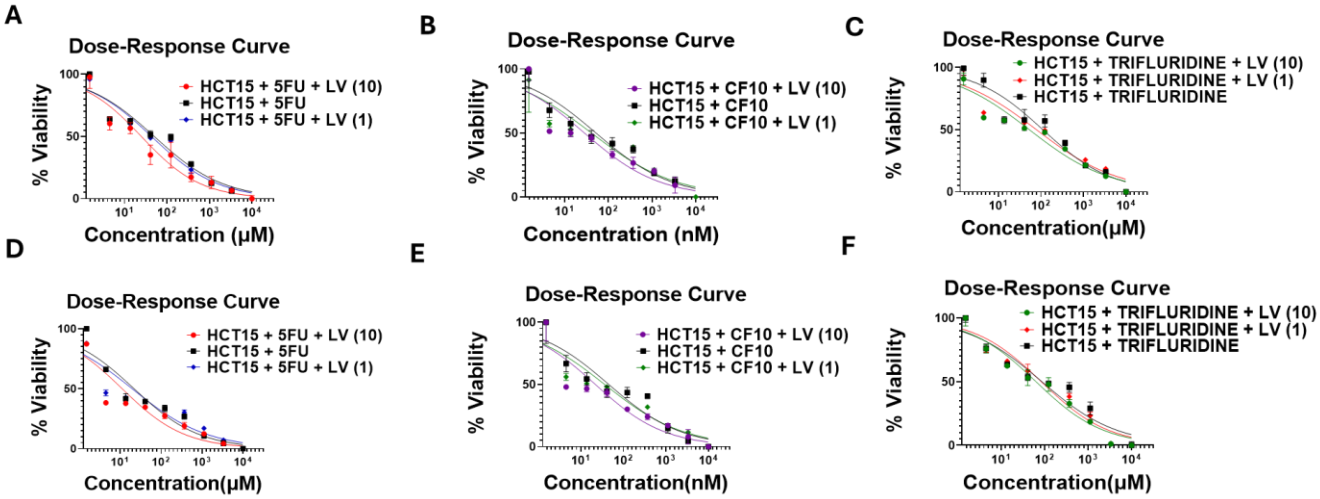

Supplementary Fig. S6. Summary of GI50 values for HCT15 CRC cell line for CF10, 5FU, TFT, and ± LV combination. CF10 is much more potent to CRC cell than 5-FU and TFT on both standard media and folate-restricted media. LV potentiates the cytotoxicity of CF10 to a similar extent as 5-FU.

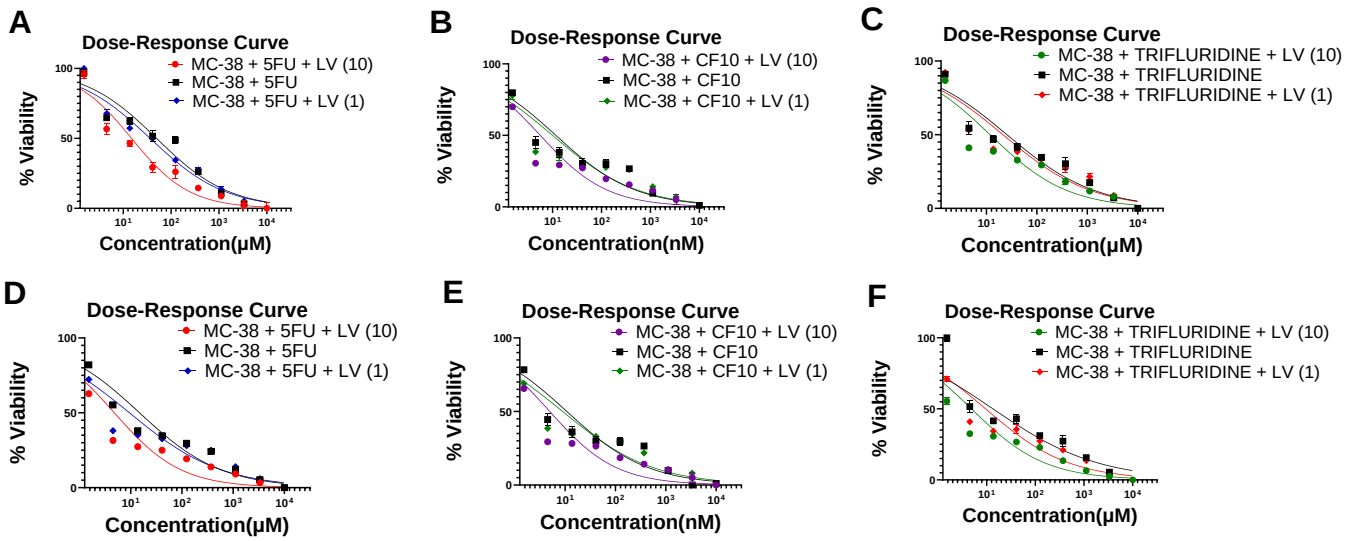

Supplementary Fig. S7. Summary of GI50 values for MC38 CRC cell line for CF10, 5FU, TFT, and ± LV combination. CF10 is much more potent to CRC cell than FP drugs.

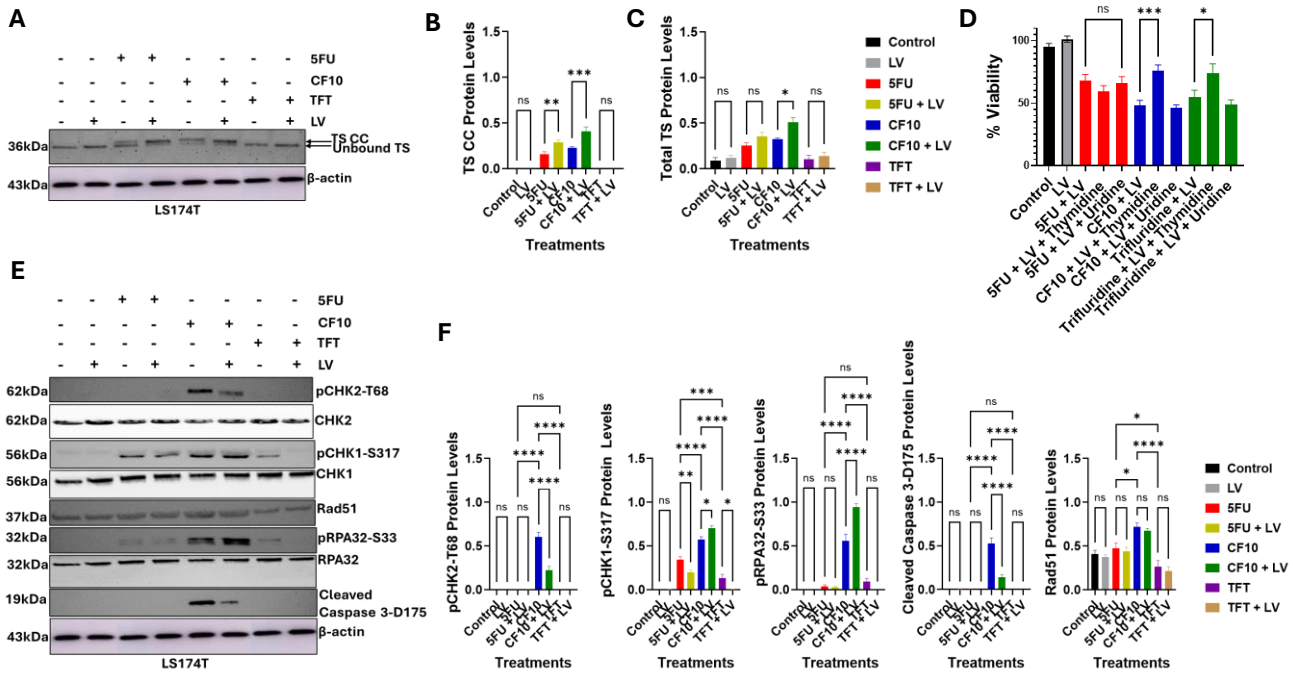

Supplementary Fig. S8. CF10 promotes TS classic complex (TS CC) formation and activates the ATR/Chk1 and ATM/Chk2 DNA damage response pathways in LS174T cells under folate-restricted culture conditions. **A**, Western blot for 5-FU ± LV, CF10 ± LV, and TFT ± LV detecting the TS CC and unbound TS; **B,C** Quantification of TS CC and total TS levels; **D**, effect of thymidine (80 uMol) and uridine (1 mMol) co-treatment on HCT-116 cell viability in FR media for 5-FU+LV (red), CF10+LV (blue), and TFT+LV (green). FP+LV was dosed at IC50 for 48h shown in Figure 2. Experiments done in triplicate ± SEM (***p ≤ 0.0002, **p ≤0.002, *p ≤ 0.03). Decreased cell viability for CF10+LV and TFT+LV is partly reversed by thymidine co-treatment but not for 5-FU+LV. **E**, Western blot for 5-FU ± LV, CF10 ± LV, and TFT ± LV detecting protein biomarkers for activation of the ATR/Chk1 (pChk1-S317, pRPA32-S33) and the ATM/Chk2 (pChk2-T68) DNA damage response pathways. Upregulation of the homologous recombination

protein Rad 51 involved in DNA double strand break repair and of cleaved caspase 3 is also shown. **F**, quantification of **E** for pChk1-S317; pRPA32-S33; Rad 51 levels from densitometry of **E**.

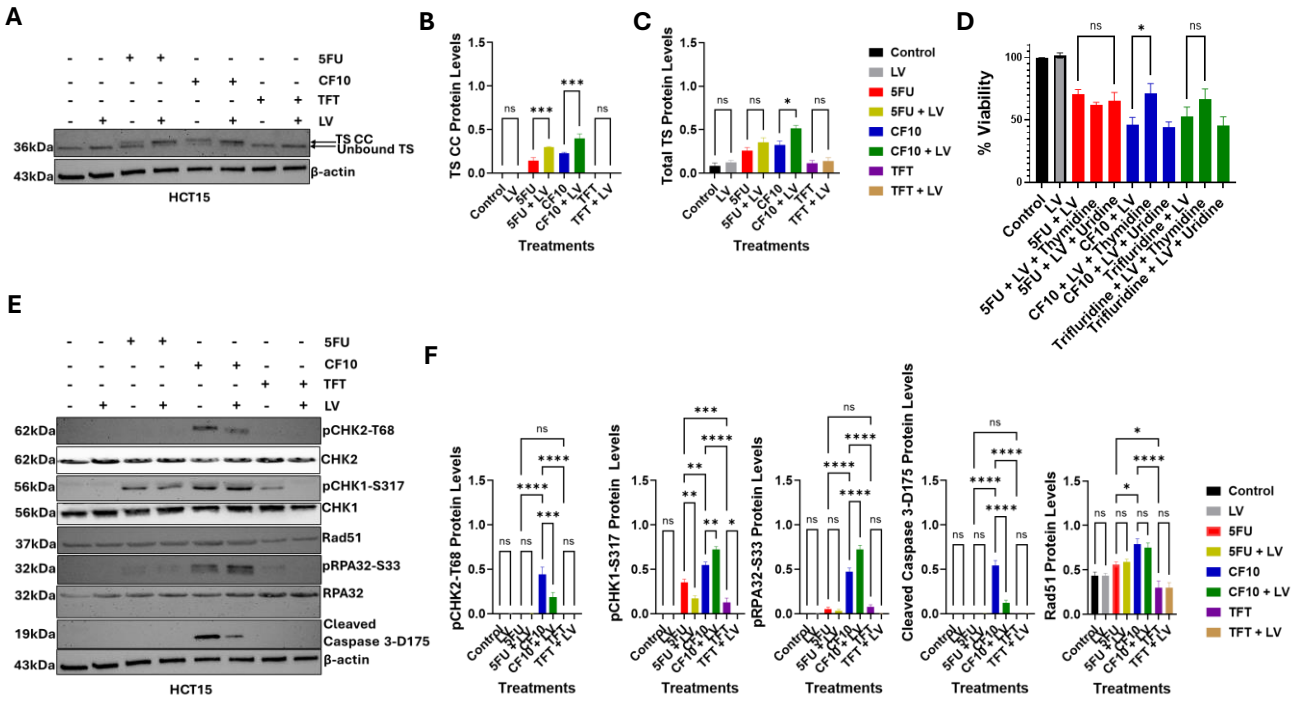

Supplementary Fig. S9. CF10 promotes TS classic complex (TS CC) formation and activates the ATR/Chk1 and ATM/Chk2 DNA damage response pathways in HCT15 cells under folate-restricted culture conditions. **A**, Western blot for 5-FU ± LV, CF10 ± LV, and TFT ± LV detecting the TS CC and unbound TS; **B,C** Quantification of TS CC and total TS levels; **D**, effect of thymidine (80 uMol) and uridine (1 mMol) co-treatment on HCT-116 cell viability in FR media for 5-FU+LV (red), CF10+LV (blue), and TFT+LV (green). FP+LV was dosed at IC50 for 48h shown in Figure 2. Experiments done in triplicate ± SEM (***p ≤ 0.0002, **p ≤0.002, *p ≤ 0.03). Decreased cell viability for CF10+LV and TFT+LV is partly

reversed by thymidine co-treatment but not for 5-FU+LV. **E**, Western blot for 5-FU ± LV, CF10 ± LV, and TFT ± LV detecting protein biomarkers for activation of the ATR/Chk1 (pChk1-S317, pRPA32-S33) and the ATM/Chk2 (pChk2-T68) DNA damage response pathways. Upregulation of the homologous recombination protein Rad 51 involved in DNA double strand break repair and of cleaved caspase 3 is also shown. **F**, quantification of **E** for pChk1-S317; pRPA32-S33; Rad 51 levels from densitometry of **E**.

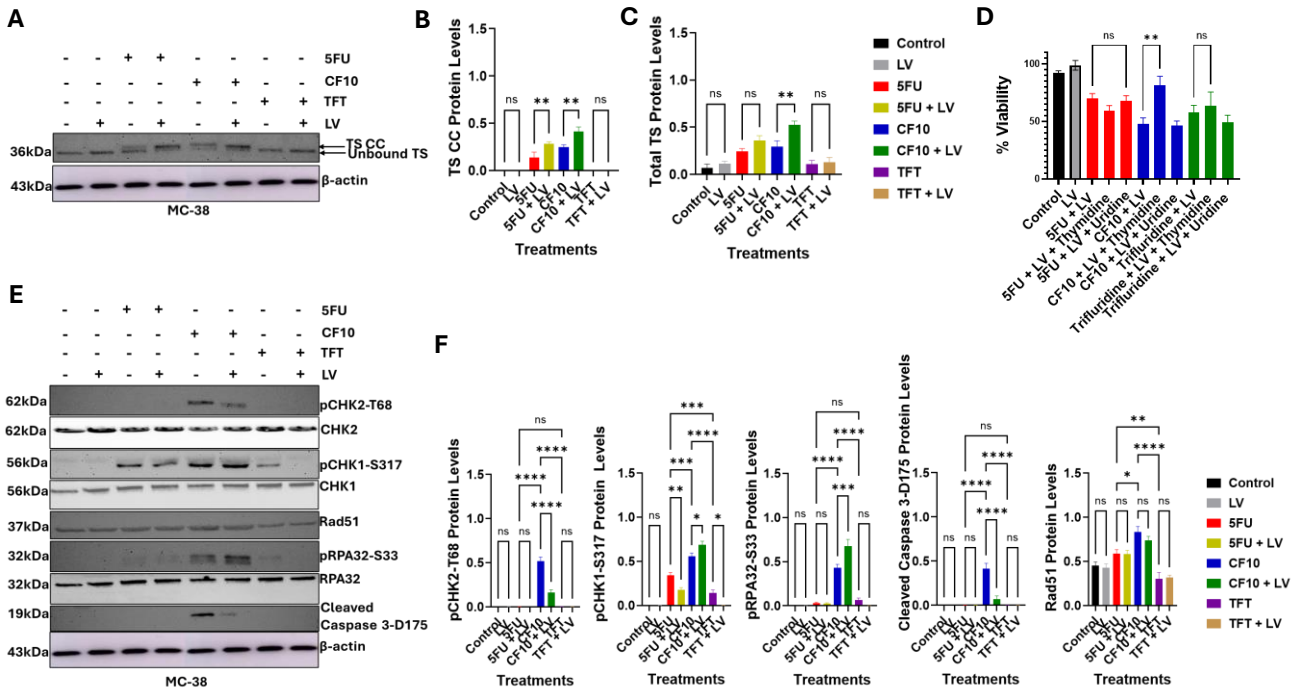

Supplementary Fig. S10. CF10 promotes TS classic complex (TS CC) formation and activates the ATR/Chk1 and ATM/Chk2 DNA damage response pathways in MC38 cells under folate-restricted culture conditions. **A**, Western blot for 5-FU ± LV, CF10 ± LV, and TFT ± LV detecting the TS CC and unbound TS; **B,C** Quantification of TS CC and total TS levels; **D**, effect of thymidine (80 uMol) and uridine (1 mMol) co-treatment on HCT-116 cell viability in FR media for 5-FU+LV (red), CF10+LV (blue), and TFT+LV (green). FP+LV was dosed at IC50 for 48h shown in Figure 2. Experiments done in triplicate ± SEM (***p ≤ 0.0002, **p ≤0.002, *p ≤ 0.03). Decreased cell viability for CF10+LV and TFT+LV is partly reversed by thymidine co-treatment but not for 5-FU+LV. **E**, Western blot for 5-FU ± LV, CF10 ± LV, and TFT ± LV detecting protein biomarkers for activation of the ATR/Chk1 (pChk1-S317, pRPA32-S33) and the ATM/Chk2 (pChk2-T68) DNA damage response pathways. Upregulation of the homologous recombination

protein Rad 51 involved in DNA double strand break repair and of cleaved caspase 3 is also shown. **F**, quantification of **E** for pChk1-S317; pRPA32-S33; Rad 51 levels from densitometry of **E**

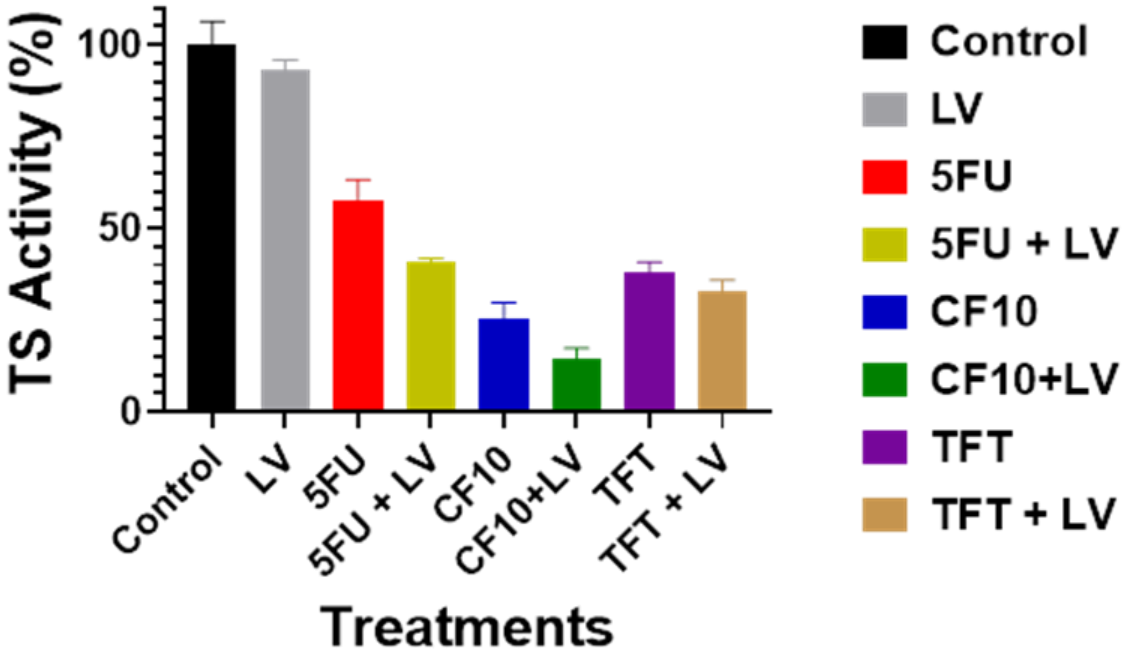

Supplementary Fig. S11. CF10 and CF10/LV are effective at reducing TS enzymatic activity. CF10 and LV were used at 10 nM while 5-FU and TFT were used at 100 nM. TS activity was determined using a ^{3}H-release assay by scintillation counting with activity expressed as %-activity relative to untreated controls. Drug treatment was for 24h in HCT-116 cells.

.

(A)

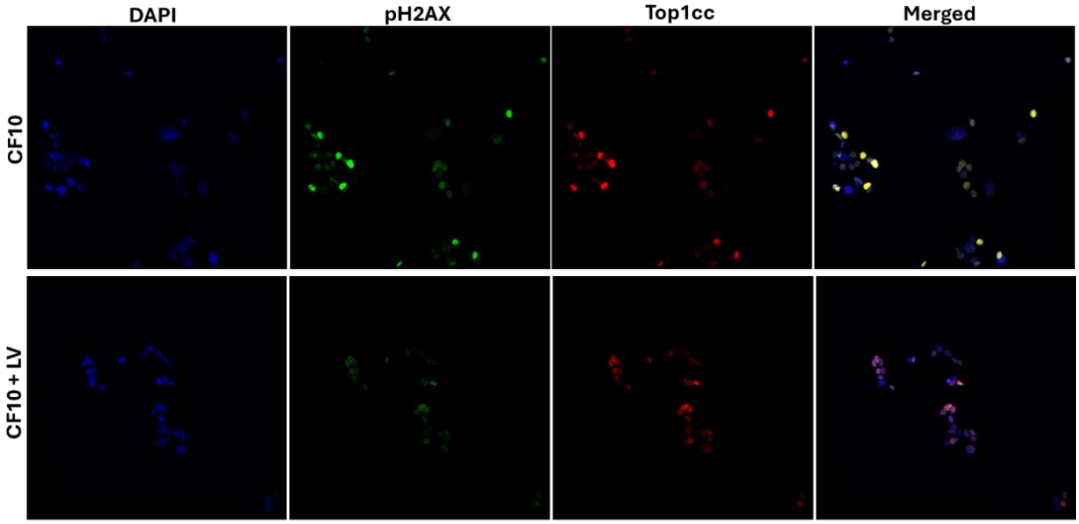

Immunofluorescence imaging of pH2AX and Top1cc in HCT-116 cells following treatment with CF10 or CF10 + LV

(B)

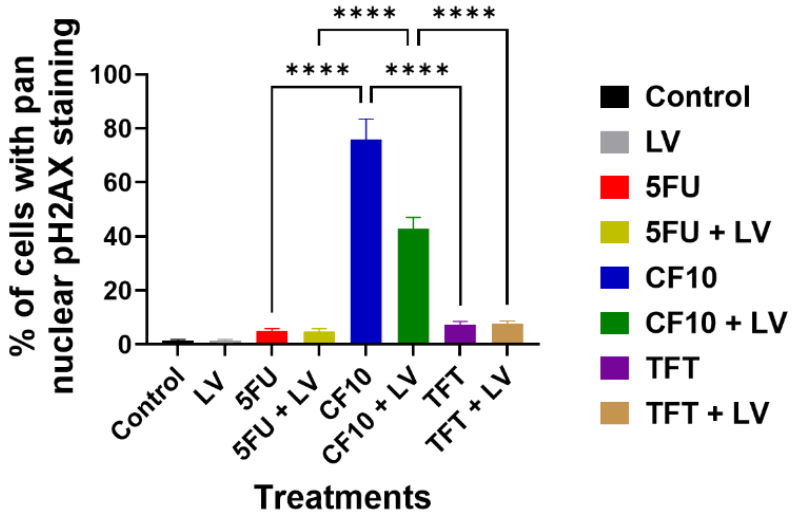

Quantification imaging of pH2AX in HCT-116 cells. ****p ≤ 0.0001

Supplementary Fig. S12. CF10 and CF10/LV induce Top1cc in HCT-116 cells (A) and are much more potent than 5-FU±LV or TFT± LV at inducing pH2AX, a marker of DNA DSBs (B).

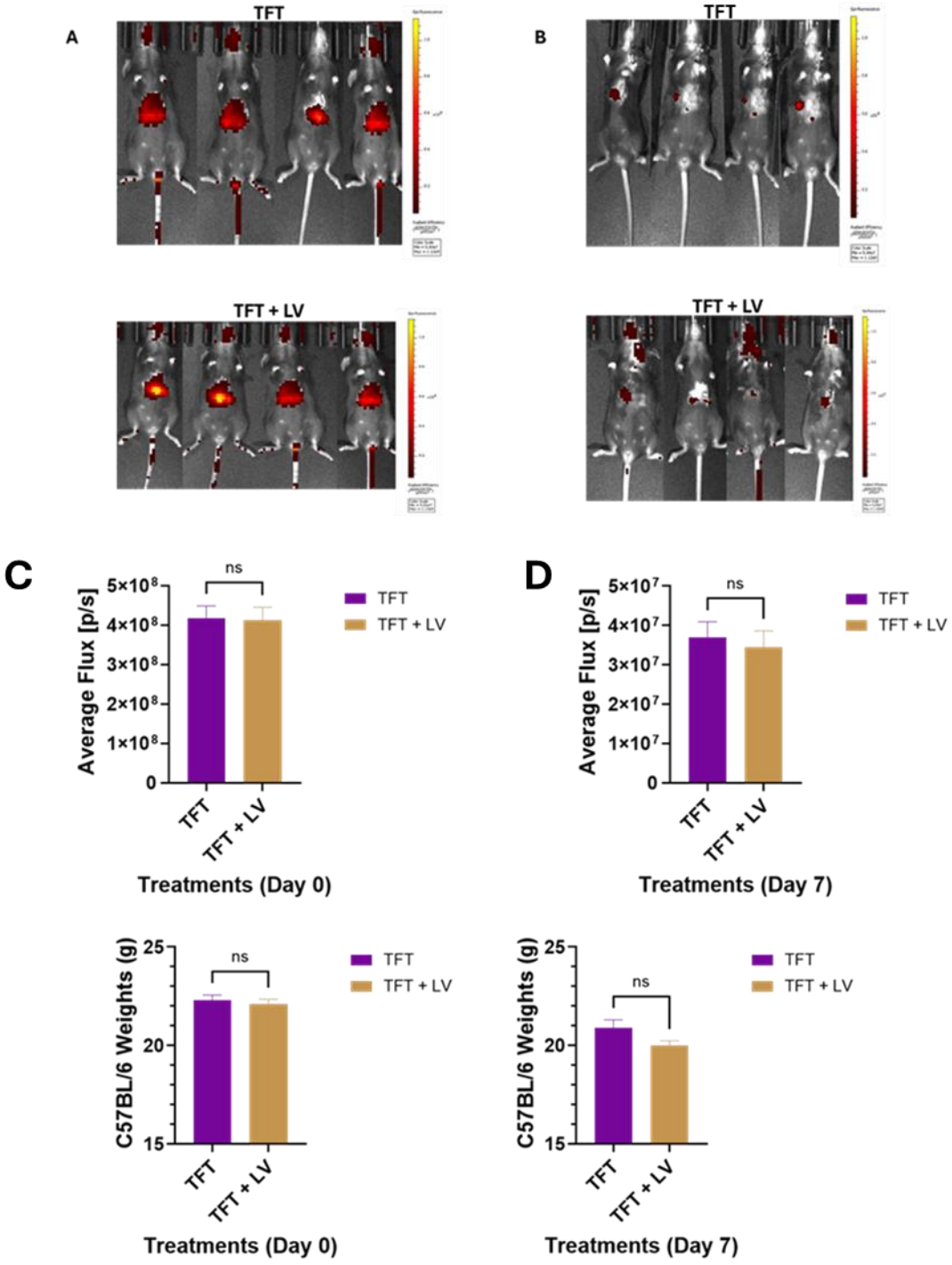

Supplementary Fig. S13. TFT and TFT/LV are effective in a liver-metastatic CRC model under conditions of human-like folate levels. **A,B** IVIS images of tumor burden for indicated treatments at day 0 (**A**) and day 7 (**B**) post-treatment.

(**C**) Tumor flux pre-treatment (top) and post-treatment (bottom). (**D**) Mice weights pre-treatment (top) and post-treatment (bottom).

CHAPTER 5

CF10/LV Overcomes Acquired Resistance to 5-FU/LV in Colorectal Cancer Cells Through Downregulation of the c-Myc/ABCB5 Axis

Charles Chidi Okechukwu[1,2], William H. Gmeiner[2]

[1]Integrative Physiology and Pharmacology Graduate Program, Wake Forest University School of Medicine, Winston-Salem, NC 27157 USA

[2]Department of Cancer Biology, Wake Forest University School of Medicine, Winston-Salem, NC 27157 USA

Correspondence to: Prof. William H. Gmeiner, Wake Forest University School of Medicine, Medical Center Blvd, Winston-Salem, NC 27055. Phone: 336-716-6216; Fax: 336-716-0255; E-mail bgmeiner@wakehealth.edu

Received: date month year

Abstract

Aim: Acquired resistance to 5-fluorouracil/leucovorin (5-FU/LV) frequently develops during treatment of metastatic colorectal (mCRC) but the causes are incompletely understood. We aim to: (i) identify the causes of 5-FU/LV resistance under physiological folate; and (ii) to determine if a polymeric fluoropyrimidine (FP) CF10 remains potent to CRC cells selected for 5-FU/LV-resistance.

Methods: 5-FU/LV-resistant CRC cells were selected by repeated passage with increasing 5-FU/LV concentrations and resistance factors were calculated from dose response studies. Basal and treatment-induced thymidylate synthase (TS), Myc, and ABCB5 were determined by RT-qPCR and Western blot. TS activity was determined using an *in situ* ^{3}H-release assay. DNA topoisomerase 1 cleavage complexes (Top1cc) and DNA double strand breaks (DSBs) were determined by immunofluorescence.

Results: Acquired resistance to 5-FU/LV with physiological folate was associated with a <1.5-fold increase in basal TS levels however with either 5-FU/LV or CF10/LV treatment TS levels were elevated ~5-fold by Western blot but only ~2-fold by RT-qPCR. CF10 remained very potent to CRC cells selected for 5-FU/LV resistance and CF10 effectively induced TS ternary complex formation and inhibited TS catalytic activity in 5-FU/LV-resistant CRC cells. c-Myc was expressed at ~4-fold higher levels in 5-FU/LV-resistant CRC cells but Myc was barely detectable with CF10/LV treatment. The Myc-target ABCB5 which is an established factor in resistance to 5-FU and other drugs was substantially downregulated with CF10/LV but not 5-FU/LV treatment.

Conclusion: Acquired 5-FU/LV resistance was associated with FP-induced TS, elevated Myc and ABCB5. There is minimal cross-resistance to CF10 in 5-FU/LV-resistant CRC cells consistent with its use in treating 5-FU/LV-resistant mCRC.

Keywords: fluoropyrimidine, thymidylate synthase, DNA Topoisomerase 1, Myc, ABCB5, CF10

Introduction

The fluoropyrimidine (FP) drug 5-fluorouracil (5-FU) is central to the management of metastatic colorectal cancer (mCRC) with 5-FU-based regimens (FOLFOX, FOLFIRI) being administered to most mCRC patients[1]. While the majority of mCRC patients initially respond to 5-FU-based chemotherapy, acquired resistance develops in nearly all patients[2] [**Figure 1**]. Thus, while survival for mCRC patients enrolled in clinical trials now exceeds 30 months during which many patients receive three or more lines of FP-based chemotherapy, long-term survival remains rare[3]. An increased understanding of the causes of acquired 5-FU resistance thus remains an important objective in cancer research as does the development of next generation FP therapeutics to overcome the limitations of current 5-FU-based therapy[4].

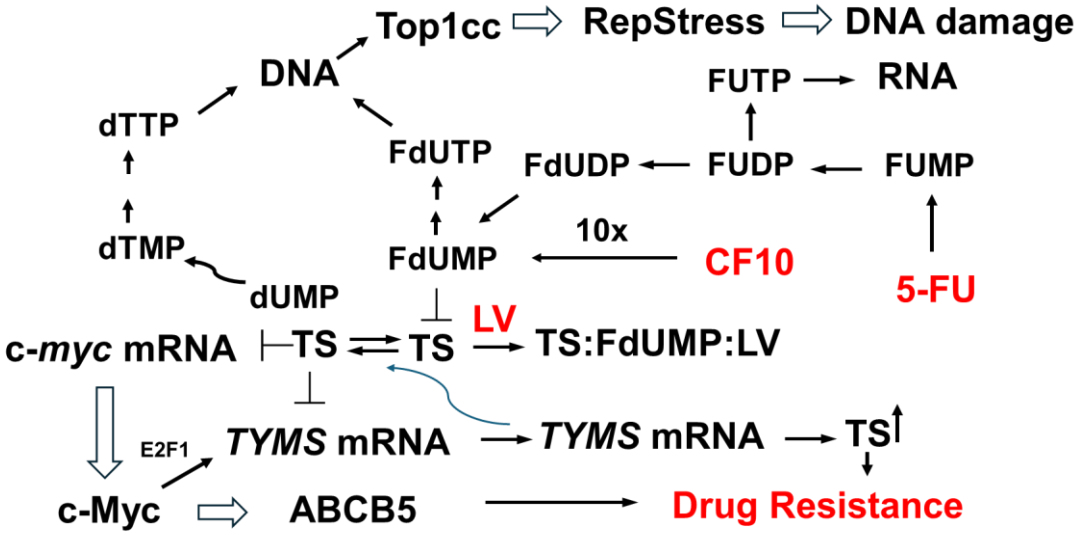

Figure 1. Resistance to 5-FU/LV converges on lack of efficacy in inhibiting TS due to: (i) elevated TS expression; (ii) inefficient conversion to the TS inhibitory metabolite FdUMP; and/or (iii) activation of the c-Myc/ABCB5 axis. CF10 is efficiently converted to FdUMP resulting in strong TS inhibition even when the enzyme is expressed at elevated levels.

patients[11]. For this reason, 5-FU is nearly always administered with leucovorin (N^5-formyl tetrahydrofolate) for cancer treatment to promote TS inhibition despite 5-FU's inefficient conversion to FdUMP[12].

Multiple studies have investigated the mechanistic basis for 5-FU resistance in CRC[2]. A common theme among the majority of studies is that 5-FU resistance generally results from decreased TS inhibition that is due to either: (i) increased TS levels; (ii) decreased conversion of 5-FU to FdUMP; or (iii) increased breakdown of FdUMP or its cellular efflux [**Figure 1**]. To overcome resistance to 5-FU we developed CF10[13-16], a 2nd generation FP polymer that directly releases FdUMP. CF10 is much more potent that 5-FU to CRC cells (>300-fold on average in the NCI60 cell line screen)[13] and increased potency corresponds to strong TS inhibition by CF10 at correspondingly lower doses relative to 5-FU. In previous studies we have shown that FP polymers such as CF10 are highly effective in CRC cells selected for acquired resistance to 5-FU due to elevated TS expression[17]. In addition to its enzymatic function TS is an RNA binding protein that autoregulates its own expression and the expression of other proteins, notably c-Myc and p53, through mRNA binding and translational repression[18]. The function of TS as an RNA-binding protein is modulated by formation of the FdUMP/MeTHF/TS ternary complex which relieves autoregulation to enable increased TS expression under conditions of TS inhibition[19]. The binding affinity of TS for its own mRNA and for c-*myc* is similar[20]. Hence, strong TS inhibition that reduces binding of TS mRNA could decrease c-Myc levels due to increased binding of c-*myc* mRNA by TS, inhibiting its translation. Decreased Myc levels in turn alter its translational program

that is fundamental to determining the balance between proliferation and cell death[21]. Among the Myc targets that have an established role in mediating resistance to 5-FU[22] and other drugs is ABCB5[23] which is involved in promoting a cancer stem cell phenotype[24].

The purpose of this study is to characterize the role of TS elevation in CRC cells selected for acquired resistance to 5-FU/LV under conditions of human-like folate levels and to determine if CF10 remains effective in these cells. Although multiple previous studies have investigated acquired 5-FU resistance[2,25-27] and shown increased TS and *TYMS* levels this is the first study to adapt cells to culture medium that includes human-like folate levels[28] and to select for resistance to 5-FU/LV in similar conditions as occur clinically. We find that in multiple CRC cell lines there is minimal constitutive change in TS at either the protein or mRNA level but that 5-FU/LV treatment results in elevated TS levels that contribute to 5-FU/LV resistance. Given the interplay between TS and Myc regulation[18] we also investigate perturbation in Myc and its direct transcriptional target ABCB5. We find that CF10 remains effective in CRC cells selected for 5-FU/LV resistance despite causing similar induction of TS and this retained potency is associated with downregulation of c-Myc and ABCB5 at both the mRNA and protein levels.

Methods

Cell lines and Drugs

All parental colorectal cancer (CRC) cells (HCT116 (RRID:CVCL_0291), HCT15 (RRID:CVCL_0292), LS174T (RRID:CVCL_1384), and MC38 (RRID:CVCL_B288)) and 5FU-LV resistant CRC cells ($HCT116^R$, $HCT15^R$, $LS174T^R$, $MC\text{-}38^R$) were cultured using folate-restricted (FR) media (folic acid-free RPMI 1640 supplemented with 40nM of 5-methyltetrahydrofolate and 0.1nM of sodium L-ascorbate)[28], confirmed by short tandem repeat analysis, and repeatedly tested negative for Mycoplasma. The 5FU/LV resistance CRC cells were generated through a repeated passage in drug-containing FR media (0.1 to10μM) containing 5FU+LV. Clinical grade 5-FU (50 mg/mL) was purchased from the Baptist Hospital clinical pharmacy, and its concentrations were calculated based on the dilution of the established stock concentration. CF10 was obtained from ST Pharma, confirmed by high-resolution mass spectrometry, and dissolved in 0.9% sterile saline. Its concentrations were matched to deliver equivalent nucleoside content to an established dose of 5-FU based on UV absorbance at 260 nm.

Cell Viability and Resistant Assay

CRC^P and CRC^R cells were plated in 96-well, white flat bottom plates, allowing 48 h for the cells to adhere to the plate and begin to grow exponentially until they reached about 25% confluency. To test for 5-FU/LV resistance, 2500 cells per well, both the CRC Parental (CRC^P) and 5-FU/LV-resistant (CRC^R) cells, were seeded

in 96 well plates and allowed to attach for 24 hours. After 24 hours, the cells were pre-treated for 2 hours with LV before adding 5-FU and then incubated for 96 hours at 37^{o}C in 5% CO_2. Cell viability was assessed using Aqueous-one (Promega) following the manufacturer's instructions. Resistance factors were calculated based on the ratio of IC50 values for CRC^P and CRC^R cells. All experiments were performed in triplicate.

Clonogenic assay

A modified clonogenic assay assessed the potency of CF10 and 5-FU in CRC^P and CRC^R cells. The CRC cells were plated in 24-well plates in FR media, and after 24 hours, they were treated with the indicated concentration of CF10 or 5-FU for 72 hours. The media were replaced after drug treatment, while the cells were allowed to grow for 168 hours. Cell proliferation was evaluated using the Aqueous One (Promega) reagent, following the manufacturer's instructions, after the cell solution was transferred to 96-well plates. Apoptosis was evaluated using Caspase 3/7-Glo reagent (Promega) following the manufacturer's instructions.

Western Blotting

Proteins were isolated, and their differential expressions were analyzed by Western blot, as described previously[15]. Briefly, both CRC^P and CRC^R treated cells (LV, 5FU, 5FU+LV, CF10, CF10+LV) were lysed using RIPA buffer (50 mM Tris HCl at pH 7.4, 150 mM NaCl, 1% Triton X-100 or NP-40, 0.5% sodium deoxycholate, 0.1% SDS, 1 mM EDTA, and 10 mM NaF freshly supplemented with protease and phosphatase inhibitors). The protein concentrations were quantified

using a Bradford assay (Bio-Rad), and the samples were normalized for equal loading. All samples were then heated to 95°C for 10 min in the presence of 6x Laemmli buffer (Boston Bio-Products; Milford, MA, USA). The proteins were resolved using SDS-PAGE, and their expression was analyzed following immunoblotting using specific antibodies. The following antibodies were used in this study: Thymidylate Synthase (Cell Signaling Technology Cat# 3766, RRID: AB_2210584), Myc (Cell Signaling Technology Cat# 18583, RRID:AB_2895543),p53 (Cell Signaling Technology Cat# 2524, RRID:AB_331743), ABCB5 (Thermo Fisher Scientific Cat# PA5-114801, RRID:AB_2899437), and β-actin (Santa Cruz Biotechnology Cat# sc-47778, RRID: AB_626632).

Immunofluorescence Assay

Immunofluorescence detection of pH2AX (Cell Signaling Technology Cat# 2577, RRID:AB_2118010) was performed in drug-treated both CRC^P and CRC^R cells that were fixed and permeabilized using 100% cold methanol and then processed as previously described[29]. Top1cc were detected using a primary antibody specific to the cleavage complex (gift of Dr. S. Kaufmann) using procedures like those previously described[29]. Top1cc foci were captured using Olympus Confocal Laser Scanning Microscope Fluoview FV3000 (RRID:SCR_017015) and Quantification of Top1cc foci was done via ImageJ by counting at least 100 cells that were declared positive if they had >50 foci per nuclei.

RNA isolation and real-time PCR

Total RNA was isolated from CRC^P and CRC^R cells treated with LV, 5-FU, 5-FU + LV, CF10, CF10 + LV using RNeasy mini kit QIAGEN (RRID:SCR_008539). The Thermo Scientific NanoDrop One/OneC Microvolume UV Vis Spectrophotometer (RRID:SCR_023005) was used to determine the quality and quantity of RNA samples. cDNA synthesis was performed using the iScript™ cDNA Synthesis Kit (Bio-Rad #:1708891). Realtime PCR was performed using Bio-Rad CFX96 Real-Time PCR Detection System (RRID:SCR_018064) and the iTaq SYBR Green supermix (Bio-Rad #: 1725121). The primers for qRT-PCR were all purchased from OriGene Technologies Inc.

TS (human): Forward: 5′-GGTGTTTTGGAGGAGTTGCTGTG-3′,

Reverse: 5′-GGAGAATCCCAGGCTGTCCAAA-3′;

Myc (human): Forward: 5′-CCTGGTGCTCCATGAGGAGAC-3′,

Reverse: 5′-CAGACTCTGACCTTTTGCCAGG-3′;

ABCB5 (human): Forward: 5′-TTTGCCTATGCGGCAGGGTTTC-3′,

Reverse: 5′-CAAAACGAGCGTTTCTCCGATGG-3′;

β-actin (human): Forward: 5′- CACCATTGGCAATGAGCGGTTC-3′,

Reverse: 5′-AGGTCTTTGCGGATGTCCACGT-3′,

β-actin were used as an internal standard to normalize the relative expressions of the mRNAs. The RT-PCR reaction settings were Stage 1: Activation: 50 °C for 2 min; Stage 2: pre-soak:95 °C for 10 min; Stage 3: Denaturation: 95 °C for 15 sec,

Annealing: 60°C for 1 min for 40 cycles; Stage 4: Melting curve: 95°C for 15 sec, 60°C for 15 sec, 95°C for 15 sec. The relative expressions were analyzed by the $2^{-\Delta\Delta Ct}$ method and experiments were performed in triplicate.

TS Activity Assay

A TS *in situ* activity assay was performed as previously described[30]; PMID: 10554030) to provide a quantitative indication of intracellular inhibition of TS activity following drug treatment. ~$0.5x10^6$ HCT-116 (RRID:CVCL_0291) and HCT116R cells were plated in each well of a 6-well plates and cells were allowed to attach for 24h then treated with either LV, 5-FU, 5-FU + LV, CF10, or CF10 + LV for 48h. For the last 2h, [5-^{3}H]-2'-deoxyuridine (Moravek) 0.16 Ci/mmol; final concentration 2.5 μM was present. 150 μL of media from each well was added to an ice-cold suspension containing 750 μL of charcoal with 0.5% T-70 dextran and 2.5% BSA) and 150 μL of 35% trichloroacetic acid. After centrifugation a portion of the supernatant was counted by liquid scintillation counting and enzyme activities were expressed as a percent relative to drug-free control.

Statistical Analysis

GraphPad Prism 10.2.0 GraphPad Prism (RRID:SCR_002798) was used for all statistical analyses. Experiments were conducted in triplicate ± SEM, used for analysis, and appropriate one-way ANOVA tests with recommended Tukey corrections were conducted, with $p < 0.05$ indicating significance.

Results

Acquired resistance to 5-FU/LV occurs through treatment-induced TS elevation

In multiple previous studies 5-FU-resistant CRC cells were generated through repeated passage in media containing increasing concentrations of 5-FU [2,25-27]. However, in the present studies we repeatedly passaged human CRC cells (HCT116, LS174T, HCT15) in the presence of 5FU/LV since 5-FU is nearly always used with LV in combination chemotherapy regimens for CRC. We also performed the selection by repeated passage in media with restricted folate levels to better simulate human physiology. After selection by repeated passage of parental cells (e.g. $HCT116^{P}$) over >4 months in 5-FU/LV, we tested cells for the extent of resistance and found HCT116 5FU/LV-resistant ($HCT116^{R}$) cells were 27.3-fold less sensitive to 5-FU/LV relative to the corresponding parental cells [**Figure 2A**] [**Table 1]**. Resistant LS174T and HCT15 cells showed similar resistance factors relative to the corresponding parental cells (27.1- and 19.9-fold [**Figure 2A**] [**Table 1**]. Importantly, all CRC cell lines selected for resistance to 5-FU/LV remained highly sensitive to CF10 and $HCT116^{R}$ cells were only 3.14-fold less sensitive to CF10 than $HCT116^{P}$ cells with other CRC cell lines showing similar moderate changes in sensitivity [**Figure 2B**] [**Table 1**].

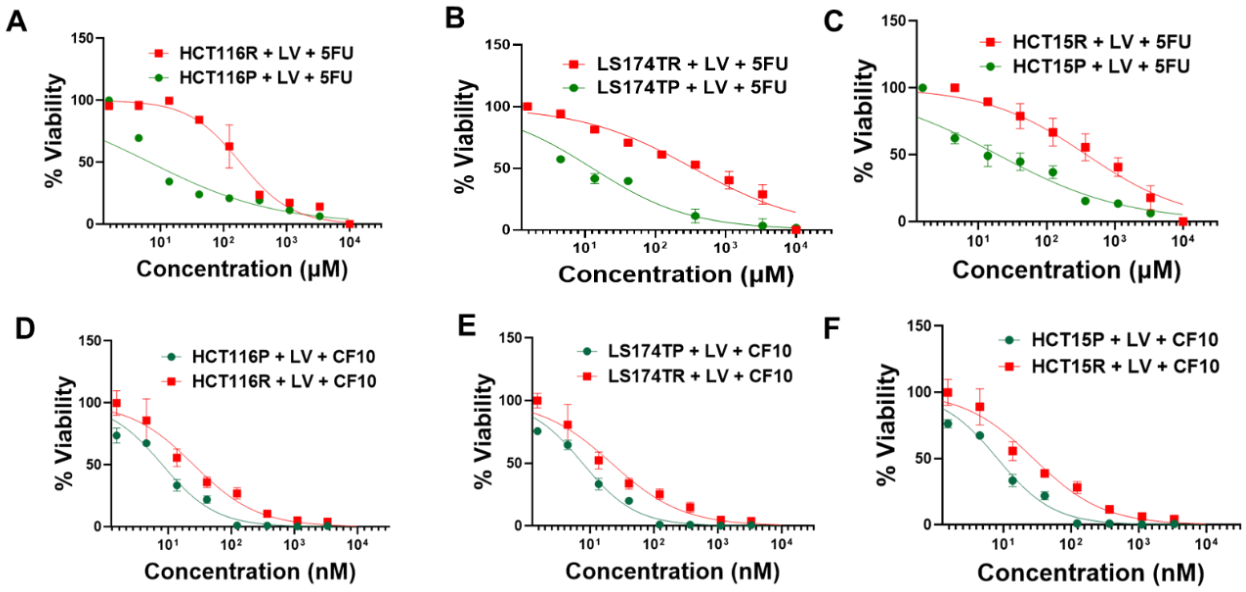

Figure 2. Dose response of parental (green) and 5-FU/LV-resistant (red) CRC cells to 5-FU/LV in HCT116 (A), LS174T (B), and HCT15 (C) cells. Dose response to CF10/LV is shown in HCT116 (D), LS174T (E), and HCT15 (F) parental (green) and 5-FU/LV-resistant (red) cells. IC50 values and resistance factors for each CRC cell line are summarized in Table 1.

Table 1. Summary of IC50 values for 5-FU/LV (μM) and CF10/LV (nM) and resistance factors.

CRC Cell line	(LV + 5FU) Treatment IC_{50} (μM)	Resistance Factor
HCT116P	6.70	27.3
HCT116R	183	
LS174TP	12.8	27.1
LS174TR	347	
HCT15P	19.2	19.9
HCT15R	383	

CRC Cell line	(LV + CF10) Treatment IC_{50} (nM)	Resistance Factor
HCT116P	8.07	3.14
HCT116R	25.3	
LS174TP	7.73	2.85
LS174TR	22.0	
HCT15P	8.23	3.40
HCT15R	28.0	

Since TS is an established target of 5-FU/LV we performed Western blot and RT-qPCR to determine to what extent resistance in selected cells was associated with increased *TYMS* expression and increased TS protein levels. Quantification of Western blot images revealed TS was upregulated ~2-fold in $HCT116^{R}$ cells [Figure 3A] and similar increases were observed for LS174T [Supplementary Figures 2 and 3], and HCT15 cells [Supplementary Figures 4 and 5]. RT-qPCR revealed less of an increase in *TYMS* mRNA, ~1.2-fold in $HCT116^{R}$ cells [Figure 3C] [Supplementary Figure 1] and in LS174T [Supplementary Figures 2 and 3], and HCT15 cells [Supplementary Figure 4 and 5]. We next investigated if TS levels were altered in response to treatment in FU/LV-R cells relative to parental cells. Treatment of $HCT116^{P}$ cells resulted in no significant change in TS mRNA or protein levels under any of the treatment conditions tested. However, TS mRNA levels were increased in $HCT116^{R}$ cells, and the magnitude of increase (~2-fold) was similar for both 5-FU/LV and CF10/LV treatment and this occurred with and without LV co-treatment [Figure 3C]. Similar trends were found for TS protein levels with 5-FU and CF10 treatment [Supplementary Figure 1], but the effects were larger at the protein level (~7-fold) than for *TYMS* mRNA (~2-fold)) in $HCT116^{R}$ cells [Figure 3A-C] and the other CRC cell lines selected for 5-FU/LV-resistance [Supplementary Figures 2-5]). Similar increases in TS were not detected with treatment in any of the parental CRC cell lines.

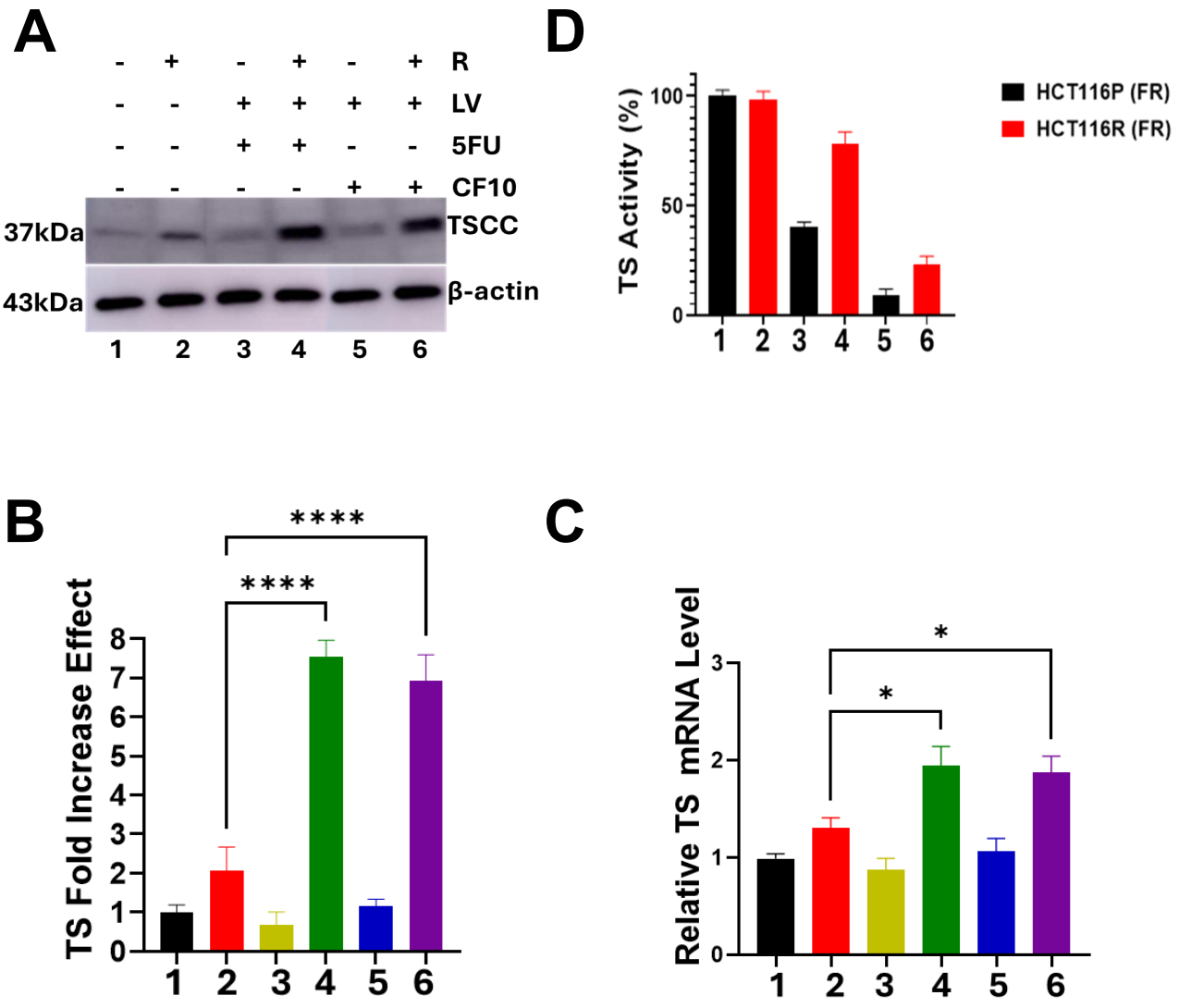

Figure 3. 5-FU/LV (10 mM, 1 mM) and CF10/LV (1 mM, 1 mM) treatment for 24h increase TS at both the protein (A,B) and mRNA (C) levels in HCT116^{R} cells but only CF10/LV promotes ternary complex formation (TSCC) and efficient inhibition of TS enzymatic activity (D). * p<0.03; **** p < 0.0001

To determine if increased TS levels induced by 5-FU/LV or CF10/LV treatment in FU/LV-R CRC cells were a cause of resistance we evaluated TS ternary complex formation based on decreased mobility on PAGE gels with Western blot detection (e.g. TS classic complex (TS CC) [**Figure 3A**]). We also evaluated TS enzymatic activity using a TS *in-situ* enzyme activity assay (TSIA) based on $^{3}H_2O$ formation from [5-^{3}H]-dUMP [**Figure 3D**]. The mobility of TS in untreated and 5-FU/LV treated cells was similar consistent with 5-FU/LV treatment (10 mM, 1 mM; 24h) not being effective in promoting TS ternary complex (TSCC) formation in HCT116^{R} cells [**Figure 3A**]. In contrast, with CF10/LV treatment (1 mM, 1 mM; 24h) TS mobility was decreased consistent with TS ternary complex formation. We also performed TSIA assays evaluating treatment effects on inhibiting TS enzymatic activity. CF10/LV was effective in reducing TS enzymatic activity in both HCT116^{P} and HCT116^{R} cells. In contrast, 5-FU/LV was less effective than CF10/LV in reducing TS enzymatic activity in HCT116^{P} cells not effective at reducing TS enzymatic activity in HCT116^{R} cells [**Figure 3D**]. The corresponding data for the single drugs in HCT116^{R} cells showed similar trends [**Supplementary Figure 1**] and in LS174T and HCT15 cells **[Supplementary Figures2-5].** Collectively these studies showed that the increased TS levels in CRC^{R} cells render 5-FU/LV ineffective at inducing TS ternary complex formation and inhibiting TS enzymatic activity while CF10/LV remains effective in TS inhibition in CRC^{R} cells despite higher enzyme levels.

Myc is elevated in 5-FU/LV-resistant cells and is downregulated by CF10/LV

Myc is elevated in multiple cancers, including CRC, driving proliferation, and upregulating a transcriptional program that contributes to drug resistance. Myc

expression is translationally regulated by TS binding to its cognate mRNA[20]; hence treatments that affect TS levels could also alter Myc, affecting proliferation and drug resistance. The pattern of Myc expression in CRC^R cells parallels that for TS at baseline in the absence of treatment with Myc levels ~4-fold higher at the protein level and ~2-fold higher at the mRNA level in $HCT116^R$ cells relative to parental cells [**Figure 4A-C**] [**Supplementary Figure 6**] with similar trends in LS174T and HCT15 cells [**Supplementary Figures 7-10**]. As for TS, treatment of parental cells with either 5-FU/LV or CF10/LV had minimal effect on Myc levels. However, in contrast to the increase in TS levels observed with treatment in $HCT116^R$ cells treatment decreased Myc at both the mRNA and protein level in $HCT116^R$ cells. 5-FU/LV treatment decreased Myc mRNA and protein relative to non-treated control cells however Myc levels were still elevated 1.5-fold (mRNA) and 2-fold (protein) in 5-FU/LV-treated $HCT116^R$ cells relative to similarly treated $HCT116^P$ cells [**Figure 4A-C**]. The effect of CF10/LV on Myc levels in $HCT116^R$ cells was striking with Myc barely detectable at either the mRNA or protein level in $HCT116^R$ cells with CF10/LV treatment [**Figure 4A-C**]. Similar effects on CF10/LV reduction of Myc levels were detected in $LS174T^R$ and $HCT15^R$ cells [**Supplementary Figures 7-10**].

The effects of elevated Myc in mediating resistance to 5-FU and other drugs have implicated ABCB5 as an important direct target of Myc that mediates drug resistance[22]. To determine if ABCB5 levels were altered in CRC cells selected for 5-FU/LV acquired resistance we evaluated ABCB5 levels both by Western blot [**Figure 4D,E**] [**Supplementary Figure 6**] and RT-qPCR [**Figure 4F**]

[**Supplementary Figure 6**]. The principal difference in Western blots for ABCB5 in 5-FU/LV-resistant cells relative to parental cells was the appearance of three additional bands with slightly increased mobility relative to the major band detected at ~89kDa. ABCB5 undergoes alternative splicing to produce multiple protein products, and the new bands detected in 5-FU/LV-resistant CRC cells are likely due to alternatively spliced products (proteomics analysis is in progress). Treatment with 5-FU/LV resulted in slight intensification of one band [**Figure 4D,E**]. In contrast, none of the additional bands attributed to ABCB5 alternative splicing were detected in $HCT116^{R}$ cells treated with CF10/LV. Further, CF10/LV treatment resulted in ABCB5 mRNA levels being decreased to barely detectable levels, similar as observed for Myc mRNA in $HCT116^{R}$ cells with CF10/LV treatment.

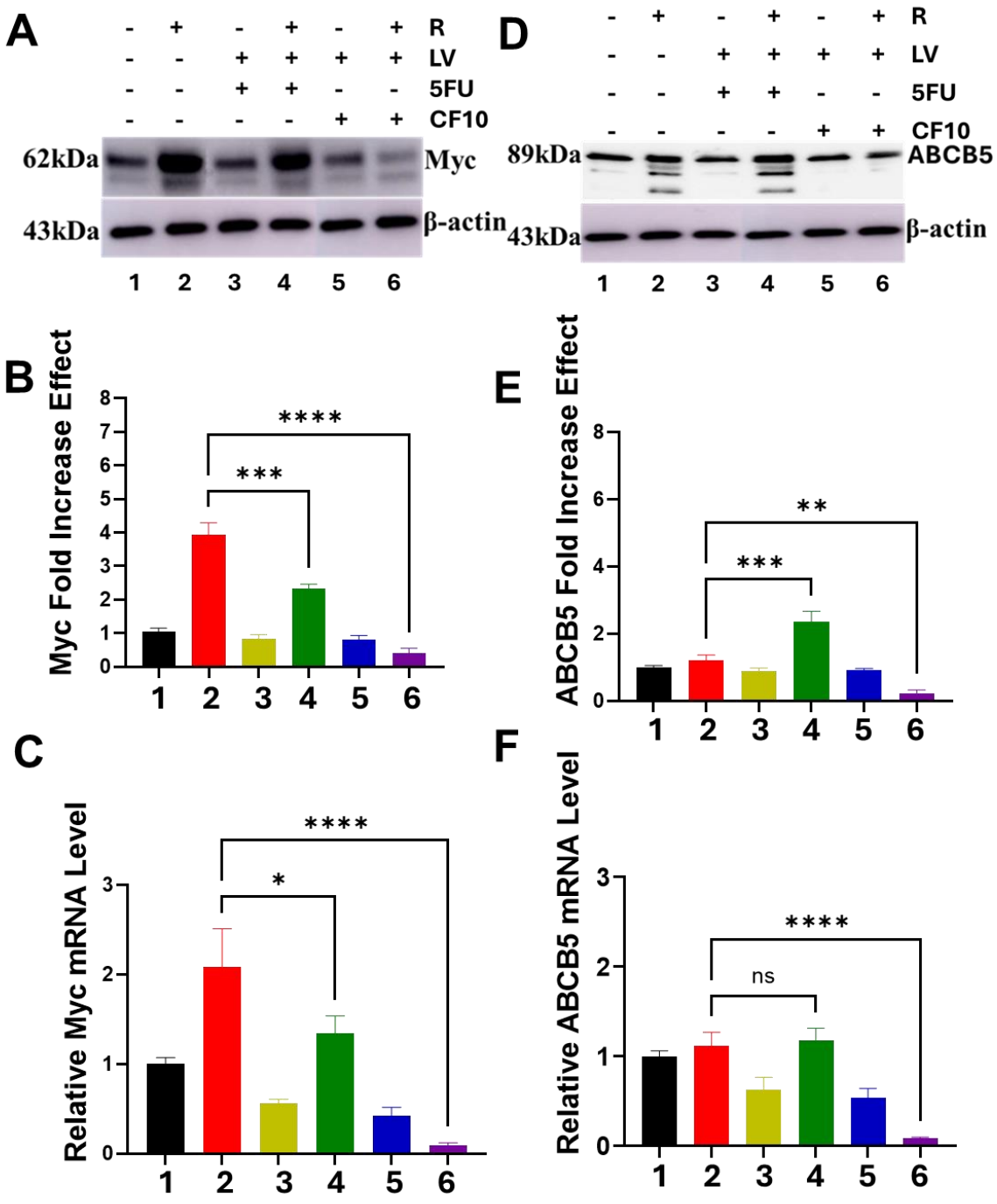

Figure 4. Myc is elevated in 5-FU/LV-resistant HCT116^{R} cells, but CF10/LV decreases levels of Myc and the Myc-target ABCB5 at both the protein and mRNA level. Western blots for Myc (A) and ABCB5 (D). Quantification of the Western blot

images by densitometry is shown for Myc (B) and ABCB5 (E). Quantification of mRNA levels by RT-qPCR is shown for Myc (C) and ABCB5 (F). *p<0.03, **p<0.002, ***p<0.002, ****p<0.0001.

CF10/LV induces Top1cc and DNA DSBs in 5-FU/LV-resistant CRC cells.

CF10 was shown to induce DNA topoisomerase 1 cleavage complex (Top1cc) formation in CRC cells[13], and it displayed mechanistic similarities to Top1cc poisons such as camptothecin in COMPARE analysis of data from the NCI60 cell line screen[31,32]. To determine if Top1cc formation and induction of DNA double strand breaks also occurs in CRC cells selected for 5-FU/LV-resistance upon treatment with CF10/LV we performed immunofluorescence studies using antibodies specific for Top1cc[29] and gH2AX, a biomarker of DNA double strand breaks [Figure 5] [Supplementary Figures 11-16]. Top1cc were evident in nearly all $HCT116^R$ cells treated with CF10/LV. Immunostaining for gH2AX was also evident in nearly all CF10/LV-treated $HCT116^R$ cells but not for 5-FU/LV-treated $HCT116^R$ cells. Our results are consistent with CF10/LV cytotoxicity being mediated through dual targeting of TS/Top1 in CRC cells selected for acquired 5-FU/LV resistance but with 5-FU/LV not effective in causing DNA DSBs in these cells.

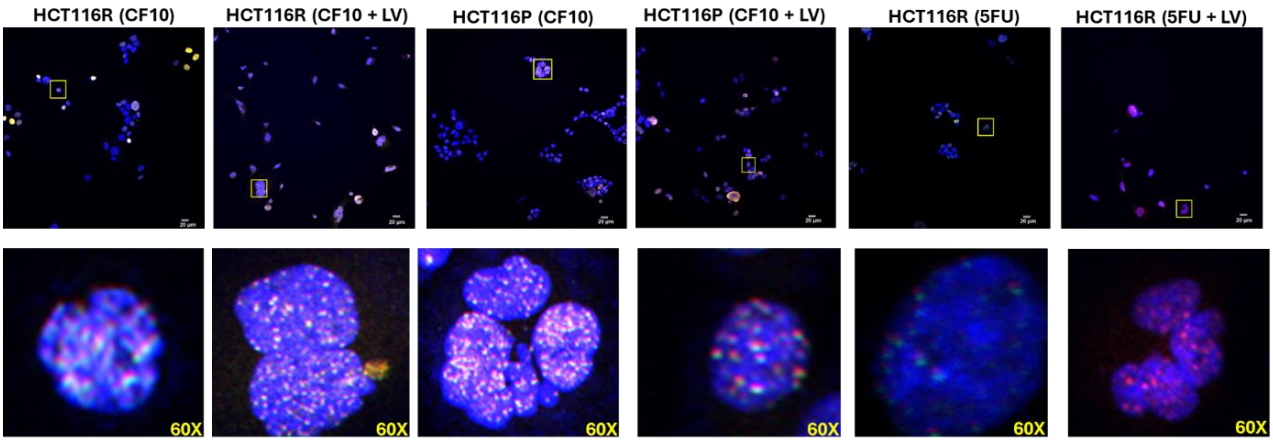

Figure 5. CF10/LV is effective at inducing Top1cc and gH2AX, a biomarker of DNA double-strand breaks in both $HCT116^{R}$ and $HCT116^{P}$ cells consistent with TS/Top1 dual targeting by CF10 in 5-FU/LV-resistant cells while 5-FU is relatively ineffective at causing DNA DSBs. Shown are merged images for DAPI (blue), gH2AX, (green), and Top1cc (red) for the indicated cell lines and treatment (5-FU 10mM, CF10 1mM, LV 1mM) for 24h. Complete images are included in [Supplementary Figures 11-16].

Discussion

This study characterizes three human CRC cell lines (HCT116, LS174T, HCT15) selected for acquired resistance to 5-FU/LV [Figure 1] in culture media that simulates human-like folate levels (FR media). All three CRC cell lines developed similar levels of 5-FU resistance (19.9-27.3-fold) [Figure 2] [Table 1] and these resistance levels were similar to CRC cell lines selected for resistance to 5-FU in standard media[2]. Because of its established role as a primary target of FP chemotherapy and mediator of 5-FU- resistance we evaluated TS expression at

the protein and mRNA levels at baseline and in response to treatment with either 5-FU or a next generation FP polymer CF10, with and without leucovorin co-treatment. In contrast to previous studies in which CRC cells selected for acquired resistance to 5-FU displayed elevated TS levels at baseline[26] the CRC^R cells selected for acquired resistance to 5-FU/LV showed no significant increase in TS at either the mRNA or protein level in the absence of treatment. However, treatment with 5-FU/LV and to a lesser extent CF10/LV increased TS levels and the effects were larger at the protein level that at the mRNA level [**Figure 3**] [**Supplementary Figures 1-5**]. The mechanism by which 5-FU/LV treatment stimulates increased TS in CRC^R cells is under investigation in our laboratory, but treatment-induced stabilization to protein degradation is one possibility. TS is stabilized from proteasome-mediated degradation through O-GlcNAc conjugation[33] and 5-FU/LV treatment could increase the extent of TS O-GlcNAc conjugation increasing protein stability.

In addition to its role in *de novo* thymidylate biosynthesis TS is an RNA-binding protein that regulates its own expression and the expression of c-Myc and p53. Myc and p53 are key proteins that regulate cell proliferation and programmed cell death and alterations in TS levels and in TS ternary complex formation could mediate drug resistance in part by modulating c-Myc and p53 levels. In fact, c-Myc is significantly elevated in CRC^R cells selected for acquired resistance to 5-FU/LV relative to parental cells [**Figure 4**]. Myc levels were also altered in response to treatment however in contrast to the increased TS levels observed in response to 5-FU/LV treatment in CRC^R cells 5-FU/LV and CF10/LV both significantly

decreased Myc protein levels. 5-FU/LV and CF10/LV treatment also significantly decreased Myc mRNA levels and for CF10/LV Myc mRNA levels were barely detectable by RT-qPCR. A possible explanation for these observations is that CF10/LV efficiently promotes TS ternary complex relieving TS autoregulation and increasing TS binding to Myc mRNA to decrease its translation. However, this process does not explain the observed decrease in Myc mRNA, particularly with CF10/LV treatment [**Figure 4A-C**][**Supplementary Figures 7-10**] indicating other processes also are involved. CF10 causes Top1cc and DNA DSB formation [**Figure 5**] and induces cell-cycle arrest, which could contribute to decreased c-Myc expression. In contrast 5-FU/LV is less effective at promoting TS ternary complex formation and causes lower levels of DNA DSBs, consistent with reduced cell-cycle arrest and correspondingly decreased Myc expression. While Myc has multiple targets with established roles in drug resistance its direct transcriptional regulation of ABCB5 expression is known to modulate resistance to 5-FU in CRC cells. We detected multiple bands of increased mobility for ABCB5 in Western blots for CRC^R cells [**Figure 4D,E**] [**Supplementary Figures 7-10**] which could be due to alternative splicing which has been described previously for ABCB5 but has not, as far as we are aware, been implicated in acquired 5-FU/LV resistance. Proteomics analysis is in progress to identify the altered forms of ABCB5 in CRC^R cells. Interestingly, CF10/LV treatment decreased ABCB5 expression to barely detectable levels by RT-qPCR and levels of the putative alternatively spliced forms of ABCB5 were decreased to undetectable levels with CF10/LV treatment. Collectively, these results are consistent with CF10/LV downregulating the

Myc/ABCB5 axis in CRC^R cells to promote strong cytotoxicity and to overcome acquired resistance to 5-FU/LV.

The mortality of CRC results almost exclusively from metastatic disease. 5-FU/LV is widely used in regimens such as FOLFOX and FOLFIRI for treatment of mCRC[1] and the majority of patients are initially responsive to front-line chemotherapy. However, acquired resistance to 5-FU/LV nearly always develops and long-term survival is not common. In previous studies we demonstrated that CF10 was very well tolerated *in vivo* inducing less weight loss and causing less GI-tract and hematological toxicities relative to equivalent doses of 5-FU. CF10 also displayed improved antitumor activity relative to 5-FU in mouse models of primary colorectal cancer[13] and in mouse and rat models of liver-metastatic CRC[15]. In these studies, we tested if CF10 remained effective in CRC cells selected for acquired resistance to 5-FU/LV. In fact, resistance factors for CF10 were only 2.85-3.40-fold, approximately an order of magnitude less than the resistance factors for 5-FU in these cell lines [**Table 1**]. The retained potency for CF10 occurs despite similar effects as 5-FU at inducing increased TS levels in CRC^R cells [**Figure 3A,B**] [**Supplementary Figures 7-10**] and is correlated with: (i) increased formation of the TS ternary complex in CRC^R cells [**Figure 3A**] and decreased TS enzymatic activity [**Figure 3D**]. The strong TS inhibition by CF10/LV in CRC^R cells corresponded to formation of Top1cc as was previously shown in CRC[13] and pancreatic cancer cells[14] and that results from FdU misincorporation into DNA inhibiting the religation step of Top1 catalysis[31]. CF10/LV was also much more potent than 5-FU/LV at inducing gH2AX foci [**Figure 5**], a biomarker of DNA double

strand breaks consistent with TS/Top1 dual targeting causing replication stress and inducing replication fork stalling and collapse. In summary, our results provide new insights into the mechanism of acquired resistance to 5-FU/LV in CRC cells and indicate CF10/LV is an effective alternative. Studies are in progress to test the efficacy of CF10/LV in in vivo models of acquired 5-FU/LV resistance and to advance CF10 into clinical trials.

Declarations

Authors' contributions

Conceptualization, writing, data analysis and interpretation: Okechukwu CC, Gmeiner WH

Performed experiments and data generation: Okechukwu CC

Writing, review, and editing: Okechukwu CC, Gmeiner WH

Availability of data and materials

All datasets and materials generated in this study can be provided by the corresponding author upon reasonable request

Financial support and sponsorship

This work was supported by NIH-NCI R42 CA254834, NIH-NCI P30 CA012197

Conflicts of interest

W. Gmeiner is an inventor on a patent application for CF10 in colon cancer. No disclosures were reported by the other authors.

Ethical approval and consent to participate

Not applicable.

Consent for publication

Not applicable.

Copyright

References

1. Gmeiner WH. Recent Advances in Therapeutic Strategies to Improve Colorectal Cancer Treatment. *Cancers (Basel)* 2024;16. [DOI: 10.3390/cancers16051029]

2. Gmeiner WH, Okechukwu CC. Review of 5-FU resistance mechanisms in colorectal cancer: clinical significance of attenuated on-target effects. *Cancer Drug Resist* 2023;6:257-72. [DOI: 10.20517/cdr.2022.136]

3. Rumpold H, Niedersuss-Beke D, Heiler C et al. Prediction of mortality in metastatic colorectal cancer in a real-life population: a multicenter explorative analysis. *BMC Cancer* 2020;20:1149. [DOI: 10.1186/s12885-020-07656-w]

4. Gmeiner WH. Chemistry of Fluorinated Pyrimidines in the Era of Personalized Medicine. *Molecules* 2020;25. [DOI: 10.3390/molecules25153438]

5. Wilson PM, Danenberg PV, Johnston PG, Lenz HJ, Ladner RD. Standing the test of time: targeting thymidylate biosynthesis in cancer therapy. *Nat Rev Clin Oncol* 2014;11:282-98. [DOI: 10.1038/nrclinonc.2014.51]

6. Gmeiner WH. Novel chemical strategies for thymidylate synthase inhibition. *Curr Med Chem* 2005;12:191-202.

7. Santi DV, McHenry CS, Raines RT, Ivanetich KM. Kinetics and thermodynamics of the interaction of 5-fluoro-2'-deoxyuridylate with

thymidylate synthase. *Biochemistry* 1987;26:8606-13. [DOI: 10.1021/bi00400a017]

8. Diasio RB, Harris BE. Clinical pharmacology of 5-fluorouracil. *Clin Pharmacokinet* 1989;16:215-37. [DOI: 10.2165/00003088-198916040-00002]

9. Patel K, Yerram SR, Azad NA, Kern SE. A thymidylate synthase ternary complex-specific antibody, FTS, permits functional monitoring of fluoropyrimidines dosing. *Oncotarget* 2012;3:678-85. [DOI: 10.18632/oncotarget.554]

10. Yang C, Xie LY, Windle JJ, Taylor SM, Moran RG. Humanizing mouse folate metabolism: conversion of the dual-promoter mouse folylpolyglutamate synthetase gene to the human single-promoter structure. *FASEB J* 2014;28:1998-2008. [DOI: 10.1096/fj.13-243261]

11. Epstein-Peterson ZD, Soff GA, Fenelus M, Korenstein D. Folate Testing and Deficiency in Hospitalized Cancer Patients. *Blood* 2018;132. [DOI: 10.1182/blood-2018-99-117073]

12. Danenberg PV, Gustavsson B, Johnston P et al. Folates as adjuvants to anticancer agents: Chemical rationale and mechanism of action. *Crit Rev Oncol Hematol* 2016;106:118-31. [DOI: 10.1016/j.critrevonc.2016.08.001]

13. Gmeiner WH, Dominijanni A, Haber AO et al. Improved Antitumor Activity of the Fluoropyrimidine Polymer CF10 in Preclinical Colorectal Cancer Models

through Distinct Mechanistic and Pharmacologic Properties. *Mol Cancer Ther* 2021;20:553-63. [DOI: 10.1158/1535-7163.MCT-20-0516]

14. Haber AO, Jain A, Mani C et al. AraC-FdUMP[10] (CF10) is a next generation fluoropyrimidine with potent antitumor activity in PDAC and synergy with PARG inhibition. *Mol Cancer Res* 2021. [DOI: 10.1158/1541-7786.MCR-20-0985]

15. Okechukwu CC, Ma X, Sah N, Mani C, Palle K, Gmeiner WH. Enhanced Therapeutic Efficacy of the Nanoscale Fluoropyrimidine Polymer CF10 in a Rat Colorectal Cancer Liver Metastasis Model. *Cancers (Basel)* 2024;16. [DOI: 10.3390/cancers16071360]

16. Finan JM, Di Niro R, Park SY et al. The polymeric fluoropyrimidine CF10 overcomes limitations of 5-FU in pancreatic ductal adenocarcinoma cells through increased replication stress. *Cancer Biology & Therapy* 2024;25. [DOI: Artn 242158410.1080/15384047.2024.2421584]

17. Liu J, Kolar C, Lawson TA, Gmeiner WH. Targeted drug delivery to chemoresistant cells: folic acid derivatization of FdUMP[10] enhances cytotoxicity toward 5-FU-resistant human colorectal tumor cells. *J Org Chem* 2001;66:5655-63. [DOI: jo005757n [pii]]

18. Chu E, Allegra CJ. The role of thymidylate synthase as an RNA binding protein. *Bioessays* 1996;18:191-8. [DOI: 10.1002/bies.950180306]

19. Chu E, Koeller DM, Casey JL et al. Autoregulation of human thymidylate synthase messenger RNA translation by thymidylate synthase. *Proc Natl Acad Sci U S A* 1991;88:8977-81. [DOI: 10.1073/pnas.88.20.8977]

20. Chu E, Takechi T, Jones KL et al. Thymidylate synthase binds to c-myc RNA in human colon cancer cells and in vitro. *Mol Cell Biol* 1995;15:179-85. [DOI: 10.1128/MCB.15.1.179]

21. McMahon SB. MYC and the control of apoptosis. *Cold Spring Harb Perspect Med* 2014;4:a014407. [DOI: 10.1101/cshperspect.a014407]

22. Kugimiya N, Nishimoto A, Hosoyama T et al. The c-MYC-ABCB5 axis plays a pivotal role in 5-fluorouracil resistance in human colon cancer cells. *J Cell Mol Med* 2015;19:1569-81. [DOI: 10.1111/jcmm.12531]

23. Gerard L, Gillet JP. The uniqueness of ABCB5 as a full transporter ABCB5FL and a half-transporter-like ABCB5beta. *Cancer Drug Resist* 2024;7:29. [DOI: 10.20517/cdr.2024.56]

24. Wilson BJ, Schatton T, Zhan Q et al. ABCB5 identifies a therapy-refractory tumor cell population in colorectal cancer patients. *Cancer Res* 2011;71:5307-16. [DOI: 10.1158/0008-5472.CAN-11-0221]

25. Blondy S, David V, Verdier M, Mathonnet M, Perraud A, Christou N. 5-Fluorouracil resistance mechanisms in colorectal cancer: From classical pathways to promising processes. *Cancer Sci* 2020;111:3142-54. [DOI: 10.1111/cas.14532]

26. Copur S, Aiba K, Drake JC, Allegra CJ, Chu E. Thymidylate synthase gene amplification in human colon cancer cell lines resistant to 5-fluorouracil. *Biochem Pharmacol* 1995;49:1419-26.

27. Peters GJ, Backus HH, Freemantle S et al. Induction of thymidylate synthase as a 5-fluorouracil resistance mechanism. *Biochim Biophys Acta* 2002;1587:194-205.

28. Fischel JL, Formento P, Ciccolini J et al. Impact of the oxaliplatin-5 fluorouracil-folinic acid combination on respective intracellular determinants of drug activity. *Br J Cancer* 2002;86:1162-8. [DOI: 10.1038/sj.bjc.6600185]

29. Patel AG, Flatten KS, Peterson KL et al. Immunodetection of human topoisomerase I-DNA covalent complexes. *Nucleic Acids Res* 2016;44:2816-26. [DOI: 10.1093/nar/gkw109]

30. Peters GJ, Smitskamp-Wilms E, Smid K, Pinedo HM, Jansen G. Determinants of activity of the antifolate thymidylate synthase inhibitors Tomudex (ZD1694) and GW1843U89 against mono- and multilayered colon cancer cell lines under folate-restricted conditions. *Cancer Res* 1999;59:5529-35.

31. Liao ZY, Sordet O, Zhang HL et al. A novel polypyrimidine antitumor agent FdUMP[10] induces thymineless death with topoisomerase I-DNA complexes. *Cancer Res* 2005;65:4844-51. [DOI: 65/11/4844 [pii]10.1158/0008-5472.CAN-04-1302]

32. Gmeiner WH, Reinhold WC, Pommier Y. Genome-wide mRNA and microRNA profiling of the NCI 60 cell-line screen and comparison of FdUMP[10] with fluorouracil, floxuridine, and topoisomerase 1 poisons. *Mol Cancer Ther* 2010;9:3105-14. [DOI: 10.1158/1535-7163.MCT-10-06749/12/3105 [pii]]

33. Very N, Hardiville S, Decourcelle A et al. Thymidylate synthase O-GlcNAcylation: a molecular mechanism of 5-FU sensitization in colorectal cancer. *Oncogene* 2022;41:745-56. [DOI: 10.1038/s41388-021-02121-9]

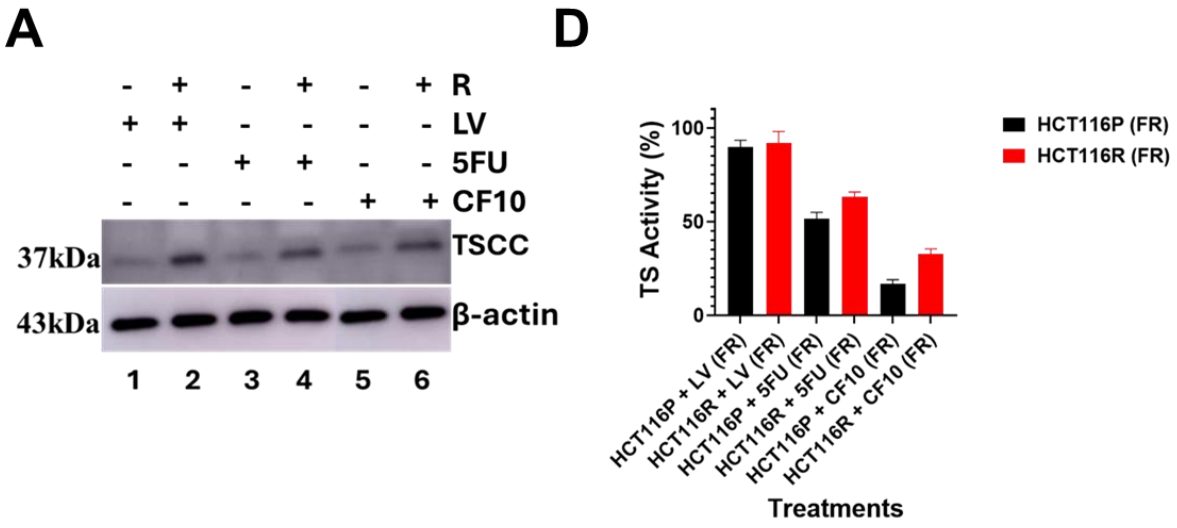

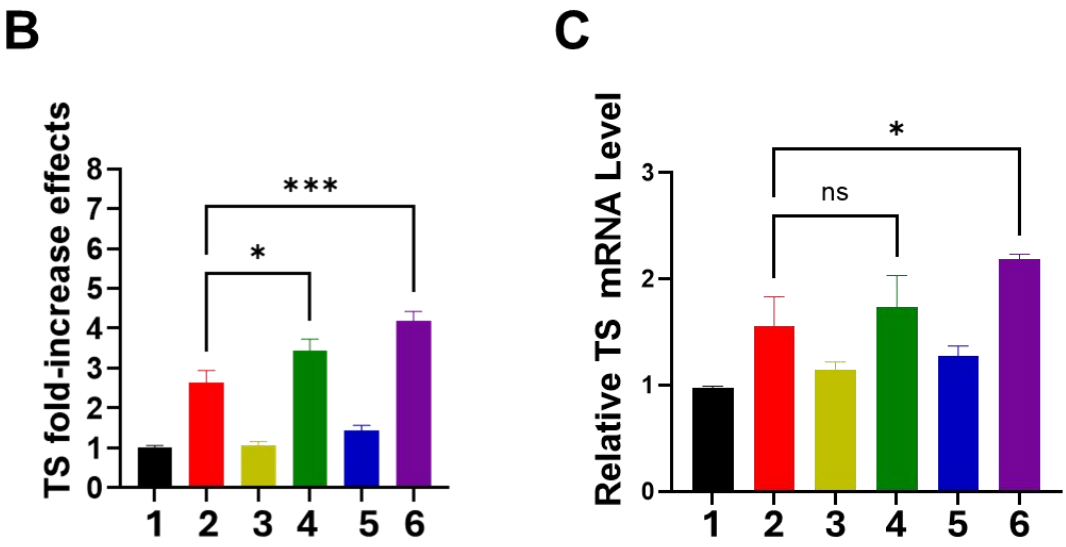

Supplementary Figure 1. 5-FU (10 mM) and CF10 (1 mM) treatment for 24h increases TS at both the protein (A,B) and mRNA (C) levels in HCT116^{R} cells but only CF10/LV promotes ternary complex formation (TSCC) and efficient inhibition of TS enzymatic activity (D). * $p<0.05$; *** $p < 0.0001$.

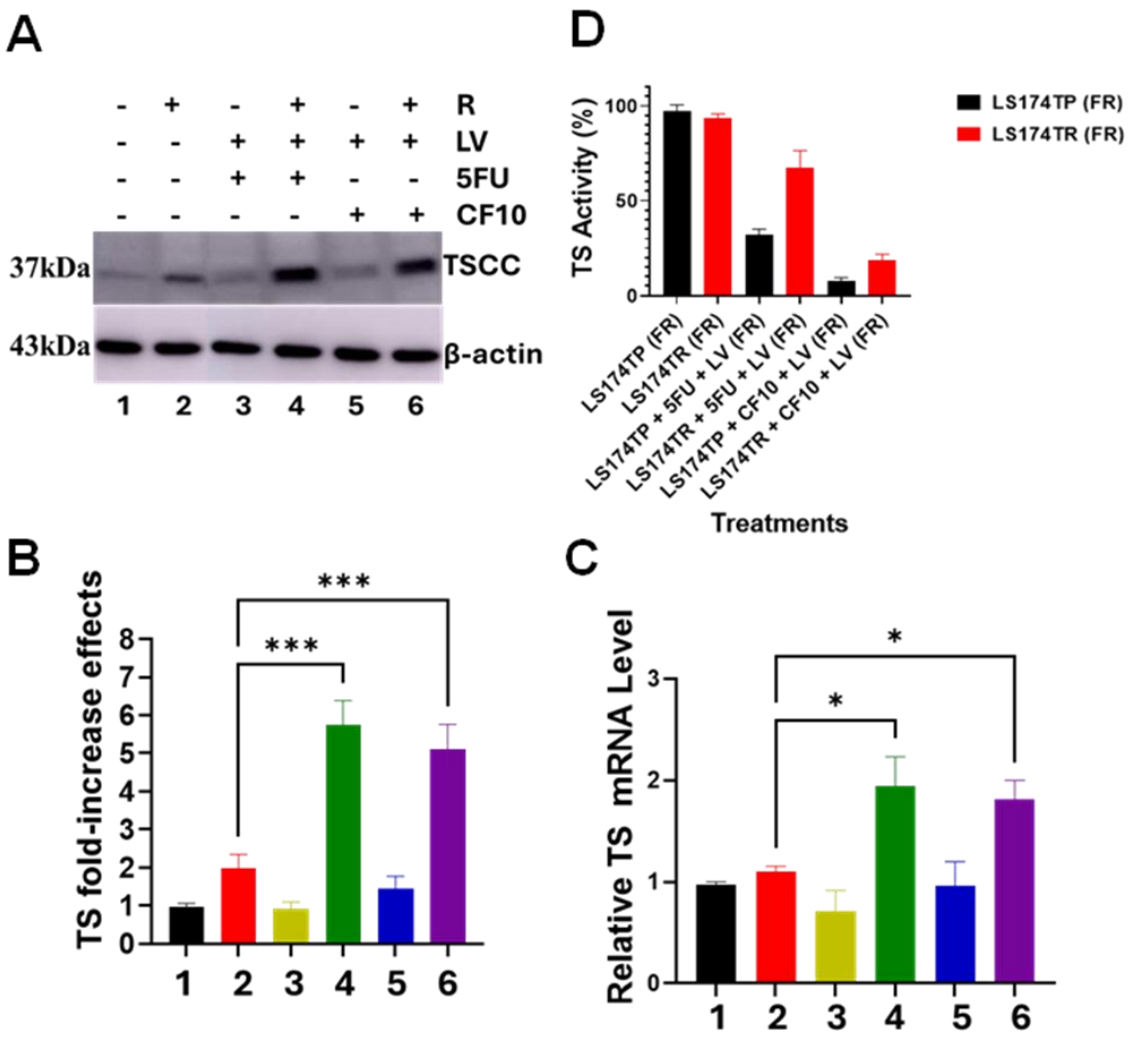

Supplementary Figure 2. 5-FU/LV (10 mM, 1 mM) and CF10/LV (1 mM, mM) treatment for 24h increases TS at both the protein (A,B) and mRNA (C) levels in LS174T^{R} cells but only CF10/LV promotes ternary complex formation (TSCC) and efficient inhibition of TS enzymatic activity (D). * $p<0.05$; *** $p < 0.0001$.

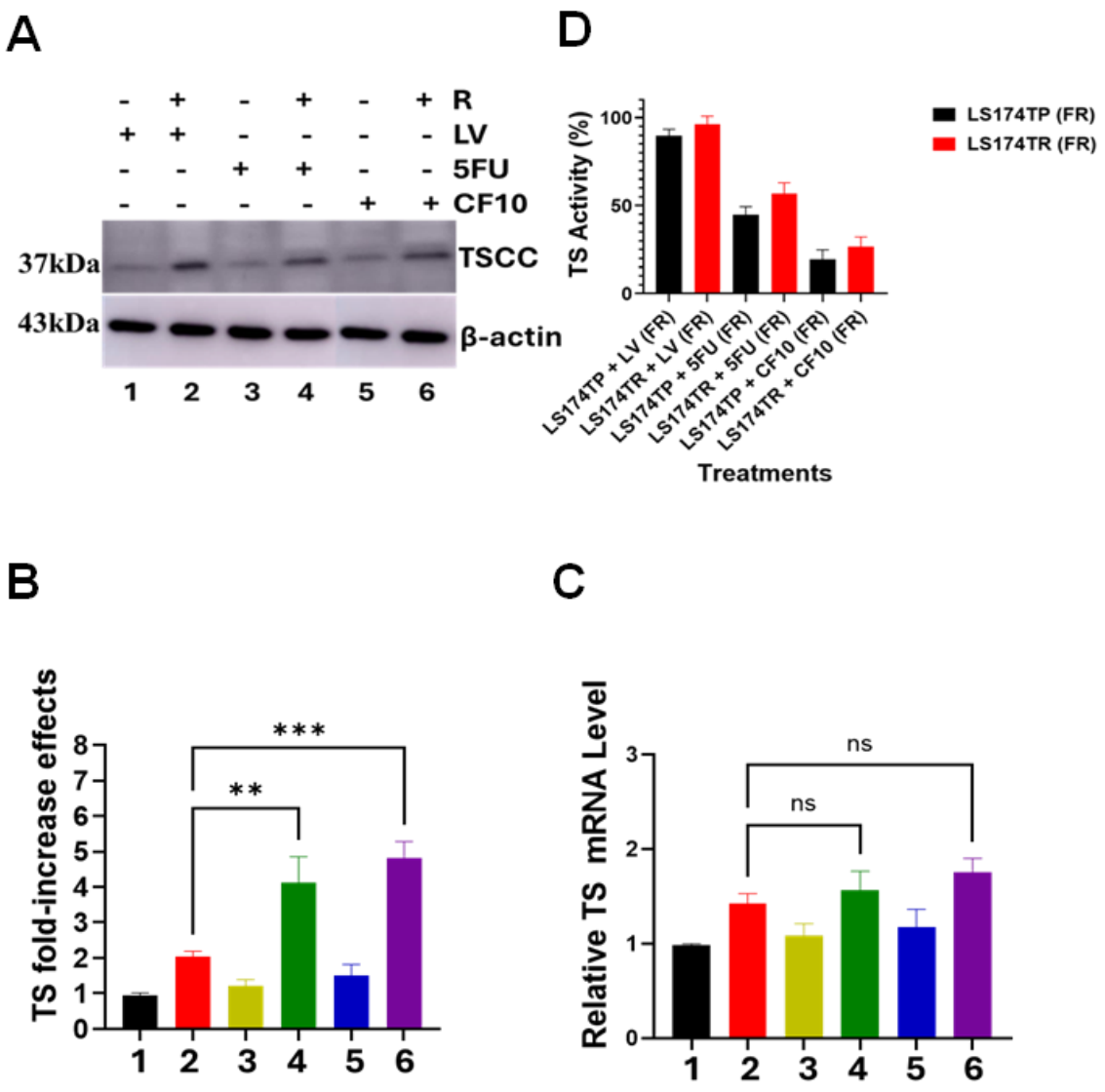

Supplementary Figure 3. 5-FU (10 mM) and CF10 (1 mM) treatment for 24h increases TS at both the protein (A,B) and mRNA (C) levels in LS174T^R cells but only CF10 promotes ternary complex formation (TSCC) and efficient inhibition of TS enzymatic activity (D). * $p<0.05$; *** $p < 0.0001$.

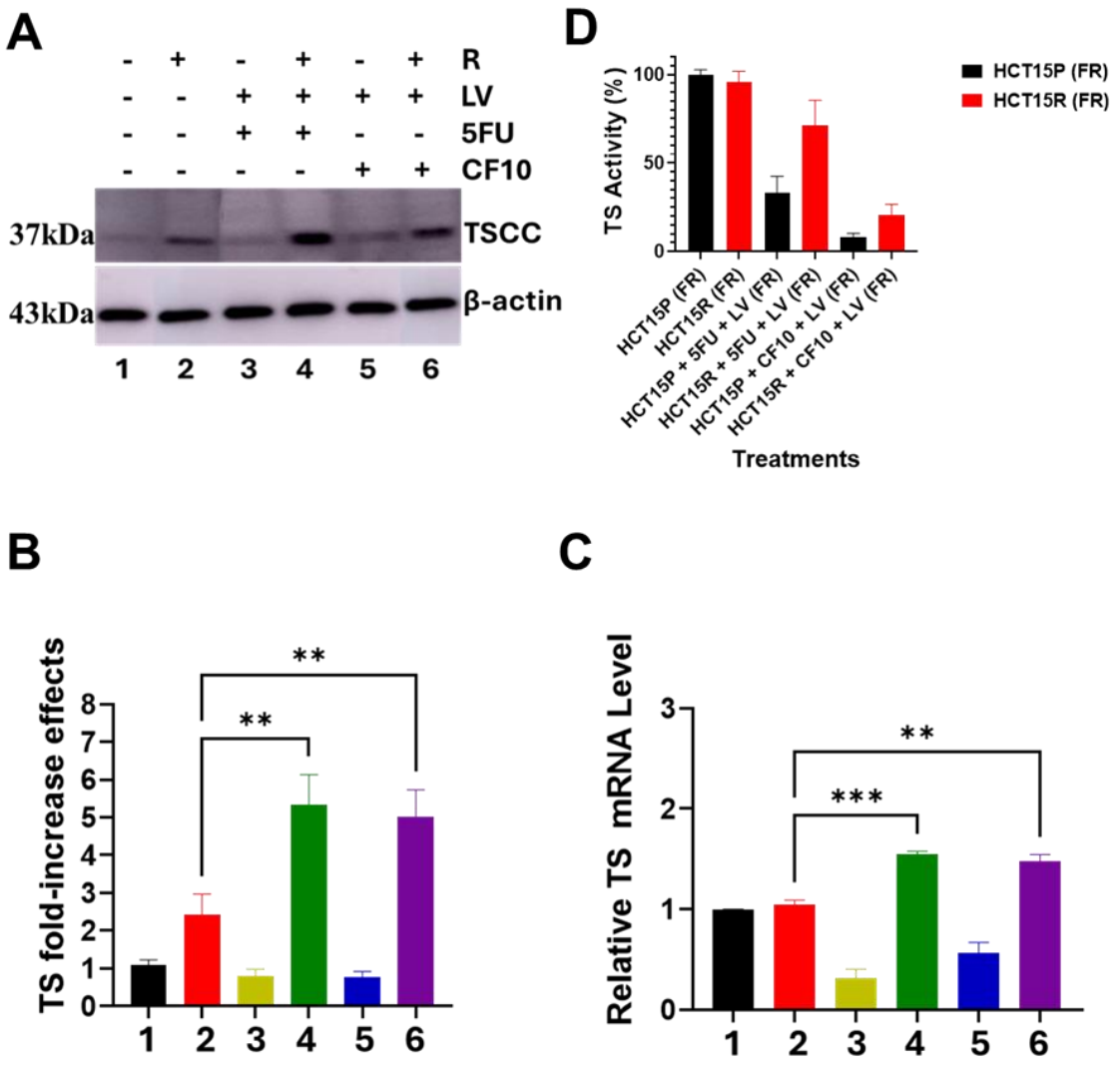

Supplementary Figure 4. 5-FU/LV (10 mM, 1 mM) and CF10/LV (1 mM, mM) treatment for 24h increases TS at both the protein (A,B) and mRNA (C) levels in HCT15^{R} cells but only CF10/LV promotes ternary complex formation (TSCC) and efficient inhibition of TS enzymatic activity (D). * $p<0.05$; *** $p < 0.0001$.

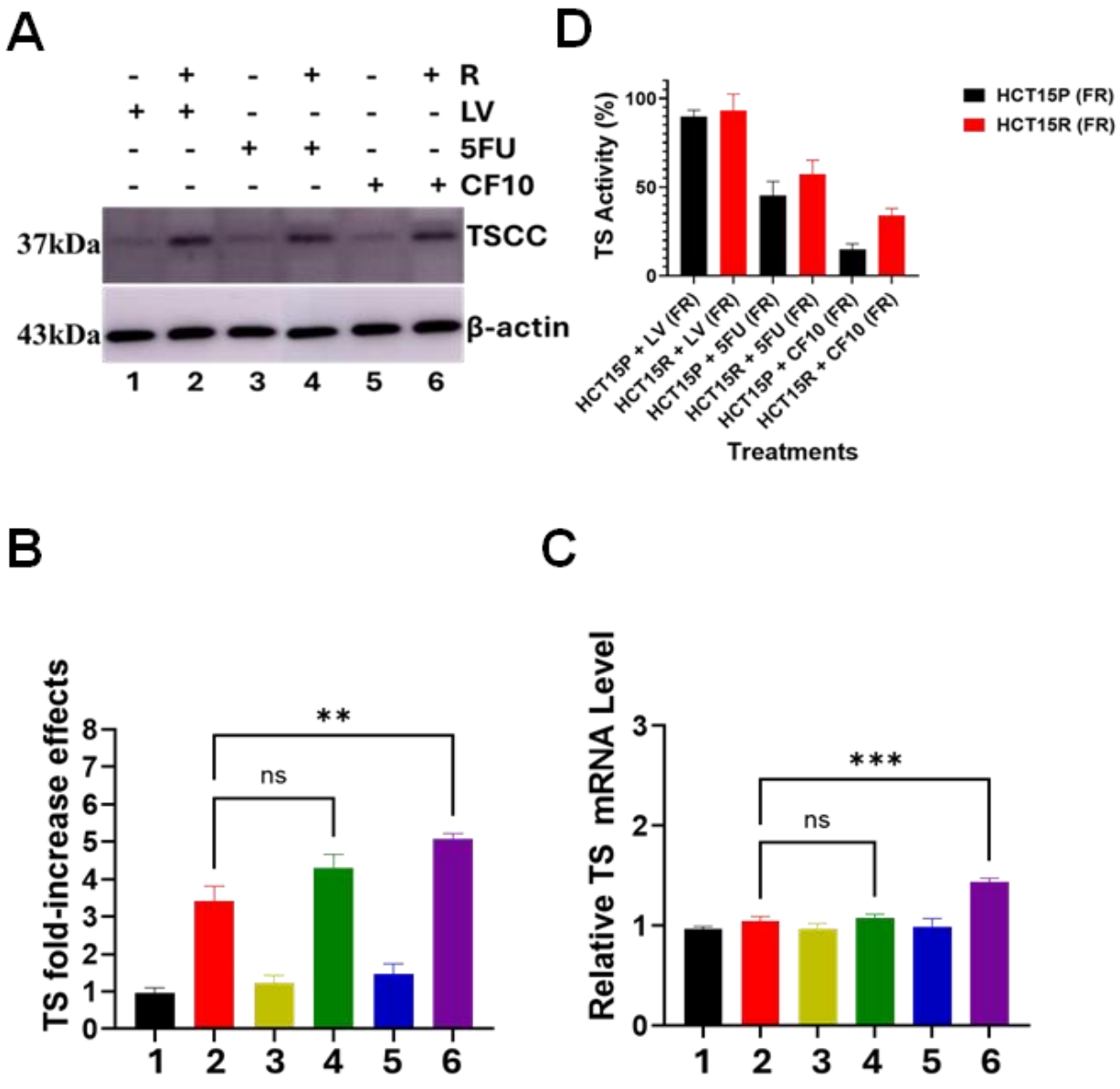

Supplementary Figure 5. 5-FU (10 mM) and CF10 (1 mM) treatment for 24h increases TS at both the protein (A,B) and mRNA (C) levels in LS174T^{R} cells but only CF10 promotes ternary complex formation (TSCC) and efficient inhibition of TS enzymatic activity (D). * $p<0.05$; *** $p < 0.0001$.

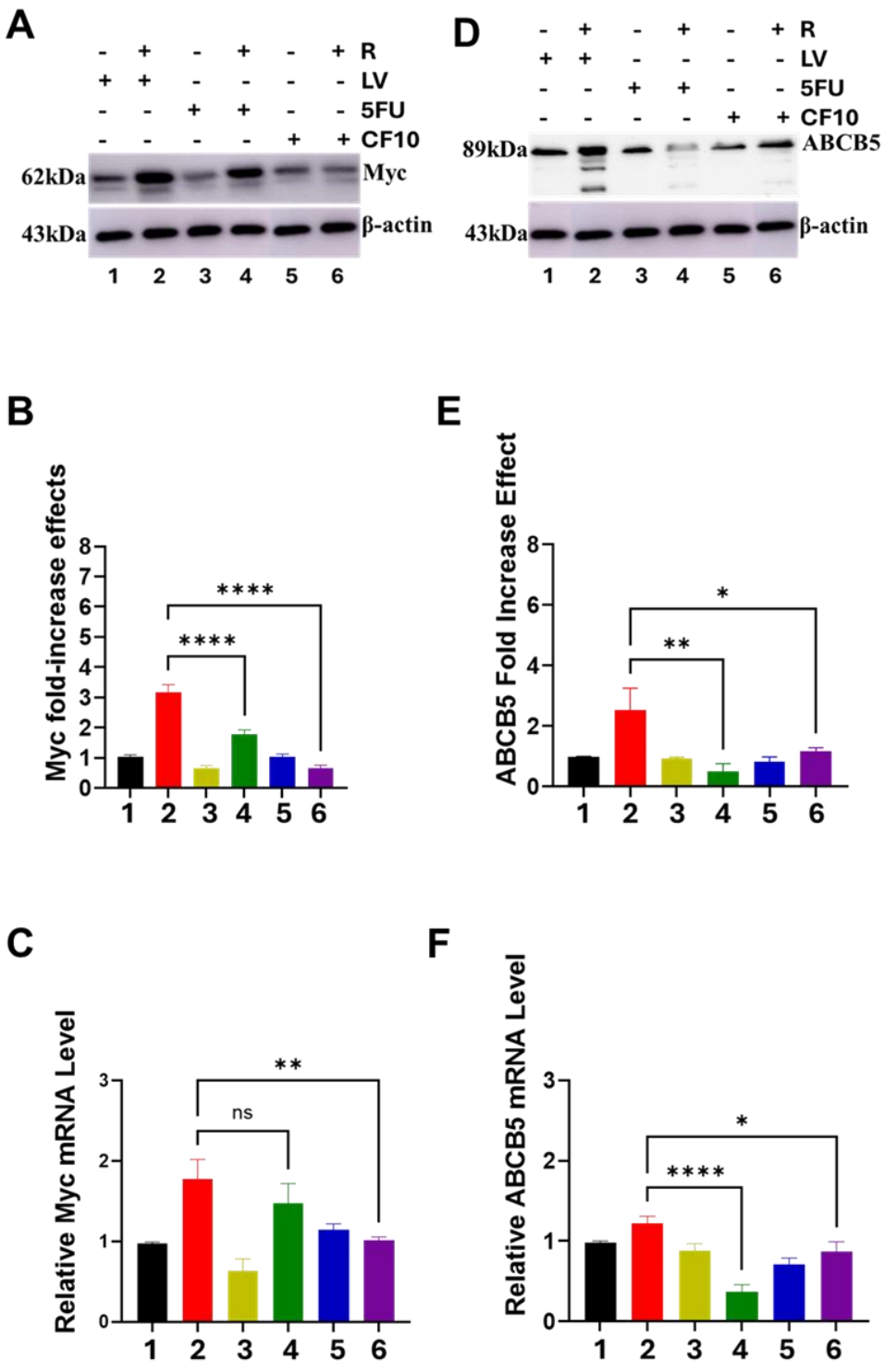

Supplementary Figure 6. Myc is elevated in 5-FU/LV-resistant HCT116^{R} cells, but 5-FU and CF10 decrease levels of Myc and the Myc-target ABCB5 at both the

protein and mRNA level. Western blots for Myc (A) and ABCB5 (D). Quantification of the Western blot images by densitometry is shown for Myc (B) and ABCB5 (E). Quantification of mRNA levels by RT-qPCR is shown for Myc (C) and ABCB5 (F). *p<0.03, **p<0.002, ***p<0.002, ****p<0.0001.

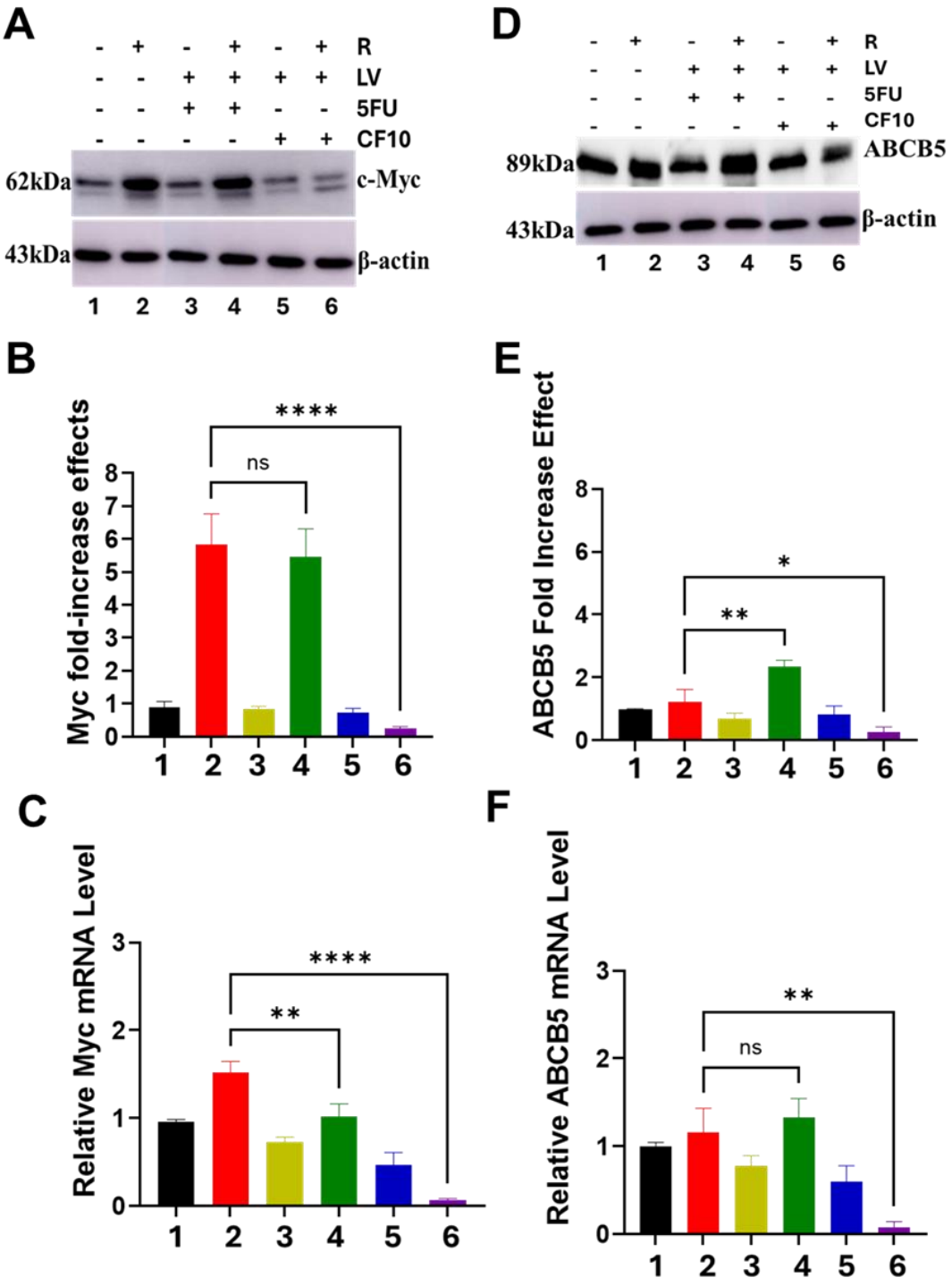

Supplementary Figure 7. Myc is elevated in 5-FU/LV-resistant LS174T^{R} cells, but CF10/LV decreases levels of Myc and the Myc-target ABCB5 at both the protein and mRNA level. Western blots for Myc (A) and ABCB5 (D). Quantification of the

Western blot images by densitometry is shown for Myc (B) and ABCB5 (E). Quantification of mRNA levels by RT-qPCR is shown for Myc (C) and ABCB5 (F). *p<0.03, **p<0.002, ***p<0.002, ****p<0.0001.

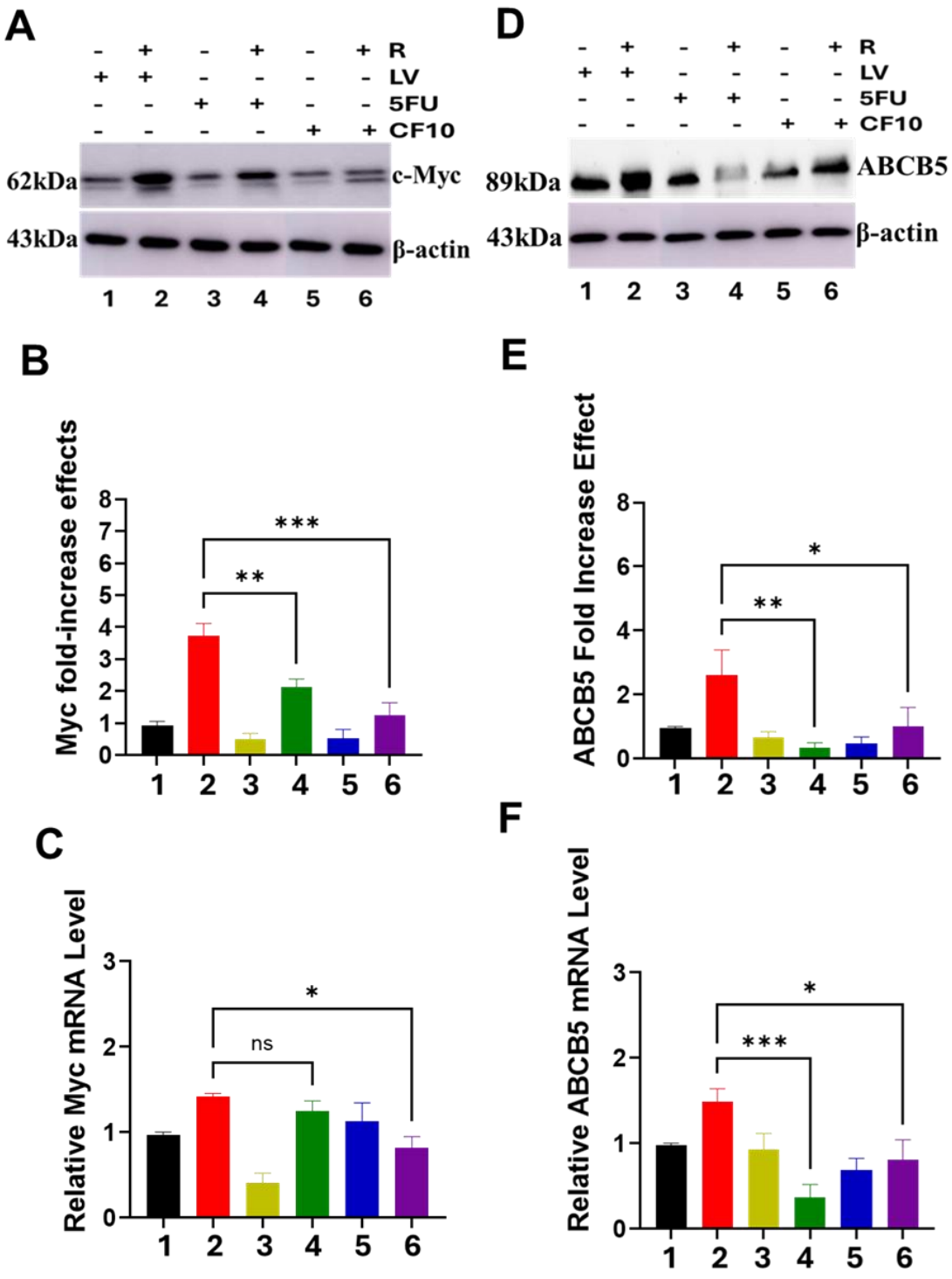

Supplementary Figure 8. Myc is elevated in 5-FU/LV-resistant LS174T^{R} cells, but 5-FU and CF10 decrease levels of Myc and the Myc-target ABCB5 at both the

protein and mRNA level. Western blots for Myc (A) and ABCB5 (D). Quantification of the Western blot images by densitometry is shown for Myc (B) and ABCB5 (E). Quantification of mRNA levels by RT-qPCR is shown for Myc (C) and ABCB5 (F). *p<0.03, **p<0.002, ***p<0.002, ****p<0.0001.

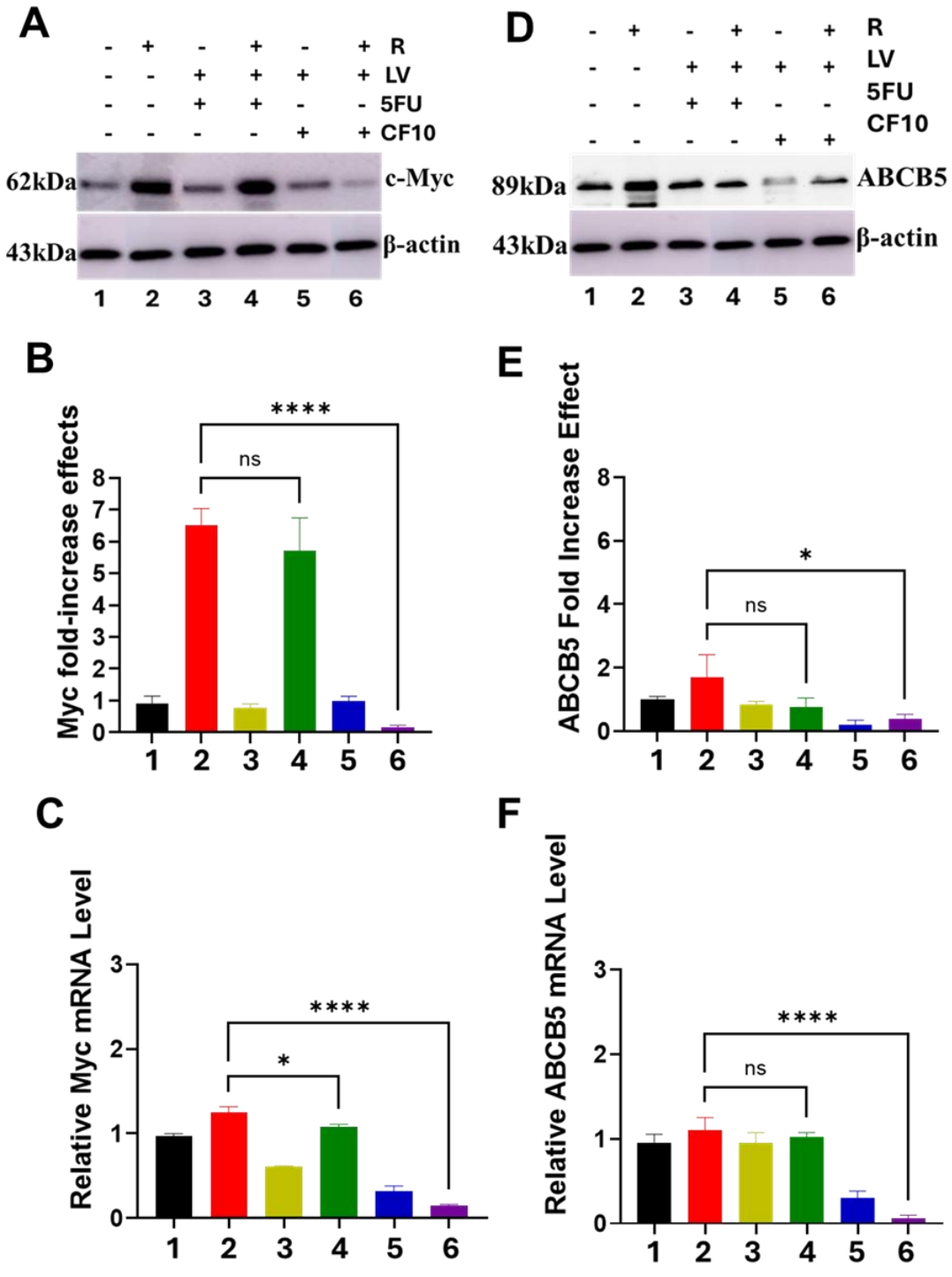

Supplementary Figure 9. Myc is elevated in 5-FU/LV-resistant HCT15^{R} cells, but CF10/LV decreases levels of Myc and the Myc-target ABCB5 at both the protein and mRNA level. Western blots for Myc (A) and ABCB5 (D). Quantification of the

Western blot images by densitometry is shown for Myc (B) and ABCB5 (E). Quantification of mRNA levels by RT-qPCR is shown for Myc (C) and ABCB5 (F). *p<0.03, **p<0.002, ***p<0.002, ****p<0.0001.

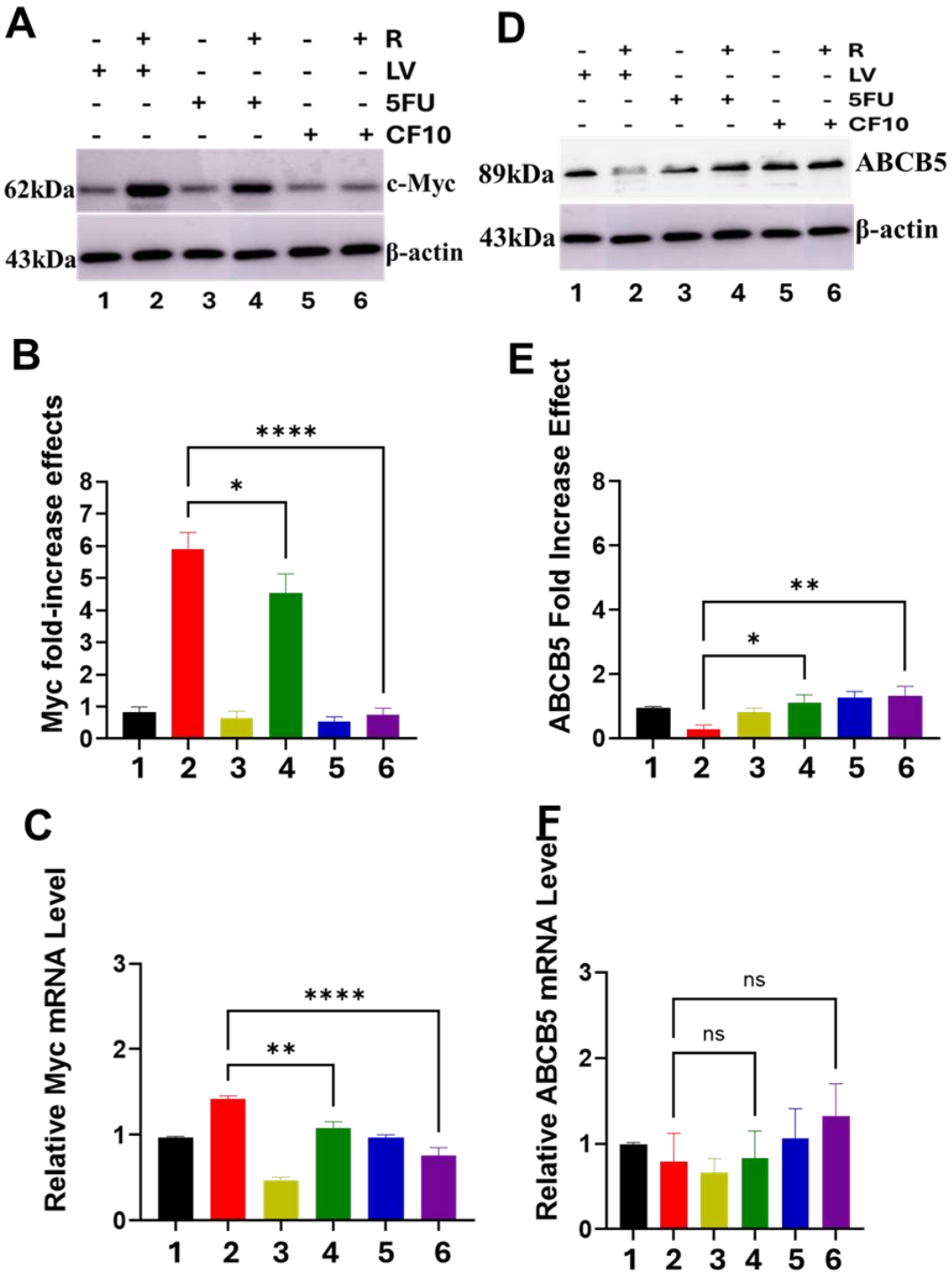

Supplementary Figure 10. Myc is elevated in 5-FU/LV-resistant HCT15^{R} cells, but 5-FU and CF10 decrease levels of Myc and the Myc-target ABCB5 at both the protein and mRNA level. Western blots for Myc (A) and ABCB5 (D). Quantification

of the Western blot images by densitometry is shown for Myc (B) and ABCB5 (E). Quantification of mRNA levels by RT-qPCR is shown for Myc (C) and ABCB5 (F). *p<0.03, **p<0.002, ***p<0.002, ****p<0.0001.

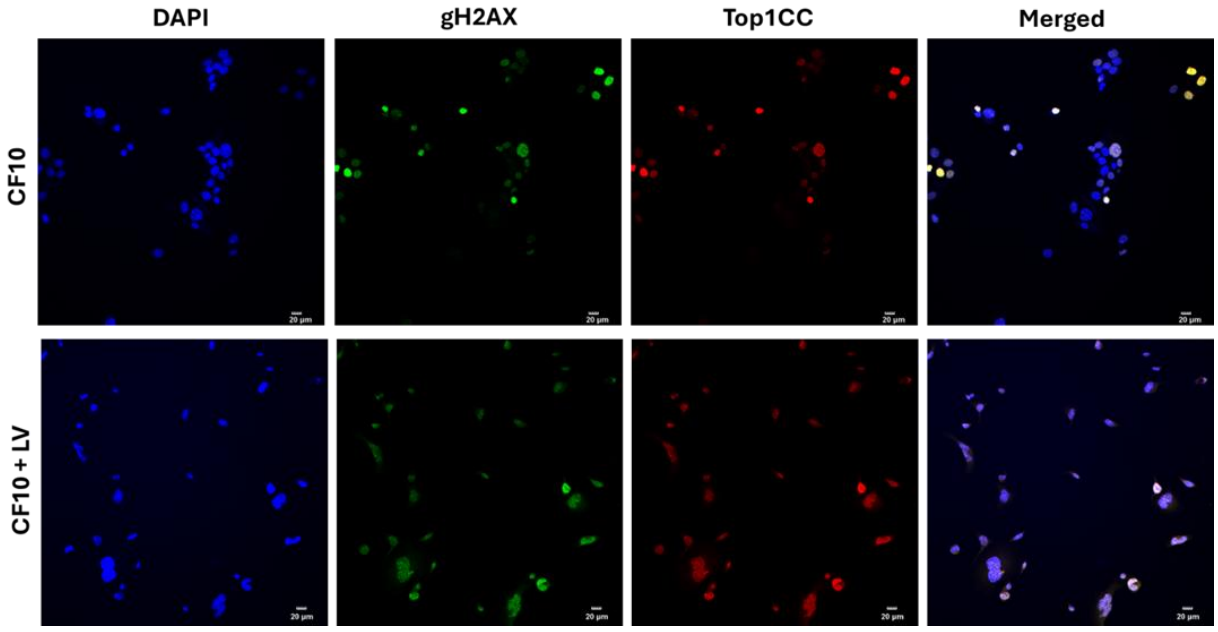

Supplementary Figure 11. Immunofluorescence Imaging of pH2AX and Top1cc in HCT116R cells following treatment with CF10 or CF10 + LV.

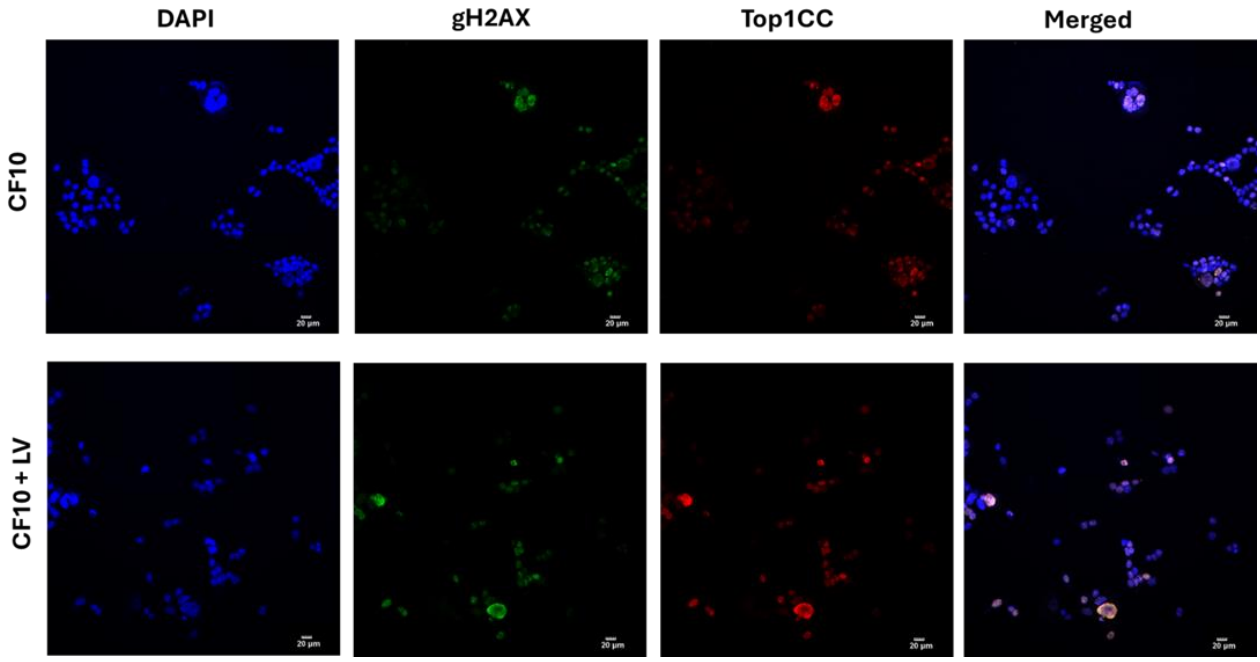

Supplementary Figure 12. Immunofluorescence Imaging of pH2AX and Top1cc in HCT116P cells following treatment with CF10 or CF10 + LV.

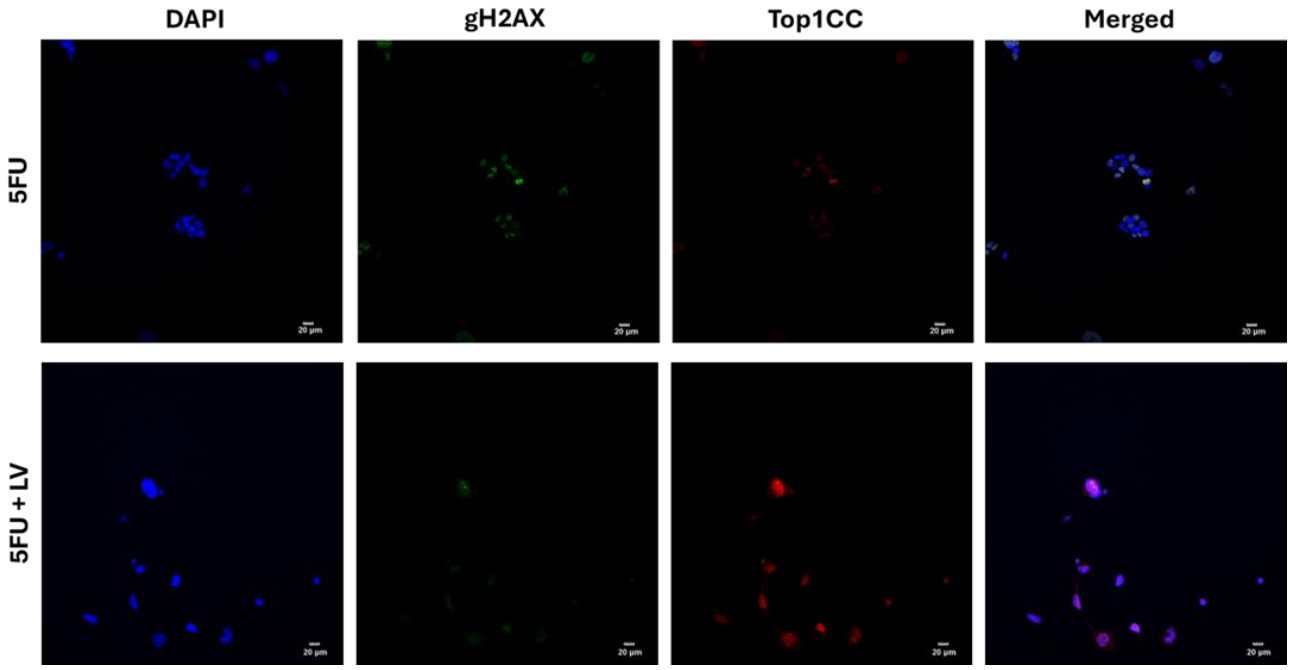

Supplementary Figure 13. Immunofluorescence Imaging of pH2AX and Top1cc in HCT116R cells following treatment with 5FU or 5FU + LV.

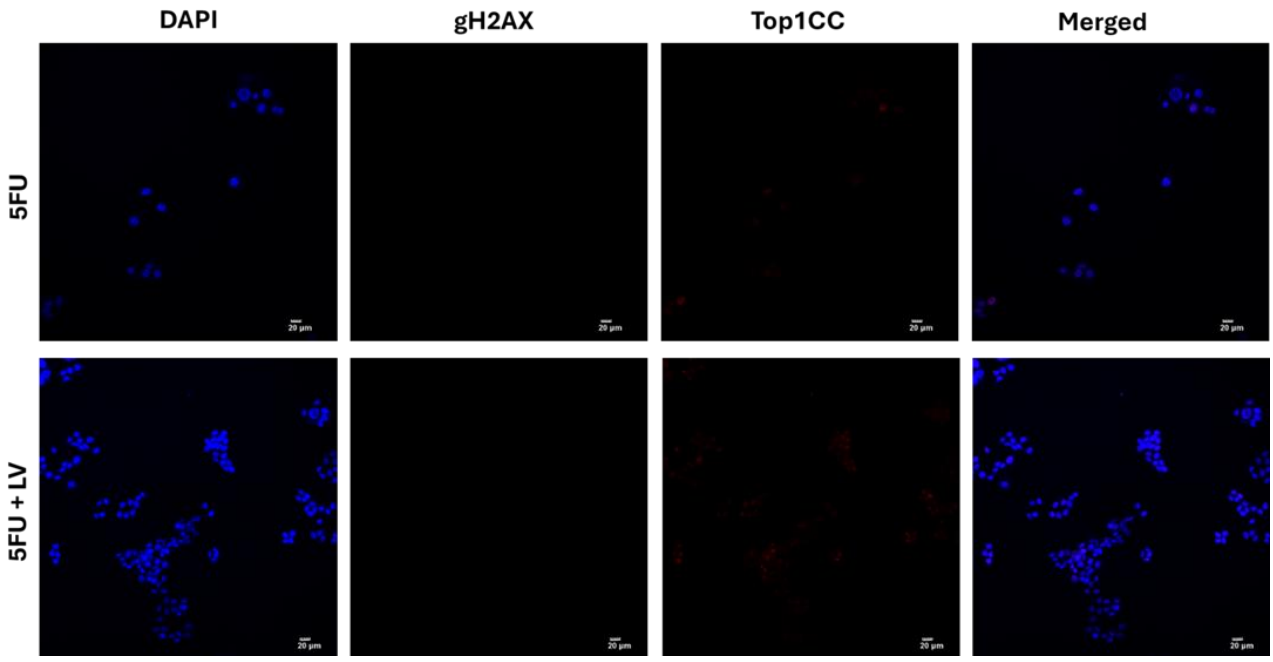

Supplementary Figure 14. Immunofluorescence Imaging of pH2AX and Top1cc in HCT116P cells following treatment with 5FU or 5FU + LV .

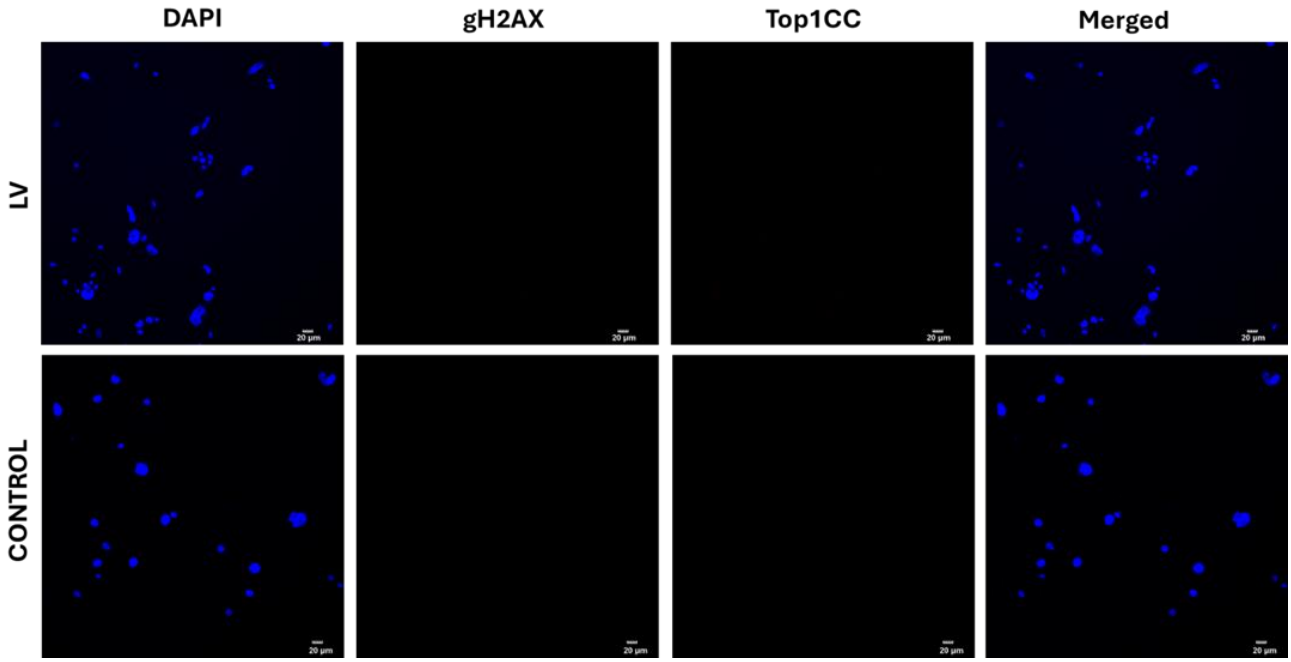

Supplementary Figure 15. Immunofluorescence Imaging of pH2AX and Top1cc in HCT116R cells following treatment with LV or no Treatment.

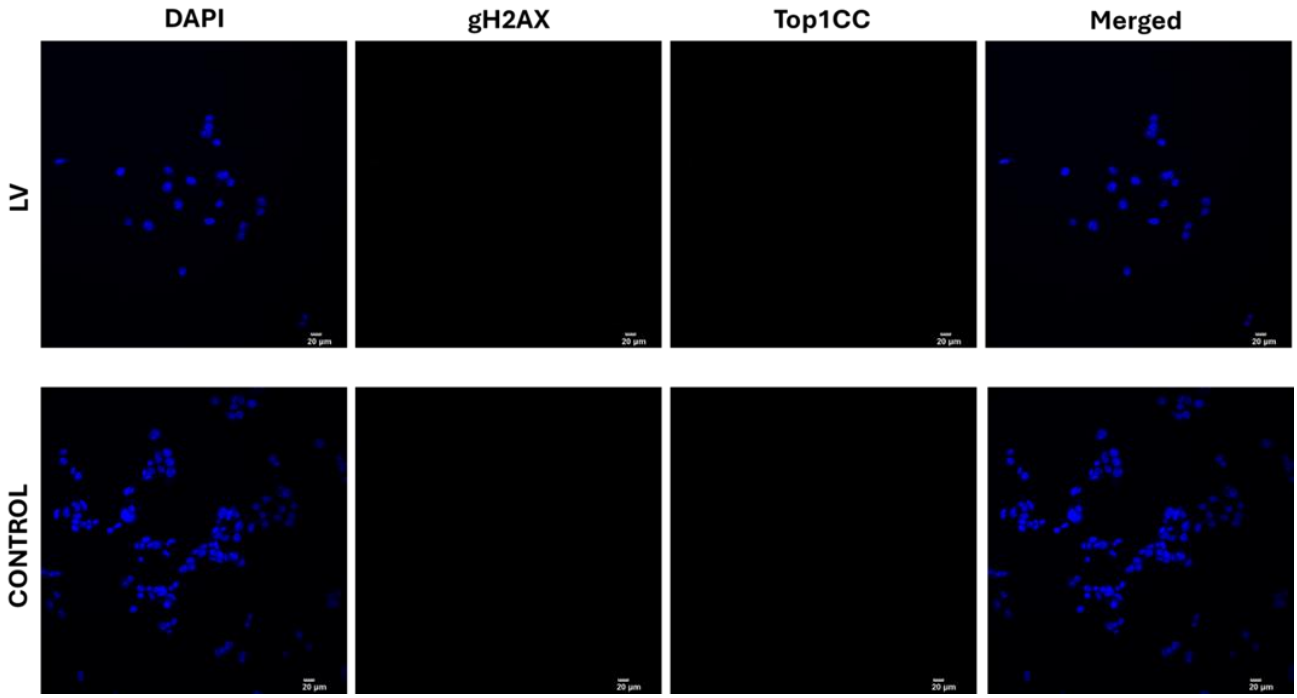

Supplementary Figure 16. Immunofluorescence Imaging of pH2AX and Top1cc in HCT116P cells following treatment with LV or no treatment

CHAPTER 6

CF10 Overcome Acquired Resistance to 5-FU/LV in a MC38:C57BL/6 Syngeneic, Orthotopic Mouse Model of Colorectal Cancer Liver Metastasis

Charles Chidi Okechukwu[1,2], Xue Ma[3], Wencheng Li[4], Ralph D'Agostino[5], Jr., and William H. Gmeiner[2*]

[1]Integrative Physiology and Pharmacology Graduate Program. Wake Forest University School of Medicine, Winston-Salem, NC 27157 USA;

[2]Department of Cancer Biology, Wake Forest University School of Medicine, Winston-Salem, NC 27157 USA;

[3]Department of Orthopedic Surgery. Wake Forest University School of Medicine, Winston-Salem, NC 27157 USA;

[4]Department of Pathology, Wake Forest University School of Medicine, Winston-Salem, NC 27157 USA;

[5]Department of Public Health Sciences and Comprehensive Cancer Center, Wake Forest University School of Medicine, Winston-Salem, NC 27157 USA;

Running Title: Improved Efficacy of CF10 in Liver-metastatic CRC

Key Words: Colorectal cancer, fluoropyrimidine, leucovorin, replication stress, thymidylate synthase, topoisomerase 1

Financial support: NIH-NCI R42 CA254834, NIH-NCI P30 CA012197, DoD PRCRP CA200460

* Corresponding Author: William H. Gmeiner, Wake Forest University School of Medicine, Medical Center Blvd, Winston-Salem, NC 27055. Phone: 336-716-6216; Fax: 336-716-0255; E-mail bgmeiner@wakehealth.edu.

Conflict of interest: W. Gmeiner is an inventor on a patent application for CF10 in colon cancer. Other authors report no conflicts.

Abstract

Metastatic disease is exclusively responsible for colorectal cancer (CRC) mortality and acquired drug resistance is a central cause as the majority of patients with metastatic CRC (mCRC) initially respond to chemotherapy with 5-FU-based regimens, but long-term survival is uncommon. In the present studies we describe development of a clinically relevant mouse model of therapy-resistant CRC liver metastasis by selecting MC38 mouse CRC cells for resistance to 5-FU/LV under human-like conditions of folate physiology and implanting the resistant cells in the liver of syngeneic C57BL6 mice. We also test a next generation fluoropyrimidine (FP) polymer, CF10, for improved activity in the resistant model. Basal TS levels were not elevated in 5-FU/LV-resistant cells but treatment with either 5-FU±LV or CF10±LV induced elevated TS expression. CF10±LV effectively reduced TS enzymatic activity and CF10±LV retained nM potency to the 5-FU/LV resistant cells. We tested CF10 and CF10/LV was effective in completely eradicating liver metastases in both MC38:C57BL/6 and MC38R:C57BL/6 CRC liver metastasis models. In both models CF10 and CF10/LV dramatically outperformed 5-FU and 5-FU/LV, and a significant survival advantage was established for CF10/LV. Collectively our studies provide new insights into the mechanisms of acquired resistance during treatment with 5-FU-based chemotherapy regimens and demonstrate the clinical potential of CF10/LV for treatment of drug-refractory mCRC.

Introduction

The efficacy of chemotherapy for treating metastatic colorectal cancer (mCRC) is limited by the development of acquired resistance [1]. Yet, an understanding of the underlying mechanisms of resistance is incomplete. 5-FU-based chemotherapy regimens (FOLFOX, FOLFIRI) are widely used in front-line chemotherapy for mCRC [2], and most patients are initially responsive; however, nearly all mCRC patients experience progressive disease within one year (median time to disease progression for FOLFOX6 is 8.6 months). Thus, while chemotherapy for mCRC is life-extending, it is rarely curative. Multiple causes of resistance to 5-FU-based therapy have been described with elevated expression or activity thymidylate synthase (TS), the primary enzymatic target, one that has been detected both in clinical samples from mCRC patients and in CRC cell lines selected in the laboratory for acquired resistance. Other causes of resistance to 5-FU include altered anabolic metabolism that limits the formation of the TS-inhibitory metabolite, FdUMP, and dysregulated programmed cell death. Understanding the relevant causes of resistance and developing new therapeutic options that overcome these mechanisms can lead to further improvements in survival for mCRC patients [3].

A challenge in studying clinically relevant causes of chemoresistance using cultured human cancer cell lines and rodent tumor models is that the conditions used for laboratory studies can be very different from cancer patients. In particular, folate levels are relatively lower in human plasma compared to those used to culture human cells and also relative to rodent pre-clinical cancer models. Folates

play an important role in cancer metabolism and folate-mediated one-carbon metabolism is central to both pyrimidine and purine biosynthesis needed to support cell proliferation. In previous studies, we showed that adaptation of cancer cells to folate-restricted media with more human-like folate levels altered response to 5-FU and the extent of potentiation by leucovorin (LV; N5-formyl tetrahydrofolate). LV is nearly always co-administered with 5-FU in chemotherapy regimens to promote formation of the TS ternary complex (TS:FdUMP:MeTHF) in cancer cells and promotes irreversible enzyme inhibition [4]. We also established that CF10, a 2nd generation fluoropyrimidine (FP) polymer that directly releases FdUMP, the TS inhibitory metabolite of FP drugs including 5-FU, retained a strong potency advantage relative to 5-FU that far exceeds its 10-fold increased FP content under folate-restricted conditions and was potentiated by by LV [5]. CF10 is advancing to clinical development based on improved antitumor activity relative to 5-FU in multiple pre-clinical tumor models including both rat and mouse syngeneic orthotopic models of colorectal cancer liver metastasis (CRLM) [6]. CF10 is also very well tolerated in vivo.

In the present studies we tested if CF10/LV could outperform 5-FU/LV in a MC38^{R}:C57BL/6 syngeneic orthotopic CRLM model. In this tumor model, MC38^{R} mouse CRC cells that were selected for acquired resistance to 5-FU/LV were used for tumor formation. MC38^{R} cells were selected for 5-FU/LV resistance by repeated passage in folate-restricted media containing increasing concentrations of 5-FU/LV to simulate clinical development of acquired resistance. This tumor model also reflects the drug-resistant state of the initial patient population likely to be

treated with CF10/LV and one for which no current therapy is adequate. The most recent FP-based drug to receive FDA approval for mCRC treatment Lonsurf which was approved based on improved activity for 3rd line mCRC in patients previously treated with FOLFOX, FOLFIRI or other regimens [2]. We anticipate a similar clinical development program for CF10. Mechanistically, we establish that acquired resistance to 5-FU/LV in $MC38^R$ cells results from induced overexpression of TS with drug treatment. CF10 through more efficient conversion to FdUMP retains strong potency to MC38R cells and CF10/LV is effective at eliminating tumor burden in the MC38R CRLM model. Our studies demonstrate that CF10/LV shows potent activity in a CRLM model that simulates both human-like folate physiology and clinically relevant therapeutic resistance supporting CF10 clinical development.

Materials and Methods

Cell lines and Drugs

Parental colorectal cancer (CRC) (MC-38 ((RRID:CVCL_B288)) and 5-FU/LV resistant CRC cells ($MC-38^R$) were cultured using Folate-Restricted (FR) media(folic acid-free RPMI 1640 supplemented with 40nM of 5-methyltetrahydrofolate and 0.1nM of sodium L-ascorbate), confirmed by short tandem repeat analysis, and repeatedly tested negative for Mycoplasma. The resistance cells were generated through a stepwise increase in drug-containing FR media (0.1 to10μM) containing 5-FU+LV. The Baptist Hospital clinical pharmacy was the vendor for the clinical grade 5-FU (50 mg/mL) and 5-FU concentrations were calculated based on the dilution of the established stock

concentration. Meanwhile, CF10 was obtained from ST Pharma, validated by high-resolution mass spectrometry, and dissolved in 0.9% sterile saline solution. CF10 concentrations were matched to deliver equivalent nucleoside content based on UV absorbance at 260 nm.

Cell Viability and Resistant Assay

MC-38 and MC-38^{R} cells were plated on 96-well, white flat bottom plates, allowing 48 h for the cells to adhere to the plate and begin to grow exponentially until they reached about 25% confluency. To test for 5FU-LV resistance, 2500 cells per well, both the MC-38 and MC-38^{R} cells, were seeded in 96 well plates and allowed to attach for 24 hours. After 24 hours, the cells were pre-treated for 2 hours with LV before adding 5 FU and then incubated for 96 hours at 37^{o}C in 5% CO_2. Cell viability was assessed using Aqueous-one (Promega) following the manufacturer's instructions. Resistance factor was calculated based on the ratio of IC50 values for MC-38 and MC-38^{R} cells. All experiments were performed in triplicate.

Clonogenic assay

A modified clonogenic assay assessed the potency of CF10 and 5-FU in MC-38 and MC-38^{R} cells. The CRC cells were plated in 24-well plates in FR media, and after 24 hours, they were treated with the indicated concentration of CF10 or 5-FU for 72 hours. The media were replaced after drug treatment, while the cells were allowed to grow for 168 hours. Cell proliferation was evaluated using the Aqueous One (Promega) reagent, following the manufacturer's instructions, after the cell solution was transferred to 96-well plates.

Western Blotting

Proteins were isolated, and their differential expressions were analyzed by Western blot, as described previously (Okechukwu CC et al. 2024). Briefly, both MC-38 and MC-38^{R} treated cells (LV, 5FU,5FU + LV, CF10, CF10 + LV) were lysed using RIPA buffer (50 mM Tris HCl at pH 7.4, 150 mM NaCl, 1% Triton X-100 or NP-40, 0.5% sodium deoxycholate, 0.1% SDS, 1 mM EDTA, and 10 mM NaF freshly supplemented with protease and phosphatase inhibitors). The protein concentrations were quantified using a Bradford assay (Bio-Rad), and the samples were normalized for equal loading. All samples were then heated to 95 °C for 10 min in the presence of 6 x Laemmli buffer (Boston Bio-Products; Milford, MA, USA). The proteins were resolved using SDS-PAGE, and their expression was analyzed following immunoblotting using specific antibodies. The following antibodies were used in this study: Thymidylate Synthase (Cell Signaling Technology Cat# 3766, RRID: AB_2210584), c-Myc (Cell Signaling Technology Cat# 18583, and β-actin (Santa Cruz Biotechnology Cat# sc-47778, RRID: AB_626632).

Liver Tumor Cell Inoculation to Simulate CRLM Formation

All animal studies were undertaken in accordance with the protocols approved by the Institutional Animal Care and Use Committee at Wake Forest University School of Medicine (Winston-Salem, NC, USA). Immunocompetent C57BL6 (RRID:IMSR_JAX:000664) mice weighing 22–24g were used because this strain is syngeneic with the MC-38R and MC-38 (RRID:CVCL_B288) CRC cell lines. C57BL6 (RRID:IMSR_JAX:000664) mice were commercially available in the U.S.

and were obtained from Charles River Laboratories for these studies. The mice had a controlled climate and light cycles, and all had free access to a FR diet and water. For the inoculation procedure, anesthesia was obtained using 2–3% isoflurane and then maintained at 1.5% for surgery. A 2 cm midline incision was made, and both the left and right hepatic lobes were mobilized. Both MC-38^{R} and MC-38 (RRID:CVCL_B288) CRC cells were suspended at a density of 2×10^{6} cells in 200 µL and 25 µL of cell suspension, mixed 1:1 with Matrigel, and injected via a 29-gauge needle into the subcapsular portion of one of the previously specified hepatic lobes of each designated group of mice. When the needle was withdrawn, a cotton swab was used to press on the puncture site to achieve hemostasis. Once hemostasis was achieved, the wound was washed with saline, the muscle layer was closed using a 6-0 Vicryl suture, and the skin was closed using staples. An abdominal bandage was applied, and the mice were allowed to recover from anesthesia before returning to the animal facility. The tumors were allowed to grow for a week and fluorescence imaging was performed using an RGD peptide Cy5.5 conjugate to establish tumor formation prior to initiating treatments.

Treatment and Fluorescence Imaging of Tumor Progression

Both C57BL6/MC-38 and C57BL6/MC-38^{R} syngeneic orthotopic mice model fluorescence tumor images were undertaken using an IVIS Lumina LT Series III system (RRID:SCR_014247) under isoflurane anesthesia. All images were analyzed using Living Image software (v4.7.4.) with an identical size region of interest for each mouse. To assess therapeutic efficacy, groups of $n = 4$ mice with similar initial tumor levels based on fluorescence imaging were treated with (1) no

treatment, (2) 5-FU, (3) CF10, (4) LV, (5) 5-FU+LV, (6) CF10+LV. 5-FU was administered at 100 mg/kg and CF10 were dosed to deliver equivalent nucleoside content based on UV absorbance at 260 nm. LV was infused together with the FP. Mice in each group were treated on a 7-day mini-osmotic pump. All mice underwent a final imaging procedure at the end of the seventh day and were then euthanized, and their important organs (livers, G.I, etc.) were harvested and prepped for other procedures. For each of the six treatments, the difference in flux or weight values were calculated (Day 7 minus Day 0). Next, a general linear model was fit to compare the 6 groups (Control, LV, 5-FU, CF10, 5-FU+LV, CF10+LV). We first examined the overall test for the model and if that was significant, pairwise comparison between groups were made. Given the large number of potential pairwise comparisons that could be made, we conservatively used a Bonferroni Correction when comparing groups. For maintaining mice on a FR diet, the FR diet purchased from Envigo Teklad Diets (Madison, WI) composed of 35.0g/Kg AIN-93G-MX (94046), 10.0g/Kg Succinyl sulfathiazole, 195.0g/Kg Casein, 3.0g/Kg L-Cystine, 304.488g/Kg Corn Starch, 0.016g/Kg Calcium Pantothenate, 0.006g/Kg Thiamin (81%), 209.749g/Kg Sucrose, 130.0g/Kg Maltodextrin, 60.0g/Kg Soybean Oil, 50.0g/Kg Cellulose, 0.007g/Kg Pyridoxine HCl, 0.012g/Kg TBHQ (antioxidant), 2.5g/Kg Choline Bitartrate, 0.03g/Kg Niacin, 0.006g/Kg Riboflavin, 0.0002g/Kg Biotin, 0.025g/Kg Vitamin B12 (0.1% in mannitol), 0.0008g/Kg Vitamin K1 phylloquinone, 0.15g/Kg Vitamin E, DL-alpha tocopheryl acetate (500 IU/g), 0.008g/Kg Vitamin A Palmitate (500,000 IU/g), and 0.002g/Kg Vitamin D3 cholecalciferol (500,000 IU/g).

In-Vivo Resistant Survival Study

The C57BL6/MC-38^{R} and C57BL6/MC-38 syngeneic orthotopic mice model fluorescence tumor images were undertaken using an IVIS Lumina LT Series III system (RRID:SCR_014247) under isoflurane anesthesia and maintained in an FR diet as described in the Treatment and Fluorescence Imaging of Tumor Progression section. All images were analyzed using Living Image software (v4.7.4.) with an identical size region of interest for each mouse. To assess therapeutic efficacy, groups of n = 5 mice with similar initial tumor levels based on fluorescence imaging were treated with (1) no treatment, (2) 5-FU+LV, (3) CF10+LV. 5-FU was administered at 100 mg/kg and CF10 were dosed to deliver equivalent nucleoside content based on UV absorbance at 260 nm. LV was infused together with the FP . Mice in each group were treated on a 14-day mini-osmotic pump. For the resistant group study, only CF10 + LV group mice survived and underwent a final imaging procedure at the end of the fourteenth day and were then euthanized, and their important organs (livers, etc.) were extracted and prepped for other procedures. Unfortunately, mice in both control group and 5FU + LV group were unable to survive through the end of the fourteenth day of the survival study due to uncontrolled growth of the tumors and organ damages. For the parental syngeneic group, mice in groups 5FU + LV and CF10 + LV survived with more animal survival in group CF10 + LV compared to group 5FU + LV at the end of the fourteenth day of the study.

TS Activity Assay

A TS in situ activity assay was performed as previously described [7]; to provide a quantitative indication of intracellular inhibition of TS activity following drug treatment. ~$0.5x10^6$ MC-38 (RRID:CVCL_B288) and MC-38^R cells were plated in each well of a 6-well plates and cells were allowed to attach for 24h then treated with either LV, 5-FU, 5-FU + LV, CF10, or CF10 + LV for 48h. For the last 2h, [5-3H]-2'-deoxyuridine (Moravek) 0.16 Ci/mmol; final concentration 2.5 µM was present. 150 µL of media from each well was added to an ice-cold suspension containing 750 µL of charcoal with 0.5% T-70 dextran and 2.5% BSA) and 150 µL of 35% trichloroacetic acid. After centrifugation a portion of the supernatant was counted by liquid scintillation counting and enzyme activities were expressed as a percent relative to drug-free control.

Statistical Analysis

GraphPad Prism 10.2.0 (RRID:SCR_002798) was used for statistical analyses of cell-based assays. Experiments were conducted in triplicate ± SEM. For all in vitro experiments, three biological replicates were used for analysis, and appropriate one-way ANOVA tests with recommended Tukey corrections were conducted, with $p < 0.05$ indicating significance. For in vivo studies, one-way analysis of variance (ANOVA) models were fit to compare the three groups on the outcomes of change in treatment response based on IVIS imaging and weight.

Results

Acquired resistance to 5-FU/LV in MC38 cells through treatment induced increased TS levels.

Multiple previous studies demonstrated that acquired resistance to 5-FU in human cells occurs through elevated TS levels which may occur through gene amplification[1, 8]. We recently described selection for 5-FU/LV in human CRC cells cultured under conditions of human-like folate levels and observed that basal TS levels were not significantly changed despite resistance factors of ~30-fold. However, TS levels detected by Western blot were significantly increased with 5-FU/LV treatment of the selected resistant cells (manuscript submitted). In order to study therapy response in a syngeneic orthotopic model of CRC liver metastasis with human-like folate levels we selected MC38 mouse CRC cells for acquired resistance to 5-FU/LV by first adapting these cells to culture conditions with human-like folate levels and then repeatedly passaging the cells in FR media with increasing concentrations of 5-FU/LV over several months. The IC50 value for 5-FU increased from 26.6 μM in parental MC38P to 346 μM in 5-FU/LV-resistant MC38R cells, a resistance factor of 13. We have previously shown that CF10/LV remained highly effective in human CRC cells selected for 5-FU/LV resistance with nM potency and resistance factors approximately 1/10 that for 5-FU/LV in these cells (manuscript submitted). Similar trends were detected in MC38R cells with CF10/LV displaying nM potency in these cells (**Figure 1**).

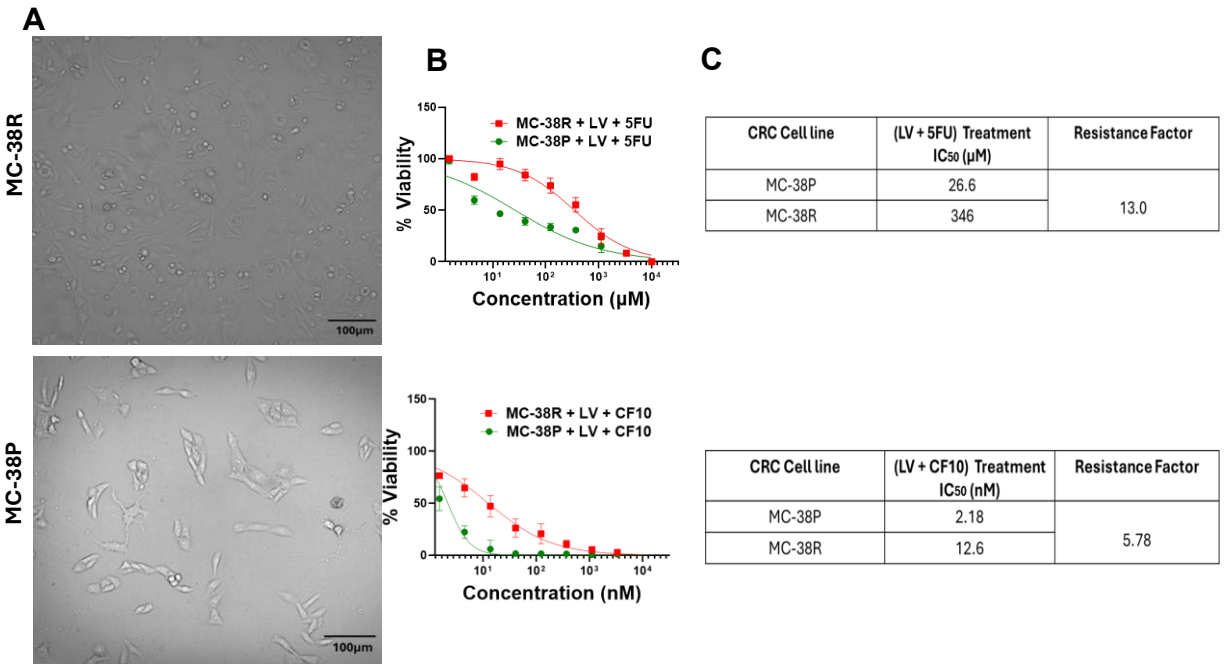

Figure 1. MC38^{R} cells selected for resistance to 5-FU/LV display limited cross-resistance to CF10/LV. (A) Bright-field microscopy images of MC38^{R} (top) and parental MC38 (MC38^{P}) cells (bottom). (B) Dose response curves for the indicated 5-FU (top – uM) and CF10 (bottom – nM) together with 10 uM LV in MC38^{R} cells (red) and MC38^{P} cells (green). (C) Summary of IC50 values and resistance factors for 5-FU/LV (top) and CF10/LV (bottom).

Western blot for TS did not reveal significant increase in MC38R vs MC38P cells and while single agent 5-FU (10 uM, 24h) did not significantly increase TS levels treatment with 5-FU/LV (10 uM/1 uM, 24h) did significantly increase TS levels (**Figure 2**). In contrast both single agent CF10 (1 uM, 24h) and CF10/LV (1 uM/1uM, 24h) did result in significantly increased TS levels. TS is an RNA-binding protein that autoregulates its expression by binding its mRNA and the results are consistent with treatments that inhibit TS activity through TS ternary complex formation stimulating increased TS expression. In particular TS mobility in gels for Western blot was reduced with CF10/LV treatment consistent with TS ternary complex formation (TSCC) (**Figure 2A,D**). To determine if treatment was sufficient

to reduce TS catalytic activity, we performed TS in situ activity assay (**Figure 2C,E**). For all treatments TS catalytic activity was reduced more effectively in MC38P vs MC38R cells. CF10 and CF10/LV were more effective than 5-FU and 5-FU/LV in reducing TS catalytic activity in both MC38 and MC38R cells and while CF10 and CF10/LV were less effective in MC38R cells TS activity was still reduced by ~80%. In contrast 5-FU and 5-FU/LV resulted in >50% reduction in TS activity despite a 10-fold higher concentration of 5-FU relative to CF10. The results are consistent with increased expression of TS with treatment with either 5-FU±LV or CF10±LV but with only CF10 remaining effective at inhibiting TS catalytic activity in the MC38R cells.

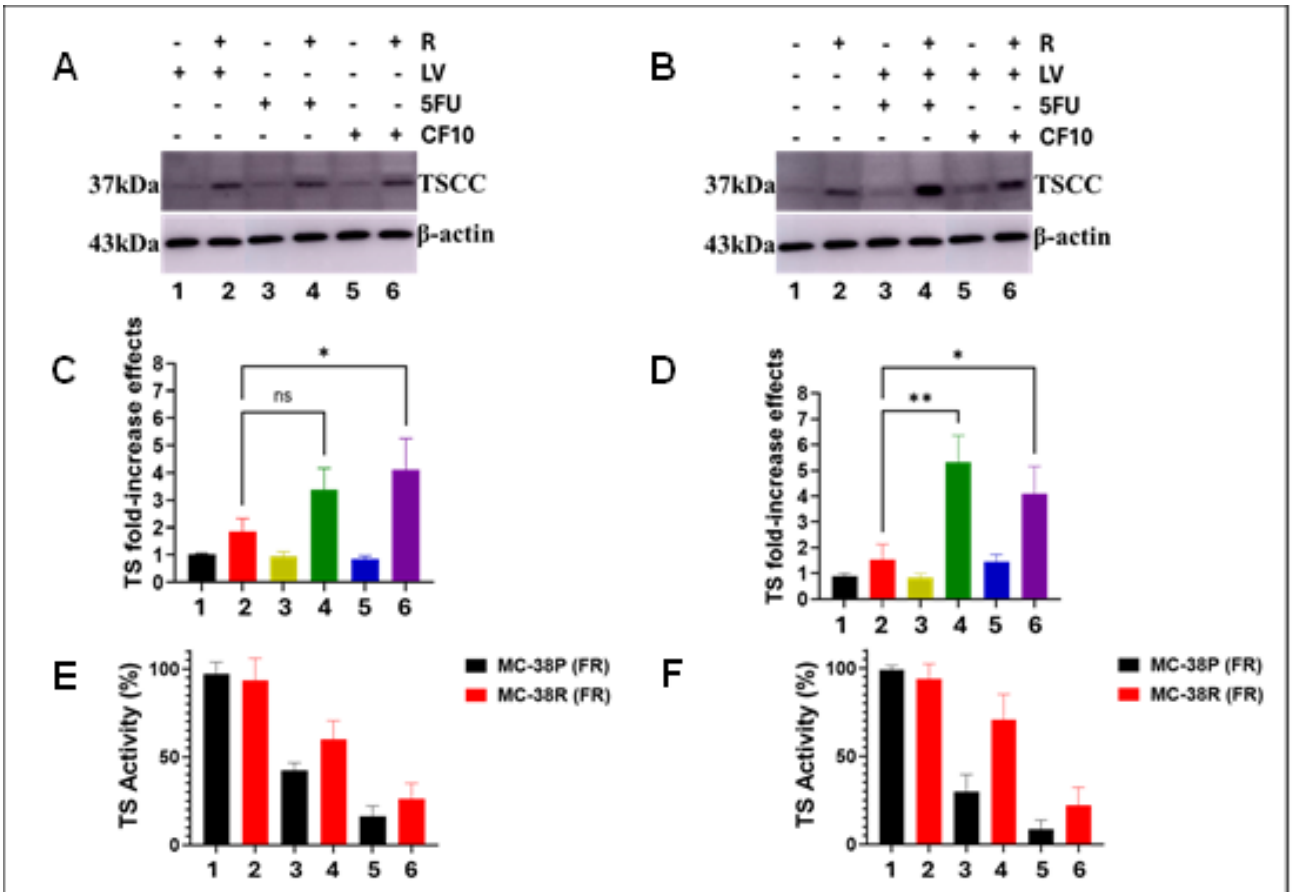

Figure 2. Fluoropyrimidine treatment induces increased TS levels in 5-FU/LV-resistant MC38R cells. (A,B) Western blots for TS in MC38R and MC38P cells with indicated treatments. TSCC indicates the TS ternary complex that migrates with reduced mobility. (C,D) Quantification of increased TS intensity for (A,B). (E,F) Reduced TS enzymatic activity in MC38P (black) and MC38R (red) cells with the same treatments as shown in the Western blot (A,B).

CF10/LV displays strong antitumor activity in MC38^{R} CRLM model.

Liver-metastatic disease is a principal cause of CRC mortality and chemotherapy with 5-FU-based regimens is often the best available therapeutic option. While current chemotherapy improves outcomes, long-term survival remains rare (<14% 5-year survival) because of the development of acquired resistance. To simulate the development of FU/LV-resistant CRLM, we developed orthotopic CRC liver metastases in mice by injecting MC38^{R} cells that were selected for acquired

resistance to FU/LV into one lobe of the liver in host syngeneic C57BL/6 mice. We evaluated the response to 5-FU/LV and CF10/LV in the MC38^{R} CRLM model using a similar approach to that recently described for the corresponding parental MC38 CRLM model in which parental MC38 cells (not selected for acquired resistance) were injected into one liver lobe of C57BL/6 mice (manuscript submitted). Since plasma folate levels affect response to fluoropyrimidine drugs seven days before tumor cell injection mice were adapted to a folate-restricted diet to develop human-like folate physiology.

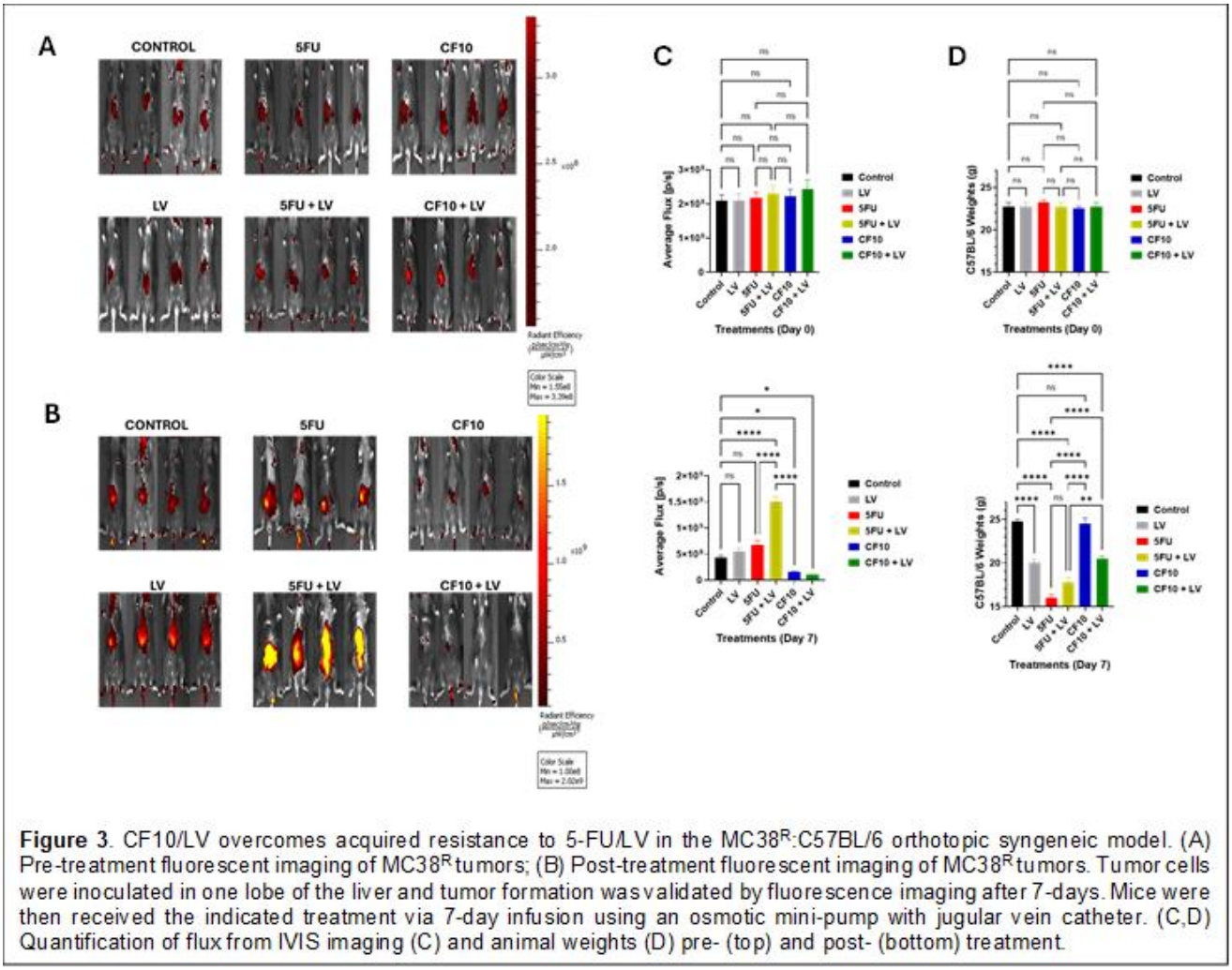

Figure 3. CF10/LV overcomes acquired resistance to 5-FU/LV in the MC38^{R}:C57BL/6 orthotopic syngeneic model. (A) Pre-treatment fluorescent imaging of MC38^{R} tumors; (B) Post-treatment fluorescent imaging of MC38^{R} tumors. Tumor cells were inoculated in one lobe of the liver and tumor formation was validated by fluorescence imaging after 7-days. Mice were then received the indicated treatment via 7-day infusion using an osmotic mini-pump with jugular vein catheter. (C,D) Quantification of flux from IVIS imaging (C) and animal weights (D) pre- (top) and post- (bottom) treatment.

After validating establishment of MC38^{R} tumors in the liver by IVIS imaging 7 days post tumor cell inoculation mice were divided into groups for treatment. Groups of n=4 mice received (1) no treatment, (2) LV, (3) 5-FU, (4) 5-FU/LV, (5) CF10, (6) CF10/LV. Initial tumor levels were similar in all groups (**Figure 3A,C**), and the tumor was localized to the liver. 5-FU was administered at 100 mg/kg and the CF10 dose was matched to the 5-FU dose based on equal A260 absorbance. For all treatment groups mice were fitted with a jugular vein catheter and drugs (5-FU±LV, CF10±LV) were administered over 7 days using an Alzet mini-pump. Tumor burden was assessed by IVIS imaging at day 0 (pre-treatment; (**Figure 3A,C**)) and day 7 (post-treatment; (**Figure 3B,C**). The removal of the Alzet pump and jugular vein catheter was performed as a terminal procedure following IVIS imaging on day 7 in all mice. While all treatments were tolerated mice in all groups except vehicle and single agent CF10 experienced significant weight loss (**Figure 3D**). The largest weight loss occurred with 5-FU, and despite mice treated with single-agent LV losing weight, mice treated with 5-FU+LV lost less weight than for single-agent 5-FU. Weight loss for mice treated with CF10+LV was slightly less than for single-agent LV (**Figure 3D**) (Supplementary Table S1, S2; Supplementary Figure S1). The change in flux from fluorescent imaging (day 7 vs day 0) was analyzed to assess treatment effects on progression of drug-resistant liver metastatic disease. Substantial flux reductions occurred with CF10 and CF10/LV treatment consistent with CF10 and CF10/LV being effective in treating CRC cells selected for resistance to 5-FU/LV. In contrast single agent LV and single agent 5-FU both increased flux relative to control. Intriguingly 5-FU/LV

strongly promoted tumor growth in the MC38^{R} CRLM model which was selected for resistance to 5-FU/LV.

To gain further insight into the effects of treatment on tumor progression, mice were euthanized post-treatment following IVIS imaging and livers were excised. H&E-stained sections from livers of all treatment groups were analyzed by a pathologist to evaluate tumor progression (**Figure 4A**).

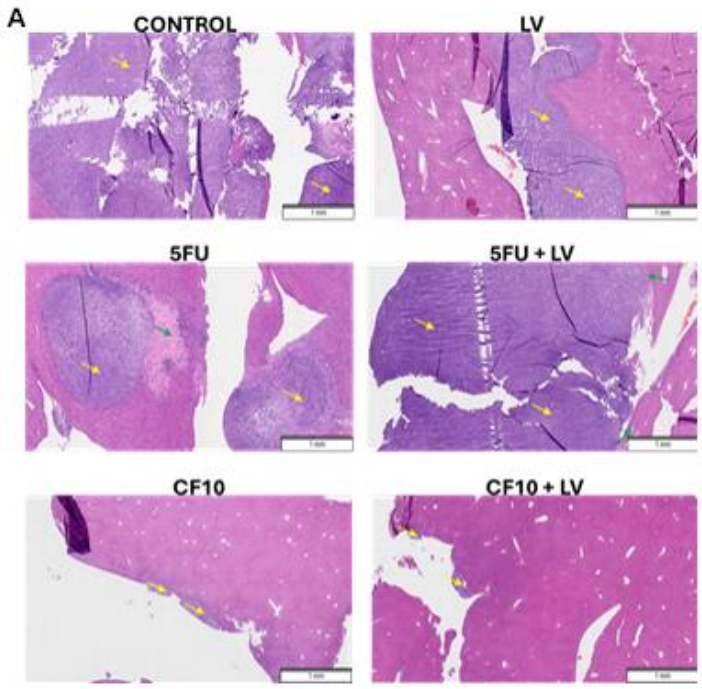

B

Treatment Group	Early Scarring/ Inflammation (Green)	% Tumor Burden (Yellow)
Control	Negative	88 ± 3.6
LV	Negative	44 ± 4.3
5FU	Positive	52 ± 3.1
5FU + LV	Positive	91 ± 3.2
CF10	Negative	9 ± 1.8
CF10 + LV	Negative	5 ± 1.3

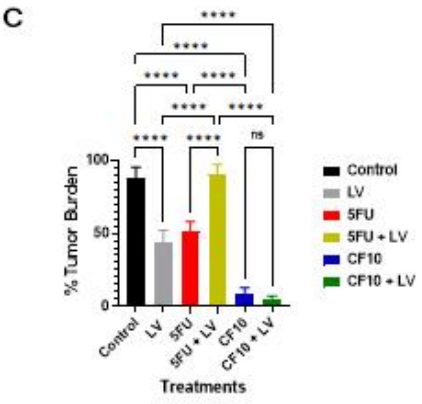

Figure 4. CF10 demonstrates potent activity to overcome resistance to 5-FU/LV. (A) H&E images depicting tumor burden in MC38R tumors following treatment with vehicle, LV, 5FU ± LV, or CF10 ± LV. (B) Table showing % tumor burden and early scarring/inflammation upon FP drugs with/without LV. (C) Qualification of A. p-values were calculated using GraphPad Prism (n = 4, ****p ≤ 0.0001,***p≤ 0.0002, **p ≤ 0.002, *p ≤ 0.01)

Extensive tumor burden was found in livers from all control mice (88±3.6%; **Figure 4B**). Single agent LV and single agent 5-FU significantly decreased MC38^{R} tumor burden (44±4.3% and 52±3.1%; **Figure 4B**) however tumor burden in 5-FU/LV-treated mice was greater than for control (91±3.2%; **Figure 4B**). In contrast both

CF10 (9±1.8%; **Figure 4B**) and CF10/LV (5±1.3%; **Figure 4B**) strongly decreased $MC38^R$ tumor burden (Supplementary Table S3, S4; Supplementary Figure S2). In addition to being significantly more effective than 5-FU and 5-FU/LV CF10 and CF10/LV did not cause scarring or inflammation in the liver which was observed with 5-FU and 5-FU/LV treatment. Our results are consistent with a lack of efficacy for 5-FU and 5-FU/LV in treating drug-resistant mCRC and in contributing to liver inflammation and scarring while CF10 and CF10/LV display potent anti-tumor activity without evidence of inflammation or scarring. Similar results were found in the parental MC38 CRLM model (manuscript submitted).

CF10/LV displays improved survival relative to 5-FU/LV in $MC38^R$ CRLM model.

Our results in the MC38R CRLM model demonstrated that CF10 and CF10/LV displayed significant therapeutic advantages relative to 5-FU and 5-FU/LV with 7-day infusion however the time period investigated was not sufficient to establish whether CF10/LV could provide a survival advantage. Since drug infusion via osmotic pump and jugular vein catheterization does not permit long-term study because removal of the jugular vein catheter is done as a terminal procedure, we conducted analogous studies for both the MC38 and MC38R tumor models with 14-day infusion. Groups of n=5 mice received (1) no treatment, (2) 5-FU/LV, (3) CF10/LV. Drug concentrations were the same as for the 7-day study (preceding section; **Figure 4**) except drugs were administered over 14 days rather than 7 days. Tumor burden was assessed by IVIS imaging at day 0 (pre-treatment and day 7 and day 14 (post-treatment) (**Figure 5A, 6A**) including body weights

(**Figures 5B, 6B**). A 14-day infusion was sufficient to investigate whether treatment impacted survival since in the absence of treatment CRLM mice in both MC38 (**Figure 5C**) and MC38R (**Figure 6C**) models survive ≤10 days. In the parental MC38 CRLM model 5-FU/LV provided a survival advantage relative to control with 2/5 mice surviving until day 14, both with substantial tumor burden (**Figure 5**). CF10/LV provided a significant survival advantage relative to both control and 5-FU/LV with 5/5 mice surviving until day 14 and with all five mice displaying minimal tumor burden (**Figure 5**). In contrast, in the $MC38^R$ CRLM model 5-FU/LV did not provide a survival advantage relative to control with 5/5 mice deceased due to tumor burden by day 9 while in control 5/5 mice were deceased due to tumor burden by day 10. However, CF10/LV provided a significant survival advantage relative to both control and 5-FU/LV in the MC38R CRLM model with 5/5 surviving until day 14 and minimal tumor burden (**Figure 6**). MC-38P histology representation showed huge tumor burden and early inflammatory scarring tissues due to 5FU treatment (**Figure 5**). Log-rank test demonstrated significantly improved survival for CF10/LV relative to 5-FU/LV and control ($p \leq 0.0059$, Gehan-Breslow-Wilcoxon test). The results demonstrate CF10/LV display strong antitumor activity in the $MC38^R$ CRLM model consistent with potential clinical use in the treatment of liver metastases following progression with treatment with 5-FU/LV-based regimens (e.g. FOLFOX, FOLFIRI).

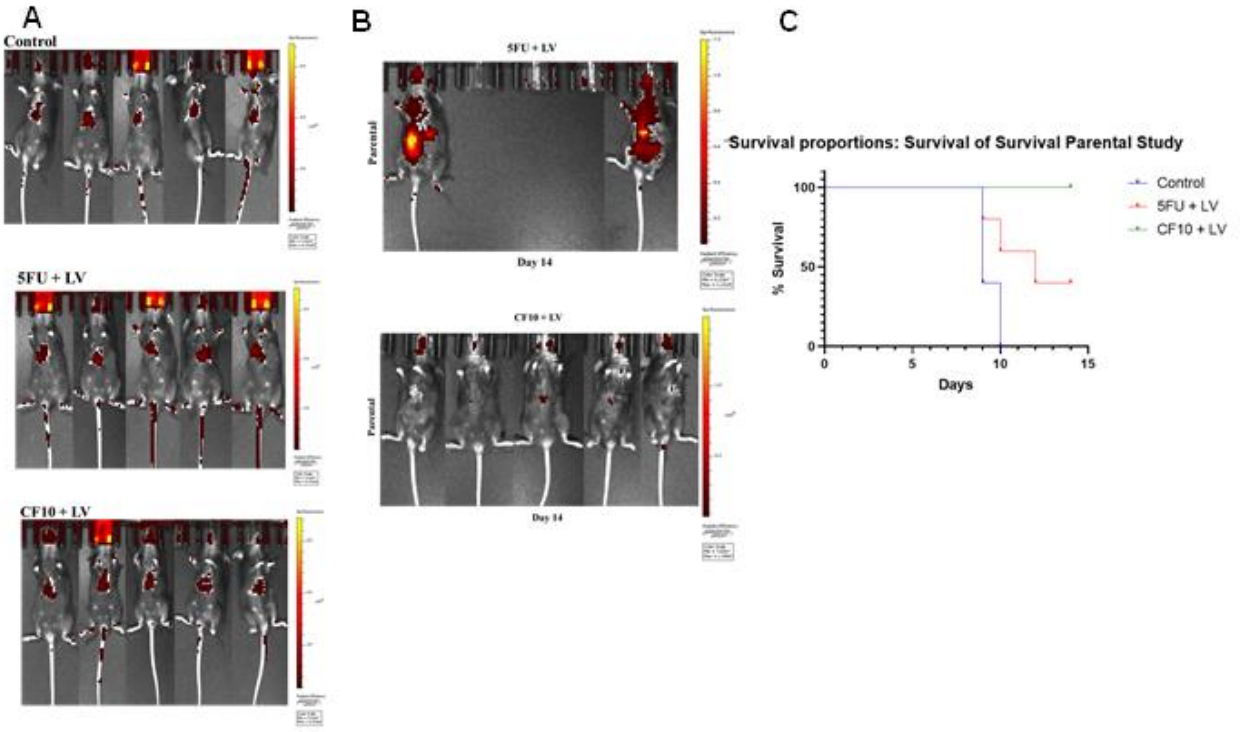

Figure 5. CF10/LV provides a survival advantage in the MC38:C57BL6 syngeneic orthotopic CRLM model.

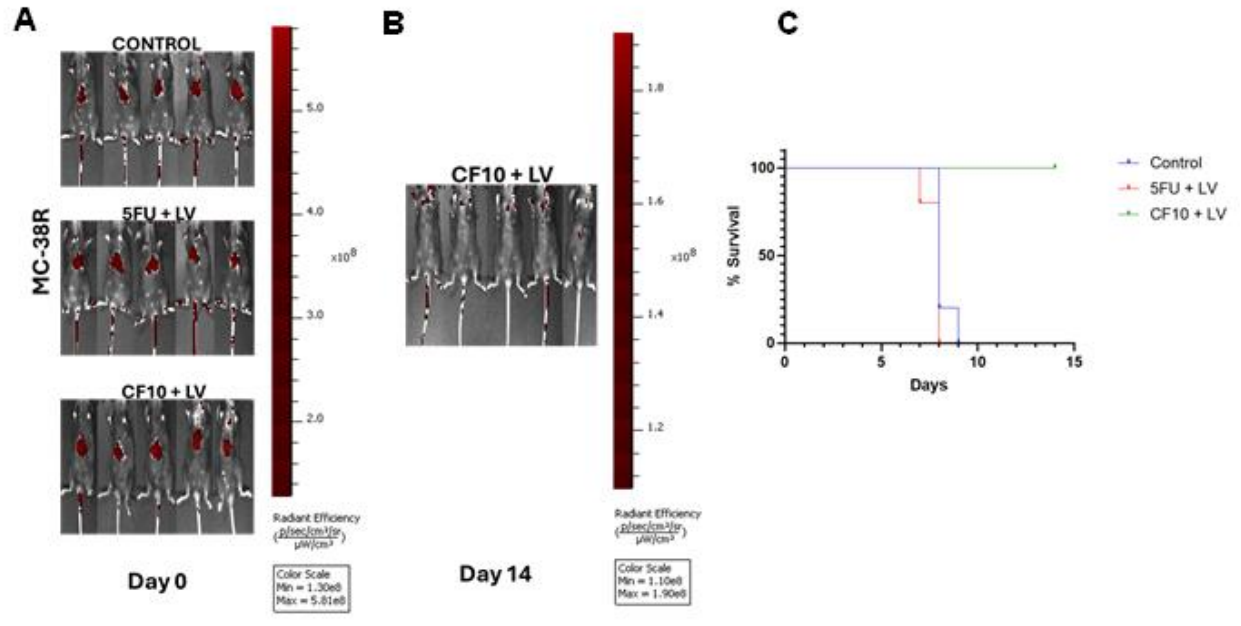

Figure 6. CF10/LV provides a survival advantage in the MC38R syngeneic orthotopic CRLM model.

CF10/LV inhibits metastasis in MC38^{R} CRLM model.

To gain further insight into the therapeutic benefit of CF10 and CF10/LV in the MC38R:C57BL6 CRLM model we extracted tissues from mice following 14-day treatment and interrogated GI-tract tissue and other organs for signs of metastatic progression (**Figure 7**). Evidence of extensive metastasis to bowel was evident in control, LV and 5-FU±LV treatment groups however there was no evidence of metastasis to bowel with CF10 or CF10/LV treatment. With 5-FU and 5-FU/LV treatment there was also extensive degradation of normal tissue while with CF10 and CF10/LV in addition to an absence of tumor tissues appeared healthy and robust.

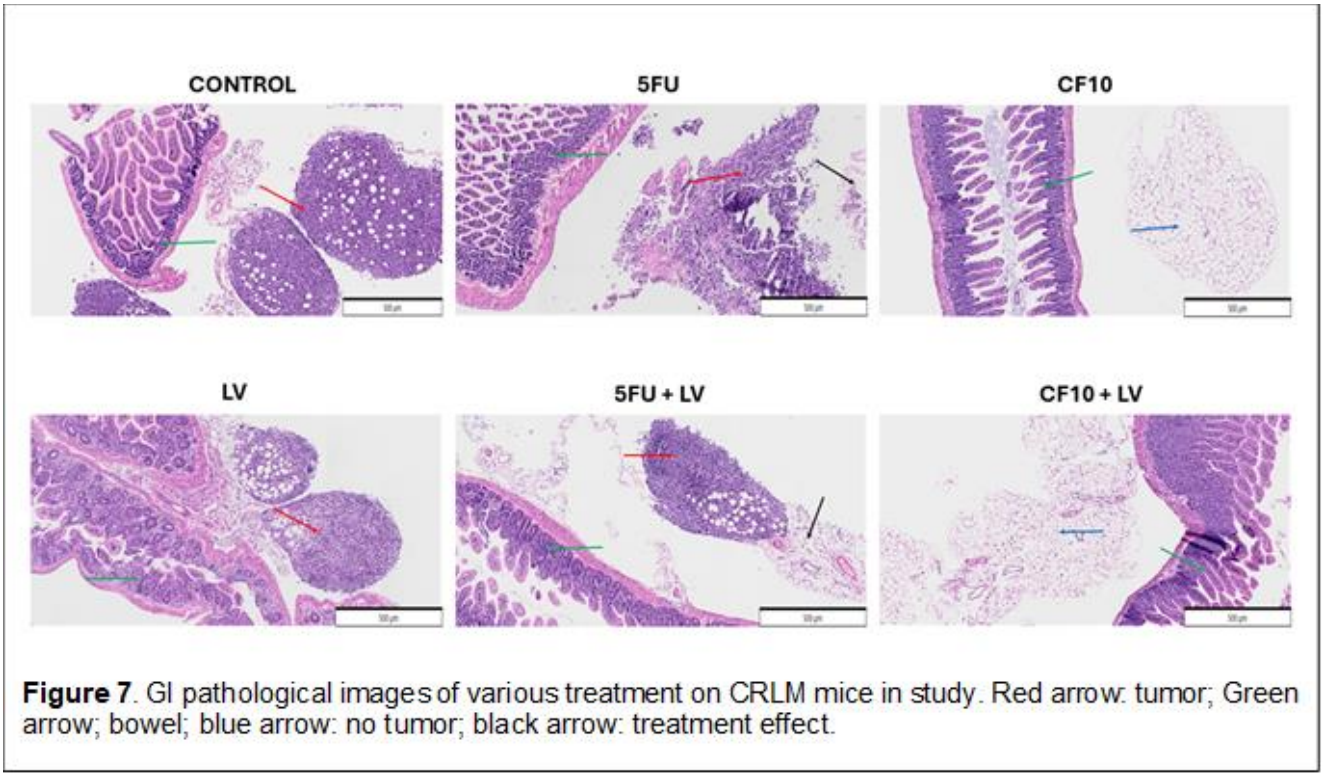

Figure 7. GI pathological images of various treatment on CRLM mice in study. Red arrow: tumor; Green arrow; bowel; blue arrow: no tumor; black arrow: treatment effect.

Discussion

Acquired drug resistance is a central cause of colorectal cancer mortality as the majority of patients with metastatic CRC initially respond to chemotherapy with 5-FU-based regimens (e.g. FOLFOX, FOLFIRI) however long-term survival is uncommon with <14% of mCRC patients surviving 5-years post-diagnosis [2, 9]. In the present studies we sought to develop a clinically relevant mouse model of therapy-resistant CRC liver metastasis since this would allow testing of next generation FP chemotherapies to evaluate their potential to overcome resistance. We previously established a syngeneic orthotopic MC38:C57BL/6 CRC liver metastasis model by sub-capsular injection of MC38 cells into one hepatic lobe. Since mice have higher folate levels than humans we maintained the mice on a folate-restricted diet. We also adapted the MC38 cells for growth in folate-restricted media prior to tumor formation. We demonstrated in this model that 5-FU was potentiated by leucovorin (LV) consistent with the clinical use of 5-FU/LV for mCRC treatment. In the present studies we modified the MC38:C57BL/6 CRC liver metastasis model by first adapting MC38 cells to culture in conditions of human-like folate levels and then selected cells for resistance to increasing concentrations of 5-FU/LV. This approach more closely reflects the conditions encountered by tumor cells *in vivo* during the course of extensive therapy with 5-FU-based chemotherapy regimens. The resulting $MC38^{R}$ cells were ~13.8-fold resistant to 5-FU/LV (**Figure 1**). As we previously showed for human CRC cell lines selected for acquired resistance to 5-FU/LV reduced cross-resistance to CF10 (5.78-fold) was observed in these cells and CF10 was highly potent to $MC38^{R}$ cells with IC50 =

12.6 nM, a result consistent with the potential of CF10 to be effective in treating mCRC patients who were previously treated with 5-FU/LV-based chemotherapy regimens.

The causes of chemoresistance are multifactorial however multiple studies investigating acquired resistance to 5-FU both in patients and in cultured cancer cells identified elevated levels of thymidylate synthase (TS), the primary molecular target of 5-FU, as a significant contributing factor [10]. Since in the present studies we first adapted cells to more human-like folate levels and then selected for resistance to 5-FU/LV rather than single-agent 5-FU an altered mechanistic basis for resistance could develop. As in our studies in human CRC cell lines that were selected for 5-FU/LV resistance using similar methods basal TS levels in $MC38^{R}$ cells did not differ significantly from $MC38^{P}$ cells. However, treatment with 5-FU±LV or CF10±LV significantly increased TS levels ~4-5-fold by Western blot (**Figure 2**) consistent with induced expression of TS with FP treatment. One mechanism for increased TS expression with FP treatment involves formation of a TS ternary complex (TS+FdUMP+N^5,N^{10} methylene tetrahydrofolate – TS classic complex) since TS ternary complex formation relieves autoregulatory inhibition of TS expression through binding of the uncomplexed protein to TS mRNA [11]. Increased TSCC was detected with CF10±LV treatment relative to 5-FU±LV treatment and CF10±LV resulted in decreased TS enzymatic activity at ~1,000-fold lower concentrations relative to 5-FU±LV despite CF10 having only a 10-fold greater FP content. Our results are consistent with the increased potency of CF10

relative to 5-FU in MC38^{R} cells resulting from strong TS inhibitory activity despite induced upregulation of TS levels with FP treatment.

In previous studies we established an improved therapeutic benefit for CF10 relative to 5-FU in a rat syngeneic orthotopic CRC liver metastasis model. We also previously established improved therapeutic benefit for CF10 relative to 5-FU in the MC38:C57BL/6 CRC liver metastasis model and in an orthotopic primary CRC and other cancer models. Mechanistically, we established that the improved potency of CF10 results from direct release of the TS inhibitory metabolite FdUMP, strong TS inhibition and formation of DNA topoisomerase 1 cleavage complexes (Top1cc) [12-14]. Top1cc are formed when FdUTP is misincorporated into DNA under thymineless conditions as Top1 can cleave FdU-substituted DNA but cannot re-ligate it. CF10-induced Top1cc cause replication fork stalling and collapse and DNA double strand breaks and initiation of apoptotic cell death(15). In these studies, we tested if CF10+LV would be more effective than 5-FU/LV in the MC38^{R}:C57BL/6 CRC liver metastasis model. 5-FU and CF10 were dosed to deliver equivalent fluoropyrimidine content based on A260 absorbance. We first tested the activity using a 7-day infusion together with LV. In this model both 5-FU and 5-FU/LV treatment actually enhanced tumor growth relative to a no treatment control. In contrast CF10 and CF10/LV resulted in complete tumor regression (**Figure 3**). We also assessed whether treatment caused scarring or inflammation as this is an established side effect with 5-FU-based chemotherapy regimens. We found that the strong efficacy of CF10 and complete eradication of liver metastasis was achieved without evidence of scarring or inflammation (**Figure 4**).

The 7-day infusion model provides valuable information on the potential of CF10 to be effective in treating drug-resistant mCRC however a limitation of the model is that it does not allow a survival advantage to be established because mice are required to be euthanized following removal of the jugular vein catheter because of the number of invasive surgeries involved in the study. To determine if CF10 and CF10/LV could provide a survival advantage relative to 5-FU and 5-FU/LV we used a 14-day infusion model and evaluated survival in both the MC38:C57BL/6 (**Figure 5**) and the MC38^{R}:C57BL/6 CRC liver metastasis models (**Figure 6**). In both models CF10 and CF10/LV were effective in complete tumor eradication with 5/5 mice surviving 14 days in both models. In contrast, 5-FU/LV showed only limited efficacy in the MC38:C57BL/6 CRLM model with only 2/5 mice surviving to the end of treatment at 14 days and with both surviving mice displaying substantial tumor burden. Further, in the MC38^{R}:C57BL/6 CRC liver metastasis model 5-FU/LV showed no benefit compared to no-treatment control will all mice deceased by day 8. Collectively, these studies confirm the therapeutic benefit of CF10 and CF10/LV in treatment of liver metastatic CRC and demonstrate its potential to be both well tolerated and to provide a substantial survival benefit relative to current therapy. We performed H&E staining on tissues from treated mice in the 14-day infusion study and assessed tissues for metastasis to GI-tract tissue and the overall appearance of tissues for drug-related toxicity and inflammation. In the absence of treatment or with treatment with LV, 5-FU, or 5-FU/LV there was evidence of metastatic spread from the liver back to GI tissue. There was also considerable degradation of the intestine with 5-FU and 5-FU/LV treatment. In

contrast, with CF10 and CF10/LV there was no evidence of metastatic progression and GI appeared tissue appeared normal as in non-treated, non-tumor bearing mice. Overall, our studies demonstrate that CF10 and CF10/LV are effective in treatment of liver metastatic CRC including in tumor models of 5-FU/LV-resistant mCRC.

In summary, we established the first model of 5-FU/LV resistance in CRC cells where cells were selected for resistance to 5-FU/LV under human-like conditions of folate physiology. Basal levels of TS were not elevated in 5-FU/LV-resistant cells but treatment with either 5-FU±LV or CF10±LV induced elevated TS expression possibly through disrupting autoregulation of TS through binding its own mRNA. CF10±LV reduced TS enzymatic activity and CF10±LV retained nM potency to the 5-FU/LV resistant cells. We tested CF10 and CF10/LV in vivo in both MC38:C57BL/6 (Figure 5) and $MC38^{R}$:C57BL/6 CRC liver metastasis models (Figure 6). In both models CF10 and CF10/LV dramatically outperformed 5-FU and 5-FU/LV. A significant survival advantage was established for CF10/LV in both models. Collectively our studies provide new insights into the mechanisms of acquired resistance during treatment with 5-FU-based chemotherapy regimens and demonstrate the clinical potential of CF10/LV for treatment of drug-refractory mCRC.

Disclosure of Potential Conflicts of interest

W. Gmeiner is inventor on a patent application for CF10 in colon cancer.

Authors' Contributions

Conception and design: W.H. Gmeiner

Development of methodology:

Acquisition of data (provided animals, acquired and managed patients, provided facilities, etc.): W.H. Gmeiner, X. Ma, C. Okechukwu

Analysis and interpretation of data (e.g. statistical analysis, biostatistics, computational analysis): R. D'Agostino Jr, W.H. Gmeiner, W. Li, C. Okechukwu

Writing, review, and/or revision of the manuscript: R. D'Agostino Jr, W.H. Gmeiner, W. Li, C. Okechukwu, X. Ma

Administrative, technical, or material support (i.e., reporting or organizing data, constructing databases): W.H. Gmeiner

Study Supervision: W.H. Gmeiner

Acknowledgements

This study was performed with grant support from 1R42 CA254843 (to W.H. Gmeiner), Department of Defense Peer Reviewed Cancer Research Program CA200460 (to W.H. Gmeiner). This work was also supported, in part, by a National Cancer Institute of the National Institutes of Health Cancer Center Support Grant P30CA012197 (AHWFBCCC). The authors wish to acknowledge the support of the Wake Forest Baptist Comprehensive Cancer Center Biostatistics Shared Resource, Cell, and Viral Vector Shared Resource, the Proteomics and Metabolomics Shared Resource, and the WFU Mass Spectrometry facility.

REFERENCES

1. Gmeiner WH, Okechukwu CC: **Review of 5-FU resistance mechanisms in colorectal cancer: clinical significance of attenuated on-target effects**. *Cancer Drug Resist* 2023, **6**(2):257-272.

2. Gmeiner WH: **Recent Advances in Therapeutic Strategies to Improve Colorectal Cancer Treatment**. *Cancers (Basel)* 2024, **16**(5).

3. Gmeiner WH: **Chemistry of Fluorinated Pyrimidines in the Era of Personalized Medicine**. *Molecules* 2020, **25**(15).

4. Danenberg PV, Gustavsson B, Johnston P, Lindberg P, Moser R, Odin E, Peters GJ, Petrelli N: **Folates as adjuvants to anticancer agents: Chemical rationale and mechanism of action**. *Crit Rev Oncol Hematol* 2016, **106**:118-131.

5. Gmeiner WH, Dominijanni A, Haber AO, Ghiraldeli LP, Caudell DL, D'Agostino R, Jr., Pasche BC, Smith TL, Deng Z, Kiren S *et al*: **Improved Antitumor Activity of the Fluoropyrimidine Polymer CF10 in Preclinical Colorectal Cancer Models through Distinct Mechanistic and Pharmacologic Properties**. *Mol Cancer Ther* 2021, **20**(3):553-563.

6. Okechukwu CC, Ma X, Sah N, Mani C, Palle K, Gmeiner WH: **Enhanced Therapeutic Efficacy of the Nanoscale Fluoropyrimidine Polymer CF10 in a Rat Colorectal Cancer Liver Metastasis Model**. *Cancers (Basel)* 2024, **16**(7).

7. Peters GJ, Smitskamp-Wilms E, Smid K, Pinedo HM, Jansen G: **Determinants of activity of the antifolate thymidylate synthase inhibitors Tomudex (ZD1694) and GW1843U89 against mono- and multilayered colon**

cancer cell lines under folate-restricted conditions. *Cancer Res* 1999, **59**(21):5529-5535.

8. Peters GJ, Backus HH, Freemantle S, van Triest B, Codacci-Pisanelli G, van der Wilt CL, Smid K, Lunec J, Calvert AH, Marsh S *et al*: **Induction of thymidylate synthase as a 5-fluorouracil resistance mechanism**. *Biochim Biophys Acta* 2002, **1587**(2-3):194-205.

9. Koroukian SM, Booker BD, Vu L, Schumacher FR, Rose J, Cooper GS, Selfridge JE, Markt SC: **Receipt of Targeted Therapy and Survival Outcomes in Patients With Metastatic Colorectal Cancer**. *JAMA Netw Open* 2023, **6**(1):e2250030.

10. Varghese V, Magnani L, Harada-Shoji N, Mauri F, Szydlo RM, Yao S, Lam EW, Kenny LM: **FOXM1 modulates 5-FU resistance in colorectal cancer through regulating TYMS expression**. *Sci Rep* 2019, **9**(1):1505.

11. Brody JR, Gallmeier E, Yoshimura K, Hucl T, Kulesza P, Canto MI, Hruban RH, Schulick RD, Kern SE: **A proposed clinical test for monitoring fluoropyrimidine therapy: detection and stability of thymidylate synthase ternary complexes**. *Cancer Biol Ther* 2006, **5**(8):923-927.

12. Gmeiner WH, van Waardenburg R: **Targeting DNA topoisomerases: past & future**. *Cancer Drug Resist* 2021, **4**(4):758-761.

13. Pommier Y, Leo E, Zhang H, Marchand C: **DNA topoisomerases and their poisoning by anticancer and antibacterial drugs**. *Chem Biol* 2010, **17**(5):421-433.

14. Pommier Y: **Drugging topoisomerases: lessons and challenges**. *ACS Chem Biol* 2013, **8**(1):82-95.

15. Sordet O, Nakamura AJ, Redon CE, Pommier Y: **DNA double-strand breaks and ATM activation by transcription-blocking DNA lesions**. *Cell Cycle* 2010, **9**(2):274-278.

Supplementary Table S1. Least squares means analysis of change in weight change during treatment (6 groups: (i) control; (ii) LV; (iii) 5-FU; (iv) 5-FU/LV; (v) CF10; (vi) CF10/LV. 2 time points (day 0, day 7).

treat	day	weight LSMEAN	LSMEAN Number
CF10	**0**	22.5000000	1
CF10	**7**	24.5000000	2
CF10_LV	**0**	22.7500000	3
CF10_LV	**7**	20.5000000	4
Control	**0**	22.7500000	5
Control	**7**	24.7500000	6
LV	**0**	22.7500000	7
LV	**7**	20.0000000	8
fFU	**0**	23.2500000	9
fFU	**7**	16.0000000	10
fFU_LV	**0**	22.7500000	11
fFU_LV	**7**	17.7500000	12

Supplementary Figure S1. Interaction plot for outcomes day 7 (red) vs day 0 (blue) depicting change in weight.

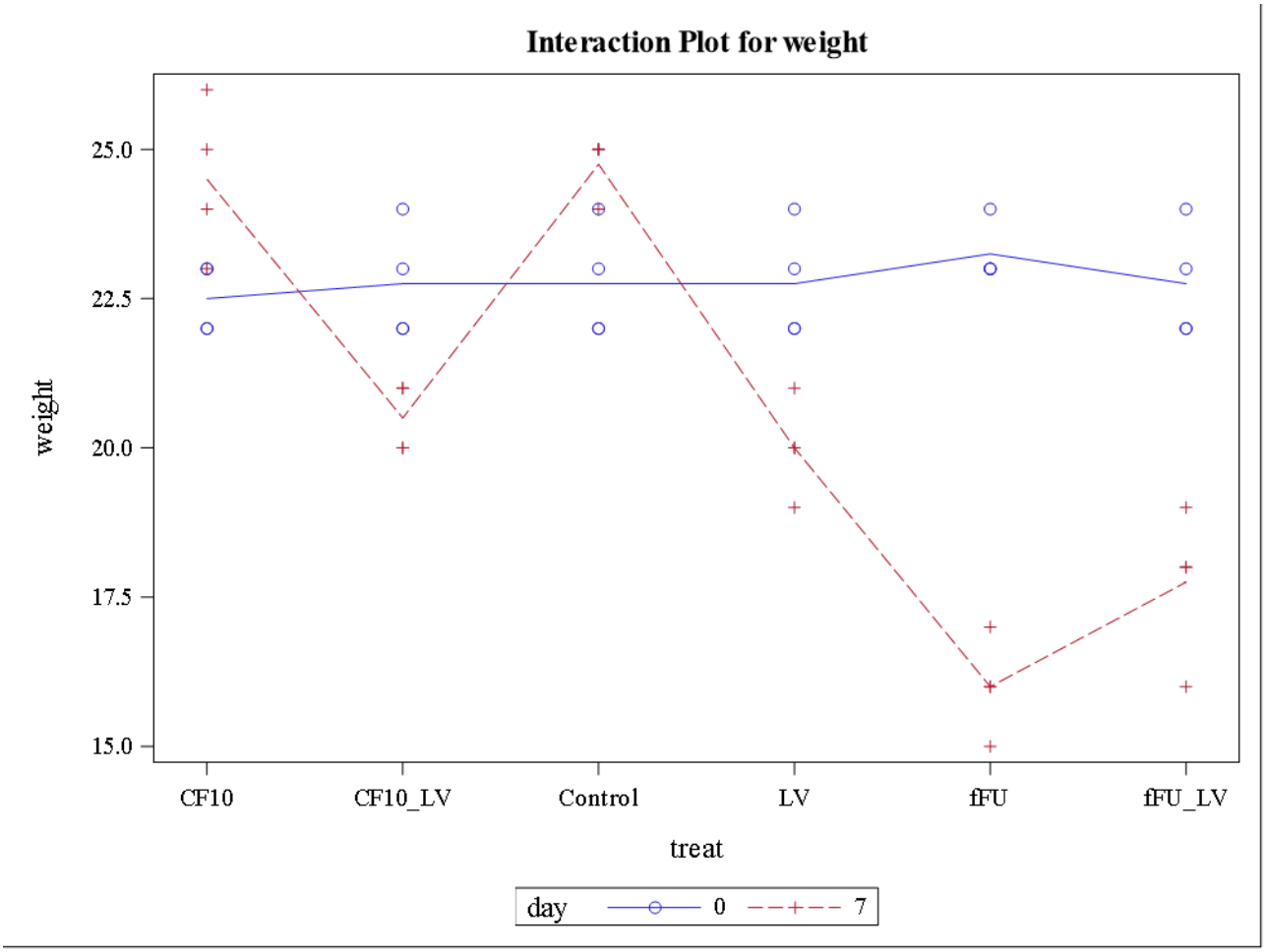

Supplementary Table S2. Least squares means analysis of change in weight during treatment (IVIS Flux – 6 groups: (i) control; (ii) LV; (iii) 5-FU; (iv) 5-FU/LV; (v) CF10; (vi) CF10/LV. 2 time points (day 0, day 7).

Least Squares Means for Effect treat*day
t for H0: LSMean(i)=LSMean(j) / Pr > |t|

Dependent Variable: weight

i/j	1	2	3	4	5	6	7	8	9	10	11	12
1		-3.19291 0.0029	-0.39911 0.6922	3.192913 0.0029	-0.39911 0.6922	-3.59203 0.0010	-0.39911 0.6922	3.991141 0.0003	-1.19734 0.2390	10.37697 <.0001	-0.39911 0.6922	7.583167 <.0001
2	3.192913 0.0029		2.793798 0.0083	6.385825 <.0001	2.793798 0.0083	-0.39911 0.6922	2.793798 0.0083	7.184053 <.0001	1.99557 0.0536	13.56988 <.0001	2.793798 0.0083	10.77608 <.0001
3	0.399114 0.6922	-2.7938 0.0083		3.592027 0.0010	0 1.0000	-3.19291 0.0029	0 1.0000	4.390255 <.0001	-0.79823 0.4300	10.77608 <.0001	0 1.0000	7.982281 <.0001
4	-3.19291 0.0029	-6.38583 <.0001	-3.59203 0.0010		-3.59203 0.0010	-6.78494 <.0001	-3.59203 0.0010	0.798228 0.4300	-4.39025 <.0001	7.184053 <.0001	-3.59203 0.0010	4.390255 <.0001
5	0.399114 0.6922	-2.7938 0.0083	0 1.0000	3.592027 0.0010		-3.19291 0.0029	0 1.0000	4.390255 <.0001	-0.79823 0.4300	10.77608 <.0001	0 1.0000	7.982281 <.0001
6	3.592027 0.0010	0.399114 0.6922	3.192913 0.0029	6.784939 <.0001	3.192913 0.0029		3.192913 0.0029	7.583167 <.0001	2.394684 0.0220	13.96899 <.0001	3.192913 0.0029	11.17519 <.0001
7	0.399114 0.6922	-2.7938 0.0083	0 1.0000	3.592027 0.0010	0 1.0000	-3.19291 0.0029		4.390255 <.0001	-0.79823 0.4300	10.77608 <.0001	0 1.0000	7.982281 <.0001
8	-3.99114 0.0003	-7.18405 <.0001	-4.39025 <.0001	-0.79823 0.4300	-4.39025 <.0001	-7.58317 <.0001	-4.39025 <.0001		-5.18848 <.0001	6.385825 <.0001	-4.39025 <.0001	3.592027 0.0010
9	1.197342 0.2390	-1.99557 0.0536	0.798228 0.4300	4.390255 <.0001	0.798228 0.4300	-2.39468 0.0220	0.798228 0.4300	5.188483 <.0001		11.57431 <.0001	0.798228 0.4300	8.780509 <.0001
10	-10.377 <.0001	-13.5699 <.0001	-10.7761 <.0001	-7.18405 <.0001	-10.7761 <.0001	-13.969 <.0001	-10.7761 <.0001	-6.38583 <.0001	-11.5743 <.0001		-10.7761 <.0001	-2.7938 0.0083
11	0.399114 0.6922	-2.7938 0.0083	0 1.0000	3.592027 0.0010	0 1.0000	-3.19291 0.0029	0 1.0000	4.390255 <.0001	-0.79823 0.4300	10.77608 <.0001		7.982281 <.0001
12	-7.58317 <.0001	-10.7761 <.0001	-7.98228 <.0001	-4.39025 <.0001	-7.98228 <.0001	-11.1752 <.0001	-7.98228 <.0001	-3.59203 0.0010	-8.78051 <.0001	2.793798 0.0083	-7.98228 <.0001	

Supplementary Table S3. Least squares means analysis of change in IVIS flux intensities during treatment (IVIS Flux – 6 groups: (i) control; (ii) LV; (iii) 5-FU; (iv) 5-FU/LV; (v) CF10; (vi) CF10/LV. 2 time points (day 0, day 7).

treat	day	outcome LSMEAN	LSMEAN Number
CF10	**0**	222500000	1
CF10	**7**	157500000	2
CF10_LV	**0**	242500000	3
CF10_LV	**7**	102500000	4
Control	**0**	210000000	5
Control	**7**	437500000	6
LV	**0**	210000000	7
LV	**7**	550000000	8
fFU	**0**	217500000	9
fFU	**7**	675000000	10
fFU_LV	**0**	230000000	11
fFU_LV	**7**	1500000000	12

Supplementary Figure S2. Interaction plot for outcomes day 7 (red) vs day 0 (blue) depicting change in IVIS flux intensities.

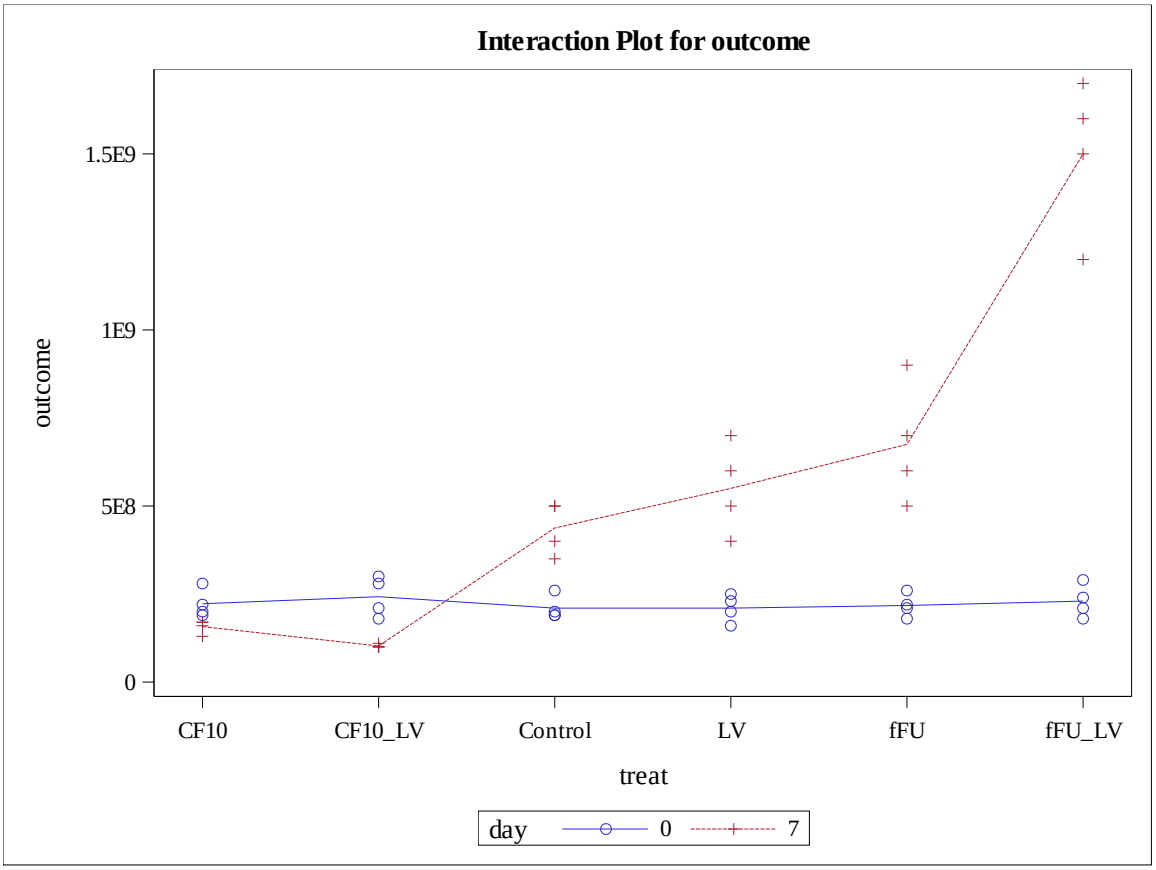

Supplementary Table S4. Least squares means analysis of change in IVIS flux intensities during treatment (IVIS Flux – 6 groups: (i) control; (ii) LV; (iii) 5-FU; (iv) 5-FU/LV; (v) CF10; (vi) CF10/LV. 2 time points (day 0, day 7).

Least Squares Means for Effect treat*day
t for H0: LSMean(i)=LSMean(j) / Pr > |t|

Dependent Variable: outcome

i/j	1	2	3	4	5	6	7	8	9	10	11	12
1		0.96311 0.3419	-0.29634 0.7687	1.778049 0.0838	0.185213 0.8541	-3.18567 0.0030	0.185213 0.8541	-4.85259 <.0001	0.074085 0.9414	-6.70473 <.0001	-0.11113 0.9121	-18.9288 <.0001
2	-0.96311 0.3419		-1.25945 0.2160	0.814939 0.4205	-0.7779 0.4417	-4.14878 0.0002	-0.7779 0.4417	-5.8157 <.0001	-0.88902 0.3799	-7.66784 <.0001	-1.07424 0.2899	-19.8919 <.0001
3	0.296341 0.7687	1.259451 0.2160		2.07439 0.0453	0.481555 0.6330	-2.88933 0.0065	0.481555 0.6330	-4.55625 <.0001	0.370427 0.7132	-6.40838 <.0001	0.185213 0.8541	-18.6325 <.0001
4	-1.77805 0.0838	-0.81494 0.4205	-2.07439 0.0453		-1.59284 0.1199	-4.96372 <.0001	-1.59284 0.1199	-6.63064 <.0001	-1.70396 0.0970	-8.48277 <.0001	-1.88918 0.0669	-20.7069 <.0001
5	-0.18521 0.8541	0.777896 0.4417	-0.48155 0.6330	1.592835 0.1199		-3.37088 0.0018	1.77E-15 1.0000	-5.0378 <.0001	-0.11113 0.9121	-6.88994 <.0001	-0.29634 0.7687	-19.114 <.0001
6	3.185671 0.0030	4.148781 0.0002	2.889329 0.0065	4.96372 <.0001	3.370884 0.0018		3.370884 0.0018	-1.66692 0.1042	3.259756 0.0024	-3.51905 0.0012	3.074543 0.0040	-15.7431 <.0001
7	-0.18521 0.8541	0.777896 0.4417	-0.48155 0.6330	1.592835 0.1199	-177E-17 1.0000	-3.37088 0.0018		-5.0378 <.0001	-0.11113 0.9121	-6.88994 <.0001	-0.29634 0.7687	-19.114 <.0001
8	4.852592 <.0001	5.815701 <.0001	4.55625 <.0001	6.63064 <.0001	5.037805 <.0001	1.666921 0.1042	5.037805 <.0001		4.926677 <.0001	-1.85213 0.0722	4.741463 <.0001	-14.0762 <.0001
9	-0.07409 0.9414	0.889024 0.3799	-0.37043 0.7132	1.703963 0.0970	0.111128 0.9121	-3.25976 0.0024	0.111128 0.9121	-4.92668 <.0001		-6.77881 <.0001	-0.18521 0.8541	-19.0029 <.0001
10	6.704726 <.0001	7.667835 <.0001	6.408384 <.0001	8.482774 <.0001	6.889939 <.0001	3.519055 0.0012	6.889939 <.0001	1.852134 0.0722	6.778811 <.0001		6.593598 <.0001	-12.2241 <.0001
11	0.111128 0.9121	1.074238 0.2899	-0.18521 0.8541	1.889177 0.0669	0.296341 0.7687	-3.07454 0.0040	0.296341 0.7687	-4.74146 <.0001	0.185213 0.8541	-6.5936 <.0001		-18.8177 <.0001
12	18.92881 <.0001	19.89192 <.0001	18.63247 <.0001	20.70686 <.0001	19.11402 <.0001	15.74314 <.0001	19.11402 <.0001	14.07622 <.0001	19.0029 <.0001	12.22409 <.0001	18.81768 <.0001	

Supplementary Table S5. MC38-P Survival Study summary statistics

Table of group by dead			
group	**dead**		
Frequency **Percent** **Row Pct** **Col Pct**	**0**	**1**	**Total**
A:Contro	0 0.00 0.00 0.00	5 33.33 100.00 62.50	5 33.33
B:ffu_lv	2 13.33 40.00 28.57	3 20.00 60.00 37.50	5 33.33
C:cf10_lv	5 33.33 100.00 71.43	0 0.00 0.00 0.00	5 33.33
Total	7 46.67	8 53.33	15 100.00

Statistics for Table of group by dead

Statistic	DF	Value	Prob
Chi-Square	2	10.1786	0.0062
Likelihood Ratio Chi-Square	2	13.9976	0.0009
Mantel-Haenszel Chi-Square	1	9.3750	0.0022
Phi Coefficient		0.8238	
Contingency Coefficient		0.6358	
Cramer's V		0.8238	
WARNING: 100% of the cells have expected counts less than 5. Chi-Square may not be a valid test.			

Fisher's Exact Test	
Table Probability (P)	0.0016
Pr <= P	0.0093

Sample Size = 15

Supplementary Table S6. MC38-R Survival Study summary statistics

Table of group by dead			
group	**dead**		
Frequency **Percent** **Row Pct** **Col Pct**	**0**	**1**	**Total**
A:Contro	0 0.00 0.00 0.00	5 33.33 100.00 50.00	5 33.33
B:ffu_lv	0 0.00 0.00 0.00	5 33.33 100.00 50.00	5 33.33
C:cf10_lv	5 33.33 100.00 100.00	0 0.00 0.00 0.00	5 33.33
Total	5 33.33	10 66.67	15 100.00

Statistics for Table of group by dead

Statistic	DF	Value	Prob
Chi-Square	2	15.0000	0.0006
Likelihood Ratio Chi-Square	2	19.0954	<.0001
Mantel-Haenszel Chi-Square	1	10.5000	0.0012
Phi Coefficient		1.0000	
Contingency Coefficient		0.7071	
Cramer's V		1.0000	
WARNING: 100% of the cells have expected counts less than 5. Chi-Square may not be a valid test.			

Fisher's Exact Test	
Table Probability (P)	0.0003
Pr <= P	0.0010

Sample Size = 15

CHAPTER 7

CONCLUSION/FUTURE DIRECTIONS

CF10 is effective in vivo in orthotopic CRLM models. CF10/LV is more effective than 5-FU/LV in a CRLM model under conditions of human-like folate levels. CF10/LV displays strong antitumor activity in MC38R CRLM model. H&E pathology showed that both CF10/LV and CF10 inhibit metastasis in MC38R CRLM model. CF10/LV is significantly more effective than 5-FU/LV at promoting increased survival in MC-38R and MC-38P CRLM model. Acquired drug resistance is a central cause of colorectal cancer mortality as most patients with metastatic CRC initially respond to chemotherapy with 5-FU-based regimens (e.g. FOLFOX, FOLFIRI) however long-term survival is uncommon with <14% of mCRC patients surviving 5-years post-diagnosis. Our 7-day infusion model provides valuable information on the potential of CF10 to be effective in treating drug-resistant mCRC however the limitation of the model is that it does not allow a survival advantage to be established because mice are required to be euthanized following removal of the jugular vein catheter because of the number of invasive surgeries involved in the study. On the other hand, our 14-day infusion model evaluated the survival in both the MC38:C57BL/6 and the $MC38^{R}$:C57BL/6 CRC liver metastasis models and the results revealed that CF10 and CF10/LV could provide a survival advantage relative to 5-FU and 5-FU/LV including complete tumor eradication in both the liver and GI according to our H&E pathological investigation. Our results also provided new insights into the mechanism of acquired resistance to 5-FU/LV in CRC cells and indicate CF10/LV is an effective alternative.

Overcoming 5-FU resistance affects mCRC treatment efficacy by understanding its consolidative mechanism. As a result, the involvement between increased TS levels, genetic polymorphisms, and programmed cell death gave an extensive background for clarifying the resistance model. CF10 displays potentiate characteristics to overcome current 5-FU-based regimes, as it is one of the significant keys to addressing the foremost problems in CRC treatment.

In general, our findings demonstrate that CF10 is much more potent for CRC cells than FPs used in treatment regimens for mCRC. The increased potency for CF10 relative to 5-FU and TFT is general, as evidenced by lower AUC values over multiple CRC cell lines included in the Broad Institute PRISM screen, is maintained with folate restriction, and is associated with stronger TS inhibition and potent Top1cc formation consistent with mechanistic similarities to Top1 poisons. LV co-treatment increases CF10 cytotoxicity to CRC cells, and while the effect is less pronounced than for 5-FU, our results support LV co-treatment during CF10 development. The promising results obtained from the TFT study, particularly eradicating tumors in the model, suggest that CF10 could improve long-term survival outcomes for patients with mCRC. Acquired 5-FU/LV resistance was also associated with FP-induced TS, elevated Myc and ABCB5. There is minimal cross-resistance to CF10 in 5-FU/LV-resistant CRC cells consistent with its use in treating 5-FU/LV-resistant mCRC.

I propose further investigating the mechanism associated with 5-FU/LV CRC resistance selective using our RNA sequencing (RNA seq) data to address the difference between non-resistant and resistant CRC. This can be achieved by

selecting the first two Hits on our RNA seq and using key molecular biology techniques like immunoprecipitation, western blotting, spheroid, and GSEA gene enrichment analysis to identify potential drug targets and examine the changes in protein expression related to 5-FU/LV metabolism and apoptosis involved in drug resistance.

Curriculum Vitae

Charles Okechukwu, M.S
cokechuk@wakehealth.edu**.** (919) 282-6135**.**
https://www.linkedin.com/in/charles- okechukwu-29515145/

EDUCATION

Ph.D., Integrative Physiology and Pharmacology **2019-2025**
Wake Forest University School of Medicine Winston Salem, NC, USA

Master of Science, Biological and Biomedical Sciences **2017-2019**
North Carolina Central University (NCCU) Durham, NC, USA
Magna Cum Laude

Bachelor of Science, Chemistry and Pharmaceutical Science **2010-2014**
North Carolina Central University (NCCU) Durham, NC, USA
Cum Laude

EXPERIENCE

Wake Forest University School of Medicine Graduate Student **2021-2025**
Advisor: Dr. William Gmeiner
My research is to determine the effects CF10 will display to improve anti-metastatic activity for the treatment of colorectal-liver metastasis through improved pharmacokinetics and exosomes mediated uptake. Rats underwent portal vein injection of colorectal cells and infused 0.9% saline as vehicle control. Rats were weighed for approximately 4weeks, including tumor growth, using IVIS imaging after RGD peptide injection. After approximately 4weeks, rats were euthanized with isoflurane, and extracted liver tumors weighed. All the tissues were fixed in 10% neutral buffered formalin for 24 hours followed by 70% ethanol, processed with xylene, sectioned, and stained with Hematoxylin and Eosin. Tumor localization via light microscopy.

Also, I developed CRC resistant cells to 5-FU/LV in folate restricted media and tested for resistance. My results confirmed 5-FU/LV CRC cell lines being resistant to 5-FU and CF10 overcomes it.

Wake Forest University School of Medicine Graduate Student 2019-2021
Advisor: Dr. Mark Chappell.

My primary research area began with a focus on the cardiovascular system, and I am interested in understanding the mechanisms of fetal programming events in kidney function and cellular injury. We conducted studies that have resulted in the characterization of the soluble prorenin receptor (sPRR) to inflammatory cytokines in the HK-2 proximal tubule cells. With the emergence of the COVID pandemic, our research refocused on ACE2 characterization in human urinary exosomes after acute or chronic kidney injury. Our study's goal was to identify unique urinary exosomal markers that can be utilized as future therapeutic targets.

North Carolina Central University Graduate Assistant 2017-2019
Thesis Research Mentor: Dr. Emmanuel Awumey.

My thesis title, "Calcium-sensing receptor (CaSR) and renin angiotensin system (RAS) expression in salt-sensitive rats". I am testing the effects of a high salt/hypertensive diet on female Dahl salt-sensitive (SS) and CaSR mutant (SS-CaSR) rats on the expression of CaSR, and its downstream signaling complements and proteins in the RAS in kidneys. My results showed significant differences in the expression of these proteins between the SS and mutants. These results were calculated using Sigma-plot to analyze their mean and standard deviations.

Student Services Contractor 2014-2017
United States Environmental Protection Agency (USEPA) Durham, NC, USA
Research Mentor: Sey Yusupha.

USEPA Pharmacokinetic Branch

This project *XAD Resin Extraction of Disinfectant By-Products in Drinking Water* proposes to extract and concentrate large volumes of water for identification of trace organic compounds used to disinfect drinking water. My responsibilities include:

- Percolating acidified water through bed of macroreticular resins (XAD-8 and XAD-2).
- Using CFT-25 refrigerated recirculator to evaporate ethyl acetate.
- Using the microtox to identify its effective concentration(s).

This project Method development and toxicity assay on Contaminated Candidate list (CCL) and Phenol Standard using the microtox. My responsibilities include:

- Determine a repeatable effective concentration for the Phenol standard.
- Determine the effective concentration for the CCL.
- Write the standard operating procedure for the microtox.

North Carolina Central University Durham, NC 2011-2014

Under the direction of Research Mentor, Dayami Lopez, Ph.D., Director of the Lopez Laboratory, my responsibilities on the project to determine the role of T_3 and/or estrogen agonists in the cell proliferation and viability of breast cancer cells, were to:

- Use a tetrazolium-based colorimetric assay (MTT) to demonstrate that triiodothyronine (T_3) reduced the viability of MDA-MB-231(triple negative breast cancer) cells but enhanced the viability of T47D (triple positive breast cancer) cells.
- Show proliferation of T47D cells but had little to no effect on the viability of MDA-MB-231 cells by both estrogen receptor agonists' diaryl propionitrile (DPN) and propyl-pyrazole-triol (PPT).

Under the direction of Research Mentor, Williams-Devane ClarLynda, Ph.D., Director of the Williams-Devane Laboratory, my responsibilities on the project to show the effect of two types of stressors:(daily hassles and stressful life events), were to:

- Determine whether these stressors differentially increase blood pressure.
- Show significant difference between them by using R to analyze their slopes and standard deviations.

University of North Carolina at Chapel Hill, NC 2011 - 2012

I participated in this 2-year collaborative program between UNC-CH Lineberger Cancer Center and North Carolina Central University, where students conducted cancer-related research at Lineberger during the summers and additional research during the academic year. In addition, Partners students took special courses (Cancer Biology, Epidemiology, Introduction to Public Health) to better understand the causes, cures, and prevention strategies for cancers.

As an intern in the summer of 2011 under the direction of Keku Temitope, Ph.D., Director of the Keku Laboratory, my responsibilities on the project to comparison of microbiota in rectal mucosal biopsies and rectal swabs were to:

- Use the bacterial 16s ribosomal gene Terminal Restriction Fragment Length Polymorphism (TRFLP) and quantitative Polymerase Chain Reaction (qPCR) to show differences in species richness, evenness and diversity in swabs compared to biopsies from the same patient.
- Show significant differences in samples from the same patient, indicating that swabs and biopsies provide different views of the microbial biota along the intestine.

As an intern in the summer of 2012 under the direction of Whitehurst Angelique, Ph.D., Director of the Whitehurst Laboratory, my responsibilities on the project to reveal the role of cancer-testes (CT) in HIF signaling were to:

- Confirm CT - antigens using siRNA to inhibit expression of hit proteins.
- Use Western blots to determine whether Hif1 protein levels were reduced due to gene inhibition.

Technical Expertise:

Cell biology: Human primary and immortalized cell culture; cytotoxicity assays; siRNA transfection; 5-FU/LV Resistance CRC cell-line selection and development.

Molecular Biology and Biochemistry: Real-time quantitative RT-PCR; Western blotting, ELISA assays; RNA isolation; Targeted RNA sequencing array design; Ultracentrifugation; Size Exclusion Chromatography; Flow Cytometry.

In Vivo – Rodents: Handling and necropsy techniques; Tissue collection; cell differential counts; Body composition measurements; Animal Breeding.

Imaging/ Bioluminescence: Microtox; Immunofluorescence staining; Absorbance and fluorescence microplate reader; Histology preparation, Immunohistochemistry, IVIS.

Administrative Skills :

Data analysis using (R, SAS, SPSS); Prism; NIH Image J; Endnote; Microsoft; Good written and oral communication; Ability to organize, lead, and participate in a diverse team environment; Time and people management.

Awards and Honors

1. American Association Cancer Research Minority Scholar in Cancer Research Award Recipient (2024)

2. Deal Fund Travel Awardee, Wake Forest Baptist Comprehensive Cancer Center (2024)

3. Burroughs Wellcome Fund Graduate Diversity Enrichment Program Award Recipient (2023-2025)

4. Deal Fund Travel Awardee, Wake Forest Baptist Comprehensive Cancer Center (2023)

5. HHMI Gilliam Fellowship nominee from Wake Forest University (2020)

6. American Physiological Society (APS): Martin Frank Diversity Travel Award Recipient (2019)

7. American Physiological Society/American Society of Nephrology (APS/ASN): Martin Frank Diversity Travel Award Recipient (2019)

8. Award Finalist Cell and Molecular Physiology Section (CAMPs)/APS Conference on my Master's research "CaSR and RAS expression in salt-sensitive rats" (2019)

9. American Chemical Society (ACS): National Scholarship Award and Student Service Impact Award Recipient (2014)

10. 20th Annual International Society of Pharmaceutical Engineers (ISPE) - Carolina South Atlantic Chapter (CASA) Life Sciences Technology Conference: 1ST Place Poster Undergraduate Competition (2013)

11. AmeriCorps President's Volunteer Service (THE WHITE HOUSE): President's Volunteer Service Award Recipient(2013)

12. University of Missouri-Columbia: Medical Preparation workshop Award Recipient(2013)

13. NCCU Foundation Scholarship Award Recipient(2012-2013)

14. BRITE Scholarship Award Recipient(2012-2013)

15. Society of Toxicology (SOT): Undergraduate Education Awardee (2012)

Publications:

Charles Chidi Okechukwu, Xue Ma, Wencheng Li, Ralph D'Agostino, Jr., and William H. Gmeiner
"CF10 Overcome Acquired Resistance to 5-FU/LV in a MC38:C57BL/6 Syngeneic, Orthotopic Mouse Model of Colorectal Cancer Liver Metastasis" In Preparation April 2025.

Charles Chidi Okechukwu, William H. Gmeiner "CF10/LV Overcomes Acquired Resistance to 5-FU/LV in Colorectal Cancer Cells Through Downregulation of the c-Myc/ABCB5 Axis" Cancer Drug Research Submitted March 2025.

Charles Chidi Okechukwu, Xue Ma, Wencheng Li, Ralph D'Agostino, Jr., Matthew G. Rees, Melissa M. Ronan, Jennifer A. Roth, and William H. Gmeiner "CF10 Displays Improved Activity Relative to 5-FU in a Mouse CRLM Model Under Conditions of Physiological Folate" AACR Clinical Cancer Research MCT submitted March 2025.

Okechukwu, C.C.; Ma, X.; Sah, N.; Mani, C.; Palle, K.; Gmeiner, W.H. Enhanced Therapeutic Efficacy of the Nanoscale Fluoropyrimidine Polymer CF10 in a Rat Colorectal Cancer Liver Metastasis Model. Cancers 2024, 16, 1360. https://doi.org/10.3390/cancers16071360.

Gmeiner WH, **Okechukwu CC.** Review of 5-FU resistance mechanisms in colorectal cancer: clinical significance of attenuated on-target effects. Cancer Drug Resistance. 2023; 6(2):257-72. doi: 10.20517/cdr.2022.136. PMID: 37457133; PMCID: PMC10344727.

Okechukwu CC, Pirro NT, Chappell MC. Evidence that angiotensin II does not directly stimulate the MD2-TLR4 innate inflammatory pathway. Peptides. 2021 Feb;136:170436. doi: 10.1016/j.peptides.2020.170436. Epub 2020 Nov 9. PMID: 33181267; PMCID: PMC7855779**.**

Araujo-Perez, F., McCoy, A. N., **Okechukwu, C.,** Carroll, IM., Smith, KM., Jeremiah, K., Sandler, RS., Asher, GN., Keku, TO. Differences in microbial signatures between rectal mucosal biopsies and rectal swabs. Gut Microbes. 2012 Nov-Dec;3(6):530-5. doi: 10.4161/gmic.22157. Epub 2012 Oct 11. PMID: 23060016; PMCID: PMC3495790.

Invited Talks and Presentations:

Charles C. **Okechukwu, M.Sc.,** Xue Ma, MD, Ph.D., William H. Gmeiner, Ph.D., MBA. "Role of O-GlcNac Conjugation and TS Translational Repression in 5-FU/LV Resistance in CRC and CF10 response" AACR Annual Meeting, San Diego, California (2024).

Charles Okechukwu, M.Sc., William H. Gmeiner Ph.D., MBA. "Role of Translational Regulation of TS, Myc, and p53 in Mediating 5-FU Resistance CRC and CF10 Response" Burroughs Wellcome Fund Conference, Raleigh, North Carolina (2023).

Charles Okechukwu, M.Sc., William H. Gmeiner Ph.D., MBA. "Role of Translational Regulation of TS, Myc, and p53 in Mediating 5-FU Resistance CRC and CF10 Response" ABRCMS, Phoenix, Arizona (2023).

Charles Okechukwu, M.Sc., William H. Gmeiner Ph.D., MBA. "Improved Anti-Metastatic Activity of CF10 in The Treatment of Colorectal-Liver and Colorectal-Cecal Metastasis" Three-minute thesis presentation at the Wake Forest University Graduate School Research Day (2023).

Charles Okechukwu, M.Sc., Mark Chappell Ph.D. "Angiotensin II Does Not Directly Stimulate The TLR4-MD2-MyD88 Inflammatory Pathway" Hypertension Scientific Session Virtual Event (2020).

Charles Okechukwu, M.Sc., Emmanuel M. Awumey Ph.D. "High Salt and Aldosterone: Focus on CaSR-RAS on Plasma and Urinary Outcomes in Dahl Salt-Sensitive Rats" APS Aldosterone and ENaC in Health and Disease: The Kidney and Beyond conference, Estes Park, CO. (2019)

Teaching Experience

2012-2013 Student Teaching Assistant (Department of Pharmaceutical Sciences, NCCU)
I was a student teaching assistant for biostatistics. I tutored students after class and addressed any question problems they have. I helped the class instructor to co-ordinate the class and make sure the students understand each class material presented to them prior to either quizzes or exams.

2017 Graduate Teaching Assistant (Department of Biological and Biomedical Sciences, NCCU)
I set up the class materials for Bio1000 Genetics class, and brought the course director(who is medically blind) to the class

to deliver the early part of the course material while I teach most of the class. I address any questions from the students and prepare both quizzes and exam questions. I graded all the quizzes, test questions, and exams. I also upload all quizzes, test questions, and exams scores on the school blackboard so that students can see their grades. I also tutor the students after hours to make sure they understand the class materials before each of the exams. The class size was over 300 students, and the class has two sessions which I teach for 90 minutes each. The class meet every Tuesdays and Thursdays.

Leadership and Community Service Experiences:

2023	Moore Outreach event hosted by Magnet Elementary School Winston-Salem, NC (Mentor)
2023	ePoster Presentation Judge ABRCMS Conference
2023	Science Night hosted by Union Cross Elementary School Kernersville, NC (Mentor)
2022	Mentor Friends-in-Stem Mentoring Program
2022	IPP Graduate Student Honors Council Representative
2021	IPP Graduate Student Honors Council Representative
2020	IPP Graduate Student Honors Council Representative
2019-2025	Graduate Student Ambassador Wake Forest Graduate School
2019	Member/Black Graduate Student Association
2014	NCCU American Chemistry Society (ACS) President
2014	AmeriCorps-North Carolina Literacy Corps (NCLC) NCCU Student site Coordinator/tutor/volunteer
2013	NCCU Louis Stokes Alliance for Minority Participation (LSAMP) students
2013	NCCU Golden Key International Society Vice-President
2013	AmeriCorps-North Carolina-Activating Citizenship Through Service (NC-ACTS!) student service/co-ordinator

Certifications:

2020	Human Research Biomedical Investigators 1-Basic Course
2020	Good Clinical Practice for Clinical Trials with Investigational Drugs and Biologics (ICH Focus) 1-Basic Course

Membership:

2024-Present	American Association Cancer Research Associate Member